Expression and regulation of N-Myc Downstream-Regulated Gene 1 in squamous cell carcinoma of the oesophagus

Jacqueline Claire Bracher

Thesis Presented for the Degree of
DOCTOR OF PHILOSOPHY

in the Department of
Clinical Laboratory Sciences
Division of
Medical Biochemistry
UNIVERSITY OF CAPE TOWN

Supervisor: Assoc. Professor D.T. Hendricks
Co-supervisor: Dr. V. Leaner

November 2009

ACKNOWLEDGMENTS

I would like to express my sincere gratitude to the following people:

My supervisor, Assoc. Prof. Denver Hendricks for his excellent supervision, constant encouragement and support

My co-supervisor, Dr. Virna Leaner, for her amazing guidance and contribution of ideas

Dr. Michael Birrer, for inviting me to, and generously hosting me, in his laboratory at the National Cancer Institute/NIH for ten months

Dr. Howard Donninger for his excellent supervision and Dr. Fred Wamunyokoli and Aaron Bell, for their advice and candid discussions at the NCI/NIH

Members of the Cancer Research Group, UCT, both past and present for creating such a dynamic and enjoyable working environment

In particular, Drs. Catherine Whibley, Widaad Zemanay and Michelle Skelton for their friendship, passing on their wisdom and willingness to discuss ideas

Also, to Dr. Pauline van der Watt, Michelle Ward, Luke Esau, Nelusha Shunmoogam- Gounden and Nina Holderness for their help in the laboratory

Dr. Sharon Prince and Prof. M. Iqbal Parker, for their contribution of ideas

Hajira Guzgay, for her meticulous management of the laboratory and for her friendship

Robert Samuels for his valuable assistance in the laboratory

Nafisa Allie and Heather McLeod for assistance with immunohistochemistry

Prof. Thérèse Commes for kindly donating the anti-NDRG1 antibody, Prof. Alan Knox for kindly donating the VEGF-A reporter, Dr. Neil Davies for generously donating the HUVEC cells and Dr. Nikki Mulder for her assistance with bioinformatics techniques

The National Institutes of Health, National Research Foundation, DAAD, the Ernst and Ethel Eriksen Trust and UCT for financial assistance

My family for their steadfast love and encouragement

My partner, Till, for his unwavering love, support and encouragement, for believing in me and teaching me to believe in myself

For my family

CONTENTS

CHAPTER 6: MATERIALS AND METHODS

ABBREVIATIONS

ADC	Adenocarcinoma
Amp	Ampicillin
Ang	Angiopoietin
AP-1	Activating Protein 1
APS	Ammonium Persulphate
ASR	Age-Standardised Incidence Rate
BCA	Bicinchoninic acid
BSA	Bovin Serum Albumin
Bp	Base pairs
cDNA	Complementary DNA
ChIP	Chromatin Immunoprecipitation
CO_2	Carbon Dioxide
°C	Degrees Celcius
C_T	Threshold cycle
Ctl	Control
DAB	Diaminobenzidine
DAPI	4',6'-diamidino-2'-phenylindole dihydrochloride
DDRT-PCR	Differentail display RT-PCR
DMEM	Dulbecco's Modified Eagle's Medium
DMSO	Dimethyl sulphoxide
DNA	Deoxyribonucleic acid
dNTP	Deoxynucleoside triphosphate
ECL	Enhanced Chemiluminescence
EDTA	Ethylenediaminetetraacetic Acid
EGF	Epidermal Growth Factor
EGFR	Epidermal Growth Factor Receptor
EGR-1	Early Growth Response Gene-1
ELISA	Enzyme-Linked Immunosorbent Assay

ERK	Extracellular-signal-related kinase
FCS	Fetal Calf Serum
GusB	β-glucuronidase
HIF	Hypoxia-Inducible Factor
HPV	Human Papilloma Virus
Hr	Hour
HRP	Horse Radish Peroxidase
HUVEC	Human Umbilical Vein Endothelial Cells
IKK	Inhibitor of κB kinase
JNK	Jun amino-terminal kinase
kDa	Kilodaltons
LB	Luria Broth
Luc	Luciferase
M	Molar
MAPK	Mitogen-Activated Kinase
mg	Milligram
min	Minutes
ml	Millilitre
MMP	Matrix Metalloproteinase
MTT	3'-(4',5'-Dimethylthiazol-2'-yl)-2',5'-diphenyltetrazolium bromide
NDRG1	N-Myc Downstream-Regulated Gene 1
NF-κB	Nuclear Factor κB
ng	Nanogram
nm	Nanometers
nM	Nanomolar
nt	Nucleotides
OC	Oesophageal Cancer
OD	Optical Density
OSCC	Oesophageal Squamous Cell Carcinoma
PAGE	Polyacrylamide Gel Electrophoresis

PBS	Phosphate Buffered Saline
PCR	Polymerase Chain Reaction
PDGF	Platelet-Derived Growth Factor
PKC	Protein Kinase C
PLB	Passive Lysis Buffer
PMSF	Pheylmethanesulfonyl Fluoride
Poly-HEMA	Poly(2-hydroxyethyl methacrylate
p/s	Penicillin and Streptomycin
RIPA	Radioimmunoprecipitation assay
RNA	Ribonucleic Acid
RNAsin	Ribonuclease inhibitor
rpm	Revolutions per minute
RT-PCR	Reverse transcription Polymerase Chain Reaction
SD	Standard Deviation
siRNA	Small interfering RNA
T_a	Annealing temperature
TBST	Tris-Buffered Saline Tween-20
TK	Thymidine kinase
TNM	Tumour-Node-Metastasis
TPA	12-*o*-tetradecanoylphorbol-13-acetate
µl	Microlitre
VEGF	Vascular Endothelial Growth Factor
VHL	Von Hippel-Lindau

ABSTRACT

Squamous cell carcinoma of the oesophagus is a formidable disease which poses a significant health risk in developing countries where the incidence is frequently high and access to health care facilities is often limited. The identification of genes involved in oesophageal tumourigenesis may provide new targets for therapy and improved diagnostics techniques, thereby improving the prognosis of this pernicious disease. In this study, real-time RT-PCR and immunohistochemistry described the overexpression of N-Myc Downstream-Regulated Gene 1 (NDRG1) in oesophageal squamous cell carcinoma (OSCC) tissue compared to normal tissue in a cohort of South African cancer patients. Despite more than ten years of research into the role of NDRG1 in cancer, the precise function of this protein remains enigmatic. Reports have been contentious, suggesting both tumour suppressor and tumour promoter functions for NDRG1, implicating it in tumourigenic processes such as metastasis and angiogenesis. Our immunohistochemical analysis if NDRG1 expression in OSCC tissue and matched normal epithelium (n=83) showed that NDRG1 expression is elevated by 2.6-fold in cancer tissue compared to normal tissue. Moreover, the expression and localisation of NDRG1 appeared to track with epithelial cell maturation where basal cells of normal oesophageal epithelium displayed plasma membrane-associated NDRG1 while maturing cells were mostly positive for NDRG1 in the cytoplasm and nucleus. Likewise, NDRG1 displayed interesting patterns of localisation in tumour tissue of the

oesophagus. Dysplastic tissue and poorly differentiated tumour tissue stained positively for NDRG1 in the plasma membrane, while moderately and well differentiated tumours displayed mixed staining for NDRG1 in the plasma membrane, cytoplasm and nucleus. Analysis of NDRG1 expression in cell lines cultured under anchorage-independent conditions revealed that NDRG1 expression is strongly induced when cells are prevented from adhering to the surface of culture dishes. Induced NDRG1 expression correlated inversely with mRNA expression of invasion genes, MMP-2 and MMP-9, as well as the mRNA expression of angiogenic factors Ang-1, PDGF-B and VEGF-C but, in contrast, showed positive correlation with the angiogenesis cytokine, VEGF-A. Knock-down of NDRG1 expression with siRNA had no effect on anchorage-independent cell proliferation or apoptosis but did inhibit VEGF-A expression. Moreover, VEGF-A promoter activity, induced by culturing cells under anchorage-independent conditions was shown to be NDRG1-dependent. In order to identify factors that may drive NDRG1 transcription in cultured OSCC cell lines we cloned and partly characterised the NDRG1 promoter. Through the generation of promoter deletion constructs, site-directed mutagenesis and Chromatin Immunoprecipitation (ChIP) assays, we showed that both EGR-1 and cJun/AP-1 are capable of driving transcription of NDRG1 in response to 12-*o*-tetradecanoylphorbol-13-acetate (TPA) through activation of PKC/MEK/ERK1/2 and JNK MAPK pathways. Taken together, we describe the regulation of NDRG1 expression by EGR-1 and AP-1 and we show that NDRG1 is overexpressed in squamous cell carcinoma of the oesophagus compared to normal oesophageal tissue. We associate NDRG1 with an

oncogenic function in OSCC through its potential role in angiogenesis via modulation of VEGF-A expression.

CHAPTER 1

LITERATURE REVIEW

1.1. Cancer

It is projected that in the year 2030 there will be 27 million new cases of cancer diagnosed and nearly 17 million deaths. In 2008 an estimated 7.6 million people succumbed to cancer. Of these, more than half of the cancer cases and 60% of the deaths occurred in less-developed countries. The global cancer burden, which has more than doubled in the last thirty years, poses a growing and devastating threat to health and economic systems. Developing countries will be the hardest hit as they generally present with a high background of communicable diseases, patients have limited access to health care facilities and governments often have inadequate health care budgets. This scenario, presented in the World Cancer Report 2008[1], highlights the urgent need for translational cancer research, particularly in developing countries.

1.2. Oesophageal cancer

Data from 2002 ranked oesophageal cancer (OC) as the eighth most common malignancy and the sixth most common cause of cancer-related death[2](Fig 1.1). Indeed, the incidence of OC continues to increase despite widespread efforts to improve diagnosis and treatment[3]. The majority of malignant tumours of the oesophagus may be classified into two different histological subtypes, namely adenocarcinoma (ADC) and oesophageal squamous cell carcinoma (OSCC). ADC occurs in the distal third of the oesophagus, usually at the gastro-oesophageal junction, and

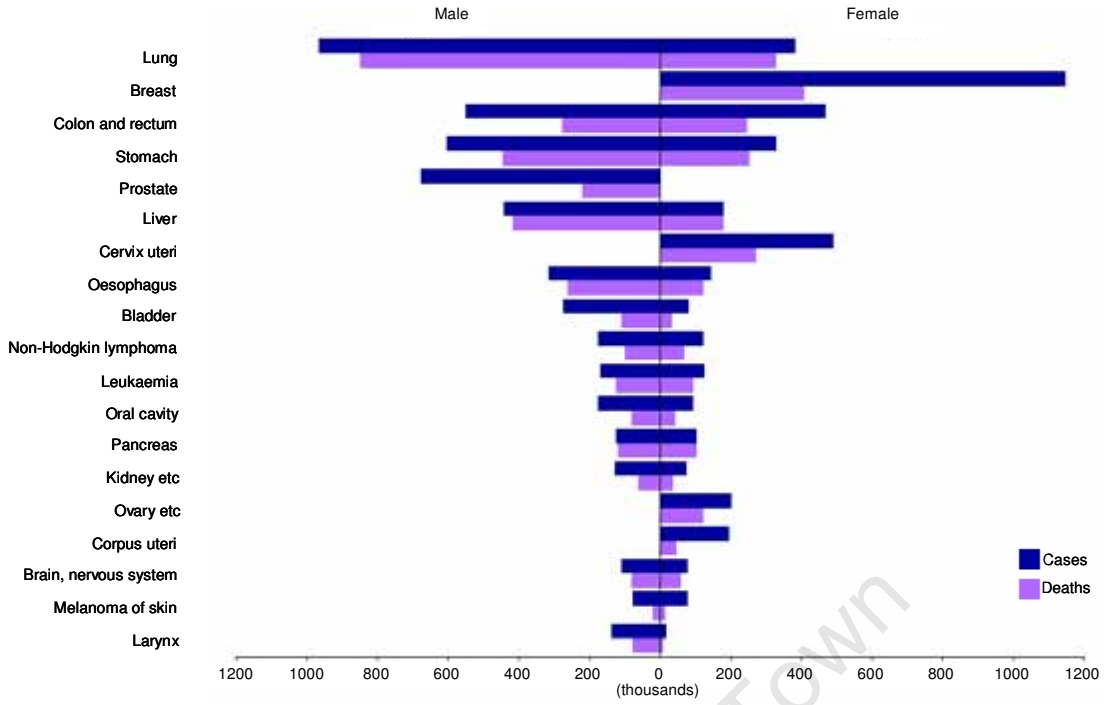

Figure 1.1. Cancer incidence and mortality rates for the world. Oesophageal cancer is the eighth most common cancer in the world and the sixth leading cause of cancer-related death. From Ferlay *et al.*, 2004 [4])

arises through the metaplastic transformation of epithelium due to continual acid reflux, a condition referred to as Barrett's oesophagus[5]. The characterisation of Barrett's oesophagus as the precursor lesion to ADC is suggested by the 95% correlation between these two conditions and is attributed to a western diet and obesity[6;7]. OSCC, which is more prevalent in developing countries is the predominant form of oesophageal cancer and primarily occurs in the upper two thirds of the oesophagus[1;8].

1.3. Oesophageal squamous cell carcinoma progression, staging and grading

Squamous cell carcinoma of the oesophagus progresses in a multi-step fashion. The pathological staging of OSCC, described in detail in Figure 1.2, is performed according

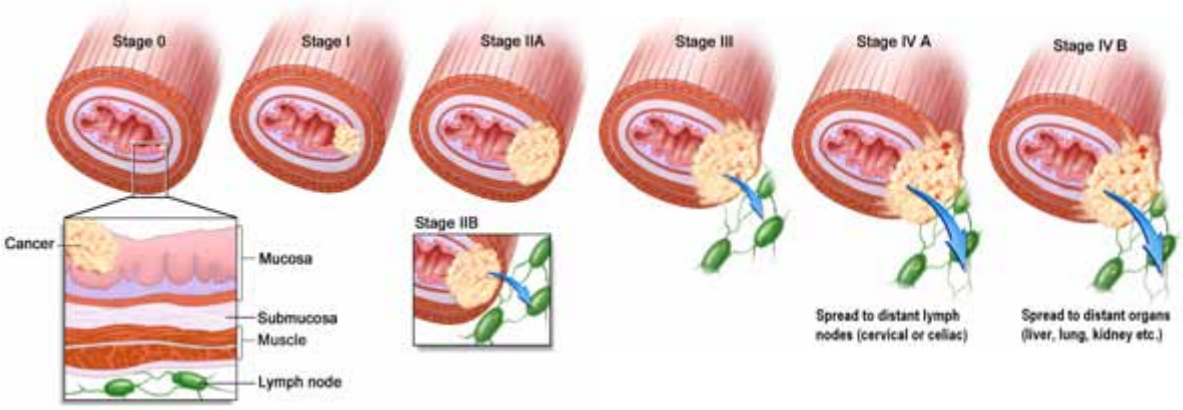

Figure 1.2. The neoplastic progression of OSCC according to the American Joint Committee on Cancer. Stage 0 is characterised by evidence of intraepithelial neoplasia (dysplasia and carcinoma *in situ*) which gives rise to the invasion of the tumour into the submucosal layer, described as Stage I. Stage II is separated into two categories namely, A, typified by the infiltration of the muscle layer, and B, signifying a tumour that has invaded all layers of the oesophagus as well as the lymph nodes. Stage 3 and 4 tumours have metastasised to the proximal and distal lymph nodes and organs, respectively. From www.cancer.gov[9].

to the 2002 American Joint Committee on Cancer tumour-node-metastasis (TNM) classification system, which takes into account the primary tumour, regional lymph node involvement and extent of metastasis. The disease initiates with dysplastic precursor lesions. These lesions are often multifocal and develop into superficial squamous cell carcinomas, confined *in situ* to the mucosa. Inconspicuous and asymptomatic, these tumours rapidly progress to late or advanced carcinomas that aggressively invade the oesophageal basement membrane, giving rise to symptoms of dysphagia, and leading to the infiltration of the submucosa, proximal lymph nodes and nearby tissues such as the trachea and aorta[6;10]. OSCC most commonly spreads to the regional lymph nodes, with the likelihood of distant metastasis increasing with tumour invasion[8]. Oesophageal cancer has long been considered a formidable disease due to its asymptomatic progression. Indeed, more than half of patients

present at a late stage and have unresectable or metastatic disease[10], explaining the reported 5-year survival rate of approximately 10% and a median survival time of 9 months[11].

Tumour grading, a far more subjective classification, is based on parameters of mitotic activity, variability in size and shape of nuclei (anisonucleosis), and degree of differentiation. The differentiation status, or extent to which tumour cells resemble their normal counterparts, can vary between tumours or even within the same tumour[6]. Although well differentiated tumours exhibit features similar to those of normal epithelium, these malignancies are comprised predominantly of keratinocyte-like cells and a smaller population of basal-like cells. The cells are frequently arranged in keratinising tumour nests, termed keratin pearls. Moderately differentiated tumours display characteristics between the well and poorly differentiated tumour types and are the most common type of OSCC[8]. Poorly differentiated tumours are largely comprised of pleomorphic, basal-like cells that are arranged irregularly, exhibit high mitotic activity and no keratinisation[6]. Poorly differentiated OSCCs are often more aggressive tumours and are thus coupled with a poor prognosis[12].

1.4. A South African Perspective

1.4.1. Epidemiology

Geographically, OSCC is widespread but a feature highlighted by many studies on oesophageal cancer is regional 'hotspots' displaying high incidence of this disease. Areas of high risk include China, South Central Asia, Western Europe, as well as

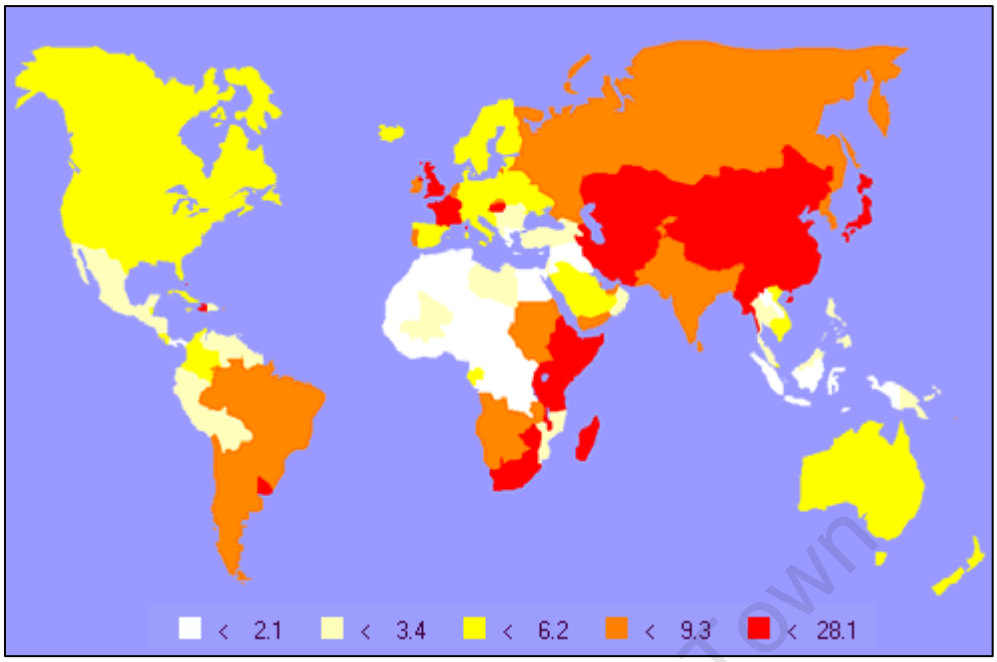

Figure 1.3. World-wide distribution of oesophageal cancer in males. Age-standardised incidence rates of oesophageal cancer per 100 000 males. Areas of high incidence include China, South Central Asia, Western Europe, as well as Southern and Eastern Africa. (Image reproduced from [4]).

Southern and Eastern Africa[2](Fig 1.3). In South Africa, cancer of the oesophagus is the third leading cancer in males, with a life time risk of 1 in 73[13]. The high incidence of OSCC in South Africa is by no means a new phenomenon. Since the 1950s it has been documented that a large number of black South Africans, particularly from the former Ciskei and Transkei regions of the Eastern Cape Province, suffer from this condition[14-16]. Today, incidence rates within the Eastern Cape have improved, yet there is still cause for concern, considering ASR of 31.3/100 000 in males and 18.0/100 000 in females[17]. Despite an increase in the worldwide incidence of OC, certain regions have shown an improved frequency of this disease. This is likely due to reduced smoking habits[18;19] as well as improved socio-economic conditions [20]

and access to health care[21]. However, one can also not exclude the effect of the HIV epidemic on life expectancy, which may result in an apparent improvement of OC incidence. Indeed the average life expectancy of South Africans has decreased from 59.6 years (1990-1999) to 47.7 years (2000-2004)[22], well below the 65 year median age of OC sufferers[8;13]. However, accounting for between 40% and 45%[17;23] of total cancer cases in the in Ciskei and Transkei region of South Africa, it is often heads of households and breadwinners that succumb to this disease – a scenario that no doubt has significant socio-economic repercussions in a developing country.

1.4.2. Aetiology

Of the aetiological factors identified as risk for OSCC, the most common is tobacco and alcohol consumption[8]. However, since the use of tobacco and alcohol is widespread and not confined to regions of high incidence, the regional hotspots of OSCC likely arise through interplay between dietary, cultural, genetic and socio-economic factors[24]. Dietary risk factors identified include nutritional deficiencies such as a lack of trace minerals (e.g. zinc and magnesium), folic acid[25;26] and vitamins A, C and E[27]. In developing countries, such as South Africa, maize is a staple source of nutrition in many rural areas. In addition to containing low levels of vitamins and trace minerals, this maize is often contaminated with various fungi (e.g. *Fusarium verticilloides* or *Aspergillus flavus*)[28-30] which produce dangerous mycotoxins that have tumourigenic potential[31] and the ability to form DNA adducts[32]. In addition to nutritional risk factors, cultural practices such as drinking extremely hot beverages[33;34] and the frequent use of emetics (herbal brews used to induce

vomiting) have been identified[35]. Polymorphisms in xenobiotic metabolising enzymes may contribute to the risk of developing OSCC[36-39], while there is also evidence that Human Papilloma Virus (HPV) may be associated, where some 30% to 75% of tumours from Chinese and South African populations were reported to carry HPV DNA[40;41].

1.5. Poor prognosis – a challenge in oesophageal cancer

Prevention rather than cure is the underlying principle of the primary health care ethos, that many health systems presently subscribe to[42;43]. The identification of risk factors for oesophageal cancer has however had little effect on improving the prognosis associated with OSCC over the last couple of decades[13;44]. Indeed, a study performed on nearly 2000 OSCC patients reported that more than 77% of these patients presented with Stage III disease, 62% had difficulty swallowing food, and the mean tumour length was between 5 cm and 10 cm[45]. The prognosis of Stage I and II OSCC is generally favourable, where treatment comprises of surgery and often neoadjuvant chemotherapy[46]. However, detection is most often at a late stage where prognosis is poor[24]. Here, metastatic involvement usually excludes surgery, and chemo- and radiotherapy are the remaining options, and in many cases serve as palliative therapy[47]. Indeed, the asymptomatic progression of OSCC coupled with limited or poor access to health care[21;48] are the predominant contributors to the poor survival rate of OSCC.

Identification of aetiological risk factors may enable the implementation of preventative measures against the development of OSCC; however the likelihood of lowering mortality rates may be more attainable than improving the incidence of OSCC. Indeed, to effectively reduce the impact of OSCC on South Africans, as well as other affected populations, more efficient diagnostic techniques, screening programs, as well as more specific therapeutic methods must be developed and implemented simultaneously. This requires an in depth understanding of the multi-gene, multi-step, multi-factorial progression to a malignant tumour and a detailed understanding of cellular processes that have gone awry in cancer.

1.6. The properties of cancer

The development and progression of cancer is associated with the acquisition of a cohort of characteristics that most cancer cells express. In general these characteristics override the systems that maintain the fine balance of tissue homeostasis. Hanahan and Weinberg[49] detailed the hallmark capabilities of cancer cells (Fig 1.4). These are:

i. Self-sufficiency in growth signals

Malignant cells acquire the ability to mimic normal mitogenic growth signals, thereby facilitating continued proliferation.

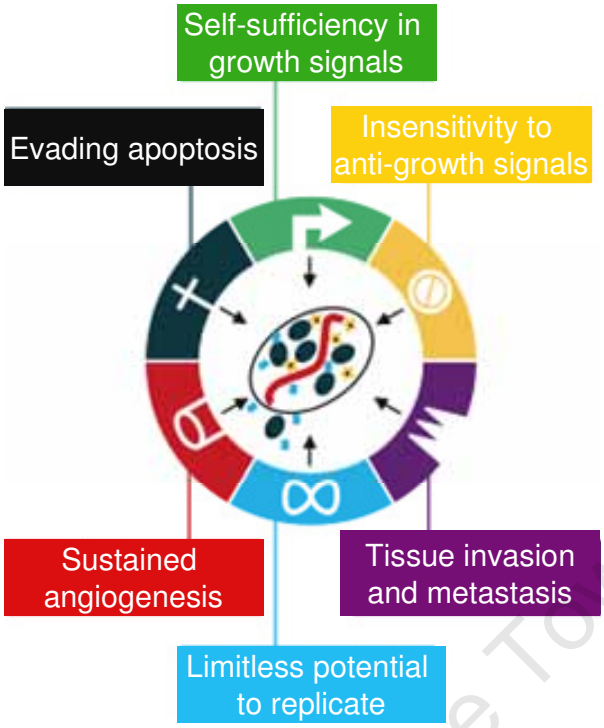

Figure 1.4. The Hallmarks of Cancer. Self-sufficiency in growth signals, insensitivity to anti-growth signal, limitless replicative potential, sustained angiogenesis and evading apoptosis are the six capabilities cells must acquire in order to dictate malignant growth. (Image reproduced from [49]).

ii. Insensitivity to antigrowth signals

Tissue homeostasis is maintained through the balance between growth and antigrowth signals. Cancer cells gain the ability to evade antiproliferative signals.

iii. Evading apoptosis

Apoptosis, or programmed cell death, is the process by which unwanted or damaged cells are eliminated. Through the activation of oncogenes or the inactivation of tumour suppressor genes, incipient cancer cells are able to escape this process.

iv. Limitless replicative potential

Uncontrolled cell growth or proliferation of cells is achieved through acquiring growth signal independence, insensitivity to anti-growth signals and escaping apoptosis. Moreover, cancer cells become immortalised through maintaining their telomere length, through the activation of the telomerase enzyme, thereby escaping replicative senescence[50].

v. Sustained Angiogenesis

As the malignant cell mass grows, so too does its need for oxygen and nutrients. Cancer cells therefore acquire the capability of regulating new blood vessel growth, a process called angiogenesis.

vi. Tissue invasion and metastasis

In due course and with increasing size, limited space, nutrients and oxygen, primary tumours invade surrounding tissues and shed cells that colonise in distant sites. This process is not well understood but requires the activation of extracellular proteases to facilitate cell movement.

In addition to the six hallmarks of cancer identified by Hanahan and Weinberg, a seventh, namely genomic instability, has recently been accepted as necessary to initiate and/or maintain the malignant phenotype[51]. Indeed, recent investigations have shown that partial loss of the mitotic spindle checkpoint results in aneuploidy,

which promotes tumour initiation and progression[51]. Taken together, these seven features describe the processes required to breach anti-neoplasm defence mechanisms, and highlight the complexity of the malignant phenotype. The acquisition of these characteristics is associated with the deregulation of a wide array of genes. Indeed, as genes which are deregulated in cancer are identified, so too can they be classified under one or more of the seven hallmarks.

1.7. N-Myc Downstream-Regulated Gene 1

The high incidence and poor survival rate of OSCC observed in South Africa, and indeed in many other developing countries, has driven a feverish, worldwide research initiative to elucidate the molecular mechanisms behind this disease. Certainly, through these research efforts diagnostic indicators, therapeutic targets and prognostic markers shall be revealed and improve the dismal circumstances of OSCC. Differential display and microarray analysis, performed in our laboratory, on tissue RNA from OSCC patients, revealed aberrant expression of several genes, amongst them N-Myc downstream-regulated gene 1 (NDRG1) (data unpublished). The altered expression of *NDRG1* in tumour tissue relative to that of adjacent normal tissue suggests a role for this gene in the initiation and/or maintenance of OSCC.

NDRG1 was initially implicated in vascular disease and identified as a tunicamycin and homocysteine responsive gene (denoted RTP) in human umbilical vein endothelial (HUVEC) cells[52]. Shortly thereafter it was described independently by other groups and named Drg-1[53], RTP/rit42[54], Cap43[55] and PROXY-1[56] according to its

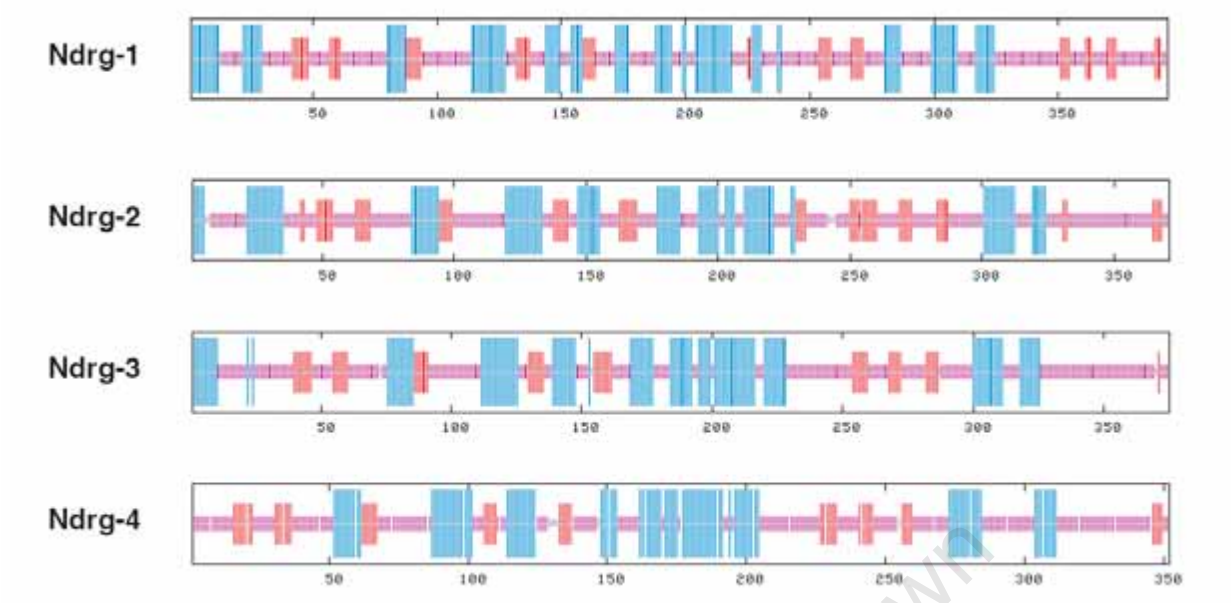

Figure 1.5. The predicted secondary structures of the NDRG family members 1-4, showing similarities and differences between family members. Blue regions signify a α-helix, red regions represent extended strands and random coils are represented by purple regions. (Figure from [57]).

alleged function. NDRG1 (as it is now accepted)[58] is a member of the NDRG family consisting of four members, namely NDRG1, NDRG2, NDRG3 and NDRG4 which share 53-65% amino acid identity between them (Fig 1.5) [59;60]. Orthologues to NDRG1 have been described in a variety of organisms including mouse[61;62], rat[63], *Caenorhabditis elegans*[64], zebra fish[65], chicken[66] and some plant species[59;67], suggesting a conserved role for this gene.

1.7.1. NDRG1 structure and post-translational modification

In humans, NDRG1 is mapped to chromosome 8q24.2[54] where the gene encodes a 3.0 kb mRNA that translates into a 43 kDa protein[53;55]. Studies examining the amino acid sequence of NDRG1 revealed three tandem deca-repeats of hydrophilic

amino acids (GTRSRSHTSE) in its C-terminal tail – a property not shared by other NDRG family members, and perhaps indicative of a unique function for this protein[52;59;60]. However, the precise function of these repeats, besides binding divalent nickel and copper ions[68;69], remains elusive. Inspection of the NDRG proteins revealed that NDRG1, as well as other family members, contains an α/β hydrolase-fold motif (Fig 1.6) [59;70]. This motif is commonly found in hydrolytic enzymes, yet the NDRG family stands unique due to its lack of residues required for catalytic activity[70]. Indeed, no predicted peptide motifs (including a putative cytochrome c family heme-binding motif and a phosphopantethein attachment motif [52;71;72]) have successfully exposed a function for NDRG1. Furthermore, examination of the NDRG1 peptide sequence, which could provide clues as to the localisation of NDRG1 at the subcellular level, revealed no significant hydrophobic

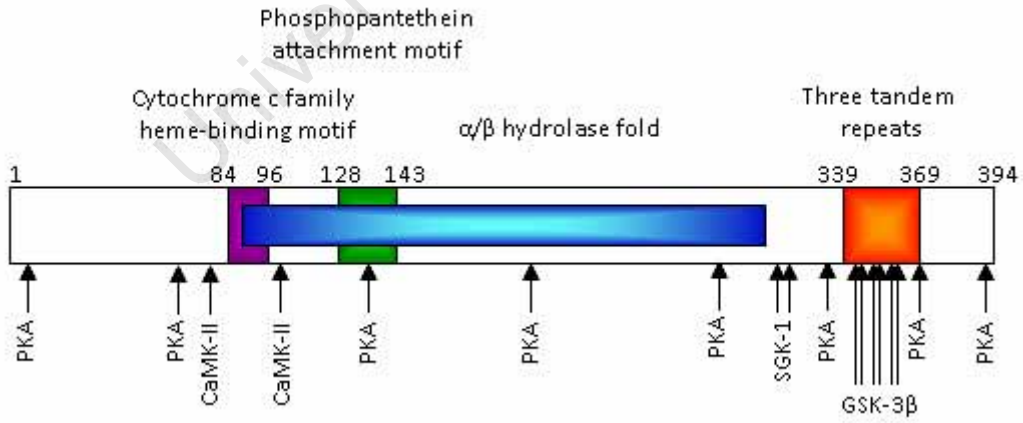

Figure 1.6. Schematic diagram of the NDRG1 protein. Positions of the hydrophilic tandem repeats, α/β hydrolase fold, phosphopantethein attachment as well as cytochrome c family heme-binding motifs are shown. Phosphorylation sites for PKA, CaMK-II, SGK-1 and GSK-3β are also shown. (Figure adapted from [72])

transmembrane domains, no signal sequence and no endoplasmic reticulum retention sequence[52]. However, NDRG1 does exist as a multi-phosphorylated protein. Two-dimensional electrophoresis identified more than seven phosphorylation sites for NDRG1[73] and experiments using kinase inhibitors have identified NDRG1 as a substrate of protein kinase A (PKA)[72;73], calmodulin kinase II[72;73], serum and glucocorticoid-induced kinase 1 (SGK-1)[74;75], and glycogen synthase kinase 3 (GSK-3) [74]. Taken together, the data on NDRG1's structure and post-translational modification does not reveal much regarding its function. NDRG1 phosphorylation has been implicated in HUVEC proliferation[73] and mast cell exocytosis[72], however the significance of NDRG1 phosphorylation should be further established. Indeed, phosphorylation may be instrumental in determining the specific functions and localisation of the NDRG1 protein.

1.7.2. NDRG1 expression and localisation

NDRG1 mRNA is ubiquitously expressed in the human body, albeit at varying levels, where notably high levels have been observed in the brain, heart, prostate, intestine, placenta and kidney[71;76]. Immunohistochemical studies on human tissue revealed that protein and mRNA levels do not necessarily correlate, where the 43 kDa NDRG1 predominates in epithelial tissues, with complete absence of the protein from the brain, heart and skeletal muscle[71]. This differs from the other members of the NDRG family which are conspicuously detected in the brain, heart, skeletal muscle and spinal chord[59;60], suggesting different but related functions for the protein family. The ubiquitous but varying levels of mRNA, and the absence of NDRG1 protein in certain

tissues, implicates both transcriptional and translational regulation for this gene, which may be tissue or cell type specific.

The subcellular localisation of NDRG1 revealed further variations in NDRG1 expression patterns. Although predominantly detected in the cytoplasm, NDRG1 has been reported to associate with the plasma membrane in cells of the intestinal epithelium, lactating breast, biliary ducts in the liver and basal cells of the oesophageal epithelium, amongst others[71]. Since NDRG1 contains no hydrophobic or transmembrane motifs, membrane localisation is probably achieved through protein-protein interactions. Closer examination of localisation by electron microscopy revealed that NDRG1 was often adjacent to adherens junctions and desmosomes, pointing to a function in cell-cell adhesion[71]. Indeed, interaction between NDRG1 and the adhesion molecules E-cadherin and β-catenin has been demonstrated[77], and exogenous overexpression of NDRG1 in colon and prostate cancer cells is capable of inducing E-cadherin expression[76;78]. Further supporting the relationship with E-cadherin, NDRG1 was identified as a Rab4a effector, involved in vesicular recycling of E-cadherin to the surface of prostate cancer cell lines[78]. Rab proteins are involved in the processing of intracellular vesicles, including budding and fusion, a mechanism by which they regulate the spatiotemporal trafficking, recycling and degradation of proteins[79]. Indeed, many signalling molecules and receptors, for example phosphoinositide 3-kinase (PI-3K) and epidermal growth factor receptor (EGFR), are recycled and redistributed in this manner. The association of NDRG1 with recycling/sorting and late

endosomes therefore opens the floor to speculation as to whether NDRG1 may be involved in regulating signal transduction.

As well as membrane-localised NDRG1, this protein was occasionally observed in the nucleus of cells, including prostate and kidney[71;80]. With no nuclear localisation sequence, it is presumed that NDRG1 enters the nucleus through interaction with one or more nuclear proteins. Molecular chaperones, such as heat shock protein 90 (HSP90) and heat shock cognate protein 70 (Hsc70) are potential NDRG1 binding partners that facilitate nuclear translocation[77;81]. Indeed, in maturing mast cells Hsc70 translocated to the nucleus, accompanied by NDRG1[81]. Moreover, DNA damaging agents have been reported to induce NDRG1 translocation from the cytoplasm to the nucleus[54]. The subcellular translocation of NDRG1 in response to stimuli, including DNA damage, suggests a role for NDRG1 in genomic stability, stress responsiveness or even transcription. Recent reports have shown, by co-immunoprecipitation, that NDRG1 does indeed associate with transcription factors, as well as DNA repair proteins ATP-dependent DNA helicase II (Ku70) and RuvB-like 2 (RUVBL2)[77]. However, the precise function of NDRG1 within the nucleus remains uncertain and requires further inspection.

Analysis of the NDRG1 protein using PSORT II software (http://psort.hgc.jp/) also predicted NDRG1 association with the mitochondrion and the cytoskeleton[57]. The cytoplasmic localisation of NDRG1 has been described as granular, and is suggestive of mitochondrial localisation[54;71]. In fact, close inspection using immunoelectron

microscopy revealed NDRG1 located at the inner mitochondrial membrane of kidney proximal tubule cells[71], which is in agreement with the reports claiming NDRG1 associates with metabolic and mitochondrial proteins[77].

Taken together, the wide range of tissues in which NDRG1 is expressed as well as the diverse subcellular localisation confounds approaches to untangle the cellular function of this protein. The lack of organelle targeting sequences suggests that NDRG1 achieves translocation via protein-protein interactions. Such interactions may also facilitate specific functionality of NDRG1 which may be cell or tissue specific.

1.7.3. NDRG1 and endoplasmic reticulum stress

The endoplasmic reticulum (ER) is an extensive membranous organelle that envelopes the nucleus and extends into the cytoplasm[82]. The ER is involved in a wide array of biologic functions that include protein folding, lipid biosynthesis and calcium storage. A rigorous control system ensures that only properly folded proteins are transported out of the ER, while misfolded or unfolded proteins are retained in the ER and degraded[82;83]. "ER stress" refers to the condition where stimuli, such as oxidative stress, calcium depletion, DNA damage or altered glycosylation (amongst others), disrupt protein folding, causing an accumulation of misfolded and/or unfolded proteins in the ER. To manage the accumulation of misfolded or unfolded proteins, the ER stress response (i) assists protein folding by elevating the levels of ER chaperone proteins and/or (ii) promotes degradation of misfolded proteins through the activation of the ER-associated protein degradation pathway[82-84].

NDRG1 expression is upregulated by several ER stress inducers, including tunicamycin[73], calcium ionophore A23187[85;86], homocysteine[52;55;87], and β-mercaptoethanol[52]. Interestingly, mass spectrometry analysis of the NDRG1 interactome in prostate cancer cells suggested that NDRG1 could interact with nuclear proteins, signaling proteins, adhesion molecules as well as endoplasmic reticulum chaperones and proteasome subunits[77]. NDRG1 reportedly complexes with ER chaperones heat shock protein 90-α (HSP90)[77;88], heat shock 70 kDa protein 5[77] and heat shock cognate protein 70[81], amongst others. Furthermore, siRNA knockdown of NDRG1 lead to a reduction in HSP90 levels in LNCaP cells[77]. On the other hand, in hepatocellular carcinoma cell lines inhibition of HSP90 with geldanamycin lead to a transcriptional increase in NDRG1 levels as well as an altered phosphorylation status[88]. Taken together, the interaction of NDRG1 with ER proteins suggests that NDRG1 may play a role in the ER stress response; however, its function therein requires further clarification.

1.7.4. NDRG1 in cancer

Since its first description in 1996[52], many studies have described the aberrant expression of NDRG1 in tumour tissue relative to that of normal tissue. However, the role of NDRG1 in the neoplastic progression of cells still remains enigmatic. Here we review the current literature that describes NDRG1 in cancer.

In the past there have been several studies that report the significant downregulation of NDRG1 expression in neoplastic tissue, labelling it a tumour and metastasis

suppressor. For instance, immunohistochemical analysis of NDRG1 expression, in tumour specimens from breast cancer patients, revealed that the NDRG1 protein levels were significantly reduced in tumour tissue compared to its high expression in its normal tissue counterpart[89]. Although no significant correlation with the histological grade or size of the tumours was observed, reduced NDRG1 expression showed a positive correlation with both lymph node and bone metastasis[89]. Moreover, the death risk for NDRG1-negative patients was 2.4 times higher than those positive for NDRG1. Taken together, this data shows that breast cancer patients with NDRG1 negative tumours have an increased likelihood of metastasis and a significantly less favourable prognosis[89;90]. Similar observations were also made in studies on colon[53;76], neuroblastoma[91], pancreas[92;93] and prostate cancers[90;94]. Consistently, these studies reported low levels of NDRG1 associated with neoplastic tissue, metastasis and a poor patient outcome. In support of these findings, Kurdistani *et al*.[54] were able to demonstrate primary tumour growth inhibition by NDRG1 in mouse xenografts, while ectopic overexpression of NDRG1 in breast and bladder cancer cell lines was able to limit soft agarose colony formation and reduce their proliferative capacity by as much as 70%. On the other hand, overexpression of NDRG1 in colon and prostate tumour cells was able to suppress liver and lung metastasis, respectively, without affecting primary tumour growth[76;94]. The results of these studies raise the question as to whether NDRG1 has differential organ-specific functions, but support the role of NDRG1 as a tumour suppressor in the development of cancer.

In contrast, there is mounting evidence suggesting that NDRG1 is in fact an oncogene, promoting the process of tumourigenesis. Cangul and associates[80;95] reported that NDRG1 levels were higher in tumour tissues of lung, liver, breast, smooth muscle, brain, kidney and skin cancers than their normal tissue counterparts. Furthermore, NDRG1 was identified by microarray analysis as a gene upregulated during the progression of cervical tissue from normal to carcinoma *in situ*, to invasive adenocarcinoma[96]. In fact, NDRG1 expression in cervical adenocarcinoma was proposed as a poor prognostic indicator as it significantly associated with tumour diameter, angiogenesis, lymph node metastasis and invasion[97]. Additionally, elevated levels of NDRG1 have been reported in colon[98;99], liver[100;101] and oral squamous cell carcinomas[102] while NDRG1 upregulation was reported during mouse and human skin tumourigenesis[91;103].

Studies on patients suffering from squamous cell carcinoma of the oesophagus have also been conflicting. In a Japanese cohort of 47 patients, real-time RT-PCR revealed that NDRG1 mRNA levels showed no correlation with histologic differentiation, lymph node metastasis or invasion. However, low NDRG1 mRNA correlated with late stage tumours and a poor prognosis[104]. In contrast, in a Chinese study, using immunohistochemistry on 49 patients, NDRG1 was found to be reduced in tumour tissue. However, no significant correlation between NDRG1 expression and tumour stage, differentiation, lymph node metastasis or prognosis was observed[105]. Again, conflicting data for the expression of NDRG1 in cancer is given. However, each of these studies measured NDRG1 expression using different methods, namely real-time

RT-PCR and immunohistochemistry. Since it has been shown that NDRG1 mRNA and protein levels do not always correlate (see section 1.7.2.) a direct comparison between these two studies cannot be made. Additionally, discrepancies in the reported data may arise through the different genetic backgrounds of each cohort studied.

As described above, reports have shown that NDRG1 is downregulated in cancer, whereas others claim the opposite. Certainly, the conflicting evidence in the literature does not clarify the role of NDRG1 in carcinogenesis but does highlight the notion that NDRG1 may have a cell or tissue-specific function. The conflicting data may also be explained through cell culture variability and artefacts reflecting diverse genetic milieus. Moreover, population based studies often emerge from varying genetic backgrounds and environments, which may influence the expression of the gene in question.

1.7.5. The role of NDRG1 in differentiation

Differentiation is best described as progressive cell maturation and specialisation of cells, and terminal differentiation is mostly associated with an irreversible and diminished proliferative capacity and is regulated by a host of spatiotemporal signalling networks, regulating the processes of proliferation, differentiation and apoptosis. Disruption of these pathways and misdirected signalling is often the cause of tumour initiation, growth and/or maintenance[106-109].

NDRG1 was first described as a differentiation associated gene through differential display technique during the *in vitro* differentiation of the colon carcinoma cell line, HT29-D4[53]. This finding has been replicated in subsequent studies using different systems of differentiation. Indeed, within specific cellular contexts transforming growth factor-β[110], nerve growth factor[39], *all-trans* retinoic acid[102;111;112] and 1,25-$(OH)_2$ vitamin D_3[113] all induced differentiated phenotypes coupled with a marked increase in NDRG1 expression. Likewise phorbol esters, well described inducers of differentiation, were able to induce NDRG1 expression in keratinocytes[114], monocytic U937 cells[113;115] and trophoblasts[116]. Furthermore, ectopic overexpression of NDRG1 in the metastatic colon carcinoma cell line, SW620, induced changes consistent with colonic epithelial cell differentiation[66]. Here, differentiation markers such as alkaline phosphatase, carcinoembryonic antigen and E-cadherin were induced by exogenous NDRG1 overexpression. Thus, not only is NDRG1 a product of the differentiation process, but also has the potential to induce the expression of markers consistent with differentiation, depending on the cellular context.

The transcription factors N-Myc and c-Myc are proto-oncogenes which have been implicated in the differentiation and maturation of tissue, particularly during embryogenesis[117;118]. Notably, increases in NDRG1 levels during tissue maturation are coupled with a decrease in N-Myc or c-Myc levels[58;62;112]. Moreover, in N-Myc deficient mice, a 20-fold increase in NDRG1 levels was recorded[62]. Conversely, treatment of estrogen receptor-α positive breast cancer cell lines with 17β-estradiol

resulted in a marked increase in cellular proliferation and c-Myc expression, while NDRG1 levels were decreased[119]. Moreover, a direct interaction of Myc proteins with the NDRG1 core promoter region (from -33 bp to +103 bp) was demonstrated in HeLa cells by chromatin immunoprecipitation[112]. In summary, this data points to a direct but inverse relationship between *NDRG1* and *MYC* genes and implicates NDRG1 in the process of cell maturation, differentiation and associated growth arrest.

1.7.6. NDRG1 in the cell cycle and apoptosis

The cell cycle consists of a series of tightly regulated events that lead to the duplication and equal distribution of genome replicas to daughter cells. The cell cycle is divided into four distinct phases, G_1 (Gap 1) phase, S (synthesis) phase and G_2 phase and M (mitosis) phase. In order to ensure that accurate, error free progeny cells are produced, a series of cell cycle checkpoints must be passed. The G_1/S checkpoint monitors DNA integrity while the G_2/M checkpoint ensures that DNA replication is complete. Finally, the spindle checkpoint ensures that distribution of chromosomes to daughter cells is equal. If errors are present in the cell, the cell has one of two fates; either arrest the cell cycle and repair errors in the cell, or undergo apoptosis if the DNA integrity cannot be restored[120].

The implication that NDRG1 may play a part in the cell cycle arose through the observation that NDRG1 levels increased during differentiation and growth arrest. Analysis throughout the cell cycle of normal mammary epithelial cells revealed that NDRG1 mRNA levels are biphasic, where expression peaked at the G_1 and G_2/M phases

and was lowest at the S phase[54]. Interestingly, in the breast tumour cell line MDAMB435, NDRG1 mRNA levels were unchanged throughout the cell cycle, suggesting that NDRG1 may contribute to carcinogenesis via deregulation of the cell cycle[54]. This biphasic, cell cycle-associated NDRG1 mRNA expression has not been reported elsewhere. The half-life of NDRG1 mRNA is approximately 4h [70], consistent with the mRNA half-life of other genes whose expression is tied to the cell cycle, such as p21[121] and $p19^{ARF}$[122]. In contrast, NDRG1 protein half-life following return to normoxic culture conditions was reportedly 16 hours and 48 hours in A549[80] and SW480[71] cells, respectively. The relatively high stability of the NDRG1 protein raises questions around the purpose of its biphasic cell cycle-regulated mRNA and needs further exploration in additional cell lines.

Further experimental evidence that NDRG1 may be involved in the cell cycle was provided when NDRG1 was shown to maintain spindle structure during cell division[123]. Here, NDRG1 was shown to be a microtubule and centrosome associated protein, which participated in the spindle checkpoint in a p53-dependent manner[123].

p53 is a tumour suppressor which is capable of inducing cell cycle arrest (at the G_1 and G_2 checkpoints) or apoptosis in response to DNA damage. Indeed, p53 has been implicated in the regulation of NDRG1. Transfection of p53 null mutant cells with a tetracycline-regulated p53-inducible system, revealed that NDRG1 mRNA increased in tandem with p53 expression levels[54]. In addition, DNA damaging agents induced

NDRG1 expression in a p53-dependent manner, coupled with nuclear translocation[54]. Similarly, Stein *et al*. identified NDRG1 as a gene necessary for p53-dependent apoptosis[124]. Using a p53-inducible colon cancer cell system, the p53 binding site, 406 bp upstream of the NDRG1 transcriptional start site, was identified[124]. Additionally, transient siRNA knockdown of p53 reduced NDRG1 expression in these cells[124]. Together, these studies provide evidence that the reduced expression of NDRG1 observed in some cancers may be explained by the frequent loss of p53 expression[54].

Paradoxically, NDRG1 has been implicated as a protective, anti-apoptotic protein in both colon cancer and acute myeloid leukaemic cells[125-127]. Irinotecan, or CPT-11, is a topoisomerase I inhibitor which is able to induce p53-mediated cell cycle arrest and apoptosis. Treatment of colon cancer cells with CPT-11 resulted in a G_2 cell cycle arrest which was characterised by a marked upregulation in NDRG1 expression. However, the same cells treated with antisense NDRG1 and CPT-11 underwent apoptosis, suggesting that NDRG1 expression has a protective, anti-apoptotic effect. Moreover, NDRG1-mediated CPT-11 resistance was shown to be independent of p53 as CPT-11 resistance was also observed in non-functional p53 SW620 cells[125]. Consistently, *in vivo* studies found that high NDRG1 expression imparted chemo-resistance to CPT-11 in patients suffering from colorectal cancer[126;127]. Similarly, in acute myeloid leukaemic cells treated with a camptothecin analog, downregulation of NDRG1 expression was associated with apoptosis[128].

1.7.7. NDRG1 in angiogenesis

The progression of a tumour cell mass to an aggressive, metastatic malignancy is a stepwise process that takes advantage of several physiological systems in the body. Indeed, as a solid tumour mass grows, so too does its need for oxygen, nutrients and waste removal. Angiogenesis (the formation of new blood vessels) and lymphangiogenesis (the formation of new lymph vessels) is an essential capability acquired by tumour cell masses to accommodate these needs[129]. In fact, tumour cells acquire the ability to produce angiogenic factors (cytokines) that are released into the tumour microenvironment and act on receptors on the surface of endothelial cells, thereby stimulating endothelial proliferation[49;130]. Not only does angio- and lymphangiogenesis alleviate resource pressure on the tumour cell mass, but also provides a portal through which shedding cancer cells may spread and metastasise to distant sites[49]. Indeed, this process is often coupled with the activation extracellular matrix (ECM) proteases, such as matrix metalloproteinases (MMPs), which remodel the ECM to facilitate tumour invasion and angiogenesis[129;131;132].

Vascular endothelial growth factors (VEGF-A, -B, -C, and –D) are well characterised angiogenic cytokines. Specifically, VEGF-A binds to its receptors, VEGFR-1 and -2 on the surface of vascular endothelial cells, inducing angiogenesis, while VEGF-C and-D that bind VEGFR-2 and -3 are predominantly responsible for lymphangiogenesis. Other factors that play a role in angiogenesis include platelet-derived growth factors (PDGFs), as well as angiopoietin-1 (Ang-1) and -2 (Ang-2) amongst many that have been extensively reviewed[133-136].

The effect of NDRG1 expression on tumourigenesis in mouse xenograft models, using colon and prostate cancer cells showed that either reduced or overexpressed NDRG1 had no effect on tumour growth[94;125]. However, while Maruyama *et al*. [93] showed that ectopic NDRG1 overexpression had no effect on cellular proliferation *in vitro*, pancreatic ductal adenocarcinoma cells overexpressing NDRG1 showed a notable decrease in tumourigenicity in a mouse xenograft model. This disparity between *in vitro* and *in vivo* effects of NDRG1 was suggested to be the result of the tumour microenvironment[93]. In fact, pancreatic cells expressing high levels of NDRG1 were shown to have reduced levels of VEGF-A, whilst *in vivo* studies showed that the angiogenic potential of pancreatic ductal adenocarcinomas was compromised in tumours expressing high levels of NDRG1[93]. The mechanism through which NDRG1 exerted this anti-angiogenic effect was through the attenuation of nuclear factor-κB (NF-κB) signalling[137]. Indeed, NDRG1 expression led to a decrease in inhibitor of κB kinase (IKK) β expression and IκBα phosphorylation, thereby reducing nuclear translocation of p65 and p50, as well as their binding to the NF-κB motif. This inhibition of NF-κB signalling, suppressed expression of VEGF-A, amongst other genes[137]. Consistently, treatment of glioblastoma and gastric cancer cell lines with the anti-tumour, anti-angiogenic drugs, ZD6474 and mycophenolic acid, was characterised by a significant induction in NDRG1 mRNA levels[138;139].

In contradiction to the above findings that NDRG1 is an anti-angiogenic factor, a report examining cervical adenocarcinoma specimens implicated NDRG1 as pro-angiogenic[97]. Here, high NDRG1 expression was significantly associated with

increased microvessel density and VEGF-A expression, making NDRG1 a poor prognostic indicator for cervical adenocarcinoma[97].

Once again, a singular role for NDRG1 in angiogenesis cannot be resolved because of contradictory observations. Reports indicating NDRG1 inhibits angiogenesis in pancreatic cancer are internally consistent and identify altered NF-κB signalling as the mechanism. Data that NDRG1 is pro-angiogenic is merely associative in cervical adenocarcinoma, however, it does highlight the fact that NDRG1s influence on angiogenesis is not simplistic, and requires further exploration.

1.7.8. Regulation of NDRG1 expression

Not surprisingly, the aberrant, albeit varying, expression of NDRG1 in a wide range of tumours, as well as its potential tumour suppressor and oncogenic functions, spurred a strong interest in the mechanisms underlying NDRG1 regulation and expression.

Analysis of the 5'-untranslated region of *NDRG1* identified two potential CpG islands. One well characterised mechanism of transcriptional silencing, often observed in different cancers, is atypical methylation of cytosines positioned 5' to guanosines (CpG) in the promoter of tumour and metastasis suppressor genes[89;140;141]. Promoter methylation was implicated in the suppression of NDRG1 expression, in both breast and colon cancer cell lines, since treatment with 5'-aza-2'-dexoycytidine (an inhibitor of DNA methylation) lead to an increase of both NDRG1 mRNA and protein

levels[76;89]. Additionally, NDRG1 induction by treatment with trichostatin A implicated histone deacetylation in NDRG1 suppression[76].

In silico analysis of the 5'-untranslated region of NDRG1 reveals the presence of multiple putative transcription factor binding sites. Indeed, research efforts have validated the direct interaction between these factors and the NDRG1 promoter, while others have merely established some form of correlative relationship. Since this data has been extensively reviewed by Ellen *et al*.[142] and Kovacevic *et al*.[57], this section will focus on transcriptional regulation most pertinent to this research project.

In addition to the evidence that NDRG1 is a target of both the Myc and p53 proteins (see sections 1.7.4 and 1.7.5), hypoxia-inducible factor 1 (HIF-1) has also been implicated in its regulation. HIF-1 is a heterodimeric transcription factor that responds to low oxygen tension by, together with co-factors (e.g. AP-1), activating transcription of target genes that alleviate this stress[143;144]. The complex is composed of two subunits α and β. HIF-1β is constitutively expressed whilst HIF-1α levels respond to the hypoxic (low oxygen) state and are largely regulated at the post-transcriptional level[143]. Although HIF-1α is constitutively expressed, under conditions of normoxia (adequate oxygen) it is targeted for degradation. This process is regulated by the prolyl-4-hydroxylases (PHD), which hydroxylate HIF-1α prolyl residues, facilitating the interaction between HIF-1α and the Von Hippel-Lindau (VHL) tumour suppressor, and thereby its proteasomal degradation[145]. In addition, HIF-1α is prevented from interacting with co-factors through the activity of Factor Inhibiting HIF (FIH), an

asparagine hydroxylase[146;147]. Under conditions of hypoxia, oxygen-dependent prolyl and asparagine hydroxylases are inhibited, HIF-1α accumulates, translocates to the nucleus where it heterodimerises with HIF-1β and activates transcription of target genes by binding to hypoxia-responsive elements, together with co-factors[148].

A number of studies have reported that NDRG1 is strongly induced by hypoxia and hypoxia mimicking agents[55;56;80;85;149;150]. Both HIF-1α regulating enzymes, FIH and PHD, require iron (Fe^{2+}) for activity. Thus, iron chelators (such as deferoxamine) and transition metals, such as cobalt (Co^{2+}) and nickel (Ni^{2+}), through competitive binding are capable of stabilising HIF-1α[151]. Indeed, the NDRG1 response, in HIF-1α double knockout mouse embryonic fibroblasts (HIF-$1\alpha^{-/-}$ MEF), to short term exposure of hypoxia, Co^{2+} and Ni^{2+} was diminished compared to HIF-1α proficient (HIF-$1\alpha^{+/+}$ MEF) cells. Moreover, hypoxia mimetics, deferoxamine and okadaic acid, were not able to induce NDRG1 core promoter activity in HIF-$1\alpha^{-/-}$ MEF cells to the same extent as in HIF-1α proficient cells[80;85;150]. What is more, in 786-O cells, which are *VHL* deficient and therefore constitutively express HIF-1α, NDRG1 had high basal, but uninducible levels compared to normal cells[152]. This data, together with the observation that the NDRG1 promoter contains putative hypoxia responsive elements, (HREs) at -1376 bp and -7503 bp[150], supports the hypothesis that HIF-1α activates NDRG1 expression in response to hypoxia. However, direct binding of HIF-1α to the HREs in the NDRG1 promoter has not been reported. Additionally, according to Zhang *et al*.[153] the HREs in the NDRG1 promoter contain only 4 (ACGT) of the nine bases of the consensus hypoxia response motif. Moreover, NDRG1 accumulation in HIF-$1\alpha^{-/-}$

MEF cells is observed after long term exposure to hypoxia[80], suggesting that NDRG1 may be upregulated in a HIF-1-independent manner.

AP-1 is a dimeric transcription factor composed of members of the Jun family of proteins, comprising of c-Jun, JunB, JunD, that form homodimers or heterodimerise with the Fos family proteins (c-Fos, Fos B, Fra-1 and Fra-2) [154;155]. AP-1 can activate or repress transcription of target genes by binding to AP-1 consensus DNA binding sites, TGAG/CTCA, also known as TPA 12-*o*-tetradecanoylphorbol-13-acetate response elements (TREs) and cAMP response elements (CREs), TGACGTCA, found in the promoter and enhancer regions of target genes [156;157]. AP-1 has been implicated in many biological processes and regulates numerous genes involved in proliferation, differentiation and apoptosis[155;158;159]. In addition, both c-Jun and c-Fos have been linked with neoplastic transformation and progression. Activation of AP-1 may be induced by a number of growth factors, stress, hormones, reactive oxygen species and ultraviolet (UV) radiation, which signal through mitogen activated protein kinase (MAPK) pathways such as Jun amino-terminal kinase (JNK), p38 MAPK and extracellular-signal-related kinase (ERK)[155]. During hypoxia, AP-1 coordinates with HIF-1 to facilitate hypoxia induced gene expression[148]. However, independently of HIF-1, hypoxia can induce and activate AP-1 through increases in intracellular calcium (Ca^{2+}). In HIF-1α proficient cells, BAPTA-AM (a Ca^{2+} chelator) completely abrogated NDRG1 upregulation by Ni^{2+} and hypoxia, implicating intracellular Ca^{2+} and its effectors (e.g. AP-1) in NDRG1 regulation[85]. In fact, Ca^{2+} ionophore was able to induce NDRG1 expression in both HIF -proficient and -deficient fibroblasts and an AP-1

dominant negative was able to abrogate hypoxia-mediated NDRG1 upregulation[86]. Thus, under hypoxic conditions, an increase in intracellular Ca^{2+} activates a HIF-1-independent, activating protein-1 (AP-1)-dependent pathway that also regulates NDRG1 expression.

Taken together, this data suggests that hypoxia-induced NDRG1 expression may be regulated by co-operative binding of transcription factors to the NDRG1 promoter and not necessarily by direct binding of HIF-1.

In addition to HIF-1 and AP-1, early growth response-1 (EGR-1) has been implicated in the hypoxic regulation of NDRG1. EGR-1 is a member of the immediate early gene family, and rapidly and transiently responds to stimuli to regulate genes implicated in cell proliferation, differentiation and survival. EGR-1 contains three zinc finger motifs and regulates transcription through binding to GC-rich elements such as 5'-GCGGGGGCG-3' or the consensus sequence '5-GCG(T/G)GGGCG-3'[160]. Under conditions of hypoxia, EGR-1 is synthesised in a HIF-1α-independent, Elk-dependent manner through the activation of protein kinase C (PKC) and ERK MAPK signalling[161;162]. In both murine RAW264.7 macrophage cells and A549 lung cancer cells, hypoxia and deferoxamine were able to induce activity of an NDRG1 reporter plasmid. Furthermore, mutation of the EGR-1 binding site, within the reporter, was able to abrogate promoter activity in RAW264.7 cells, and binding of EGR-1 to this site was demonstrated by electrophoretic mobility shift assay (EMSA)[153]. However, Zhang *et al*. did not demonstrate *in vivo* binding of EGR-1 to the NDRG1 promoter.

It has become apparent that NDRG1 must play an important role in the hypoxic response. The data above reveals that multiple pathways converge on the NDRG1 promoter in response to hypoxia. Certainly, if the role of NDRG1 in angiogenesis was more clearly defined perhaps NDRG1 and its activators could be targets for cancer therapy.

1.8. Significance

In 1985 the first formal proposal to decode the DNA sequence of the human genome was put forward[163]. Fifteen years later the first survey of the entire human genome was announced[164] - a pinnacle event in the history of modern science, which has provided us with the framework to move forward in translational research. Aptly stated by Venter *et al.* [165], "It provides the boundaries for scientific inquiry. The sequence is only the first level of understanding of the genome. All genes and their control elements must be identified; their functions, in concert as well as in isolation, defined; their sequence variation worldwide described; and the relation between genome variation and specific phenotypic characteristics determined. Now we know what we have to explain."

Our laboratory identified *NDRG1* as a gene with altered expression in oesophageal tumour tissue when compared to normal tissue. Given the elusive function of this gene as well as the conflicting evidence in the literature for its role in cancer, we sought to explain its role in OSCC, a disease that occurs with a high incidence in South Africa.

1.9. Project aims

The aims of this study are:

(i) To determine the expression status of NDRG1 in archived tissue of OSCC patients from South Africa, as well as in cultured OSCC cell lines.

(ii) To characterise the functional relevance of NDRG1 expression in cancer cells.

(iii) To determine the transcriptional regulatory mechanisms responsible for NDRG1 expression in OSCC cell lines.

CHAPTER 2

NDRG1 EXPRESSION IN OESOPHAGEAL SQUAMOUS CELL CARCINOMA PATIENT MATERIAL AND CULTURED CELLS

2.1. INTRODUCTION

The stepwise progression of a cell from a normal to a transformed, malignant state is driven by temporal and spatial changes in gene expression. In fact, progression from dysplastic precursor lesions, to carcinoma *in situ*, to invasive carcinoma, and the maintenance of the tumourigenic phenotype, is made possible through the silencing or inappropriate expression of genes that regulate cellular processes such as the cell cycle, proliferation, differentiation, apoptosis, angiogenesis and DNA repair. Procedures for monitoring genome-wide changes in gene expression and transcriptome profiling have been available for many years due to rapid technological advances and conceptual advances about cell function and molecular biology. Techniques such as differential display reverse transcription PCR (DDRT-PCR), as well as microarray analysis, deepen our understanding of the diseased state through the simultaneous examination of the expression of multiple genes, and the identification of genes that are differentially expressed[166].

Squamous cell carcinoma of the oesophagus is major problem in the developing world and a better understanding of the molecular nature of OSCC and the underpinning

tumourigenic processes is required in order to devise improved screening methods and rational drug design. In our laboratory a preliminary study was conducted, using DDRT-PCR and microaray analysis, in order to identify genes that are expressed differently in oesophageal squamous cell carcinoma tissue compared to normal oesophageal tissue. Amongst the genes deregulated, NDRG1 was identified as having altered expression in tumour tissue compared to that of normal tissue.

To date, the precise function of NDRG1, and specifically the role of NDRG1 in tumourigenesis, remains enigmatic. Paradoxically, research has suggested both a tumour-suppressor as well as an oncogenic role for NDRG1, which may be tissue or cell type specific. As presented in chapter 1, previous studies describe the downregulation of NDRG1 protein and mRNA in OSCC but report inconsistent data with respect to tumour stage, differentiation and prognosis[104;105]. While much research has been conducted on NDRG1's expression in cancer, a defined role for this protein in tumour biology, as well as normal cell and tissue systems is yet to be put defined.

This chapter describes the characterisation of NDRG1 protein and mRNA expression in normal and cancerous squamous epithelium of the oesophagus, derived from a South African cohort of patients, as well as the expression of NDRG1 in our panel of cultured oesophageal squamous cell carcinoma cells.

2.2. RESULTS

2.2.1. Quantitative real-time RT-PCR analysis of *NDRG1* expression in biopsies of oesophageal squamous cell carcinoma patients

To determine the expression status of *NDRG1* in oesophageal tumour tissue and normal tissue, RNA from a sample of normal (n=6) and oesophageal cancer (n=8) tissue biopsies was subjected to real-time RT-PCR analysis, using primers designed to specifically amplify NDRG1 mRNA. Only samples where RNA was of high quality, as determined by RNA gel electrophoresis, were included. Each RNA sample was normalised to the expression of the *cyclophilin D* (*peptidylprolyl isomerase D*) and *β-glucuronidase* (*gusB*) genes in order to accommodate for possible differences in RNA quantity and quality. In this case, two house-keeping genes were utilised as this is recommended when examining gene expression in human tissue biopsies [167].

The specificity of the real-time RT-PCR was assessed by melting curve analysis (data not shown) and electrophoresis of the PCR product (Fig 2.1.A). Real-time RT-PCR data was then analysed using the comparative threshold cycle (C_T) method to compute the expression fold change between samples[168]. Real-time RT-PCR using RNA isolated from OSCC tissue and normal tissue confirmed that the relative expression of NDRG1 was significantly higher in tumour tissue compared to normal tissue (at least 2-fold, $p < 0.05$)(Fig 2.1.B) and that a distinctly broad range of NDRG1 expression in tumour specimens was observed.

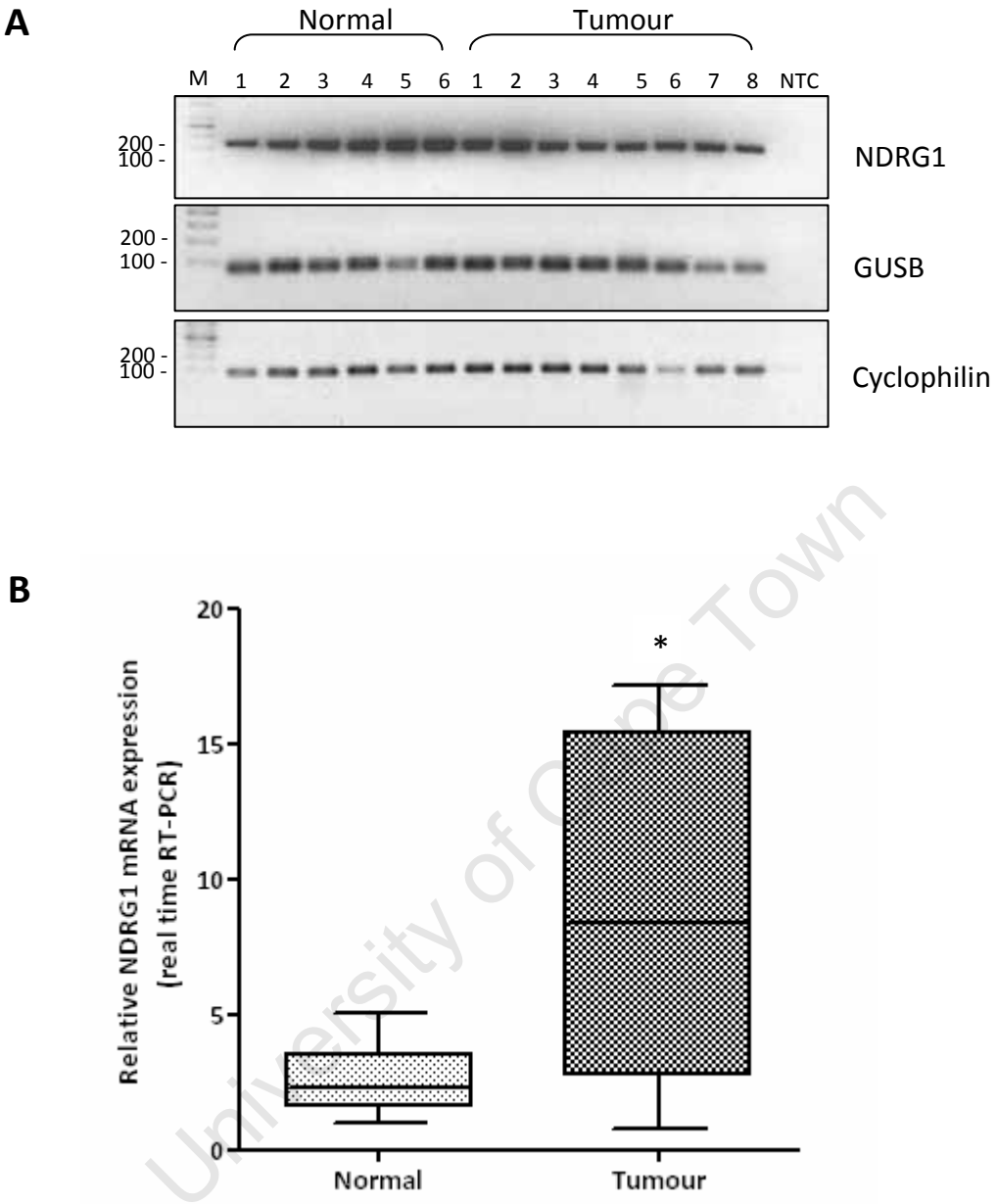

Figure 2.1. Expression of NDRG1 mRNA in normal and oesophageal cancer tissues. A. Specificity of NDRG1, GUSB and Cyclophilin D real-time RT-PCR was confirmed by agarose gel electrophoresis of real-time RT-PCR products alongside GeneRuler DNA Ladder (M; Fermentas) (NTC - no template control). B. Quantitative real-time RT-PCR analysis (using comparative threshold cycle method) revealing the upregulation of NDRG1 mRNA in oesophageal cancer tissue biopsies compared to normal tissue biopsies [normal (n = 6), tumour (n = 8), *p < 0.05]. The Box-and-Whisker plot was generated using Graphpad Prism 5 software.

2.2.2. Immunohistochemical analysis of NDRG1 expression in oesophageal squamous cell carcinoma tissue and adjacent normal tissue

Although our analysis strongly suggested an overexpression of NDRG1 mRNA levels in tumour tissue compared to normal tissue, this result could reflect the small number of samples analysed. Since additional samples could not be readily obtained, we next examined the level of NDRG1 protein expression in archived, paraffin embedded tumour and normal tissue specimens. Measuring NDRG1 protein levels directly also addressed the problem that NDRG1 mRNA and protein levels within a tissue do not always correlate[71], so it was important to determine whether NDRG1 protein levels were also upregulated in patient material.

NDRG1 protein expression was analysed using antibodies raised against NDRG1, and visualized using peroxidase/diaminobenzidine (DAB) staining on tissue sections cut from archived tissue blocks of OSCC patients. This allowed for the examination of both levels of protein expression as well as localisation of NDRG1 in the normal and oesophageal cancer tissue sections. Tissue sections of squamous cell carcinoma and adjacent normal tissue from eighty-three patients were examined. Patients ranged in age from 23 to 80 years and were comprised of twenty females and sixty-three males. The bias in the male to female ratio in the samples analysed reflect the higher incidence of the disease in males, and also the availability of tissues. The average survival time of the eighty-three patients was 3.2 years (range: 0-17 years). Five percent of patients presented with either stage 0 or I disease, 50 % with stage II and 34

% with stage III disease. Staging data for 11 % of patients was not attainable. Given the heterogenous nature of the NDRG1 stain, as well as the subjective nature of immunohistochemical scoring, Axiovision software (version 4.7) was used to quantitate NDRG1 positivity in oesophageal tissue sections. Three fields of view, per tumour or normal specimen, under 200 x maginification were analysed. Briefly, greyscale images of stained sections were captured using a Zeiss AxioCamHR camera. Using the Axiovosion software, regions containing epithelial cells/tumour cells were selected (i.e. the stroma excluded) and the average grey-scale intensity per pixel determined.

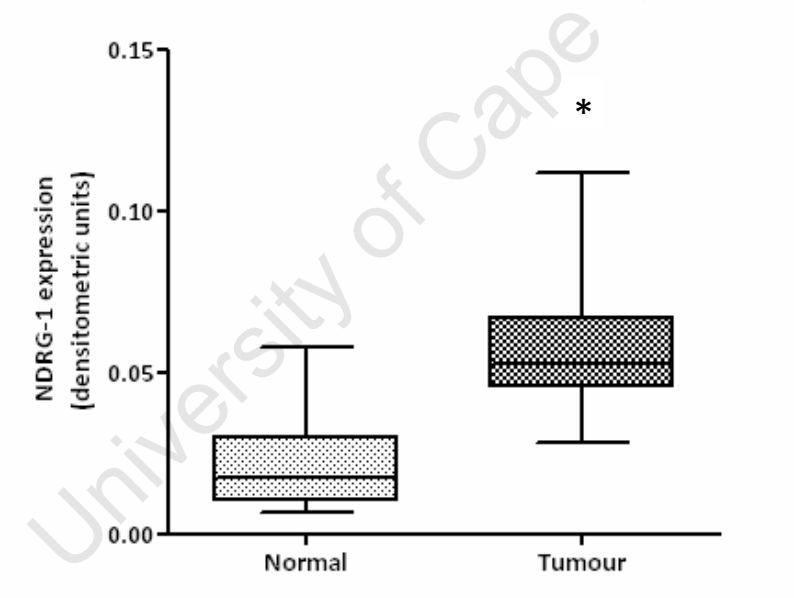

Figure 2.2. Overexpression of NDRG1 protein in squamous cell carcinoma of the oesophagus compared to normal oesophageal epithelium. Quantification of NDRG1 protein expression in normal and oesophageal cancer tissue sections. Immunohistochemistry was quantified using AxioVision version 4.7 software (*p<0.0001). A total of three views per slide (magnification 200x) were used to calculate the average signal intensity per sample.

Examination of the eighty-three patient specimens revealed that NDRG1 protein expression was approximately 2.6-fold higher ($p<0.0001$) (Fig 2.2) in cancer tissues compared to normal tissues, using the AxioVision quantification software. This confirmed our initial observations using quantitative real-time RT-PCR.

In normal esophageal epithelial tissue, NDRG1 protein displayed an interesting bi-modal pattern of expression. NDRG1 protein was exclusively associated with the plasma membrane of basal cells of the epithelium, whereas supra-basal cells exhibited nuclear staining with a blush of cytoplasmic staining as they matured towards the surface of the esophageal epithelium (Fig. 2.3.A). The flattened luminal surface epithelial cells did not stain for NDRG1. The abrupt change in the cellular location of the NDRG1 protein from plasma membrane-associated (in basal cells) to exclusively nuclear/cytoplasmic as the epithelial cells mature, suggests that the subcellular localization of NDRG1 may be associated with the differentiation status of oesophageal epithelial cells.

The NDRG1 protein was exclusively localised in the plasma membrane of dysplastic cells (Fig. 2.3.B) regardless of the stage of dysplasia. This expression pattern was identical to that displayed by the basal layer cells of the normal esophageal epithelium. In contrast, tumours of the oesophageal epithelium displayed a mixed staining pattern where membrane, cytoplasmic and nuclear localised NDRG1 was observed. Specifically, in well differentiated tumours, characterised by the presence of keratin

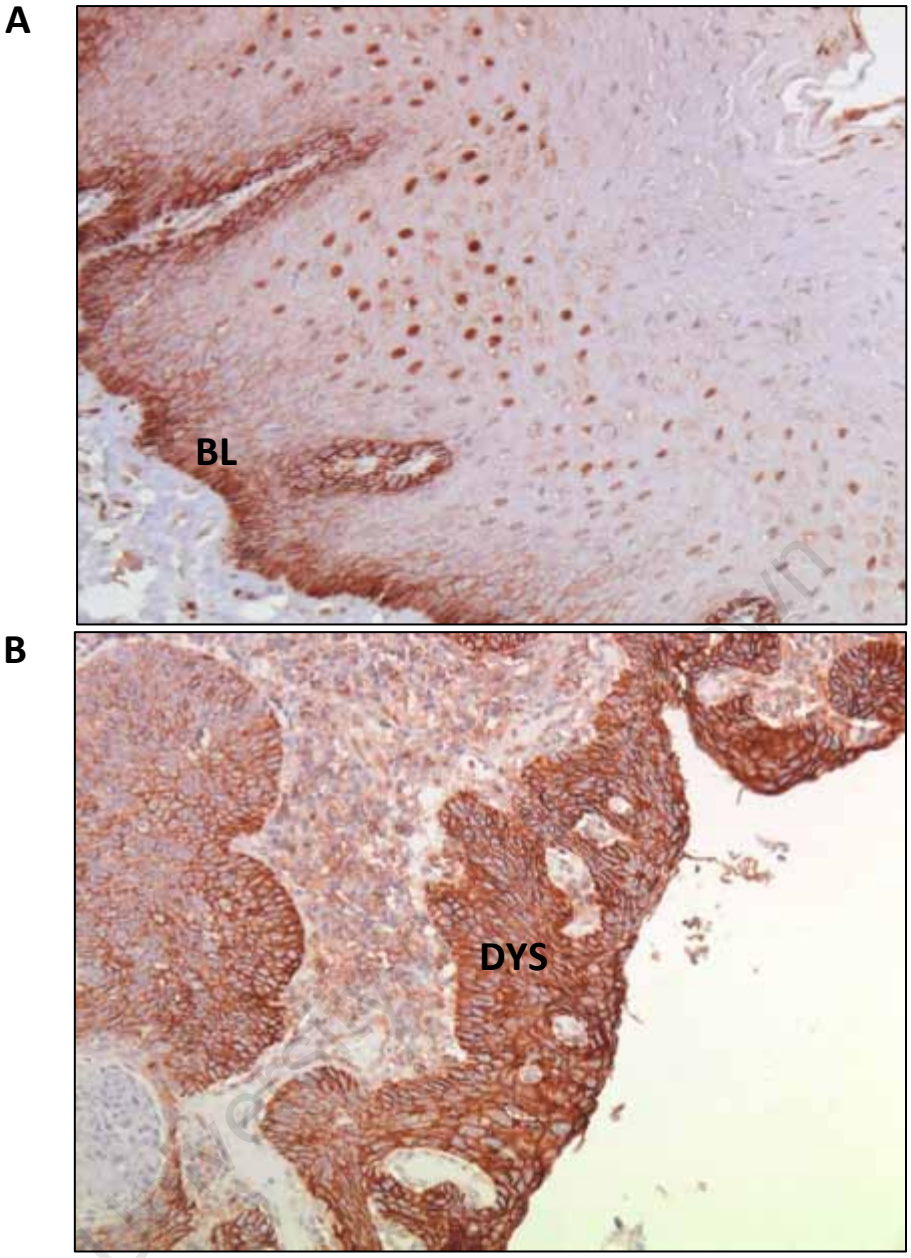

Figure 2.3. Expression and localisation pattern of NDRG1 in normal and dysplastic oesophageal epithelium. Representative images showing immunohistochemical staining for NDRG1 expression in sections of normal (A; magnification 250x) and dysplastic (B; magnification 200x) oesophageal epithelium. The basal layer of cells (BL) in normal epithelium displayed plasma membrane staining for NDRG1 protein, whereas suprabasal and mature cells displayed cytoplasmic and nuclear staining for NDRG1. Areas of dysplasia (DYS) displayed intense, plasma membrane-associated NDRG1 expression.

pearls, plasma membrane, cytoplasmic and mixed (cytoplasmic and nuclear) staining for NDRG1 was noted. This staining pattern was coupled with a marked increase in the intensity of NDRG1. Keratinised pearls at the centre of tumour nests stained predominantly negative for NDRG1. Basal-like cells, distal from the keratin pearl, display plasma membrane-associated NDRG1. Cells closer to the keratin pearl (and with a more mature appearance, morphologically) display cytoplasmic and nuclear staining with varying intensity (Fig 2.4. A and B). Correspondingly, moderately differentiated tumours also exhibit a tiered NDRG1 expression pattern. Here, keratin pearls are absent and the centre of the tumour nest is characterised by strong cytoplasmic and nuclear NDRG1 expression, with varying intensity (Fig 2.5. A). NDRG1 staining at the periphery of the tumour nest was either plasma membrane-associated or altogether lost. In contrast, poorly differentiated tumours displayed strikingly predominant plasma membrane-associated NDRG1. However, cells with nuclear and cytoplasmic positivity were also sporadically observed (Fig 2.5. B). The specificity of these staining patterns was confirmed through using NDRG1 antibodies from three different sources (see materials and methods, section 6.2), since it is possible that the variation in NDRG1 staining reported in the literature could be due to the use of different antibodies.

Since a relationship between NDRG1 expression and differentiation emerged, we wanted to determine whether this was unique to oesophageal epithelium or whether

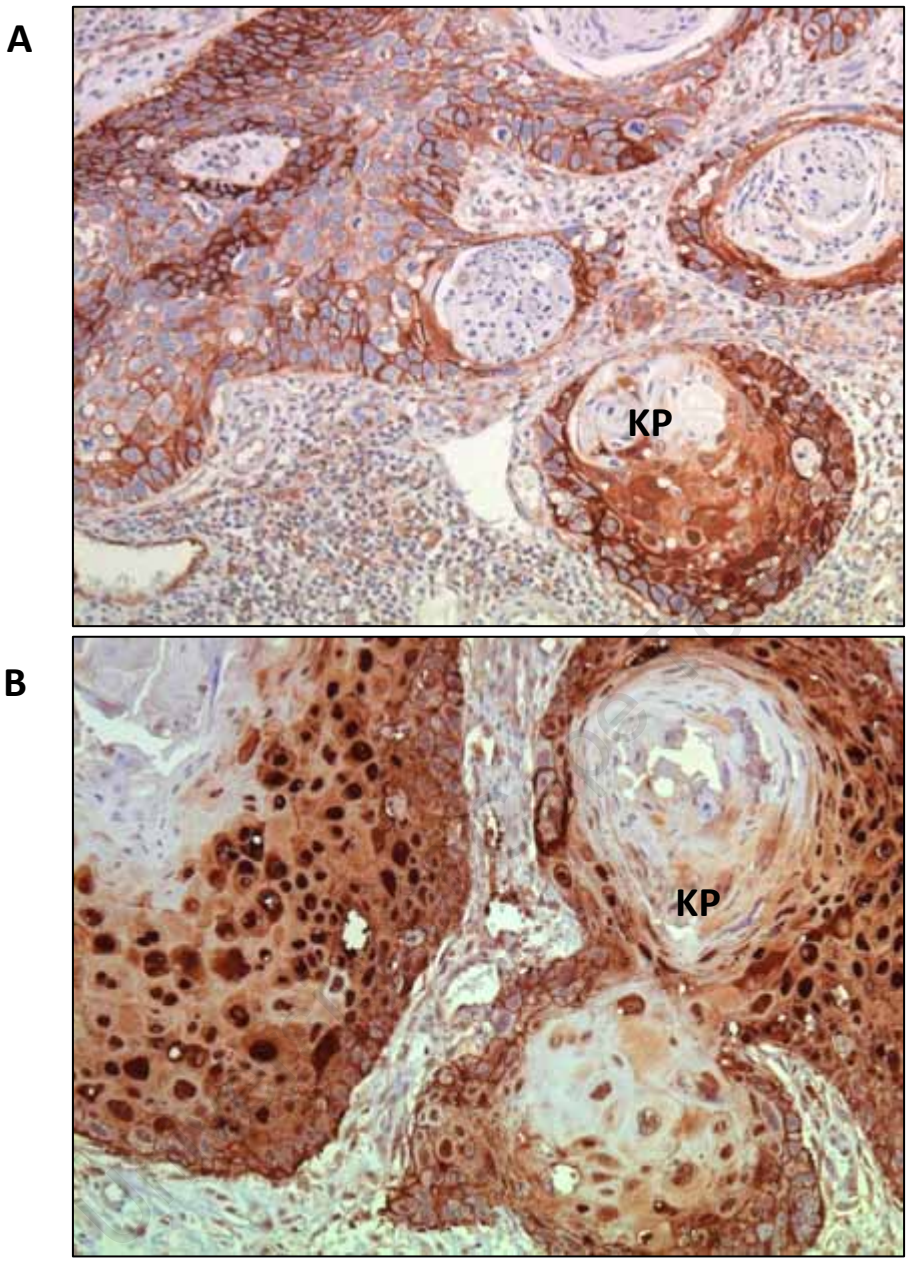

Figure 2.4. Expression and localisation pattern of NDRG1 in well differentiated squamous cell carcinoma of the oesophagus. Representative images showing immunohistochemical detection of NDRG1 expression in sections of well differentiated oesophageal cancer (A and B; magnification 200x). Tumour nests arranged around keratin pearls (KP) stained positive for NDRG1 in the nucleus, plasma membrane and cytoplasm of cells.

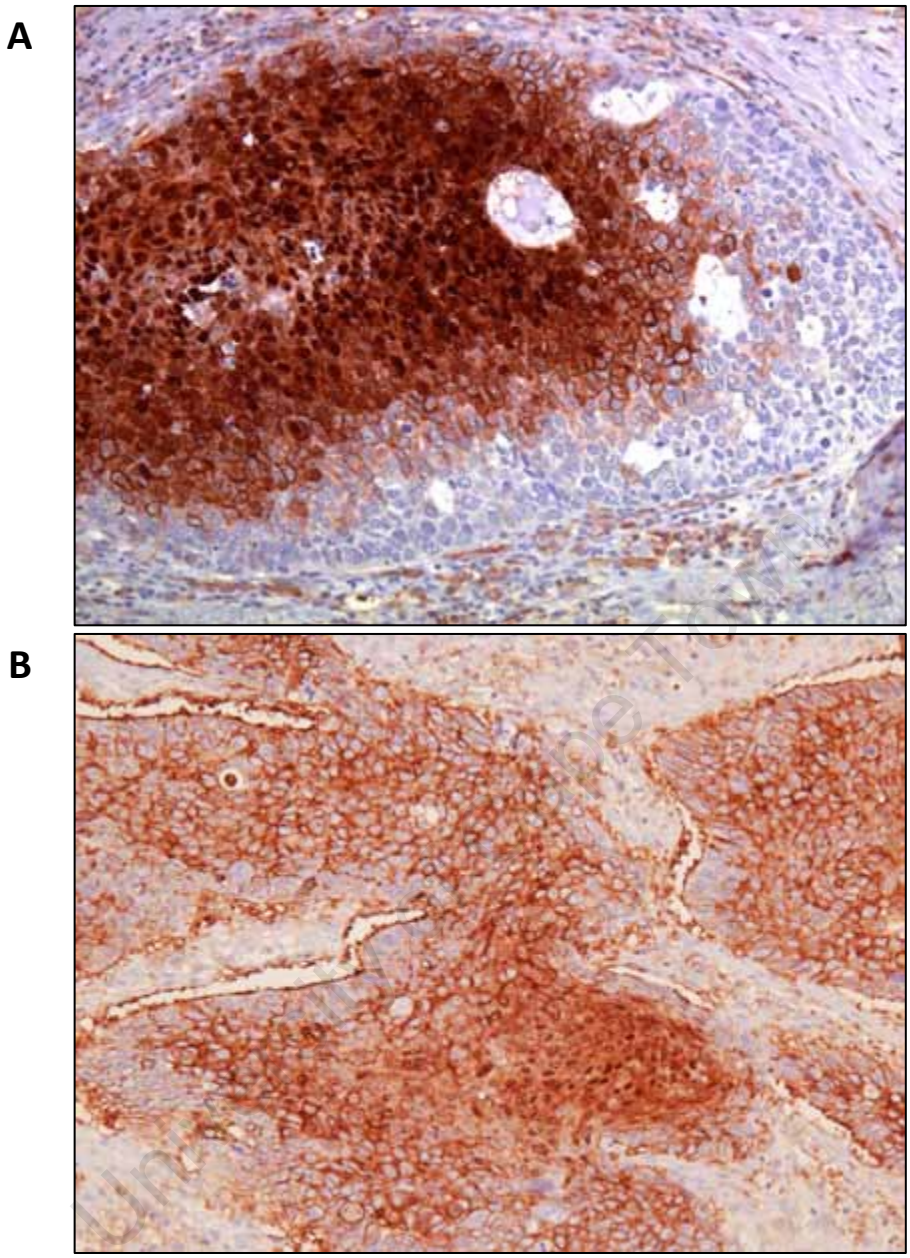

Figure 2.5. Expression and localisation pattern of NDRG1 in moderately and poorly differentiated squamous cell carcinoma of the oesophagus. Representative images showing immunohistochemical staining of NDRG1 expression in sections of moderately differentiated (A; magnification 200x) and poorly differentiated (B; magnification 200x) OSCC. Moderately differentiated tumours were characterised by the presence of mixed nuclear, cytoplasmic and plasma membrane localised NDRG1, as well as unstained cells. In poorly differentiated tumours NDRG1 predominantly localised to the plasma membrane.

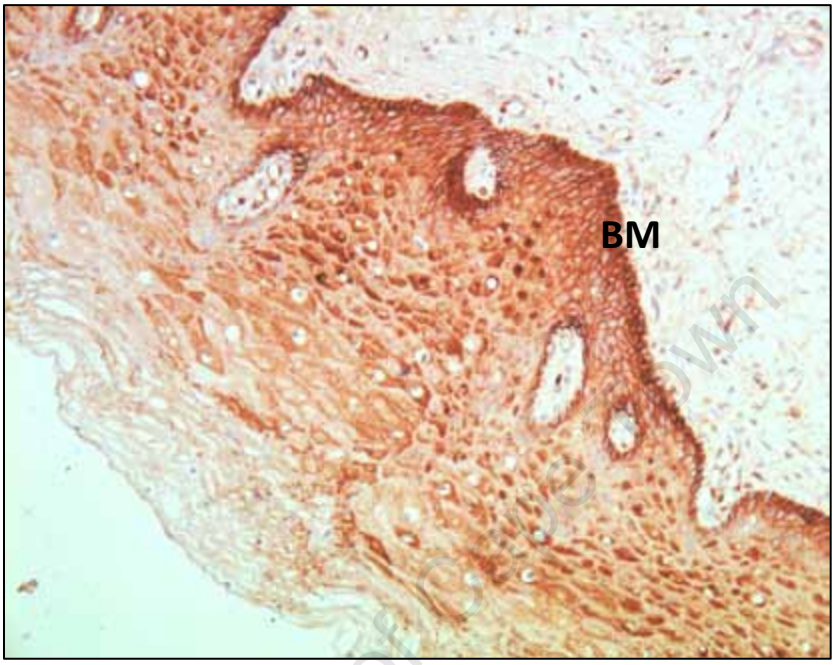

Figure 2.6. Expression and localisation pattern of NDRG1 in normal cervical squamous epithelium (magnification 200x). Cells adjacent to the basement membrane (BM) showed plasma membrane staining for NDRG1, whereas mature cells displayed cytoplasmic and nuclear staining for NDRG1.

it was present in other types of epithelium. Immunohistochemical staining for NDRG1 was therefore carried out on sections of normal cervical epithelium. As observed with normal oesophageal epithelium, NDRG1 was localised exclusively in the plasma membrane of cells adjacent to the basement membrane of the cervical epithelium. Similarly, NDRG1 expression localised in the cytoplasm and nucleus of maturing cells (Fig. 2.6.). The immunohistochemical staining of NDRG1 in normal oesophageal and cervical squamous epithelium are remarkably similar and both suggest a relationship between NDRG1, cellular localisation and differentiation.

2.2.3. Expression of NDRG1 in cultured oesophageal squamous cell carcinoma cells

Since NDRG1 was observed to be overexpressed in oesophageal cancer tissue specimens, we next investigated the expression levels of NDRG1 mRNA and protein in cultured OSCC cell lines. Protein and RNA were prepared from cultured cancer cells grown at subconfluence overnight. Western blot analysis and real-time RT-PCR was used to evaluate NDRG1 expression levels in WHCO1, WHCO5, WHCO6, KYSE70, KYSE180, KYSE450 and KYSE520 cell lines. Western blot analysis revealed that NDRG1 was expressed in all of the cell lines, with highest protein levels observed in WHCO1 and KYSE520 cells. KYSE70, KYSE180 and KYSE450 cells expressed low levels of NDRG1 while the remainder of the cell lines, WHCO5 and WHCO6, expressed moderate NDRG1 levels (Fig 2.7.A). Similarly, NDRG1 mRNA expression was highest in WHCO1 cells. Whereas KYSE70 and KYSE180 cells showed relatively low levels of NDRG1 mRNA

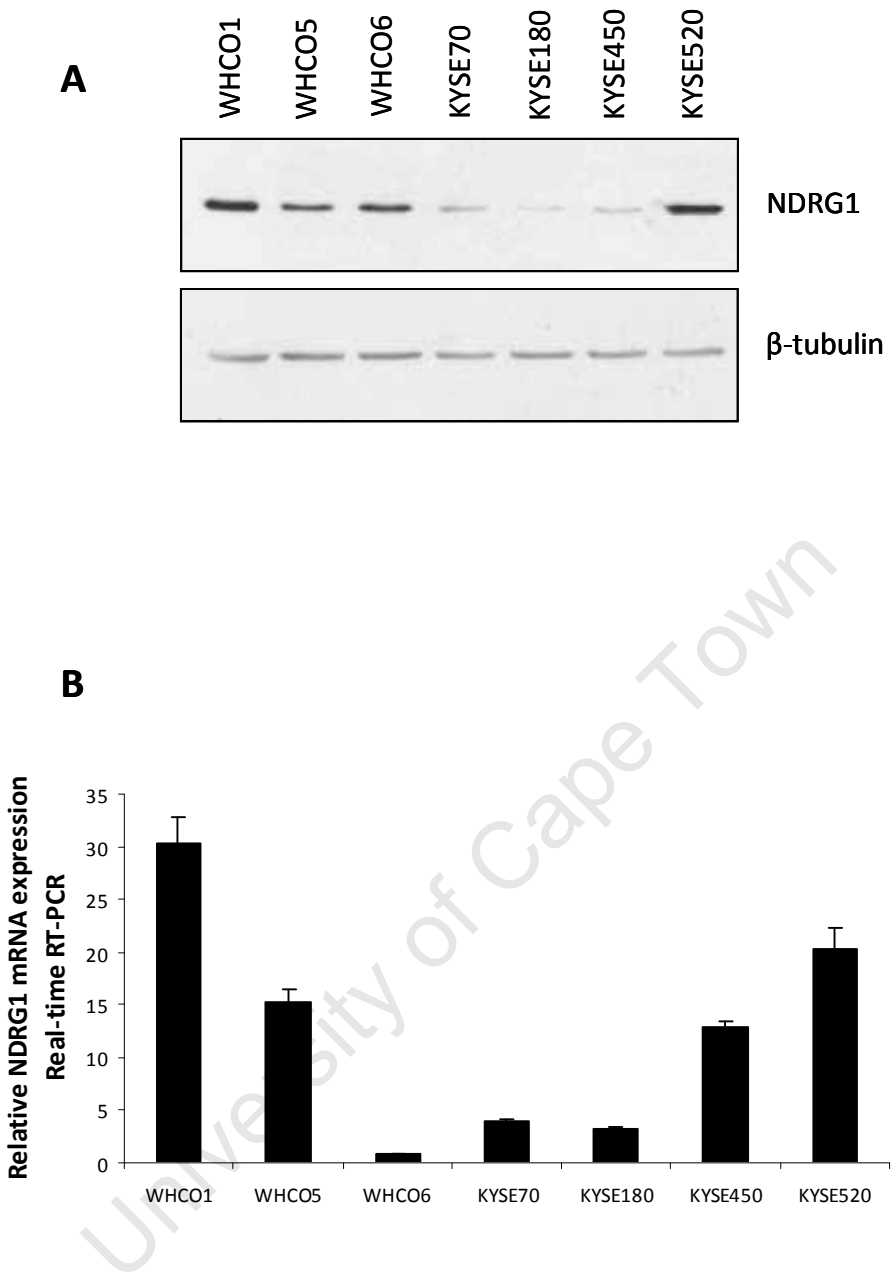

Figure 2.7. NDRG1 is differentially expressed in cultured oesophageal squamous cell carcinoma cell lines. A. Western blot analysis of NDRG1 in cultured OSCC cells reveals that NDRG1 is differentially expressed. Forty micrograms of whole cell lysate from cells cultured overnight was subjected to Western blot analysis. β-tubulin was used as a control for protein loading. Results shown are representative of Western blots performed in triplicate. B. Real-time RT-PCR analysis of NDRG1 in oesophageal cancer cell lines, WHCO1, WHCO5, WHCO6, KYSE70, KYSE180, KYSE450 and KYSE520, cultured overnight. Results shown are the mean ± SD of experiments performed in triplicate and repeated at least two times.

expression, WHCO6 cells expressed the lowest levels of NDRG1 mRNA, some 30-fold lower than that observed in WHCO1 cells, yet expressed high levels of NDRG1 protein (Fig 2.7.B). In agreement with patient-derived data, this shows that NDRG1 is differentially expressed at both the mRNA and protein level in cultured cells. However, the discrepancy between protein levels and mRNA levels in some of the cell lines are intriguing and is perhaps indicative of transcriptional as well as post-translational mechanisms of NDRG1 expression regulation. Indeed, analysis of NDRG1 protein and mRNA stability within these cells may be appropriate.

2.2.4. Subcellular localisation of NDRG1 in cultured oesophageal squamous cell carcinoma cells

In patient specimens, NDRG1 was detected in the plasma membrane, cytoplasm and nucleus and the expression patterns appeared to be related, in part, to differentiation. Given this interesting staining pattern of NDRG1 in patient tissue, we examined the localisation of NDRG1 in cultured OSCC cell lines.

NDRG1 subcellular localisation was determined by immunofluorescence staining of cultured OSCC cells, grown for 24 hours on glass coverslips. Fixed cells were probed with primary antibodies to NDRG1 as well as E-cadherin (a plasma membrane associated protein) and secondary antibodies labelled with Cy3 and Alexa-488 fluors, respectively (see materials and methods, section 6.10). 4',6'-diamidino-2'-phenylindole dihydrochloride (DAPI) was used to stain nucleic acid and reveal the

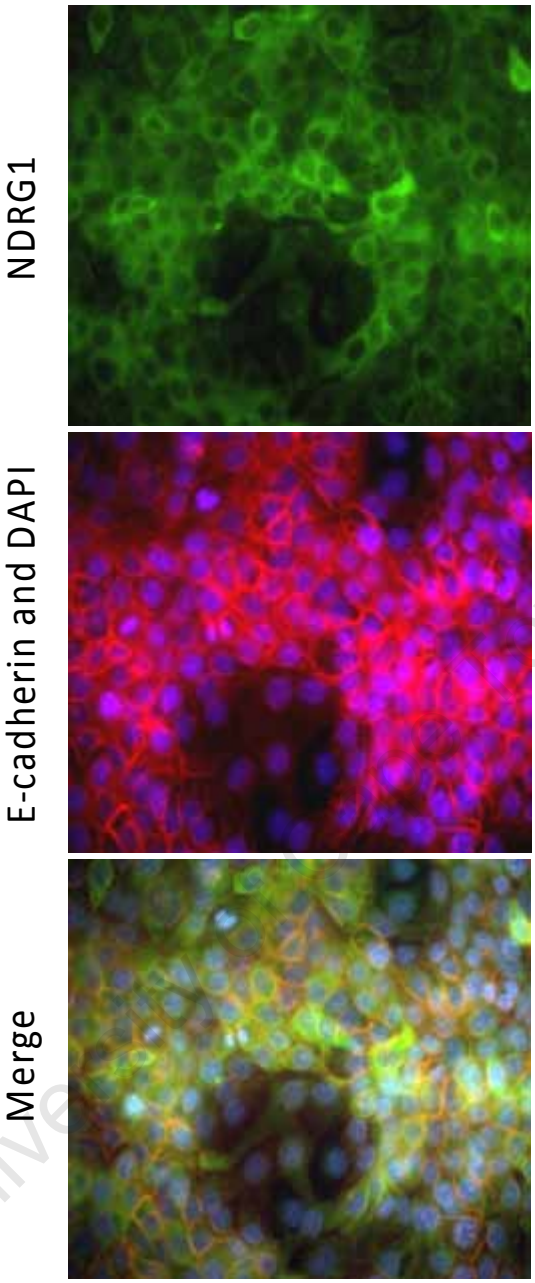

Figure 2.8. Localisation of NDRG1 in cultured oesophageal cancer cell lines. Representative fluorescent images for NDRG1 and E-cadherin expression as well as blue nuclear staining (DAPI) in cultured KYSE30 OSCC cells (maginification 400x). NDRG1 localised predominantly in the cytoplasm of cultured cells, unlike E-cadherin, which was localised to the plasma membrane.

location of cell nuclei. Whereas E-cadherin was, as expected, located in the plasma membrane, NDRG1 appeared to localise largely in the cytoplasm, with no predominant nuclear or plasma membrane localisation (Fig. 2.8.). This staining pattern was or nucleus. The cytoplasmic localisation of NDRG1 was explored further in order to ascertain which subcellular organelles may be associated with NDRG1 expression. observed across the panel of seven OSCC cell lines. In contrast to that seen in patient material, NDRG1 did not show a strong association with either the plasma membrane NDRG1 localisation in cultured cells was determined using an antibody to NDRG1 and a Cy3-labelled secondary antibody. Cells were examined under high power magnification using a Axiovert 200M microscope (Zeiss). KYSE450 and WHCO1 cells were examined based on the expression data generated by western blot, as seen in figure 2.7. Close inspection of stained cells revealed a punctate staining pattern for NDRG1, which on occasion appeared more concentrated in the perinuclear region (Fig. 2.9.).

2.3. DISCUSSION

In a preliminary study in our laboratory, DDRT-PCR and cDNA microarray technology was used to examine the global gene expression patterns of normal and oesophageal cancer tissues. Here, NDRG1 was identified as a deregulated gene in OSCC. This study, confirmed, using real time RT-PCR and immunohistochemistry, that NDRG1 mRNA and protein is overexpressed in oesophageal cancer tissue compared to normal tissue.

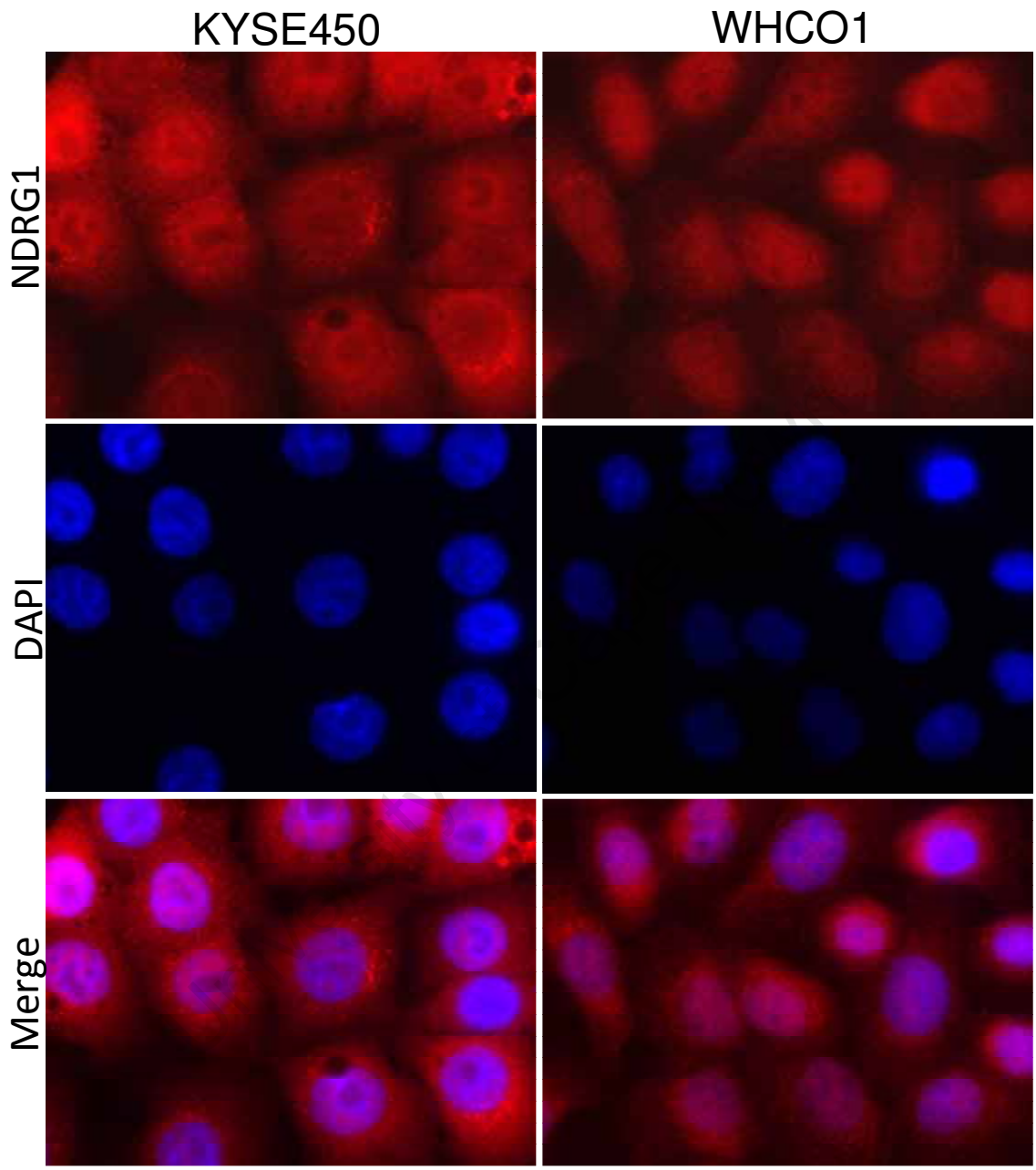

Figure 2.9. Immunofluorescent localisation of NDRG1 in KYSE450 and WHCO1 cells. Immunofluorescent analysis of NDRG1 subcellular localisation in cultured KYSE450 and WHCO1 cells (magnification 1000x) reveals a punctate pattern of NDRG1 expression, which predominates in the cytoplasm and occasionally appears perinuclear. DAPI staining for nuclei is shown.

Real-time RT-PCR of RNA isolated from patient biopsies revealed that NDRG1 was overexpressed in tumour tissue compared to normal tissue. Although our results of NDRG1 mRNA overexpression were obtained from only six normal and eight cancer biopsies, this observation was consistent with the immunohistochemical analysis of NDRG1 in a cohort of eighty-three patients reported here. This finding is in agreement with an earlier study reporting an approximate 4-fold increase of NDRG1 mRNA in OSCC[169]. In contrast, a study on a cohort of 47 Japanese OSCC patients reported NDRG1 mRNA expression levels to be significantly lower in advanced stage tumours (i.e. stage II-IV) compared to early stage tumour (stage 0-I)[104]. This discrepancy may be explained by differences in patient profiles, differences in population genetics or possibly different aetiological profiles of the cancer, although these are unlikely. A more likely scenario is that differences in reported NDRG1 expression probably reflect differences in methodological approaches. It should be noted that the majority of OSCC patients (84 %) used in our study presented with advanced cancer (stage II-III), similar to the patient sample used by Ando *et al*.[104]. However, Ando *et al*.[104] normalised their real-time RT-PCR data using the house-keeping gene, *glyceraldehyde 3-phosphate dehydrogenase* (*gapdh*). GAPDH as well as β-actin mRNA expression is reportedly deregulated in some cancers, making these genes inappropriate normalisers for real-time RT-PCR[170-172]. Moreover, GAPDH mRNA was found to have significantly different expression levels in the same tissues from different donors[173]. The reliability of the Ando *et al*.[104] study may be greatly improved if more than one house-keeping gene were used in combination with, or as an alternative to, *gapdh*. Similarly, a previous immunohistochemical study described the

downregulation of NDRG1 protein in OSCC tissue specimens[105]. However, no NDRG1 positivity was associated with the plasma membrane of normal tissues, unlike our observation, and an earlier report that examined the expression of NDRG1 in a wide range of tissues [71]. A previous PhD study in our laboratory also observed membrane staining of NDRG1 in basal cells of the oesophageal epithelium, although only one antibody to NDRG1 was used in that study[174]. So whilst the study by Ando *et al*. should not be discounted, the poor quality of He and associates[105] immunohistochemical data undermines the veracity of their report. The observation that the same staining pattern was obtained using three different antibodies for NDRG1 underscores our confidence in the immunohistochemical data presented here.

In agreement with previous reports, we describe the membrane localisation of NDRG1 in basal cells of the oesophageal epithelium[71] as well as the cytoplasmic and nuclear localisation in mature epithelial cells. Indeed, examination of normal and tumour tissue counterparts revealed a staining pattern which paralleled cellular and tumour differentiation. Our observation of a near identical staining pattern in cervical epithelium which correlates with that reported for intestinal epithelium[71] suggests that NDRG1 may function and be regulated, at least in part, in the same manner in some epithelial tissues in the body.

The proliferative stem cell compartment of the oesophageal epithelium lies adjacent to the basement membrane. Stem cells in the basal compartment divide, giving rise to

transit amplifying daughter cells whose progressive specialization culminates in terminal differentiation and is often associated with a diminished proliferative capacity[106;107;109;175]. Membrane localised NDRG1, in areas of oesophageal epithelial dysplasia, mimics the staining pattern observed in cells adjacent to the basement membrane of normal epithelium. This invites speculation that dysplastic cells could arise from the premalignant expansion of the stem cell compartment of the epithelium. Additional work is required to explore this idea further.

In the cultured OSCC cell system, NDRG1 did not localise to the plasma membrane or nucleus but rather predominated in a punctate cytoplasmic pattern. Indeed, NDRG1 has been described as an endosome-associated protein which, similarly, appears in a cytoplasmic, punctate profile in prostate cancer cells[78]. However, a punctate cytoplasmic stain could also be indicative of mitochondrial localisation. Given that NDRG1 reportedly associates with mitochondria[71] and mitochondrial proteins[77] in other tissue and cell culture systems, this too is a possibility in cultured OSCC cells. The absence of distinctly nuclear or plasma membrane-associated NDRG1 in cultured cells (unlike in patient specimens) could be explained by culture conditions and the surrounding cellular milieu. Indeed, tissue culture systems far from accurately mimic conditions within an intact tissue or tumour mass. Hypoxia has been shown to increases cytoplasmic expression of NDRG1, but is insufficient for its membrane localisation in human hepatocellular carcinoma cell lines[101]. However, grown *in vivo,* within mouse xenografts, these same cells express NDRG1 in the plasma

membrane[101]. This suggests that the tumour microenvironment may play a role in the recruitment of NDRG1 to the plasma membrane, a finding that should be considered when exploring NDRG1 function *in vitro*. Some of these issues will be explored at a later stage within this study.

Although the precise function of NDRG1 remains enigmatic, numerous studies revealing altered expression of NDRG1 in tumour tissue relative to normal tissue suggesting that this protein may have a role in tumour biology. A growing number of studies have implicated an oncogenic role for NDRG1 in neoplasia. For example, elevated NDRG1 levels have been observed in oral squamous cell carcinoma[102], cervical adenocarcinoma[96;97], liver[100;101] and colon cancer[98;99], to mention but a few, where high NDRG1 levels correlated with metastasis, enhanced vascularity and a poor prognosis. To our knowledge, our laboratory is the first to report the overexpression of NDRG1 protein in squamous cell carcinoma of the oesophagus. The significance of this finding depends on whether this overexpression is necessary to sustain the malignant phenotype; a question which is explored in the next chapter.

CHAPTER 3

IMPACT OF NDRG1 EXPRESSION IN OSCC CELL LINES CULTURED IN AN ANCHORAGE-INDEPENDENT MANNER

3.1. INTRODUCTION

In the previous chapter we reported the overexpression of NDRG1 in primary oesophageal tumour tissue at both the mRNA and protein levels, relative to normal tissue. This upregulation of NDRG1 expression suggests that it may have some functional importance in the initiation, maintenance and/or progression of oesophageal cancer. Conflicting data has been reported with regards to NDRG1 expression in OSCC[104;105;169], however, no functional *in vitro* studies have been published supporting an oncogenic or tumour suppressor role for NDRG1 in this cancer.

Recently, it was reported that hypoxia induced expression of NDRG1 in the hepatocellular carcinoma cell line, Hep3B, but was not associated with the plasma membrane localisation of this protein[101]. On the other hand, NDRG1 in Hep3B cells, grown *in vivo* in mouse xenografts, showed a strong association with the plasma membrane. Sibold *et al*.[101] therefore suggested that the tumour milieu influences the subcellular localisation of NDRG1 and may therefore have implications with

regards to NDRG1 function. In fact, they proposed that plasma membrane-associated NDRG1 within the neoplastic microenvironment may be involved in signal transduction, cell mobility and/or cell adhesion[101].

In sections of normal oesophageal tissue, we observed a change in localisation of NDRG1 from the plasma membrane, in cells adjacent to the basement membrane, to the cytoplasm and nucleus of mature cells (Chapter 2, Figure 2.3.). One might speculate that proximity to the basement membrane may influence NDRG1 localisation; however, NDRG1 is also associated with the plasma membrane in dysplastic and tumour tissue sections where the basement membrane is uninvolved. Certainly, the differential localisation of NDRG1 observed in tissue and that reported by Sibold *et al*.[101] could provide insights regarding the role of NDRG1, and suggests that tissue architecture may affect NDRG1 function.

In this study we therefore examined the impact of NDRG1 expression on selected cellular processes involved in tumourigenesis, using cells cultured in an anchorage-independent (non-adherent) manner. Using RNA interference (RNAi) we examined how targeted downregulation of NDRG1 would influence cellular processes such as cell proliferation and apoptosis, and also examined how NDRG1 may affect the tumour microenvironment through modulation of genes involved in metastasis, invasion and angiogenesis.

3.2. RESULTS

3.2.1. NDRG1 expression is induced by anchorage-independent growth

It has been reported previously that the localisation of NDRG1 in cultured hepatocellular carcinoma cells (grown *in vitro*) differs from that in mouse xenograft models, despite using the same cell lines. In the cultured cell system, NDRG1 is located in the cytoplasm, whereas this protein is located at the plasma membrane in xenografts[101]. This finding prompted us to examine the effect anchorage-independent growth on NDRG1 expression in cultured OSCC cell lines. Cells were seeded in tissue culture dishes coated with Poly(2-hydroxyethyl methacrylate) (poly-HEMA), to prevent adhesion, or grown in normal culture dishes, to allow adherence, for 24 hours. Western blot analysis of whole cell lysates showed that NDRG1 levels were strongly upregulated in cells cultured in an anchorage-independent manner (Fig. 3.1.). This upregulation was observed across the panel of seven cell lines, albeit to differing degrees. Given the strong signal obtained from NDRG1 expression in WHCO1, WHCO5 and WHCO6 cells cultured anchorage-independently, the exposure of the Western blot to x-ray film was short and gives the impression that NDRG1 is absent in KYSE70, KYSE180 and KYSE450 cells cultured under anchorage-independent conditions. Longer exposure times did however confirm that NDRG1 is present in these cells (data not shown).

To determine the time course of NDRG1 induction under anchorage-independent culture conditions, randomly selected WHCO1, WHCO6, KYSE70, KYSE180 and KYSE450

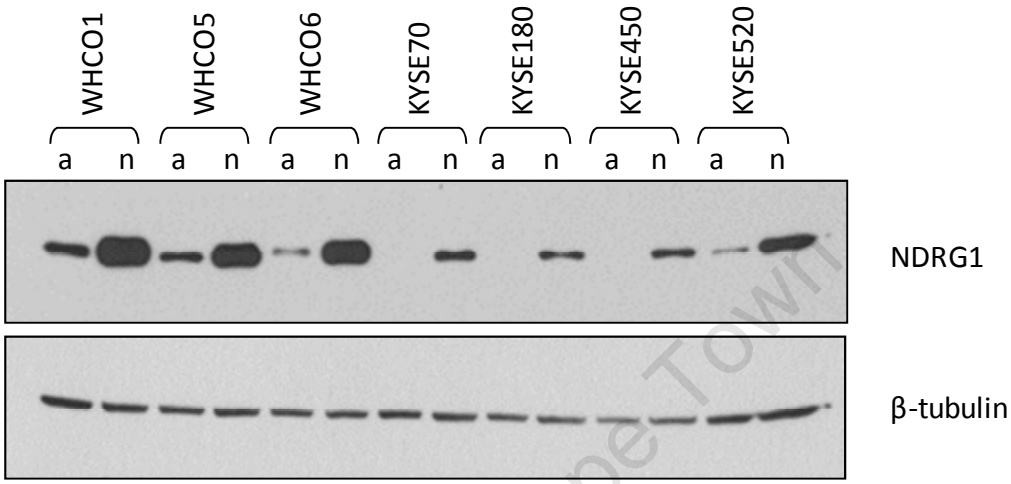

Figure 3.1. Anchorage-independent growth conditions induce NDRG1 expression in cultured OSCC cell lines. Western blot analysis of NDRG1 protein expression, performed on 20 µg of whole cell lysate, prepared from cell cultures grown under anchorage-dependent (a) or -independent (n) conditions for 24 hours. β-tubulin was used as a control for protein loading.

cells were cultured in an anchorage-independent manner for 24, 48 and 72 hours and NDRG1 mRNA and protein levels examined. Real-time RT-PCR analysis showed a strong induction of NDRG1 mRNA levels in all cell lines, with the bulk of NDRG1 mRNA induction completed within the first 24 hours. With a 12-fold increase in mRNA levels, WHCO1 cells showed the weakest NDRG1 response, while KYSE450 cells showed the strongest relative increase in NDRG1 mRNA levels of 129-fold. After 72 hours of anchorage-independent growth, NDRG1 mRNA showed a decline in all cell lines but had not yet reached basal (anchorage-dependent) levels (Fig. 3.2.). Similarly, Western blot analysis of whole cell lysates from the same cell lines demonstrated a strong upregulation in NDRG1 levels within 24 hours of anchorage-independent growth. However, in contrast to mRNA levels, NDRG1 protein levels showed no decline after 72 hours of anchorage-independent cell cultire, likely owing to its reportedly long half-life of 16-24 hours[71;80] (Fig. 3.3).

3.2.2. NDRG1 localisation is altered in oesophageal cancer cells cultured in an anchorage-independent manner

Since the three-dimensional tumour microenvironment was reportedly associated with a change in NDRG1 localisation[101], we next examined the effect of *in vitro* anchorage-independent cell culture conditions on NDRG1 subcellular localisation. WHCO1, WHCO6, KYSE70 and KYSE180 cells were cultured in an anchorage-dependent and –independent manner for 48 hours. Adherent cells were lifted from culture plates using 0.2 % w/v EDTA, to preserve membrane associated proteins. Cells were fixed,

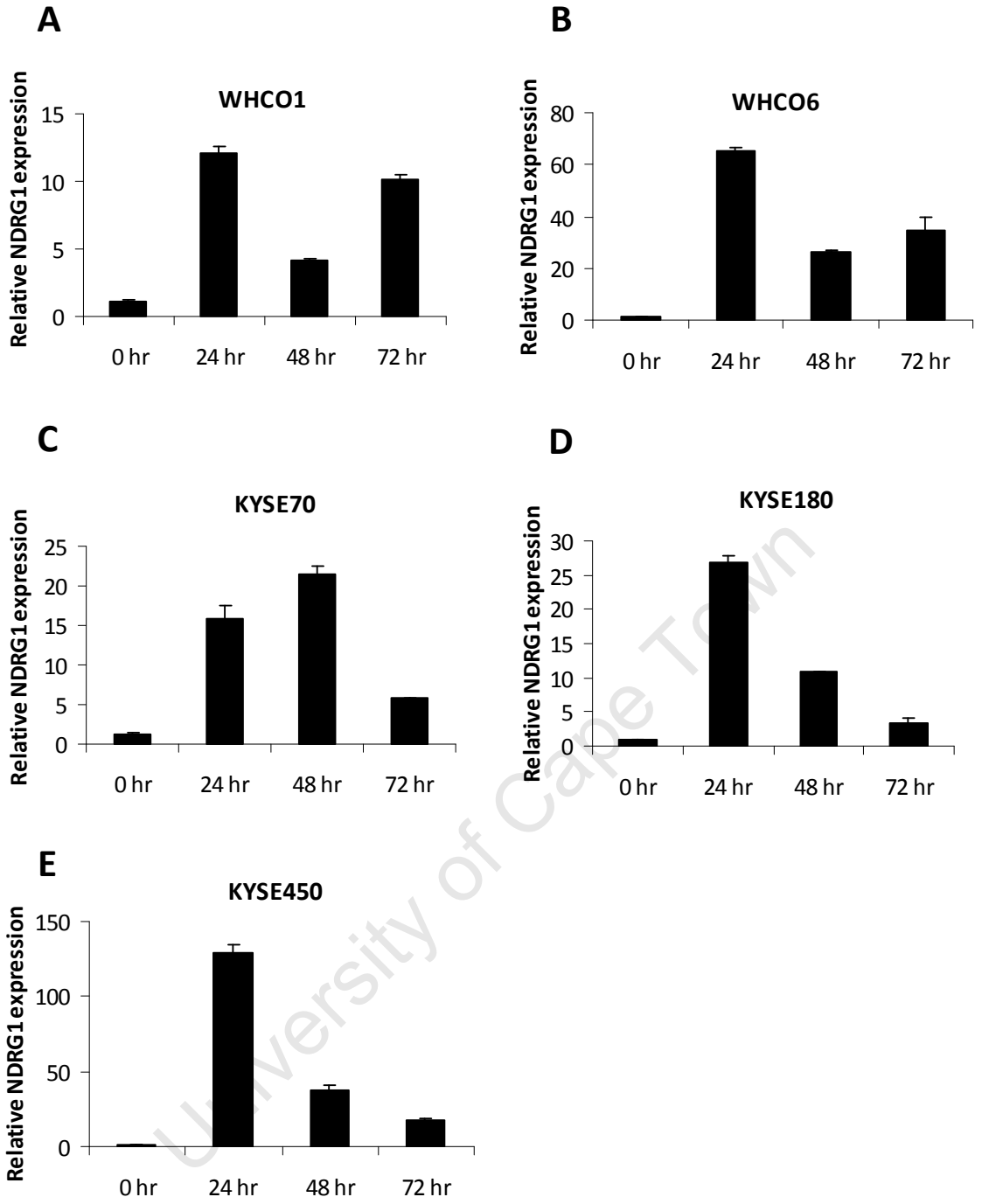

Figure 3.2. Time course of NDRG1 mRNA expression in OSCC cell lines cultured under anchorage-independent conditions. Real-time RT-PCR to determine NDRG1 mRNA expression was performed on RNA extracted from WHCO1, WHCO6, KYSE70, KYSE180 and KYSE450 cells (A-E) cultured under anchorage-dependent conditions for 24 hours (0 hr) and anchorage-independent conditions for 24, 48 and 72 hours. RNA of a high quality, determined by RNA gel electrophoresis, was used and normalised to GUSB mRNA expression. The specificity of the real-time RT-PCR was assessed by melting curve analysis. Results shown are the mean ± SD of experiments performed in triplicate and repeated at least two times.

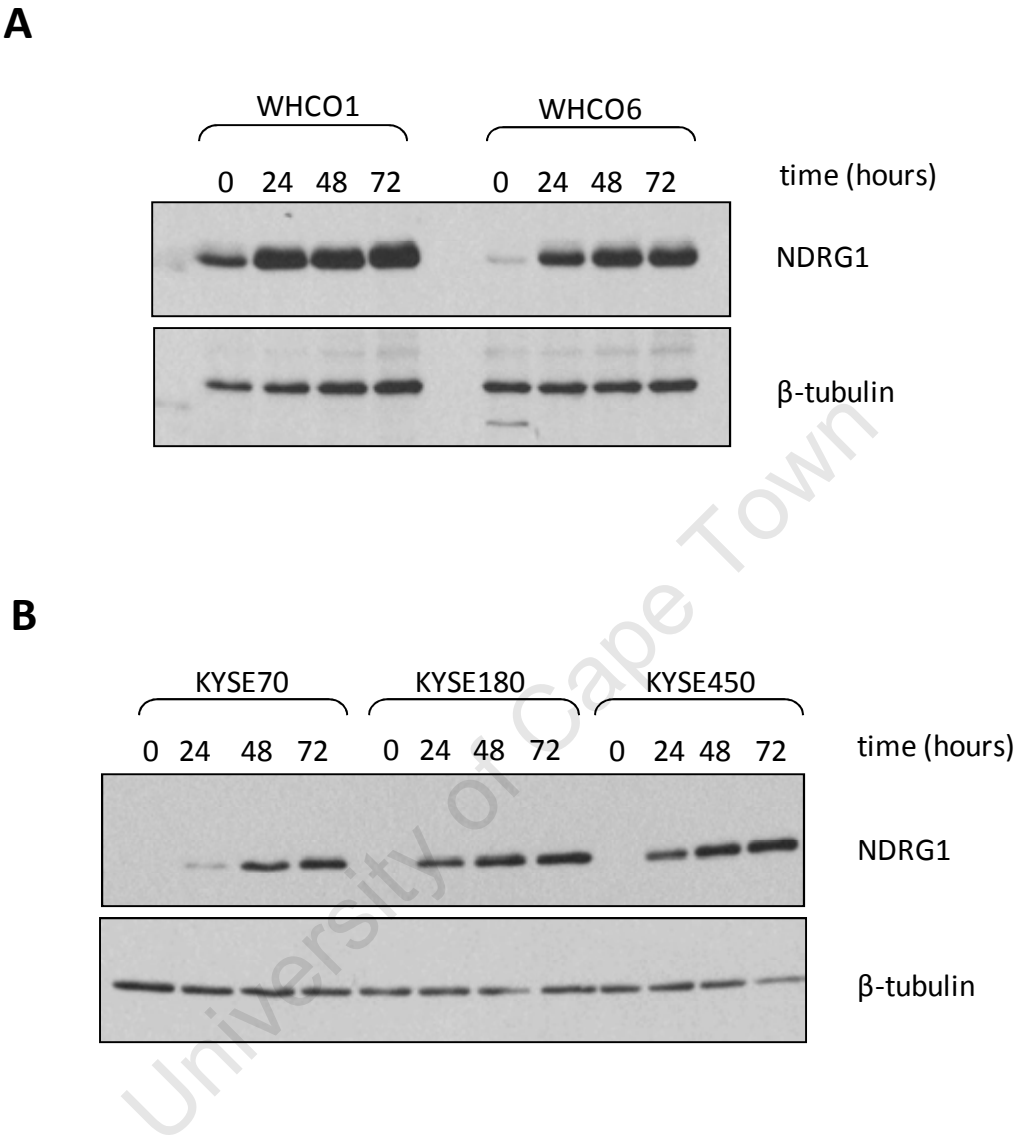

Figure 3.3. Time course of NDRG1 induction in OSCC cell lines cultured under anchorage-independent conditions. Western blot analysis of NDRG1 protein expression, performed on 20 µg of whole cell lysate prepared from WHCO (A) and KYSE (B) cell line cultures, grown under anchorage-dependent conditions for 24 hours (0) and anchorage-independent conditions 24, 48 and 72 hours. β-tubulin was used as a control for protein loading. Results shown are representative of experiments performed three times.

mounted in paraffin, sectioned and stained for NDRG1 using peroxidase/DAB staining. Compared to anchorage-dependently cultured cells, in all cases cell lines cultured in an anchorage-independent manner showed increased levels of NDRG1. In anchorage-independently cultured WHCO1 and WHCO6 cells, a strong upregulation in NDRG1 levels was evident. Here, NDRG1 localisation was cytoplasmic (albeit at varying levels) and in some cells nuclear-associated NDRG1 was observed (Fig. 3.4.1.). Likewise, immunohistochemical analysis of NDRG1 expression in KYSE70 and KYSE180 cells demonstrated an increased expression of NDRG1 protein in cells grown in an anchorage-independent manner. However, unlike WHCO1 and WHCO6 cells, NDRG1 positivity appeared to predominate at the periphery of stained KYSE70 and KYSE180 cells, reminiscent of plasma membrane localisation (Fig. 3.4.2). Taken together, these results suggest that anchorage-independent growth affects both expression levels and localisation of NDRG1.

3.2.3. Inhibition of NDRG1 expression has no effect on anchorage-independent proliferation of oesophageal cancer cells

In order to determine the biological significance of elevated NDRG1 protein levels in anchorage-independently cultured oesophageal cancer cells, small interfering RNA (siRNA) was used to inhibit its expression. The efficacy of NDRG1 siRNA in down-regulating NDRG1 expression was determined in WHCO1 and KYSE450 cells. Cells were transiently transfected with 20 nM siRNA targeted against NDRG1 or a scrambled sequence control siRNA, which served as a negative control, and then cultured in an

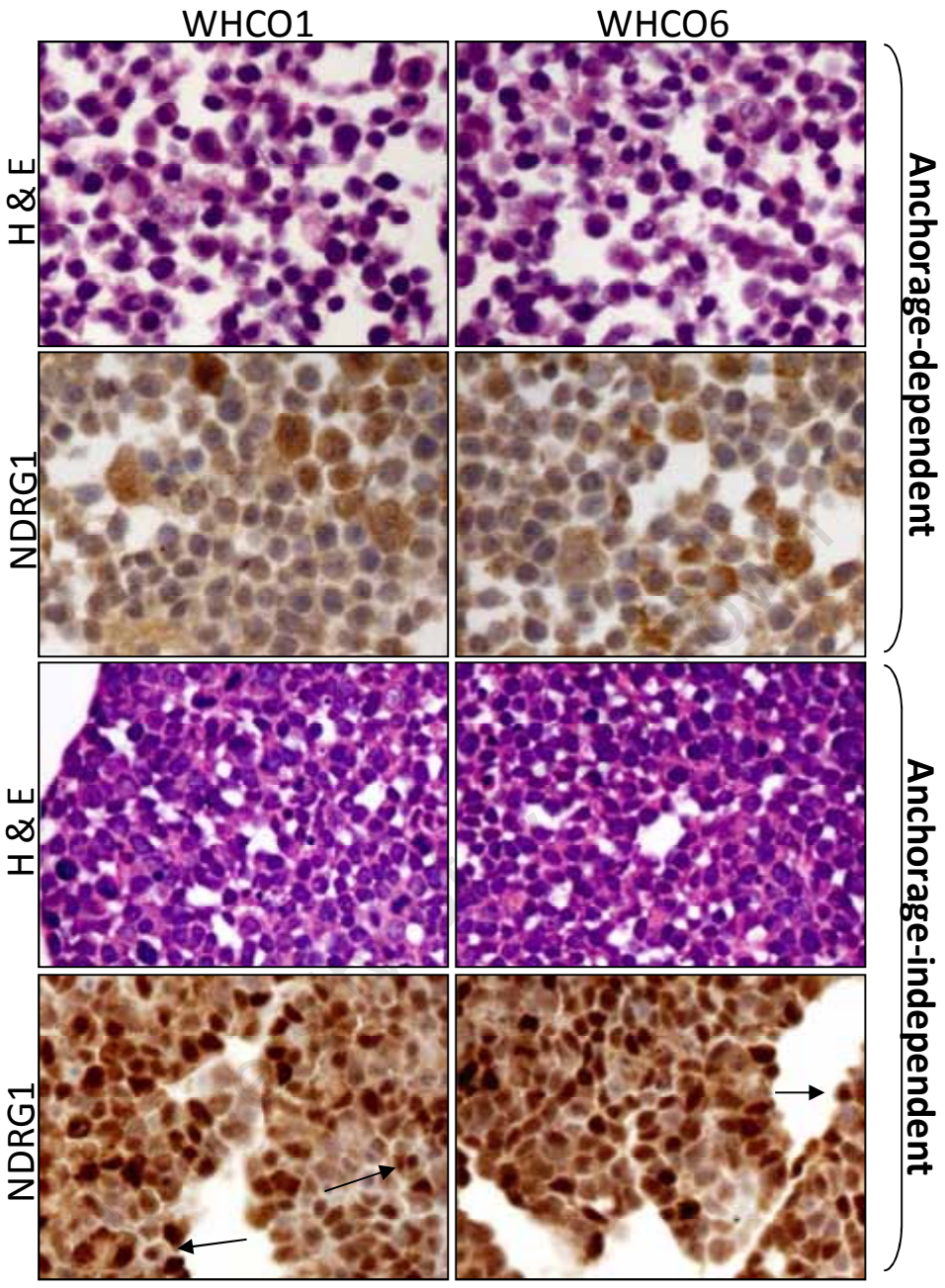

Figure 3.4.1. Immunohistochemistry of NDRG1 in WHCO1 and WHCO6 cells cultured in an anchorage-dependent and -independent manner (magnification 400x). Cell lines, cultured in an anchorage-dependent and -independent manner for 48 hours, were fixed, embedded in paraffin blocks, sectioned and stained for NDRG1. WHCO1 and WHCO6 cells displayed intense cytoplasmic, and perhaps nuclear (arrows), localised NDRG1 when cultured in an anchorage-independent manner. Representative images of hematoxylin and eosin (H&E) staining are shown.

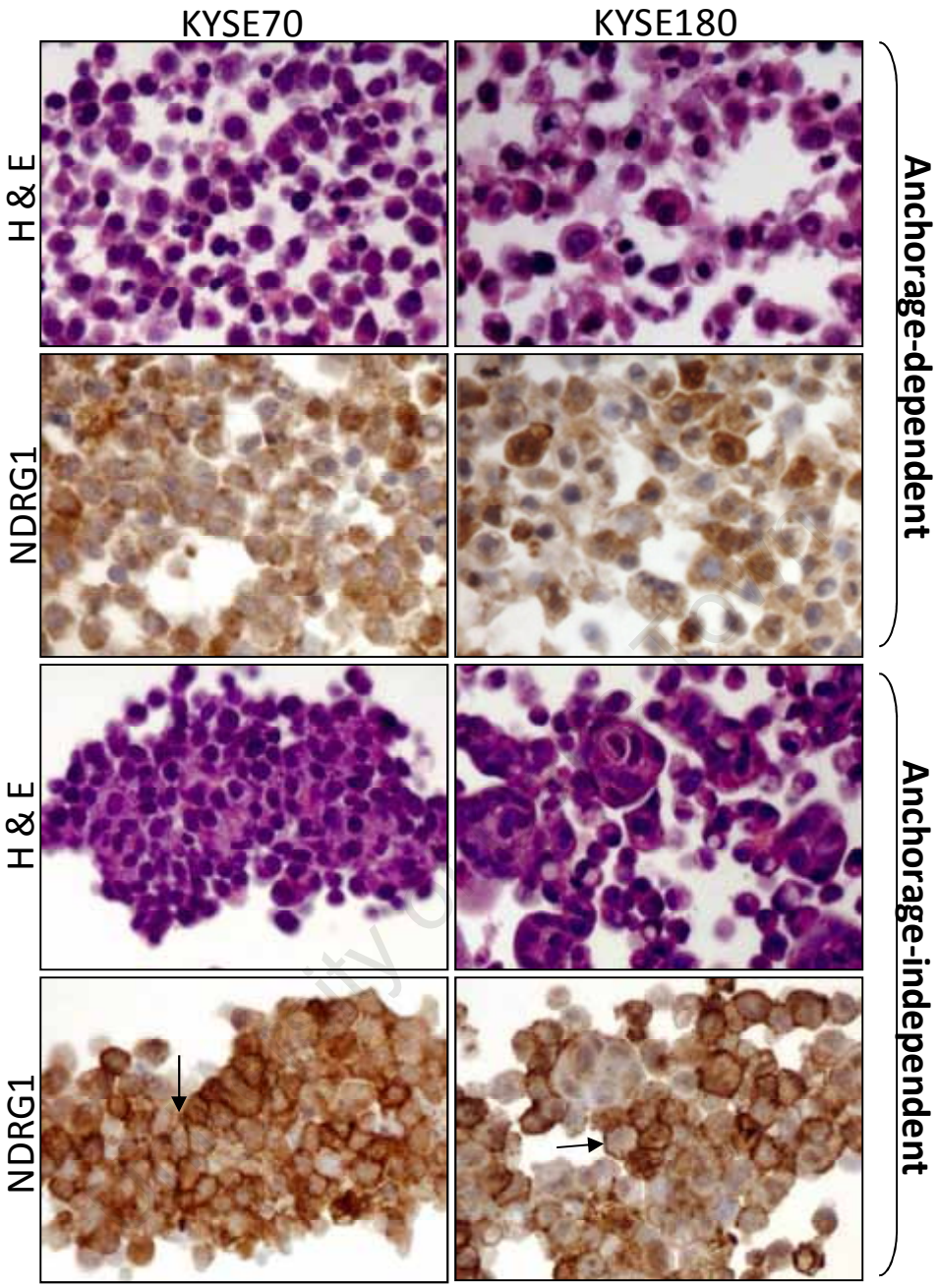

Figure 3.4.2. Immunohistochemistry of NDRG1 in KYSE70 and KYSE180 cells cultured in an anchorage-dependent and -independent manner (magnification 400x). Cell lines, cultured in an anchorage-dependent and -independent manner for 48 hours, were fixed, embedded in paraffin blocks, sectioned and stained for NDRG1. NDRG1 appeared to localise to the periphery of KYSE70 and KYSE180 cells, reminiscent of plasma membrane localisation (arrows), when cultured in an anchorage-independent manner. Representative images of hematoxylin and eosin (H&E) staining are shown.

anchorage-independent manner for 24, 48, 72 and 96 hours. The effect of NDRG1 and control siRNAs on NDRG1 protein expression was evaluated by Western blot. NDRG1 protein levels were significantly reduced in cells treated with NDRG1 targeted siRNA (Fig. 3.5.). Western blot densitometry, using Quantity One software (version 4.6.6.), showed that NDRG1 siRNA knocked down NDRG1 expression by as much as 80 %. A time-course of siRNA treatment showed that NDRG1 siRNA down-regulated NDRG1 protein levels up to five days post-transfection.

Having established that targeted siRNA was indeed effective at inhibiting NDRG1 protein expression, we next evaluated the biological effects of knocking down this protein's expression. Anchorage-independent cell proliferation assays were performed on WHCO1, WHCO6, KYSE70, KYSE180 and KYSE450 cell lines to determine the role of NDRG1 in anchorage-independent cell growth. Cells were transiently transfected with 20 nM of either NDRG1 siRNA or control siRNA and grown on poly-HEMA coated plates in media containing 1.5 % methyl cellulose. Cell proliferation was assayed one, three and seven days after anchorage-independent growth. While KYSE cell lines steadily increased in number over the seven day assay, WHCO cells showed a decline after 3 days of anchorage-independent cell culture. However, results showed that there was no significant change in anchorage-independent proliferation, in all cell lines, despite a 5-fold reduction in NDRG1 (Fig. 3.6. A-E).

A

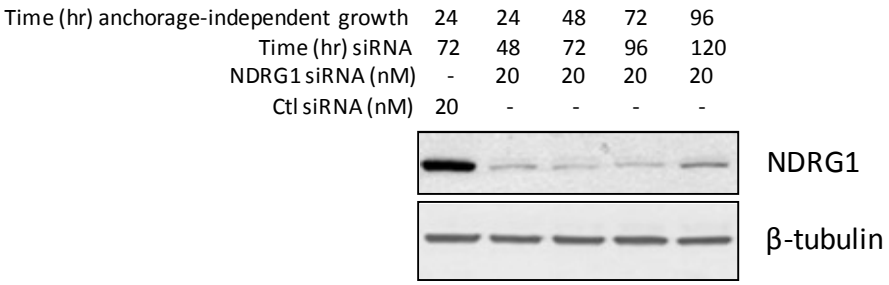

B

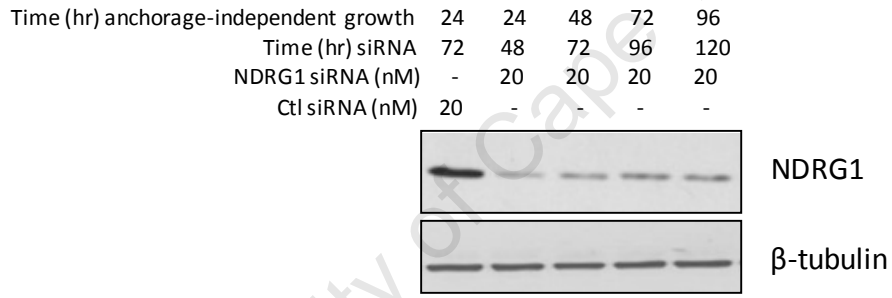

Figure 3.5. Inhibition of NDRG1 protein expression using siRNA. WHCO1 (A) and KYSE450 (B) cells were transfected with 20 nM control or NDRG1 siRNA and then cultured under anchorage-independent conditions. Whole cell lysates were harvested for 4 days following anchorage-independent growth. Western blot analysis on 30 µg of protein revealed that NDRG1 siRNA resulted in specific knockdown of NDRG1 protein expression in cells cultured in an anchorage-independent manner. The control siRNA had no effect on NDRG1 expression. Western blots shown are representative of experiments performed three times.

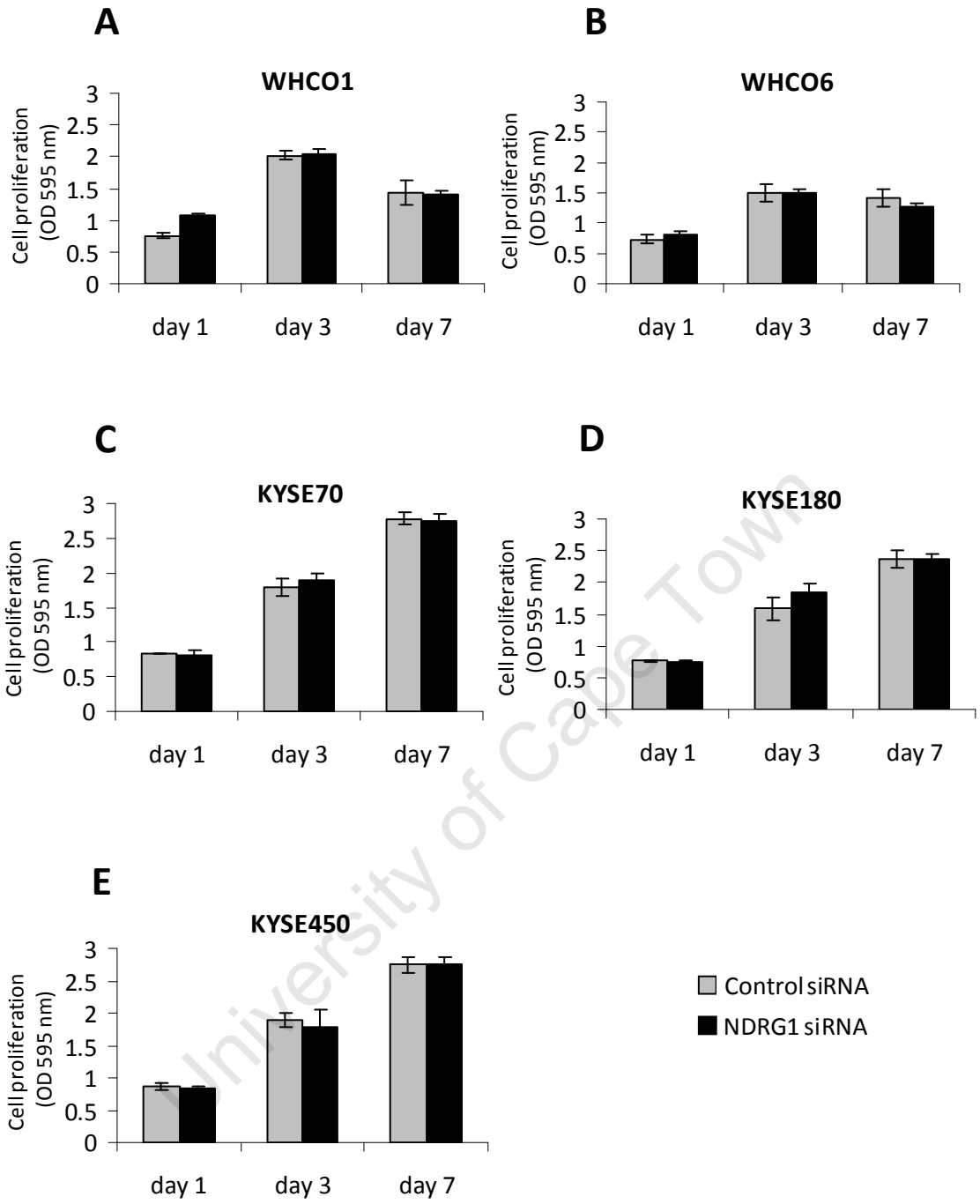

Figure 3.6. Effect of NDRG1 inhibition on anchorage-independent proliferation of OSCC cell lines. WHCO1, WHCO6, KYSE70, KYSE180 and KYSE450 cells (A-E) were transfected with 20 nM NDRG1 or control siRNA and grown under anchorage-independent conditions. Cell proliferation was monitored one, three and seven days after transfection, using MTT. No significant changes in proliferation were observed when NDRG1 expression was knocked down with siRNA. Results shown are the mean ± SD of experiments performed in triplicate and repeated at least two times.

3.2.4. Effect of NDRG1 siRNA knock-down on Caspase-3/7 activity in cancer cells cultured in an anchorage-independent manner

To determine the effect of anchorage-independent growth conditions on apoptosis, Caspase-3/7 activity was measured in WHCO1, WHCO6, KYSE70 and KYSE180 cell lines cultured under anchorage-independent growth conditions for 72 hours. A 4- and 5-fold increase in Caspase-3/7 activity was observed in anchorage-independently cultured WHCO1 and WHCO6 cells, respectively ($p < 0.001$) (Fig. 3.7.A.) In KYSE70 and KYSE180 cells Caspase-3/7 increased by 3- and 2-fold, respectively ($p < 0.001$). To determine whether NDRG1 has an affect on apoptosis in these cells, Caspase-3/7 activity was measured after NDRG1 inhibition with siRNA. Cells were transfected with control or NDRG1 siRNA and cultured in an anchorage-independent manner for 72 hours. No significant change in Caspase-3/7 activity and therefore apoptosis was observed between untransfected, control or NDRG1 siRNA-transfected cells (Fig. 3.7.B.).

Taken together these results show that NDRG1 expression does not affect proliferation or apoptosis, and suggests that it's induction under anchorage-independent growth conditions is either a by-product of this culture condition, or that NDRG1 plays a role in processes not measured in the assays used here.

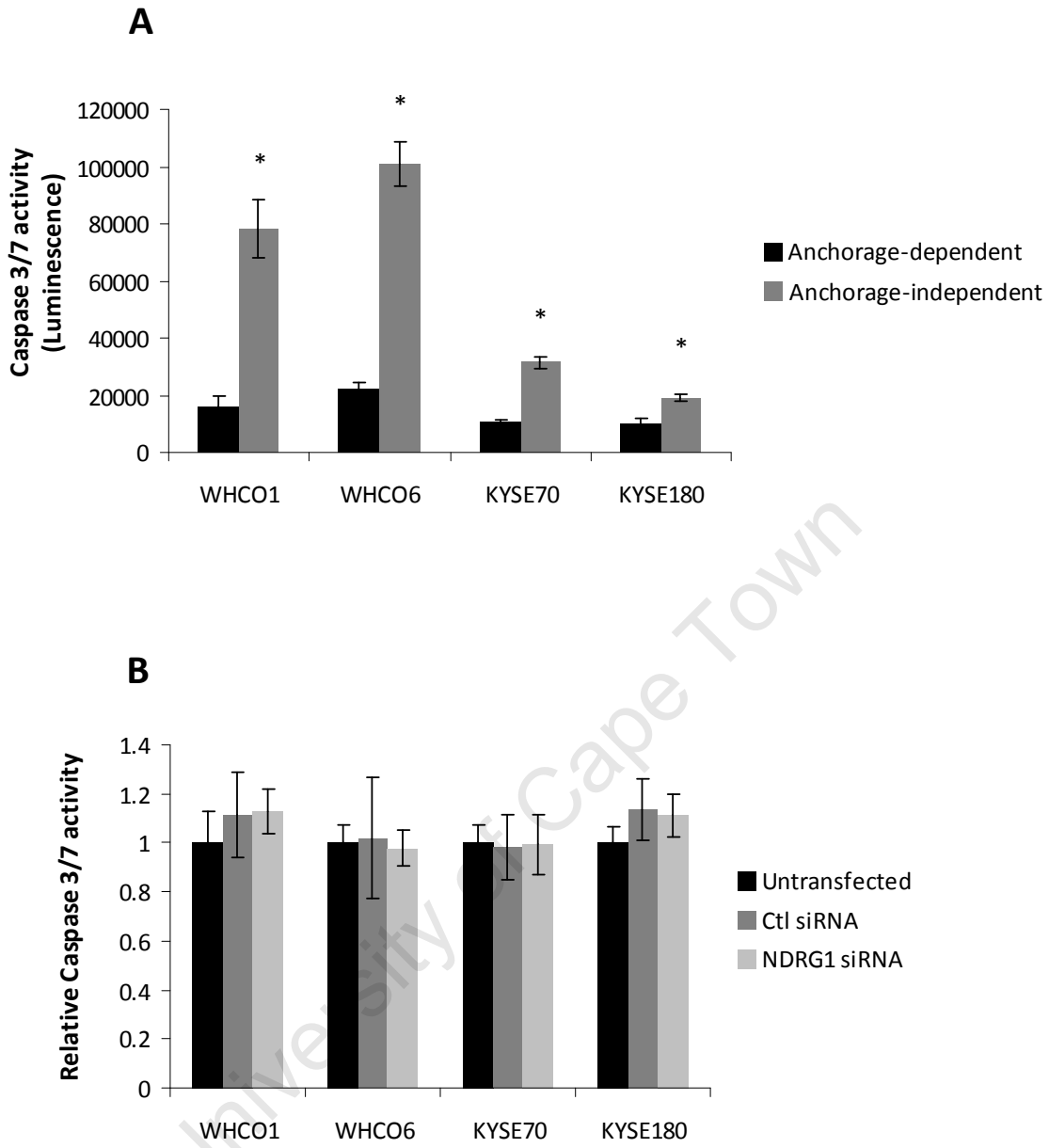

Figure 3.7. NDRG1 does not does not induce or protect cells from apoptosis under in cell lines cultured under anchorage-independent conditions. A. Caspase-3/7 activity, measured after culturing cells under anchorage-dependent or -independent conditions for 72 hours, revealed an increase in apoptosis in cells cultured in an anchorage-independent manner (*$p < 0.001$). B. Caspase-3/7 activity was measured post-transfection with NDRG1 or control siRNA, after 72 hours of anchorage-independent growth. NDRG1 knockdown with siRNA caused no significant increase or decrease in Caspase-3/7 activity. Results shown are the mean ± SD of experiments performed in quadruplicate and repeated at least two times.

3.2.5. Effect of anchorage-independent growth on the expression of invasion and angiogenesis factors

Given the above results, we sought to examine the effect of anchorage-independent cell culture conditions on processes involved in invasion and angiogenesis. Specifically, we examined the expression of MMP-2, MMP-9, Ang-1, PDGF-B, VEGF-C and VEGF-A mRNA every 24 hours for three days in OSCC cell lines cultured in an anchorage-independent manner. A panel of five cell lines was examined to identify common trends in gene expression. Real-time RT-PCR results showed a strong down-regulation of MMP-2 expression and a partial down-regulation of MMP-9 expression with increasing time of anchorage-independent culture in all cell lines (Fig. 3.8.). Similarly, when angiogenesis cytokines Ang-1, PDGF-B and VEGF-C were examined, a downward trend in mRNA expression was observed across all cell lines (albeit to differing extents), with the exception of WHCO6 which showed an increase in PDGF-B levels when cells were cultured under anchorage-independent conditions (Fig. 3.9.1. and 3.9.2.).

In contrast to the above-mentioned results, real-time RT-PCR analysis of VEGF-A mRNA expression in WHCO1, WHCO6, KYSE70, KYSE180 and KYSE450 cells cultured under anchorage-independent conditions showed an induction of VEGF-A expression in all cell lines (Fig. 3.10.), reminiscent of the increase observed in NDRG1 mRNA (section 3.2.1, Figure 3.2). WHCO1 and WHCO6 cells showed a steady increase in mRNA levels over time giving rise to a 9.9-fold and 8.8-fold increase in VEGF-A mRNA levels, respectively. KYSE450 cells showed an 8–fold increase in VEGF-A mRNA levels after

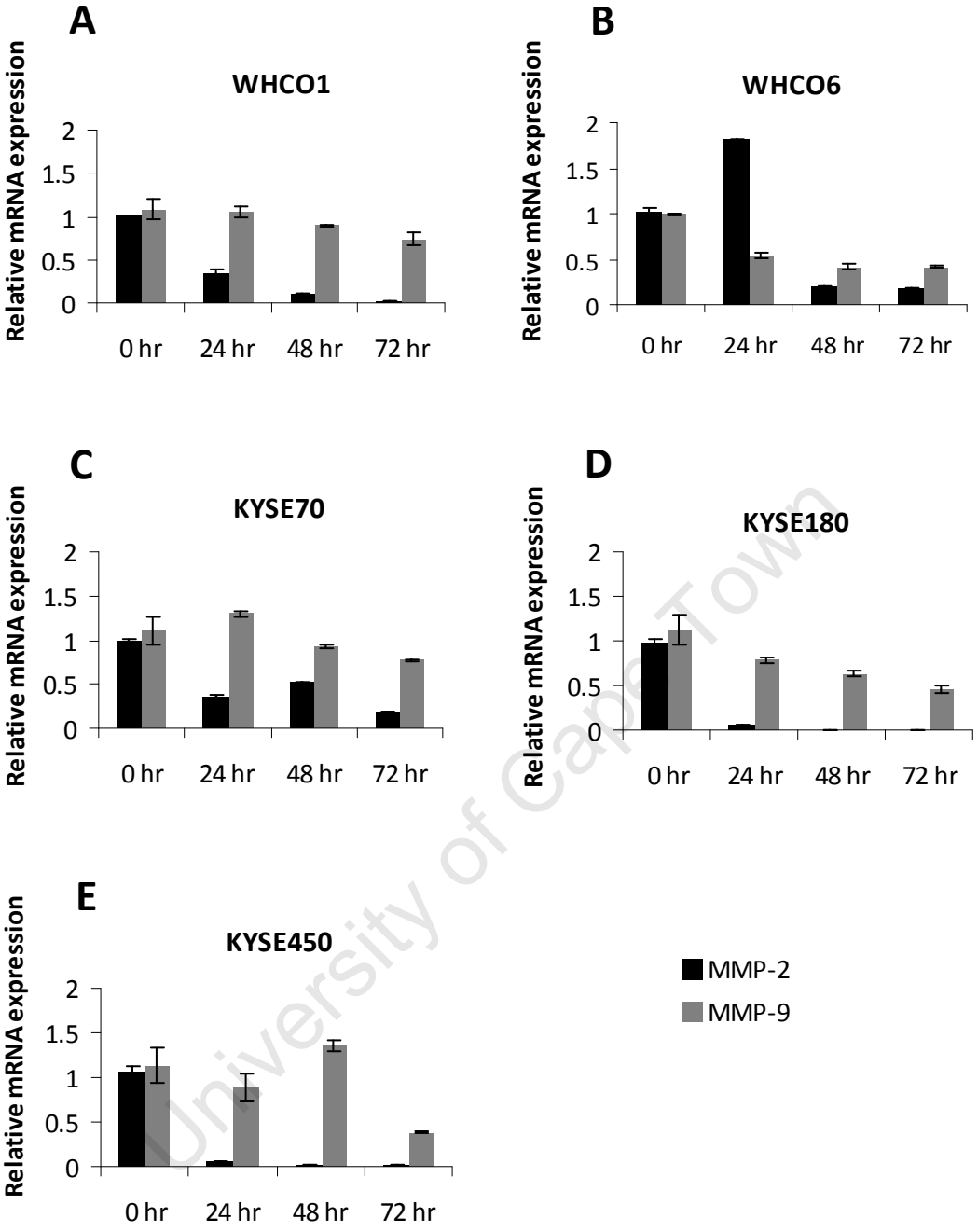

Figure 3.8. Matrix metalloproteinase mRNA expression in OSCC cell lines grown under anchorage-independent conditions. Real-time RT-PCR analysis of MMP-2 and MMP-9 mRNA expression in WHCO1, WHCO6, KYSE70, KYSE180 and KYSE450 cell lines (A-E) cultured anchorage-dependently for 24 hours (0 hr) or anchorage-independently for 24 hr, 48 hr and 72 hr. RNA of a high quality, determined by RNA gel electrophoresis, was used and normalised to GUSB mRNA expression. The specificity of the real-time RT-PCR was assessed by melting curve analysis. Results are expressed relative to anchorage-dependent (0 hr) expression levels. Results shown are the mean ± SD of experiments performed in triplicate and repeated two times.

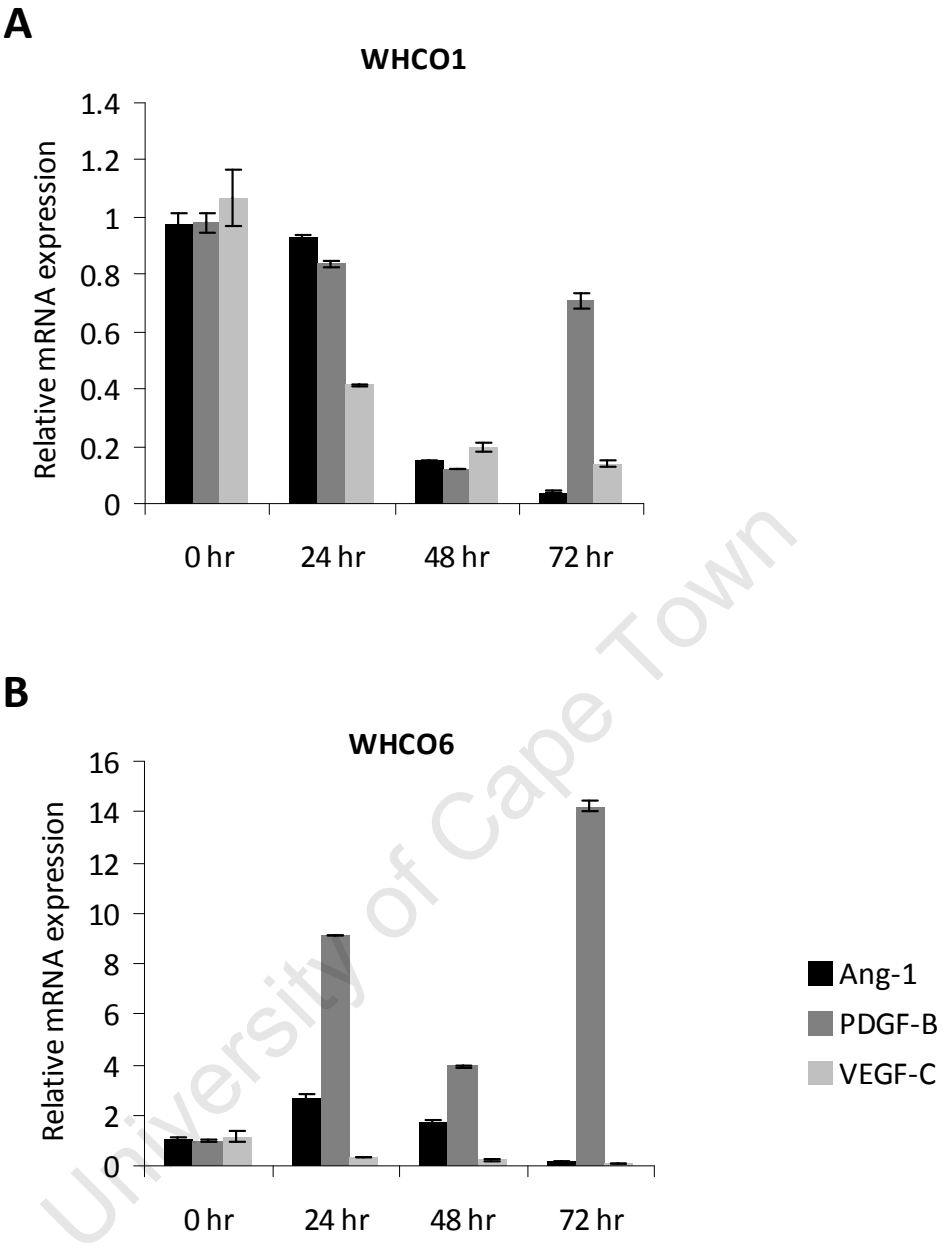

Figure 3.9.1. Messenger RNA expression of angiogenesis factors Ang-1, PDGF-B and VEGF-C in WHCO1(A) and WHCO6(B) cells grown under anchorage-independent conditions. Real-time RT-PCR analysis of Ang-1, PDGF-B and VEGF-C mRNA expression cells cultured under anchorage-dependent conditions for 24 hours (0 hr) or under anchorage-independent conditions for 24 hr, 48 hr and 72 hr, revealed a decrease in gene expression, with the exception of PDGF-B mRNA which increased in WHCO6 cells. RNA was normalised to GUSB mRNA expression. The specificity of the real-time RT-PCR was assessed by melting curve analysis. Gene expression relative to 0 hr are shown as means ± SD of experiments performed in triplicate and repeated two times.

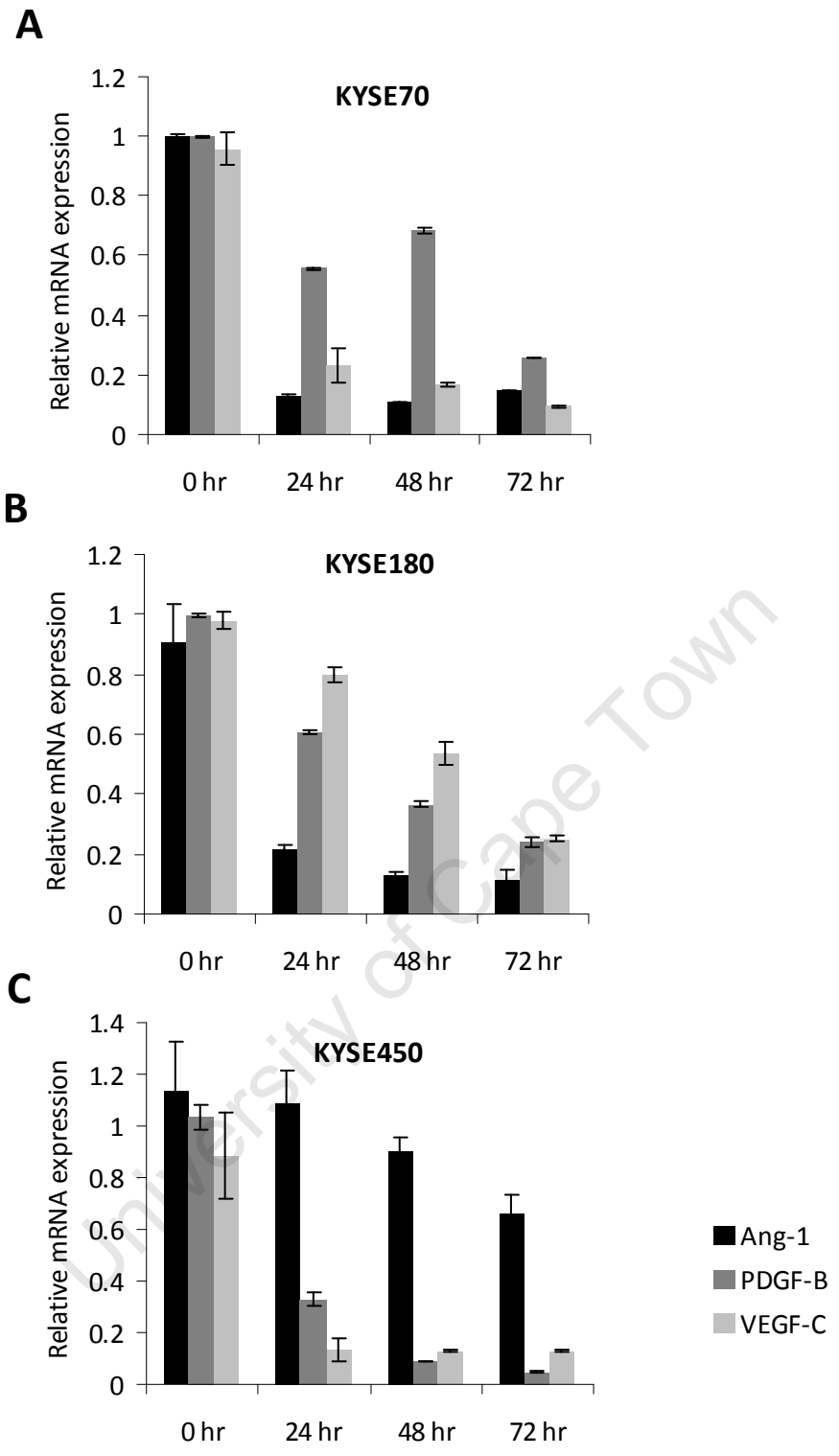

Figure 3.9.2. Messenger RNA expression of angiogenesis factors Ang-1, PDGF-B and VEGF-C in KYSE70(A), KYSE180(B) and KYSE450(C) cells grown under anchorage-independent conditions. Real-time RT-PCR analysis of Ang-1, PDGF-B and VEGF-C mRNA expression cells cultured under anchorage-dependent conditions for 24 hours (0 hr) or anchorage-independent conditions for 24 hr, 48 hr and 72 hr, revealed a decrease in gene expression. Gene expression relative to 0 hr are shown as means ± SD of experiments performed in triplicate and repeated two times.

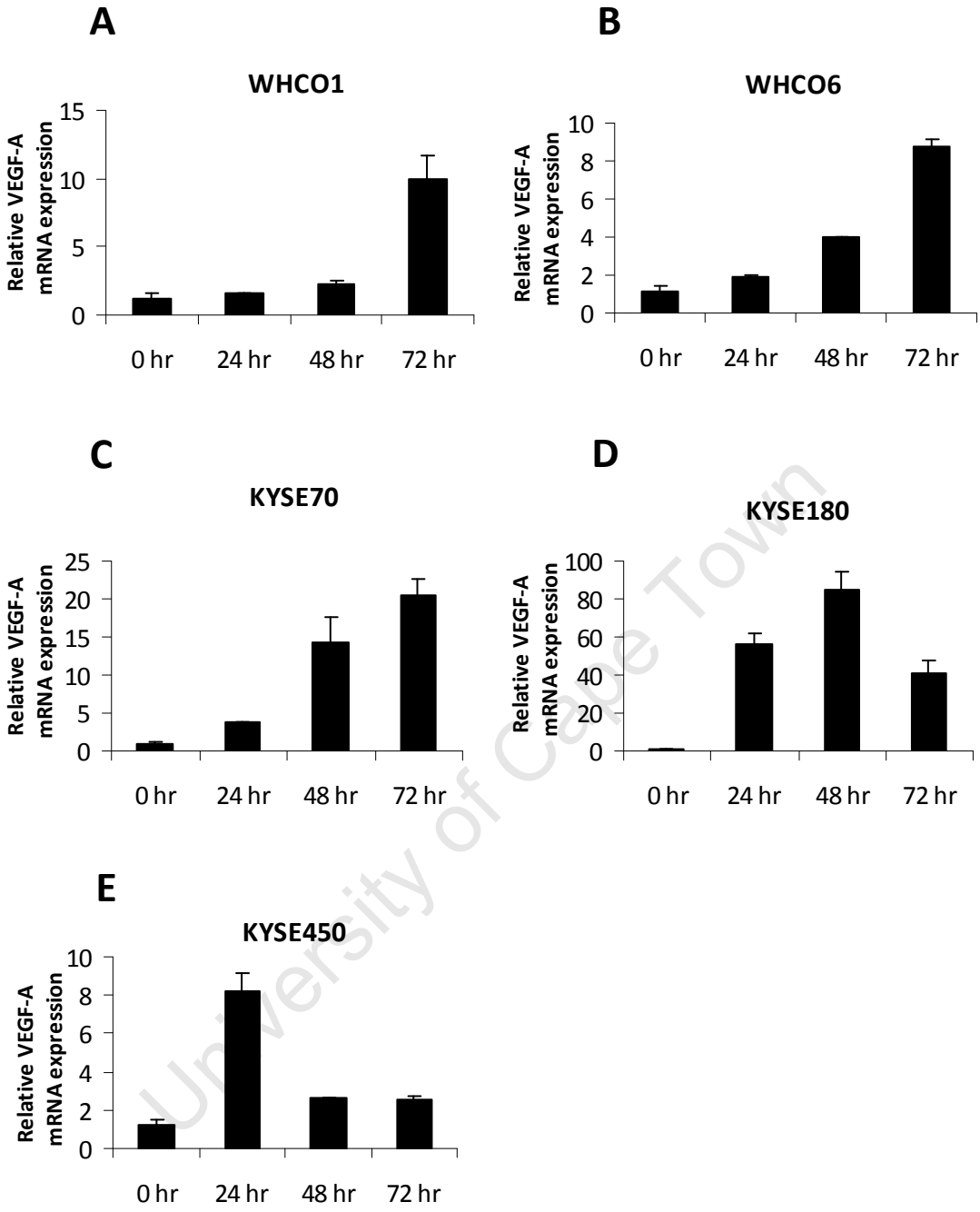

Figure 3.10. Anchorage-independent growth induces VEGF-A mRNA expression in OSCC cell lines. Real-time RT-PCR analysis showing an increase in VEGF-A mRNA expression in WHCO1, WHCO6, KYSE70, KYSE180 and KYSE450 cells (A-E) cultured under anchorage-dependent conditions for 24 hours (0 hr) or anchorage-independent conditions for 24 hr, 48 hr and 72 hr. RNA of a high quality, determined by RNA gel electrophoresis, was used and normalised to GUSB mRNA expression. The specificity of the real-time RT-PCR was assessed by melting curve analysis. Results are expressed relative to anchorage-dependent (0 hr) expression levels. Results shown are the mean ± SD of experiments performed in triplicate and repeated two times.

24 hours of anchorage-independent cell culture, which then decreased to 2.5-fold for the following two days. KYSE70 and KYSE180 cells displayed the largest change in VEGF-A mRNA levels at 20- and 85-fold, respectively.

To determine whether anchorage-independent cell culture induction of VEGF-A mRNA translates to an increase in VEGF-A cytokine release into the media of cultured cells, a VEGF-A ELISA was performed. Again, cells were cultured under anchorage-dependent conditions for 24 hours or anchorage-independent conditions and VEGF-A levels monitored every 24 hours for three days. ELISA results confirmed that VEGF-A protein, secreted into the media of cells cultured under anchorage-independent conditions, increased with time of cell culture. Of the cells cultured under anchorage-dependent conditions for 24 hours, media from WHCO1 cells contained the highest concentration of VEGF-A at 737 pg/10^6 cells while media of KYSE70 cells contained the lowest VEGF-A at 131 pg/10^6 cells (Fig. 3.11.). After 72 hours of anchorage-independent growth VEGF-A cytokine concentration in the media of anchorage-independently cultured cells ranged from 1036 pg/10^6 cells to 1321 pg/10^6 cells.

3.2.6. Anchorage-independent cell culture induction of VEGF-A expression is NDRG1 dependent

Whilst evidence in the literature suggests that NDRG1 acts as an anti-angiogenic

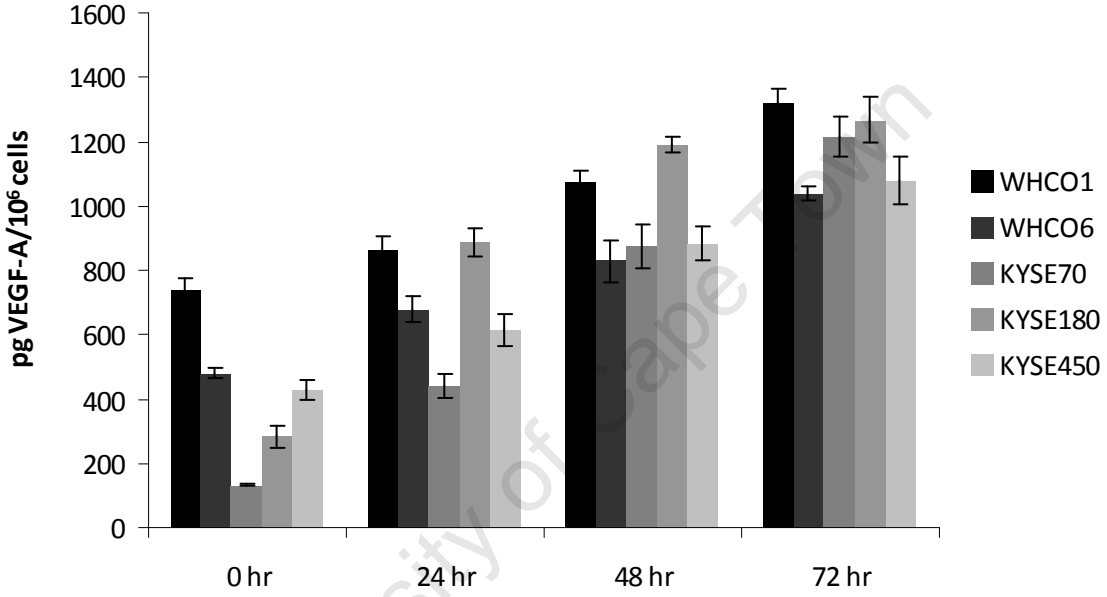

Figure 3.11. Anchorage-independent growth increases VEGF-A protein levels in the media of OSCC cell lines. VEGF-A ELISA was performed to detect levels of VEGF-A secreted into the media of OSCC cell lines cultured under anchorage-dependent conditions for 24 hours (0 hr) or anchorage-independent conditions for 24 hr, 48 hr and 72 hr. The quantity of VEGF-A was normalised to the number of cells at the time of conditioned medium harvest and reported as picograms (pg) per 10^6 cells. Results shown are the mean ± SD of experiments performed in triplicate and repeated at least two times.

factor[137-139] others have proposed that NDRG1 expression correlates positively with VEGF-A expression and tumour vasculature[97]. In our anchorage-independent cell culture system there appears to be a positive correlation between NDRG1 and VEGF-A mRNA and protein expression. We therefore explored the relationship between NDRG1 and VEGF-A expression in our anchorage-independent cell culture system, using siRNA.

To determine whether NDRG1 expression was indeed necessary for VEGF-A expression, cell lines were transiently transfected with NDRG1 siRNA and then cultured under anchorage independent conditions for 72 hours. Real-time RT-PCR, Western blot analysis and VEGF-A ELISA were all performed on the same pool of transfectants to determine the efficiency of NDRG1 knock-down and observe any effects on VEGF-A expression. Real-time RT-PCR analysis showed that NDRG1 mRNA expression was effectively inhibited by NDRG1 siRNA OSCC cell lines cultured in an anchorage-independent manner (Fig. 3.12.A.). NDRG1 knock-down was significant in all cell lines ($p < 0.01$), most efficient in WHCO1, KYSE180 and KYSE450 cells and least efficient in KYSE70 cells with only a 2-fold decrease in NDRG1 mRNA levels. Western blot analysis revealed similar results, where NDRG1 siRNA effectively inhibited NDRG1 protein expression in all OSCC cell lines cultured in an anchorage-independent manner (Fig. 3.12.B.).

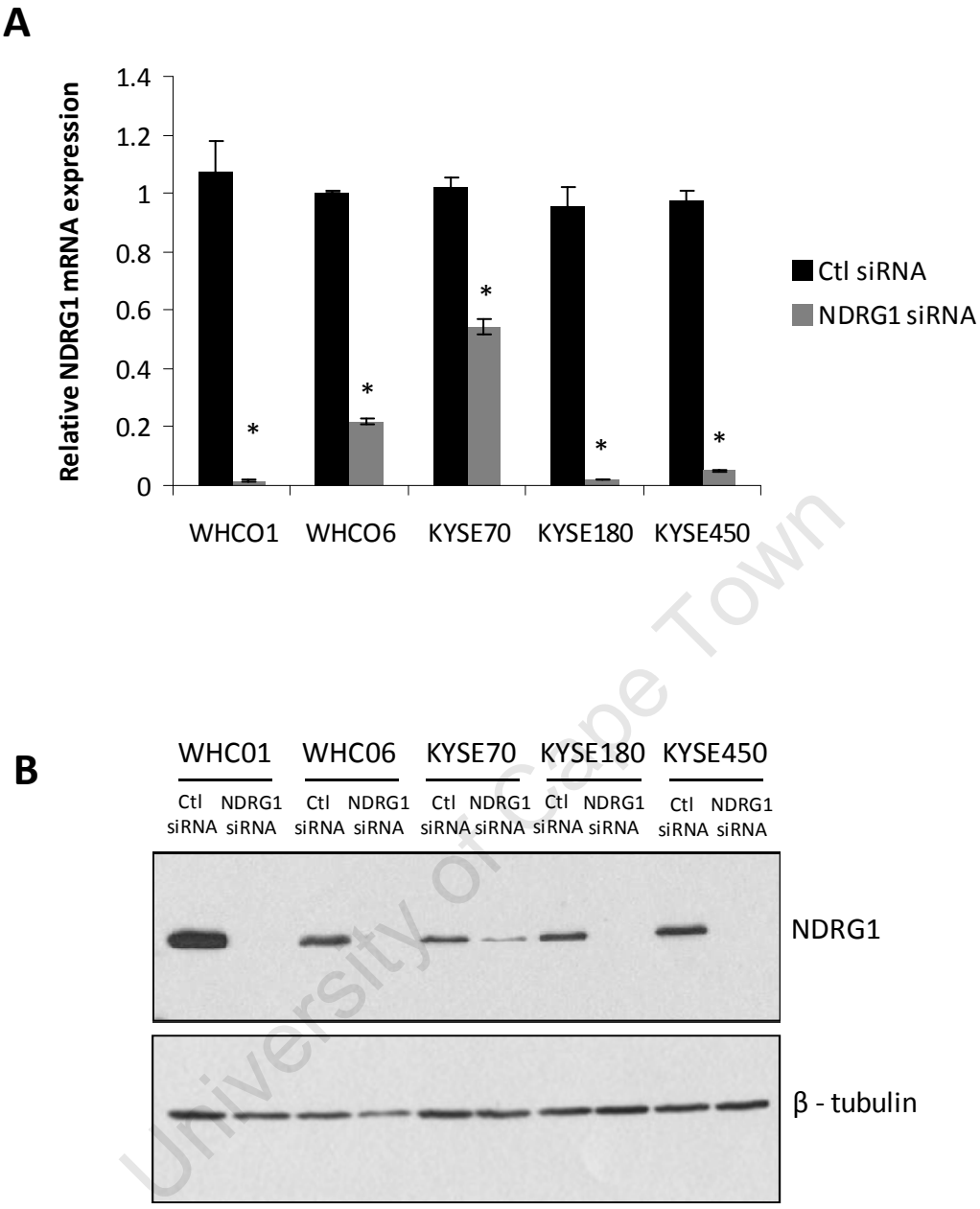

Figure 3.12. NDRG1 siRNA inhibits NDRG1 mRNA and protein expression in OSCC cell lines cultured under anchorage-independent conditions. WHCO1, WHCO6, KYSE70, KYSE180 and KYSE450 cell lines were transfected with 20 nM of control or NDRG1 siRNA and cultured in an anchorage-independent manner for 72 hours. A. Real-time RT-PCR performed on RNA. Results are normalised to GUSB expression and expressed relative to control siRNA transfected cells (*$p < 0.01$). B. Western Blot analysis on 20 µg of whole cell lysate. β-tubulin was used as a loading control. Results showed that NDRG1 siRNA effectively knocked down NDRG1 mRNA and protein expression in cell lines cultured under anchorage-independent conditions for 72 hours.

Given that NDRG1 expression was effectively downregulated with transient, target specific NDRG1 siRNA, we next examined its effect on VEGF-A expression. Real-time RT-PCR analysis showed that in all NDRG1 siRNA transfected cells, VEGF-A mRNA expression was significantly reduced ($p < 0.05$) (Fig. 3.13.A.). In fact, the extent of VEGF-A mRNA reduction was consistent with the level of NDRG1 mRNA knockdown observed in the various cell lines. Where NDRG1 inhibition was least effective (i.e. in KYSE70 cells), VEGF-A levels were the least effected (0.7-fold decrease). The most effective downregulation of VEGF-A expression was observed in WHCO1 cells at 25-fold (Fig 3.13.A.). VEGF-A ELISA performed on the media from NDRG1 siRNA transfected cells also showed a significant downregulation in VEGF-A protein levels secreted into the media ($p < 0.01$) (Fig. 3.13.B.).

3.2.7. NDRG1 affects VEGF-A expression through the modulation of its promoter activity

Through the transient downregulation of NDRG1 expression with siRNA we have shown that NDRG1 effects VEGF-A expression in OSCC cell lines cultured in an anchorage-independent manner. Potential mechanisms by which modulation of VEGF-A expression can occur include altering its promoter activity, or through stabilisation of its mRNA transcript. We addressed the former possibility by first performing a VEGF-A reporter assay, whereby the VEGF-A promoter region (-2018 to +50) fused to the luciferase reporter gene in the plasmid pVEGF-Luc (Fig. 3.14.i) was transfected into OSCC cell lines, and luciferase activity assayed after 48 hours of anchorage -

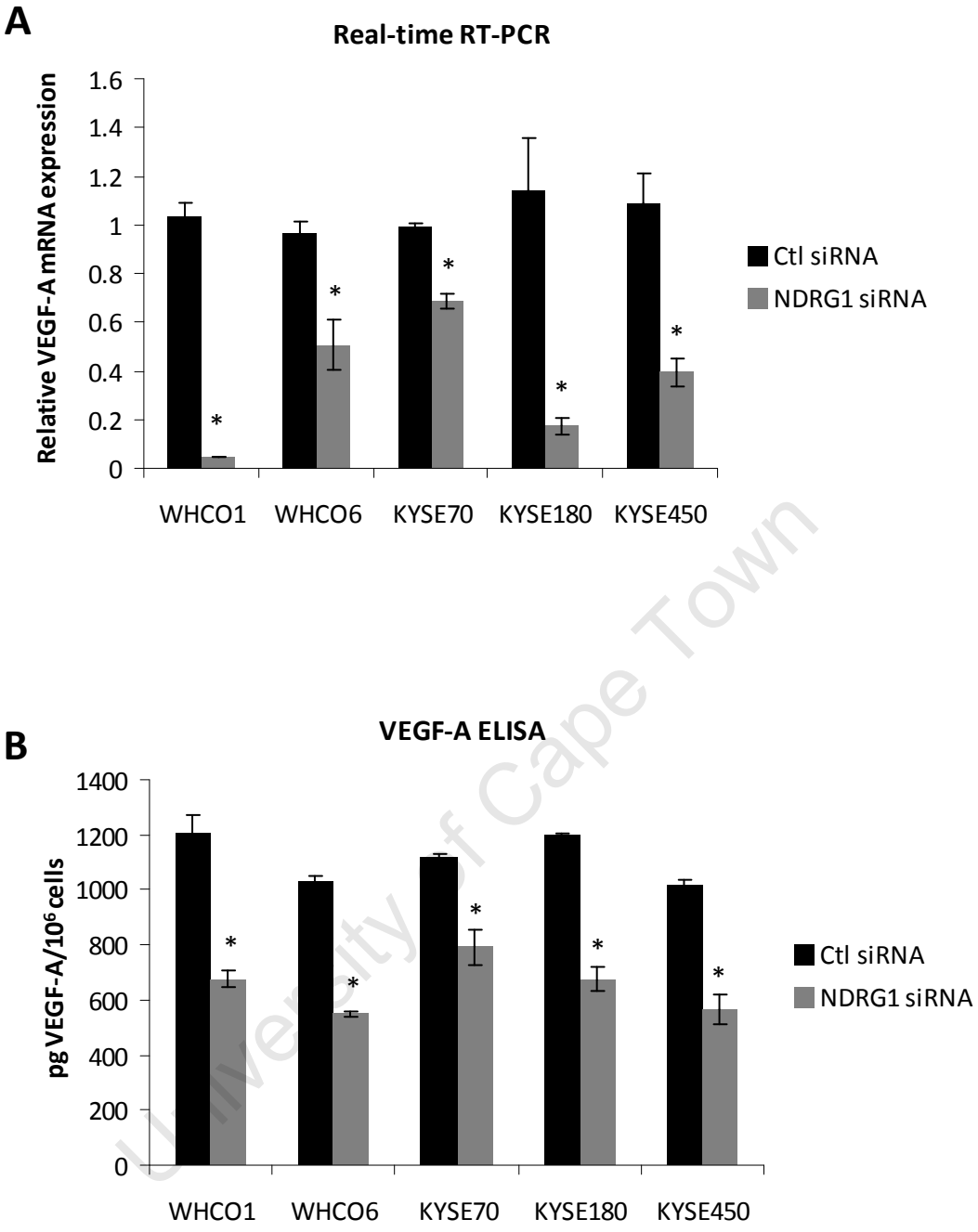

Figure 3.13. NDRG1 siRNA inhibits VEGF-A mRNA expression and VEGF-A cytokine production of OSCC cell lines cultured under anchorage-independent conditions. A. WHCO1, WHCO6, KYSE70, KYSE180 and KYSE450 cell lines were transfected with 20 nM of control or NDRG1 siRNA and cultured in an anchorage-independent manner for 72 hours. Real-time RT-PCR analysis, relative to control siRNA transfected cells, showed that NDRG1 siRNA effectively knocked down VEGF-A mRNA in cell lines cultured under anchorage-independent conditions for 72 hours (*$p < 0.05$). B. VEGF-A ELISA showed that NDRG1 siRNA was effective at knocking down VEGF-A cytokine release into the media of cells cultured in an anchorage-independent manner (*$p < 0.01$).

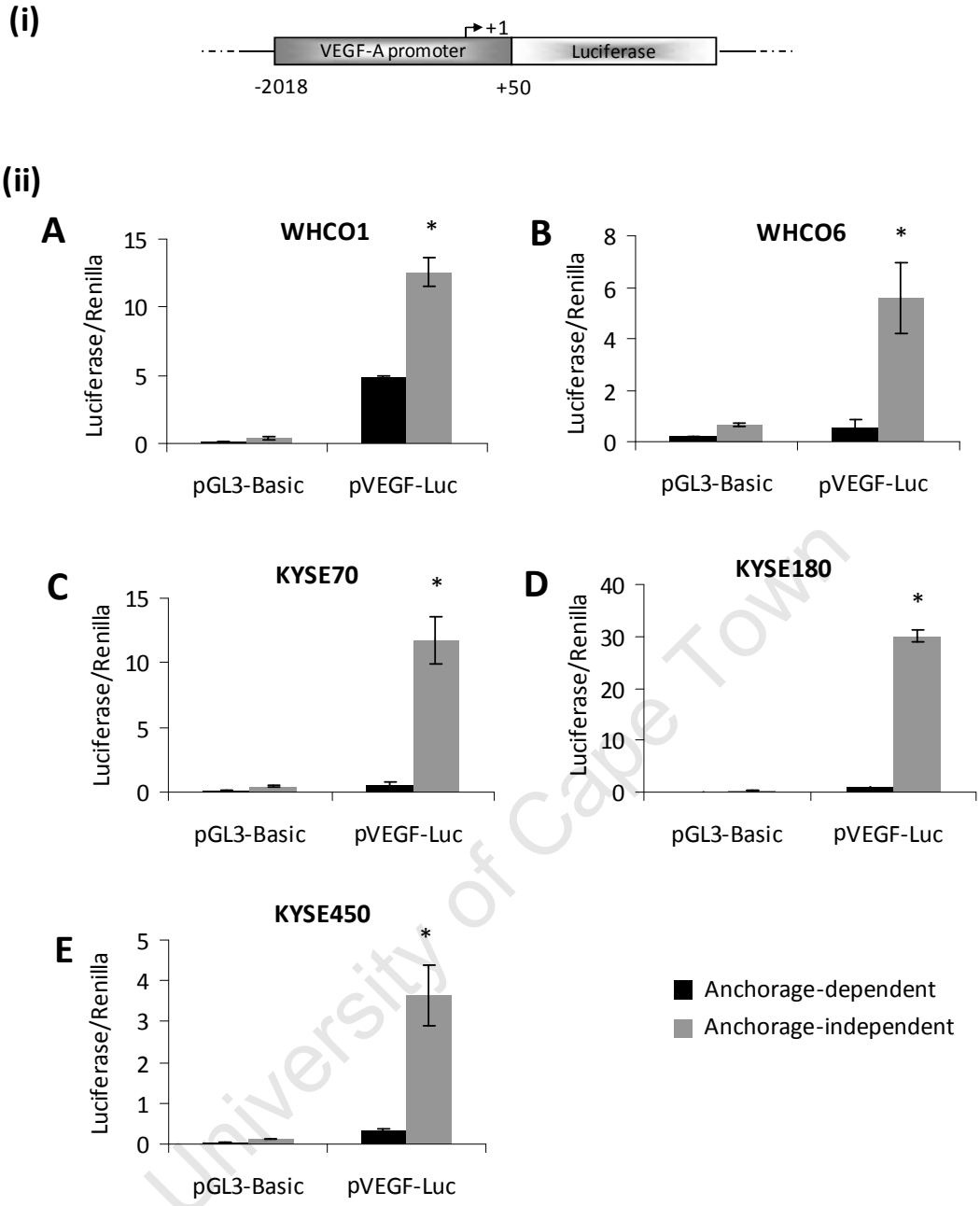

Figure 3.14. Activity of human VEGF-A (-2018 to +50) promoter in OSCC cell lines cultured under anchorage-dependent or -independent conditions. (i). Schematic representation of the VEGF-A promoter (-2018 to +50) reporter construct, pVEGF-Luc. (ii). pVEGF-Luc and pGL3-Basic plasmids were transiently transfected into WHCO1(A), WHCO6(B), KYSE70(C), KYSE180(D) and KYSE450(E) cell lines. Cell were then cultured under anchorage-dependent or -independent conditions for 48 hours. Significant induction of VEGF-A promoter activity was observed in cell lines cultured in an anchorage-independent manner (*$p < 0.05$). The pGL3-Basic vector control showed no significant activity in cells cultured in an anchorage-independent manner. pRL-TK was used as an internal control for transfection efficiency and luciferase activity was normalised to *Renilla* luciferase.

independent growth. The results showed that VEGF-A transcriptional activity was significantly increased in cells cultured for 48 hours under anchorage-independent growth conditions ($p < 0.05$) (Fig. 3.14.ii.), where the lowest fold change was observed in WHCO1 cells (3-fold) and the highest in KYSE180 cells (30-fold). Moreover, it was observed that WHCO1 showed the highest VEGF-A promoter activity under anchorage-independent conditions which is in agreement with the ELISA performed on the media of adherent cells (Fig. 3.11.).

To establish whether the increase in VEGF-A promoter activity was NDRG1-dependent, pVEGF-Luc was transfected into control or NDRG1 knock-down cells, and luciferase activity measured after 48 hours of anchorage-independent growth. The results showed that VEGF-A promoter activity was significantly decreased in cells treated with NDRG1 siRNA compared to control cells ($p < 0.05$) (Fig.3.15.). This downregulation in VEGF-A promoter activity was observed in WHCO1, WHCO6, KYSE70, KYSE180 and KYSE450 cell lines.

3.2.8. VEGF-A produced by anchorage-independent growth of OSCC cell lines is functionally active

Since we had shown that anchorage-independent growth induced VEGF-A promoter activity and expression in an NDRG1-dependent manner, we next examined whether the VEGF-A released into the media of cultured OSCC cell lines was functionally active.

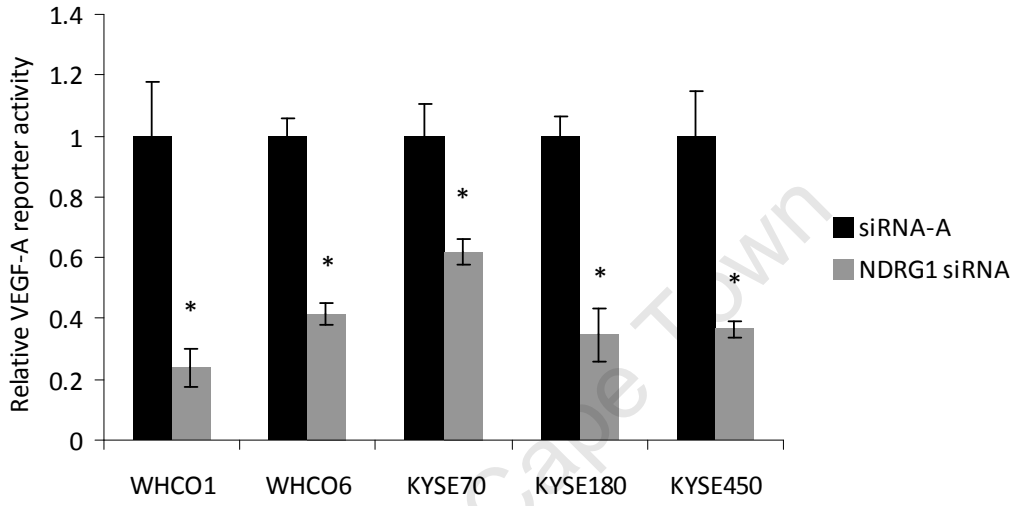

Figure 3.15. NDRG1 siRNA inhibits VEGF-A promoter activity in cells cultured under anchorage-independent conditions. Cell lines were transfected with 20 nM of control or NDRG1 siRNA, the VEGF-A reporter, pVEGF-Luc and pRL-TK. After 48 hours of anchorage-independent cell culture, luciferase levels were assayed and normalised using Renilla. NDRG1 siRNA significantly suppresses VEGF-A promoter activity in cells cultured in an anchorage-independent manner (* $p < 0.05$). Results are expressed relative to control siRNA transfected cells and represent the mean ± SD of experiment performed twice in triplicate.

Since VEGF-A acts as a chemotactic agent to endothelial cells, we explored the potential of conditioned media from OSCC cell lines to induce transwell filter migration of human umbilical vein endothelial cells (HUVECs). After 72 hours of anchorage-independent cell culture, WHCO1 and KYSE180 cells were removed from their growth media by centrifugation and the conditioned medium used in a transwell migration assay. Conditioned media from WHCO1 and KYSE180 cells was able to induce chemotaxis of HUVECs compared to the unconditioned media control (Fig. 3.16.). The extent of HUVEC migration was reduced by the inclusion of a VEGF-A neutralising antibody showing that HUVEC migration is VEGF-A-dependent.

Taken together these results show that anchorage-independent cell culture of OSCC cell lines induces VEGF-A expression in an NDRG1-dependent manner, and this VEGF-A is capable of inducing endothelial cell migration.

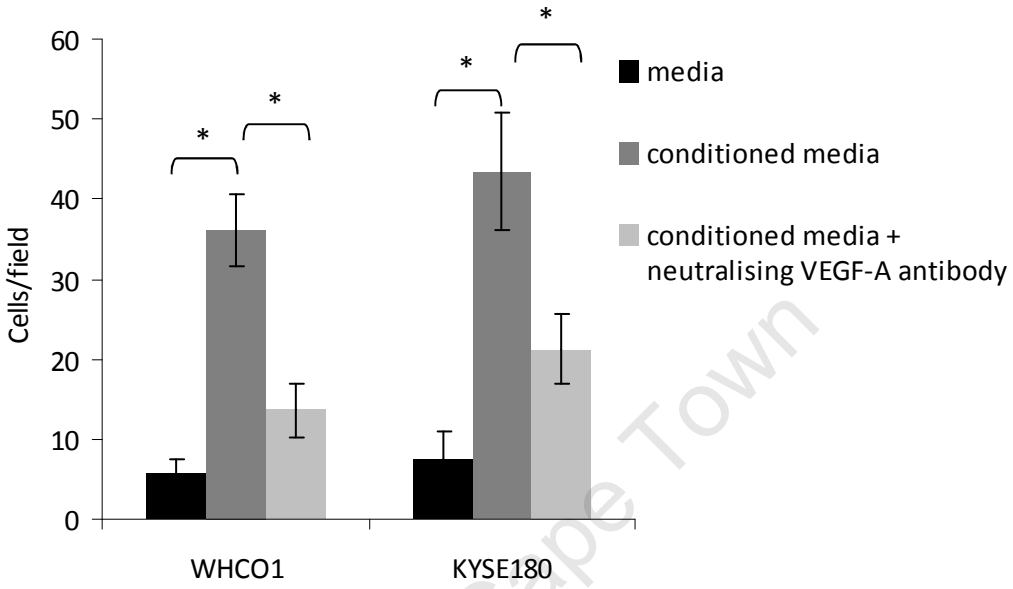

Figure 3.16. Endothelial cell migration is induced by VEGF-A secreted into the media of OSCC cell lines. Starved HUVECs were seeded into the upper chambers of a 8-µm filter transwell plates and allowed to migrate for 8 hours in response to cell culture media alone, conditioned media from WHCO1 or KYSE180 cells cultured for 72 hours under anchorage-independent conditions, or conditioned media containing 5 µg/ml neutralising VEGF-A antibody. Cells remaining in the upper chamber were removed and the migrated cells were visualised by staining with crystal violet. Results showed that HUVEC migration was VEGF-A-dependent (*$p < 0.001$). Values are mean ± SD for each condition in duplicate wells, counted in quadruplicate fields.

3.3. DISCUSSION

The raised expression of NDRG1 in the tumours of our cohort of South African OSCC patients suggests that NDRG1 plays a role in tumour biology and maintenance. We report here that anchorage-independent culture conditions induce a strong and sustained upregulation in NDRG1 expression. However, our analysis showed that this overexpression had no effect on many of the cellular processes that we measured. Specifically, NDRG1 inhibition with siRNA had no effect on anchorage-independent cell proliferation or apoptosis. Similar studies report that exogenous overexpression of NDRG1 in NIH3T3 mouse fibroblasts, as well as prostate cancer cell lines, induced no changes in the cells' ability to form colonies in soft agarose, but, in the latter, was able to suppress spontaneous lung metastasis *in vivo*[94;176]. Notably, neither of these studies reports the expression levels of NDRG1 in cells grown in an anchorage-independent manner. One could speculate that if endogenous NDRG1 is induced in these culture conditions, exogenous overexpression may be redundant due to saturation. However, in contrast, Kurdistani *et al*. [54] showed that exogenous overexpression of NDRG1 in the breast cancer cell line MCF-7, and EJ bladder carcinoma cells, compromised the cell lines' ability to form colonies in soft agarose. Indeed, this once again raises the possibility, mentioned in Chapter 1, that NDRG1 may have a tissue or cell type-specific function. To this end, when we examined the localisation of NDRG1 in OSCC cells cultured in an anchorage-independent manner, we observed differential localisation of NDRG1, despite examining cell lines derived from the same tissue type. Examination of NDRG1 localisation in anchorage-dependently cultured cells revealed that NDRG1 is largely located in the cytoplasm. However,

NDRG1, in WHCO1 and WHCO6 cells cultured under anchorage-independent conditions, was strongly upregulated and localised to the cytoplasm and possibly nucleus. This is in contrast to that observed in KYSE70 and KYSE180 cells, where anchorage-independent cell culture induced the expression of NDRG1 at periphery of cells, reminiscent of plasma membrane localisation. To our knowledge, this is the first description of NDRG1 expression and localisation in cells cultured in an anchorage-independent manner. This finding corroborates, to an extent, that reported by Sibold *et al.*[101] where *in vivo* cell growth (in mouse xenografts) was able to induce NDRG1 localisation to the plasma membrane. Indeed, taken together these results suggest that the approach to exploring NDRG1 function *in vitro* cannot be simplistic and should take into consideration the fact that *in vitro* cell culture does not effectively mimic *in vivo* tissue systems.

Interestingly, although we show that NDRG1 upregulation, in cells cultured in an anchorage-independent manner, does not contribute to cell proliferation or apoptosis, we do show a correlative relationship between NDRG1 and VEGF-A expression. In fact, anchorage-independent cell culture conditions lead to an upregulation in VEGF-A promoter activity, mRNA expression and secretion into the media of cells, in an NDRG1-dependent manner. Whilst the expression of VEGF-A has not been examined in our cohort of OSCC patients, it is reportedly overexpressed in 31 % - 93 %[177-180] of patients with squamous cell carcinoma of the oesophagus. This pro-angiogenic molecule promotes stromal degradation, through the activation of proteolytic

enzymes[181], enhances vascular permeability[182], and stimulates proliferation and migration of endothelial cells, giving rise to vessel sprouting[183]. Indeed, evidence in the literature suggests that VEGF-A expression is induced in tumours in response to low oxygen tension, and this induction is mediated by the activation of HIF-1α (amongst others)[184]. High HIF-1α expression reportedly correlates with stage, depth of invasion, lymph node metastasis, distant metastasis and poor survival in oesophageal cancer sufferers[185]. VEGF-A therefore contributes to the aggressive characteristics of oesophageal cancer, through tumour angiogenesis and, in all likelihood, facilitates the spread of the tumour through the body. A positive correlation between NDRG1, VEGF-A and tumour microvascular density (MVD) in cervical adenocarcinoma specimens was recently reported[97]. However, in contrast, Maruyama *et al.*[93] reported an inverse relationship between MVD and NDRG1 expression in specimens of pancreatic ductal adenocarcinoma. This finding was supported by *in vitro* experimental evidence where exogenous overexpression of NDRG1 in cultured PANC cells led to a downregulation in VEGF-A expression[93]. The mechanism through which NDRG1 imparted its effect on VEGF-A in was reportedly through NF-κB signalling attenuation[137] (see Chapter 1, section 1.7.6). Conversely, we report here that NDRG1 induces VEGF-A expression in OSCC cell lines cultured under anchorage-independent conditions. Since *in vitro* cell proliferation does not depend on vessel growth, it is understandable that no phenotypic effects of NDRG1 knock-down were observed in our anchorage-independent cell culture system. Nevertheless, we did show that VEGF-A secreted into the media of OSCC cell lines cultured in an anchorage-independent manner was biologically active and capable of

inducing endothelial cell migration. Interestingly, despite the variable staining pattern, reflecting NDRG1 localisation, in cell lines cultured under anchorage-independent conditions, NDRG1 knockdown imparted the same effect on VEGF-A expression. The link between NDRG1 and VEGF-A upregulation in our system has, however, not been explored. One might hypothesise that NDRG1 imparts its upregulatory effect on VEGF-A through the inverse mechanism reported by Hosoi *et al*.[137], namely through the induction of NF-κB signalling. Our group has recently reported that expression of p65 (one of the subunits of the NF-κB complex) is elevated in 78 % of tumour tissue derived from patients with OSCC, compared to normal oesophageal epithelium[186]. This may provide the link between NDRG1 and VEGF-A expression and will be explored further in our laboratory. In addition, while the increase in VEGF-A levels was explained in part by the increase in VEGF-A promoter activity, the possibility that VEGF-A mRNA levels were stabilised, under conditions of anchorage-independent cell culture, was not examined. Indeed, VEGF-A mRNA levels have been reported to be stabilised in response to hypoxia[187;188] – a stress pathway that may be induced by anchorage-independent cell culture. Interestingly, Bcl-2 overexpression in human melanoma cells was shown to induce angiogenesis through both HIF-1-mediated stimulation of VEGF-A transcriptional activity and the stabilisation of VEGF-A mRNA[187]. Thus, the potential role of NDRG1 in stabilising VEGF-A mRNA should be examined.

The results presented in this chapter support an oncogenic role for NDRG1 in oesophageal cancer. If indeed the relationship between NDRG1 and VEGF-A observed *in vitro* can be supported by *in vivo* studies, NDRG1 too will be classified under one of the hallmarks of cancer.

CHAPTER 4

INVESTIGATION OF THE TRANSCRIPTIONAL REGULATORY MECHANISMS THAT REGULATE NDRG1 EXPRESSION

4.1. INTRODUCTION

In the previous chapters we described the altered expression of NDRG1 in OSCC tumour tissue relative to that of normal oesophageal tissue and suggested that it associates with differentiation and cancer. Furthermore, we also demonstrated that NDRG1 expression may play an important role in promoting angiogenesis through the induction of VEGF-A expression. We were particularly interested in the transcriptional regulatory mechanisms that account for altered NDRG1 expression in OSCC cells. Indeed, although we examined a small cohort of patients, the identification of increased NDRG1 mRNA in cancer cells compared to normal cells (Chapter 2) suggests that its altered expression arises through deregulated transcription.

Transcription is a highly synchronised process whereby transcription (or trans-acting) factors initiate and facilitate the production of RNA from DNA. This occurs through the highly specific and co-ordinated binding of transcriptional activator, or repressor, proteins to *cis* recognition elements within the promoter of genes, in response to cellular signalling and/or an environmental stimulus. In cancer however, misdirected

cellular signalling and transcription factor activation gives rise to aberrant gene expression which, in many cases, contributes to the progression of the disease.

We suggest that the induction of NDRG1 expression observed in OSCC patients is the culmination of deregulated gene expression and altered transcriptional regulation of the NDRG1 promoter. While some studies have examined the regulation of the NDRG1 promoter (see Chapter 1, section 1.7.7) there have been no studies reporting its transcriptional control in oesophageal cancer. Since our non-adherent cell culture system is technically cumbersome, we opted to use TPA, a phorbol ester, as a stimulus to study the transcription factors that activate NDRG1 expression. Phorbol esters, well described inducers of differentiation, are able to induce NDRG1 expression in keratinocytes[114], monocytic U937 cells[113;115] and trophoblasts[116]. TPA functions as a diacyglycerol analogue, diffusing into cells, activating protein kinase C (PKC) and downstream mitogen activated protein kinase (MAPK) pathways, culminating in the transcription of many genes.

The objective of this study was therefore, using TPA as a stimulus, to analyse the NDRG1 promoter, and to identify activating transcription factors that affect the expression of NDRG1 in oesophageal epithelial cells. These results may provide clues about those genes that regulate the altered expression of NDRG1 in oesophageal cancer, and that may contribute to the tumourigenic state in this pernicious disease.

4.2. RESULTS

4.2.1. TPA induces NDRG1 expression in a subset of OSCC cell lines

Firstly, in order to establish that NDRG1 expression is induced in OSCC cell lines by TPA treatment, preliminary Western blot analysis was performed. OSCC cell lines were seeded subconfluently, and the next day, cells were either left untreated or treated for 16 hours with 20 nM TPA. Western blot analysis on whole cell lysates revealed NDRG1 protein is induced by TPA in WHCO1, WHCO6, KYSE70, KYSE180 and KYSE450 cell lines (Fig. 4.1). WHCO5 and KYSE520 cell lines showed no NDRG1 response to TPA in two independently performed experiments. The exposure time of the x-ray film in this experiment was selected to minimise overexposure of the NDRG1 bands in WHCO1 and KYSE70. The time was too short to detect basal NDRG1 expression in KYSE180 and KYSE450 cells, which were observed on longer exposures. It was therefore determined that TPA was an appropriate stimulus to further examine the transcriptional regulation of NDRG1 in a subset of OSCC cell lines.

4.2.2. Cloning the NDRG1 promoter

Two thousand one hundred base pairs upstream of the NDRG1 transcription start site, together with 12 bp of the 5' untranslated region (downstream of the transcription start site), was amplified by PCR using specific primers designed to the published sequence for NDRG1 and its contiguous regions (GenBank accession number NT_008046; appendix 1). The amplified NDRG1 (-2100 to +12) DNA fragment was cloned into the shuttle vector, TOPO-XL, and individual clones sequenced. The sequence correct 2112 bp fragment was then cloned into the *Kpn*I and *Xho*I sites

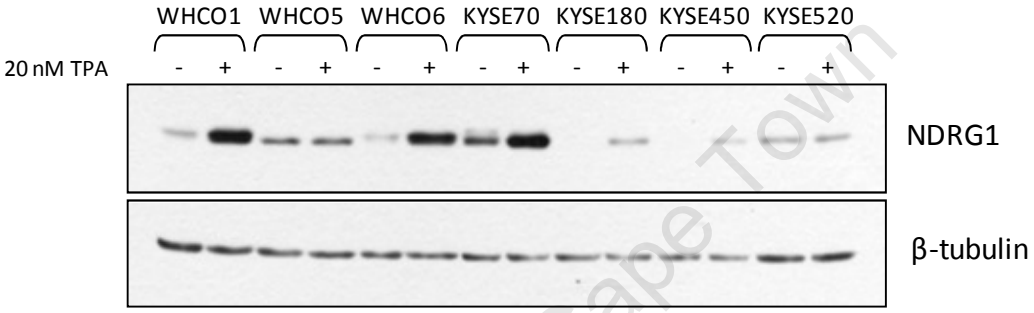

Figure 4.1. TPA induces NDRG1 expression in a subset of OSCC cell lines. Western blot analysis of NDRG1 expression in cell lines either untreated (-) or treated (+) with 20 nM TPA for 16 hours. Twenty micrograms of whole cell lysate was subjected to analysis and showed that NDRG1 is induced by TPA in WHCO1, WHCO6, KYSE70, KYSE180 and KYSE450 cell lines. β-tubulin was used as a control for equal protein loading. Results shown are representative of independent experiments performed two times.

within pGL3-Basic vector, upstream of the luciferase reporter gene. Since a recognition sequence for the restriction enzyme *Bam*HI lies in both the insert and the pGL3-Basic vector, correct clones were identified by *Bam*HI restriction digestion. This yielded two bands of the expected size, namely 2827 bp and 4166 bp (Fig. 4.2.A). The pGL3-Basic vector contains no eukaryotic promoter and enhancer sequences; therefore the luciferase generated using a cloned promoter fragment in this vector, exclusively represents the activity of the cloned promoter in question.

To determine the whether the cloned NDRG1 (-2100 to +12) promoter fragment was indeed functional, luciferase assays were performed on transiently transfected WHCO1, KYSE70 and KYSE520 cells. The pRL-TK vector was used as an internal control reporter. This vector contains the herpes simplex virus thymidine kinase promoter, which drives expression of *Renilla* luciferase, and allows for normalisation of transfection efficiency. Cells were transfected with the pGL3- NDRG1 (-2100 to +12) construct and then either left untreated or treated for 16 hours with 20 nM TPA. In addition, WHCO1 cells were transfected with the parental vector pGL3-Basic to serve as a background control. Luciferase activity derived from the -2100 to +12 NDRG1 promoter fragment in untreated WHCO1 cells was approximately 209-fold higher than that derived from the empty vector alone (the luciferase activity of which measured 0.199) indicating that the -2100 to +12 region of NDRG1 was capable of driving significant levels of transcription (Fig. 4.2. B). Moreover, treatment with 20 nM TPA was able to induce the NDRG1 -2100 to +12 promoter activity in WHCO1 and KYSE70 cells by 3- and 6.5-fold, respectively. In KYSE520 cells TPA was not, however, able to

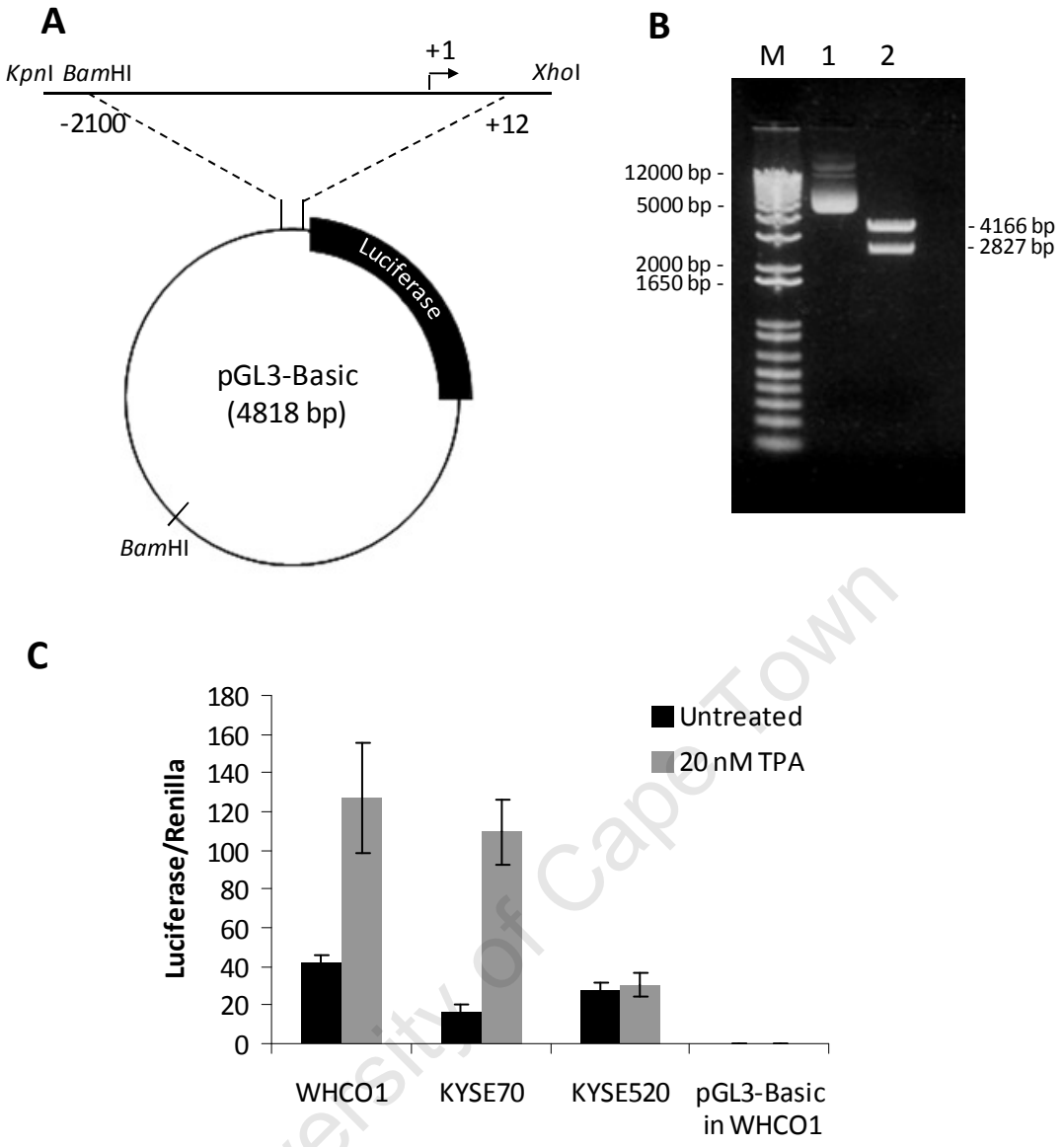

Figure 4.2. Promoter activity of human NDRG1 (-2100 to +12) cloned into the pGL3-Basic reporter vector. A. Schematic diagram of the cloned NDRG1 (-2100 to +12) promoter fragment in pGL3-Basic. The promoter fragment was inserted upstream of the luciferase reporter gene using *Kpn*I and *Xho*I restriction sites present in the multiple cloning site of pGL3-Basic. B. *Bam*HI digestion of NDRG1 (-2100 to +12) in pGL3-Basic. The undigested plasmid was electrophoresed alongside the digested product on a 1 % agarose gel using 1 Kb Plus DNA Ladder as a marker (M; Invitrogen). Lane 1). Uncut pGL3-Basic-NDRG1 (-2100 to +12); Lane 2). *Bam*HI-digested pGL3-Basic-NDRG1 (-2100 to +12). C. Luciferase assay showing significant promoter activity in the NDRG1 (-2100 to +12) cloned fragment compared to the empty vector in WHCO1 cells. Treatment for 16 hours with 20 nM TPA was able to induce NDRG1 promoter activity in WHCO1 and KYSE70 cells, but not KYSE520 cells. pRL-TK was used as an internal control for transfection efficiency and luciferase activity is normalised to *Renilla* luciferase. The results show the mean ± standard deviation of experiments performed in triplicate, three times.

induce activity of the NDRG1 -2100 to +12 fragment. This finding correlates with the data (shown in Figure 4.1) where NDRG1 protein is induced by TPA in WHCO1 and KYSE70 cells, but not KYSE520 cells.

4.2.3. TPA activates MAPK pathways and induces NDRG1 expression

Initial experiments with TPA had been carried out using an arbitrary concentration of 20 nM. We were, however, interested to see whether the NDRG1 response was TPA dose-dependent. Since it had been reported previously that 4 hours of treatment with TPA was capable of activating MAPK pathways in cultured cells[189], the effect of TPA on NDRG1 expression in KYSE450 cells was therefore determined by treating cells with increasing concentrations of TPA for 4 hours (Fig. 4.3.). Western blot analysis revealed that treatment from 10 nM up to 320 nM TPA induced NDRG1 protein expression to similar extents. In addition, as little as 10 nM TPA exposure led to the activation of the ERK, p38 and JNK MAPK pathways, whereas the AKT pathway, which was phosphorylated in the absence of TPA, was suppressed by the presence of the phorbol ester. Our next step was to determine the dose response of the NDRG1 promoter to TPA treatment so that an optimal working TPA concentration could be identified for further analysis. Cells were therefore transfected with the (-2100 to +12) NDRG1 luciferase reporter plasmid and treated with 10 nM to 320 nM TPA for 4 hours (Fig. 4.4.). A significant upregulation in NDRG1 promoter activity was achieved after exposure to as little as 10 nM TPA for 4 hours ($p < 0.005$) and, as with the protein levels, luciferase activity did not display a linear relationship with TPA dose. From this

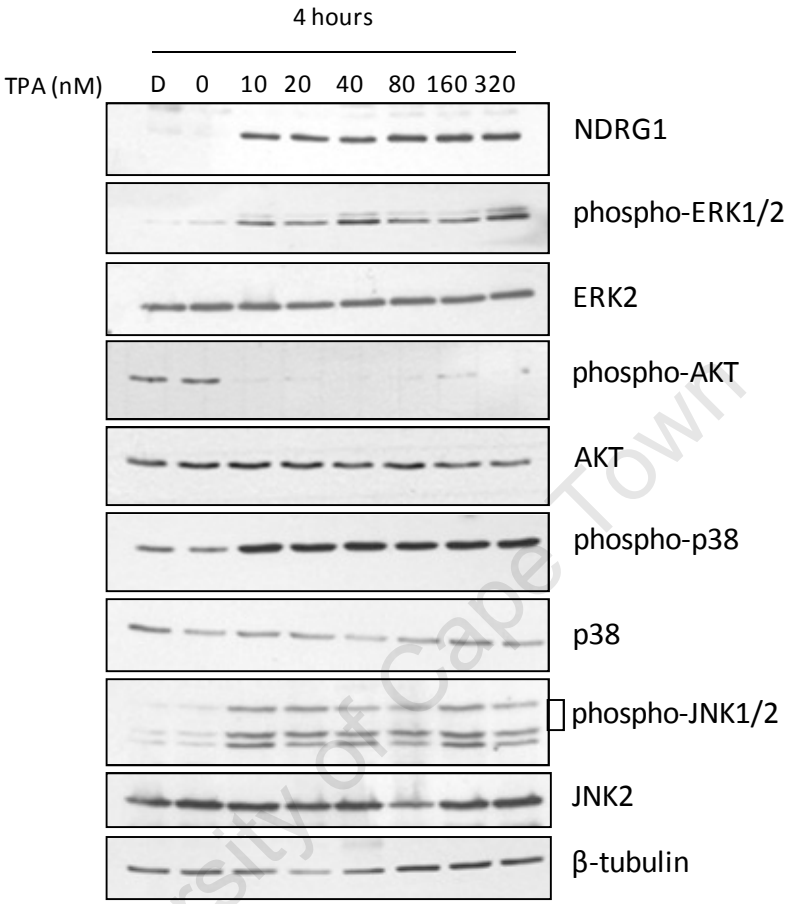

Figure 4.3. Twenty nanomolar TPA is sufficient to upregulate NDRG1 expression and induces phosphorylation of MAPK pathways. KYSE450 whole cell lysates were prepared 4 hours after treatment with various concentrations of TPA. Forty micrograms of protein were separated by SDS-PAGE and immunoblotted with antibodies against NDRG1 and phosphorylated and unphosphorylated MAPK proteins. Levels of unphosphorylated MAPK proteins and β-tubulin were used as loading controls. *D*, DMSO (0.005 %) solvent control *0*, untreated cells.

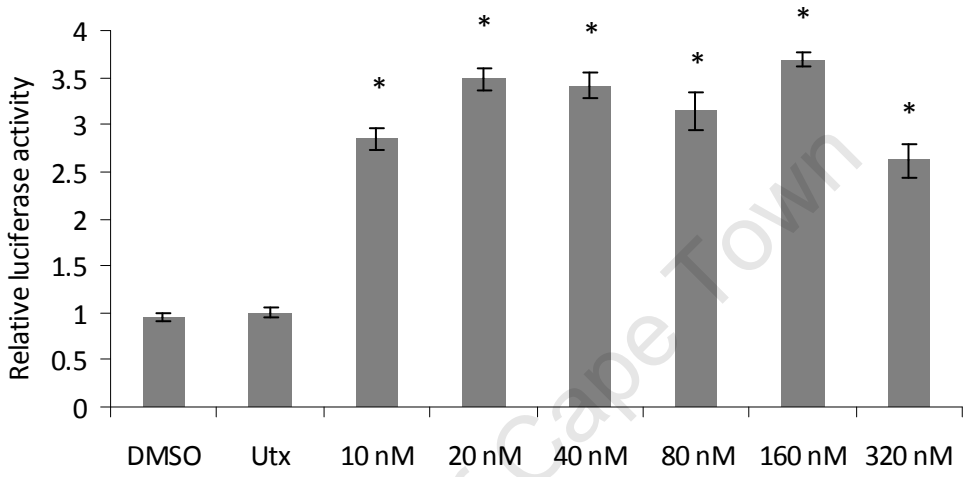

Figure 4.4. Twenty nanomolar TPA is sufficient to upregulate NDRG1 (-2100 to +12) promoter activity in KYSE450 cells. and induces phosphorylation of MAPK pathways. NDRG1 (-2100 to +12) promoter activity was analyzed by dual luciferase reporter system. KYSE450 cells were transiently co-transfected with NDRG1 reporter construct and pRL-TK. The next day cells were either left untreated (Utx) or treated with different concentrations of TPA for 4 hours. *NDRG1* relative luciferase activity is expressed as a ratio of luciferase activity of treated cells relative to untreated cells. *Renilla* luciferase was used as an internal control. The DMSO (0.005 %) solvent control showed no significant difference in promoter activity compared to untreated cells. The results show the mean ± standard deviation of experiments performed in triplicate, three times (* $p < 0.005$).

data it was decided that 20 nM TPA was a suitable concentration to continue further experiments.

To further understand the effect of TPA treatment on NDRG1 expression we treated KYSE450 cells with 20 nM TPA for various times and measured NDRG1 and MAPK pathway responses by Western blot (Fig. 4.5.). As short as 1 hour exposure to 20 nM TPA was able to induce measurable levels of NDRG1 protein, where maximal levels were observed at 8 - 10 hours of exposure, after which NDRG1 levels began to decline. Strong activation of the ERK and JNK pathways was observed between 1 and 4 hours after TPA treatment and p38 phosphorylation was also observed after TPA exposure, albeit at a later stage. Additionally, TPA resulted in a decrease in phospho-AKT levels from 1 - 8 hours of exposure. These results suggest that TPA induces NDRG1 via a MAPK pathway in a time-dependent manner. Moreover, NDRG1 upregulation is paralleled with the activation of MEK/ERK, JNK and p38 MAPK pathways, and the inhibition of AKT signalling.

4.2.4. Analysing NDRG1 promoter activity through the generation of deletion constructs and identification of evolutionary conserved regulatory regions

The NDRG1 -2100 to +12 upstream regulatory region is capable of driving transcription and responds to TPA stimulation as expected. However, one cannot exclude the possibilty that additional untranslated regions may also play a part in regulating NDRG1 expression. In order to gain a better understanding of the elements important for regulating NDRG1 transcription, additional reporter constructs were synthesised,

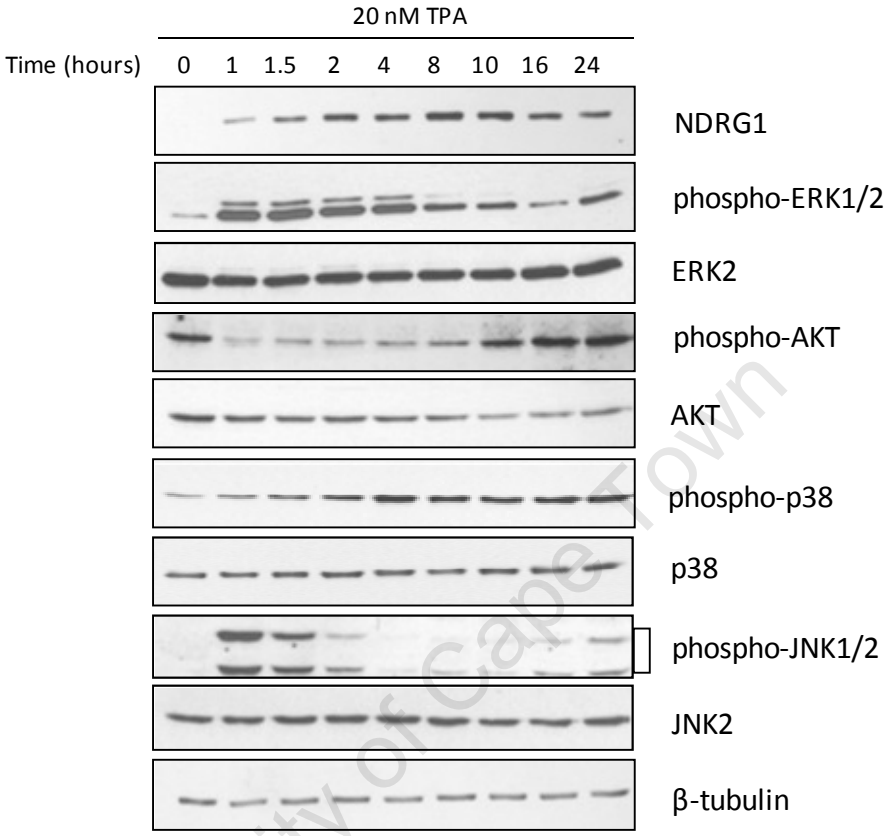

Figure 4.5. TPA rapidly induces NDRG1 expression and activates MAPK signalling pathways. Western blot analysis of whole cell lysates from KYSE450 cells treated with 20 nM TPA for the indicated times. Forty micrograms of protein were electrophoretically separated and probed with antibodies against NDRG1, β-tubulin and phosphorylated and unphosphorylated MAPK proteins. Levels of unphosphorylated MAPK proteins and β-tubulin were used as loading controls.

using PCR, and cloned into the pGL3-Basic reporter plasmid. These constructs included the NDRG1 putative promoter regions (-4819 to +305), (-4819 to +12), (-2100 to +305), (-1500 to +12), (-1200 to +12), (-900 +12), (-298 to +12), as shown in Fig. 4.6, in addition to the already cloned (-2100 to +12) NDRG1 promoter construct described earlier. All PCR amplified promoter products were confirmed by sequencing.

Since we had shown that the NDRG1 (-2100 to +12) promoter fragment was capable of driving luciferase expression in response to TPA, we again used this system, in KYSE450 cells, to explore the functionality of all promoter constructs. NDRG1 promoter deletion constructs were thus transfected into KYSE450 cells; the next day cells were either left untreated or treated with 20 nM TPA for 8 hours (where maximal induction of NDRG1 protein was observed) and luciferase activity measured. Results showed that all constructs displayed significantly more activity in the TPA-treated cells versus untreated cells (Fig. 4.6.). As little as 298 bp upstream of the transcriptional start site to +12 bp was capable of driving a 2-fold increase in promoter activity when treated with TPA, while the (-900 to +12) fragment induced a near 4-fold induction of luciferase activity ($p < 0.005$). Maximal induction of promoter activity was achieved in TPA-treated cells transfected with the NDRG1 (-1200 to +12) reporter, suggesting that transcription factor binding sites, important for inducing NDRG1 expression in response to TPA, lie within the -1200 bp to +12 bp region of the NDRG1 promoter. Both the (-4819 to +305) and (-2100 to +305) reporter constructs showed lower activity when compared to the (-4819 to +12) and (-2100 to +305) reporters, respectively. This is likely explained by the presence of the Myc repressor binding

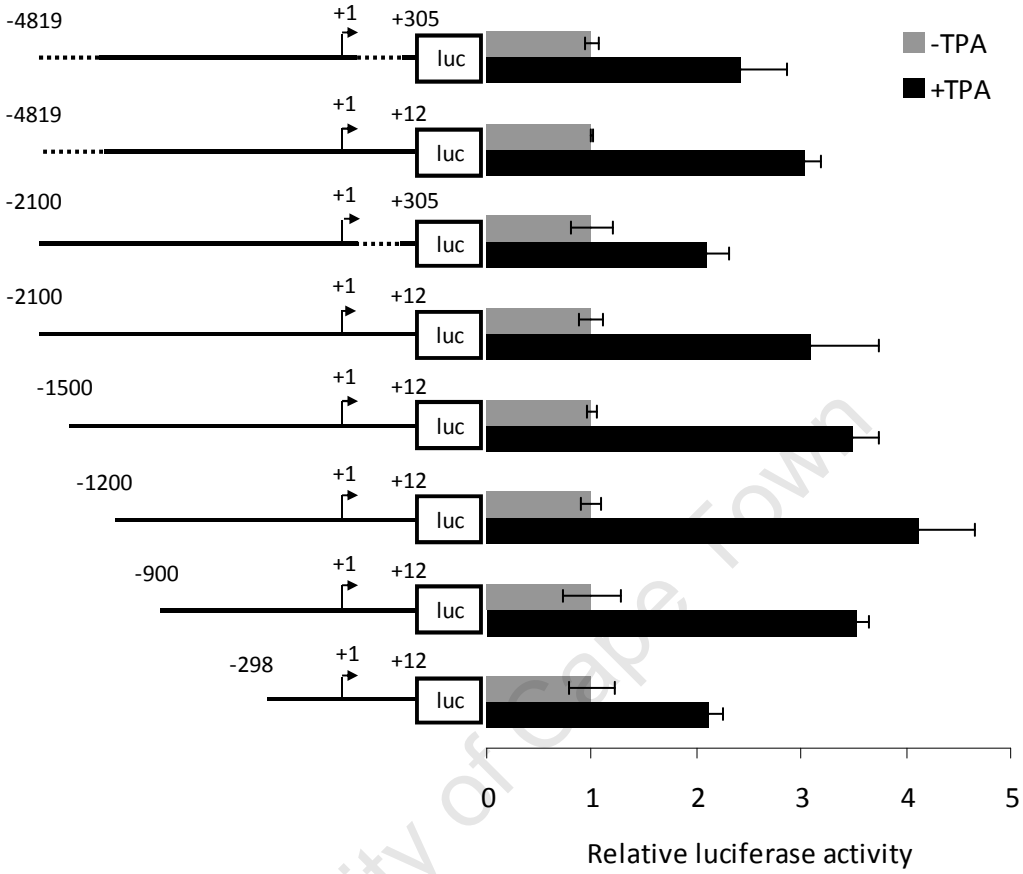

Figure 4.6. Relative luciferase activity of the NDRG1 promoter deletion contructs in KYSE450 cells. Luciferase reporter constructs containing different regions of the human NDRG1 promoter were transiently transfected into KYSE450 cells. The next day cells were either left untreated, or treated for 8 hours with 20 nM TPA. All constructs showed a response to TPA stimulation, varying from between 2- and 4-fold induction. The smallest promoter fragment (-298 to +12) showed a 2-fold response to TPA treatment. An additional 602 bp upstream (-900 to +12) induced a further and significant TPA response (*$p < 0.005$). Nucleotides are numbered relative to the transcription start site (+1). The results shown are the mean ± standard deviation of experiments performed in triplicate, three times and luciferase activity is expressed relative to untreated cells.

sequence within the NDRG1 core promoter region (from -33 bp to +103 bp) that was reported recently[112]. Interestingly, no significant upregulation in reporter activity was observed when base pairs as far as -4819 were included in reporter constructs, compared to the (-2100 to +12), (-1500 to +12), (-1200 to +12) and (-900 +12) reporter plasmids and further suggests that key NDRG1 regulatory elements lie within 2100 bp of the transcriptional start site.

Since regulatory elements, important for gene transcription are often conserved phylogenetically[190] regions of conserved 5' *cis* acting elements, potentially regulating NDRG1 transcription, were identified by performing a hierarchical sequence alignment. Sequences approximately 5 Kb upstream of the NDRG1 transcriptional start site to +1 bp for human, chimpanzee, rat, mouse and bovine NDRG1 were retrieved from the NCBI database; ClustalW multiple sequence alignment was performed, using BioEdit Sequence Alignment Editor[191;192], and showed that sequence homology increased with proximity to the transcriptional start site, notably from -500 bp to +1 bp of the putative promoter region (Fig. 4.7.).

4.2.5. TPA induces NDRG1 expression via PKC

Since we had shown that TPA induces NDRG1 expression and activates MAPK pathways we determined the role of PKC in the TPA response observed. Although it is well known that TPA is responsible for PKC activation, it may also lead to activation of other kinases, such as EGFR[193;194]. To inhibit the activity of PKC, we used the PKC antagonist GF109203x (Bisindolylmaleimide I), an inhibitor that shows high selectivity

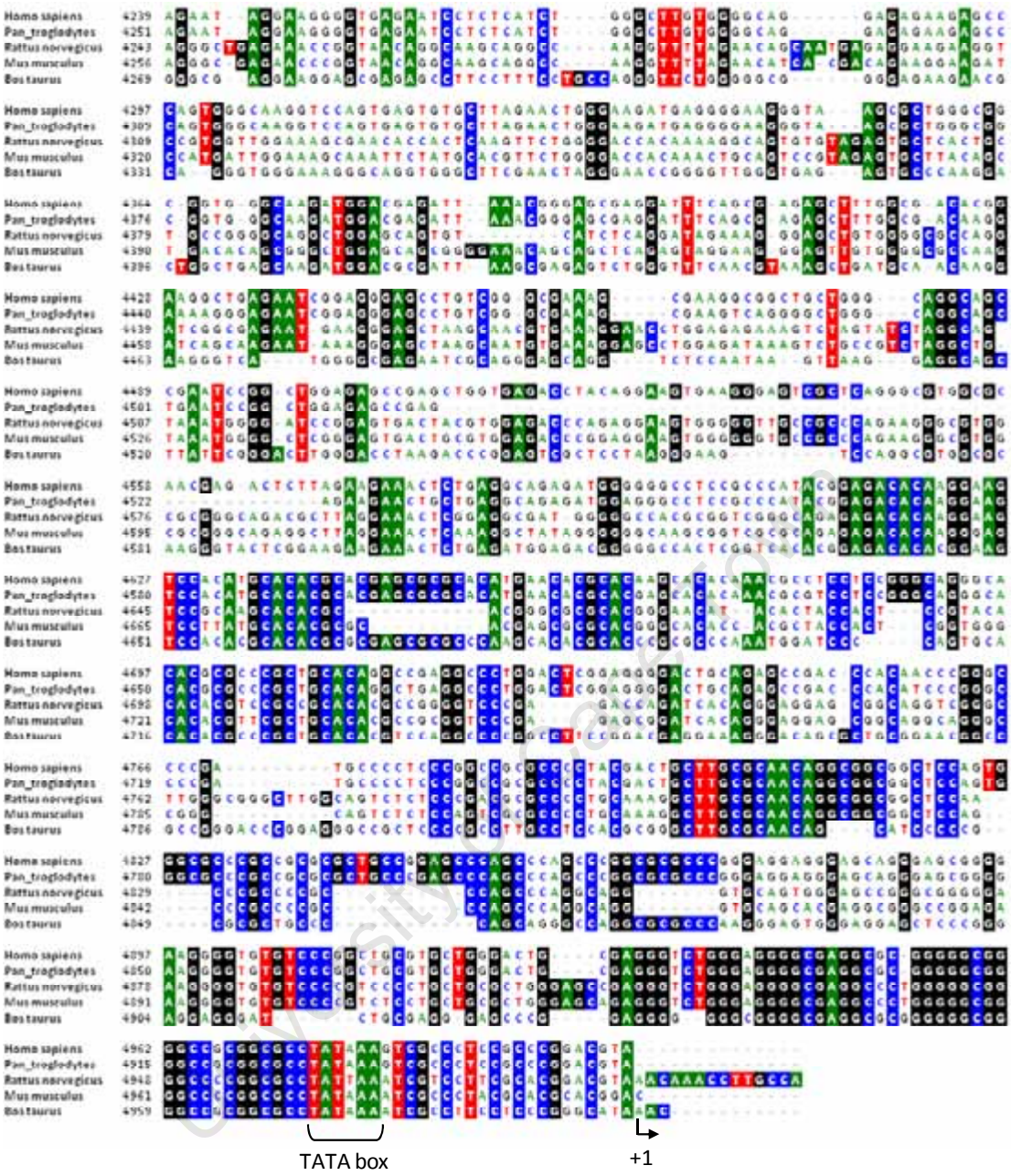

Figure 4.7. Hierachical multiple sequence alignment showing regions that are conserved in the putative NDRG1 promoter. ClustalW software was used to align the putative NDRG1 promoter sequences of human, chimpanzee, rat, mouse and bovine. Regions of 100 % homology across species are highlighted and show that identity increases with proximity to the transcriptional start site. Sequences start at approximately -762 bp (marked here as 4239) and end at +1 bp. The putative TATA box and transcriptional start site (+1) are indicated.

for PKCα, βI, βII, γ, δ, and ε isozymes. KYSE450 cells were pre-treated with 40 μM GF109203x for 1 hour and then stimulated with 20 nM TPA for 8 hours. Western blot analysis showed that the presence of the PKC antagonist inhibited TPA-induced NDRG1 protein expression (Fig. 4.8.A.). Immunoblotting with phospho-p38 antibody confirmed the activity of GF109203x.

To confirm that the TPA stimulation of NDRG1, mediated by PKC, occurred at the transcriptional level, a luciferase reporter assay was performed. Since we had shown that TPA-induced NDRG1 promoter activity did not extend beyond the -2100 bp to + 12 bp regulatory region, KYSE450 cells were transiently transfected with the NDRG1 (-2100 to +12) reporter construct along with pRL-TK. The next day cells were either left untreated, treated with PKC inhibitor alone, treated with TPA alone or pre-treated for 1 hour with PKC inhibitor, followed by 8 hours of TPA stimulation. NDRG1 (-2100 to +12) reporter activity was diminished 4-fold, to basal levels, when cells were treated with TPA in the presence of the PKC inhibitor ($p < 0.01$), compared to cells treated with TPA alone. Taken together these results suggest that the NDRG1 response to TPA is mediated by PKC and converges on the -2100 bp to +12 bp region of the NDRG1 promoter.

4.2.6. TPA signals to NDRG1 via MEK/ERK and JNK

Exposure of cells to a stimulating agent such as TPA leads to the modulation of intracellular signalling pathways and expression of transcription factors, culminating in the transcription of target genes. TPA treatment resulted in NDRG1 upregulation, and

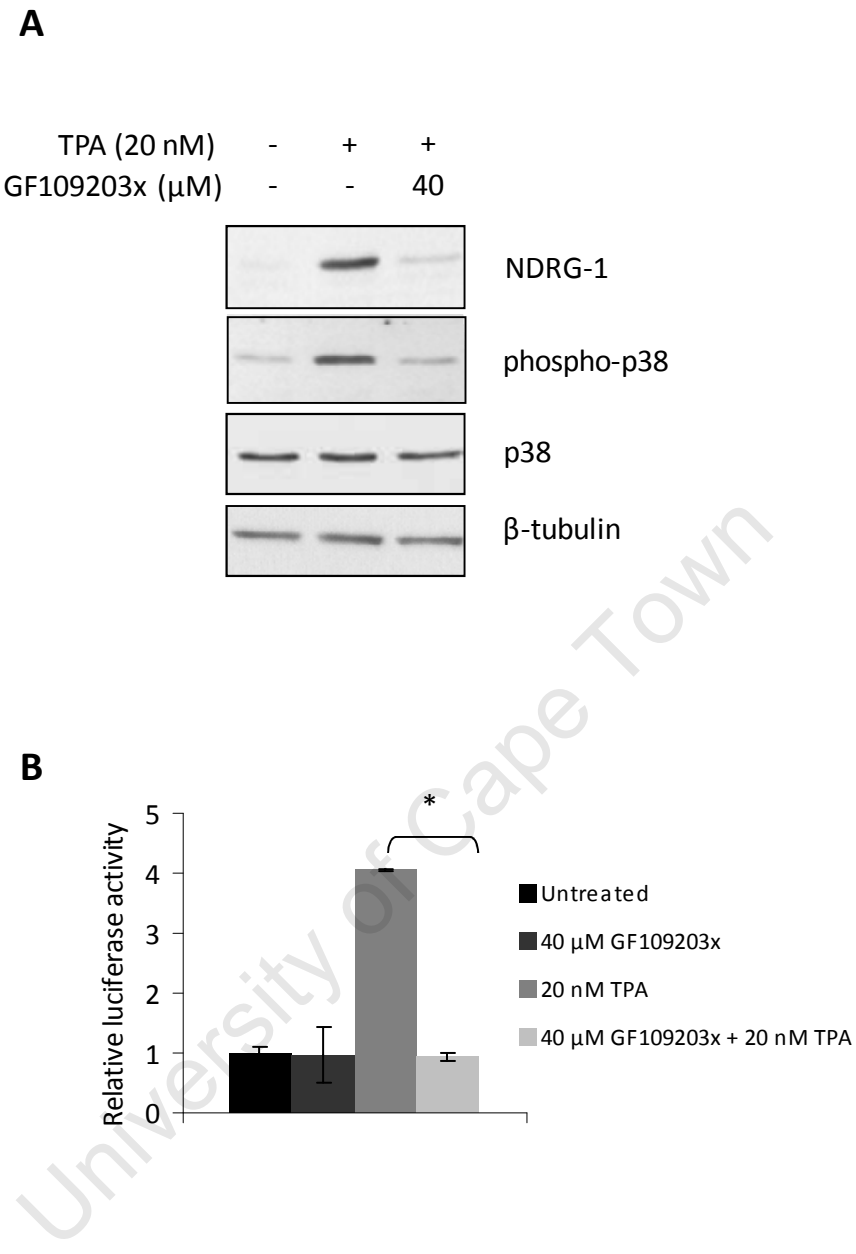

Figure 4.8. TPA induced upregulation of NDRG1 is mediated by PKC. A. Western blot analysis of KYSE450 cell lysates pre-treated for 1 hour with 40 µM PKC inhibitor (GF109203x) followed by 20 nM TPA treatment for 8 hours. Forty micrograms of protein lysates were probed with antibodies to NDRG1, β-tubulin and phosphorylated and unphosphorylated p38 proteins. B. NDRG1 luciferase reporter activity was determined in KYSE450 cells transiently co-transfected with the (-2100 to + 12) NDRG1 reporter construct and pRL-TK. The day after transfection cells were either left untreated, treated with GF109203x alone, treated with TPA alone or pre-treated for 1 hour with 40 µM PKC inhibitor (GF109203x) followed by 20 nM TPA treatment for 8 hours (* $p < 0.01$). The results shown are the mean ± standard deviation of experiments performed in triplicate, three times.

associated activation of the MEK/ERK, JNK and p38 MAPK pathways and the dephosphorylation of AKT. We sought to determine which MAPK pathways were involved in the TPA-stimulated expression of NDRG1 by utilizing target specific antagonists.

To determine which MAPK pathways play a role in the NDRG1 response to TPA treatment, KYSE450 cells, were pre-treated with either the MEK inhibitor (PD98059), AKT inhibitor (Akti-1/2), JNK inhibitor (SP600125) or p38 inhibitor (SB203580) for 1 hour followed by stimulation with 20 nM TPA for 8 hours. The levels of NDRG1 protein in cells stimulated with TPA in the presence of the MAPK inhibitors was determined by Western blot analysis and showed that the AKT and p38 inhibitors had little inhibitory effect on TPA-induced NDRG1 expression, whereas the MEK and JNK inhibitors were able to reduce the extent of TPA-stimulated induction of NDRG1 (Fig. 4.9.). Here, the MEK inhibitor suppressed NDRG1's TPA response by 80 % whilst the JNK inhibitor reduced NDRG1 expression by approximately 45 %, as determined by densitometric quantification, using Quantity One software (version 4.6.6). Immunoblotting against phosphorylated MAPK proteins and phospho-cJun confirmed inhibition of signalling pathways by the specific inhibitors. In the case of the p38 MAPK pathway and SB203580, this antagonist prevents the activity of p38 but not its transactivation, hence an apparent increase in phospho-p38 is observed[195].

To show that the MEK/ERK and JNK MAPK signalling converges on the NDRG1 -2100 bp to +12 bp promoter region, luciferase reporter assays were performed. KYSE450 cells,

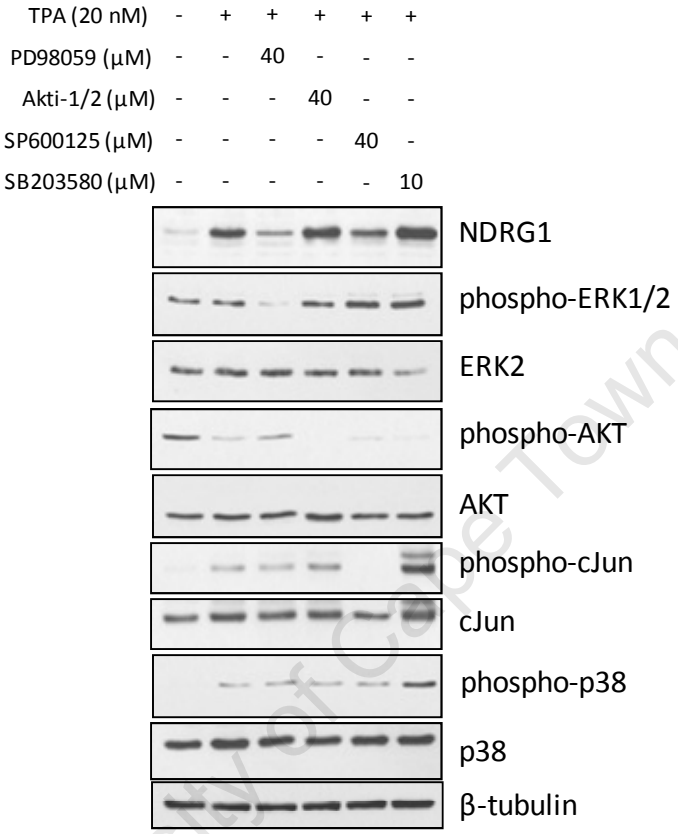

Figure 4.9. TPA induced upregulation of NDRG1 protein is suppressed by MEK and JNK inhibitors. Western blot analysis performed on 40 µg KYSE450 cell lysates pre-treated for 1 hour with MAPK inhibitors followed by 20 nM TPA treatment for 8 hours. Protein lysates were probed with antibodies to NDRG1, β-tubulin and phosphorylated and unphosphorylated MAPK proteins and revealed that MEK (PD98059) and JNK (SP600125) inhibitors were able to abrogate, albeit to differing degrees, the induction of NDRG1 by TPA treatment.

transiently transfected with the NDRG1 (-2100 to +12) luciferase reporter plasmid and pRL-TK, were pre-treated with various MAPK inhibitors for 1 hour followed by TPA stimulation for 8 hours. As observed in the Western blot analysis, the presence of either the AKT or p38 inhibitor had little effect on the TPA-induced up-regulation of NDRG1 promoter activity (Fig 4.10.). However, the presence of the MEK and JNK inhibitors abrogated the TPA-stimulated reporter response by 82 ($p < 0.005$) and 35 ($p < 0.05$) percent, respectively. Thus, it appears that MEK/ERK is the predominant MAPK mediator of the NDRG1 TPA response and JNK plays a partial role. As an aside, it was interesting to note that the AKT inhibitor alone induced basal levels of NDRG1 (-2100 to +12) reporter activity by 1.5-fold ($p < 0.005$) while the MEK inhibitor alone repressed basal NDRG1 (-2100 to +12) transcription by almost 4-fold ($p < 0.001$). This leads one to speculate that the MEK/ERK and AKT pathways may be key regulators of basal NDRG1 transcription and expression.

4.2.7. EGR-1 and cJun mediate the TPA-stimulated NDRG1 response

MAPKs transmit stimuli from the extracellular environment to the nucleus giving rise to transcription factor activation and recruitment to target genes. In KYSE450 cells the TPA stimulus is relayed to NDRG1 predominantly via the MEK/ERK MAPK pathway. In order to identify candidate transcription factors that promote NDRG1 transcription in response to TPA, an *in silico* bioinformatics analysis was perfomed. Here, the 2100 bp 5' to + 12 region was subjected to a transcription factor binding site search using MatInspector[196] and Conreal (conserved regulatory elements anchored alignment

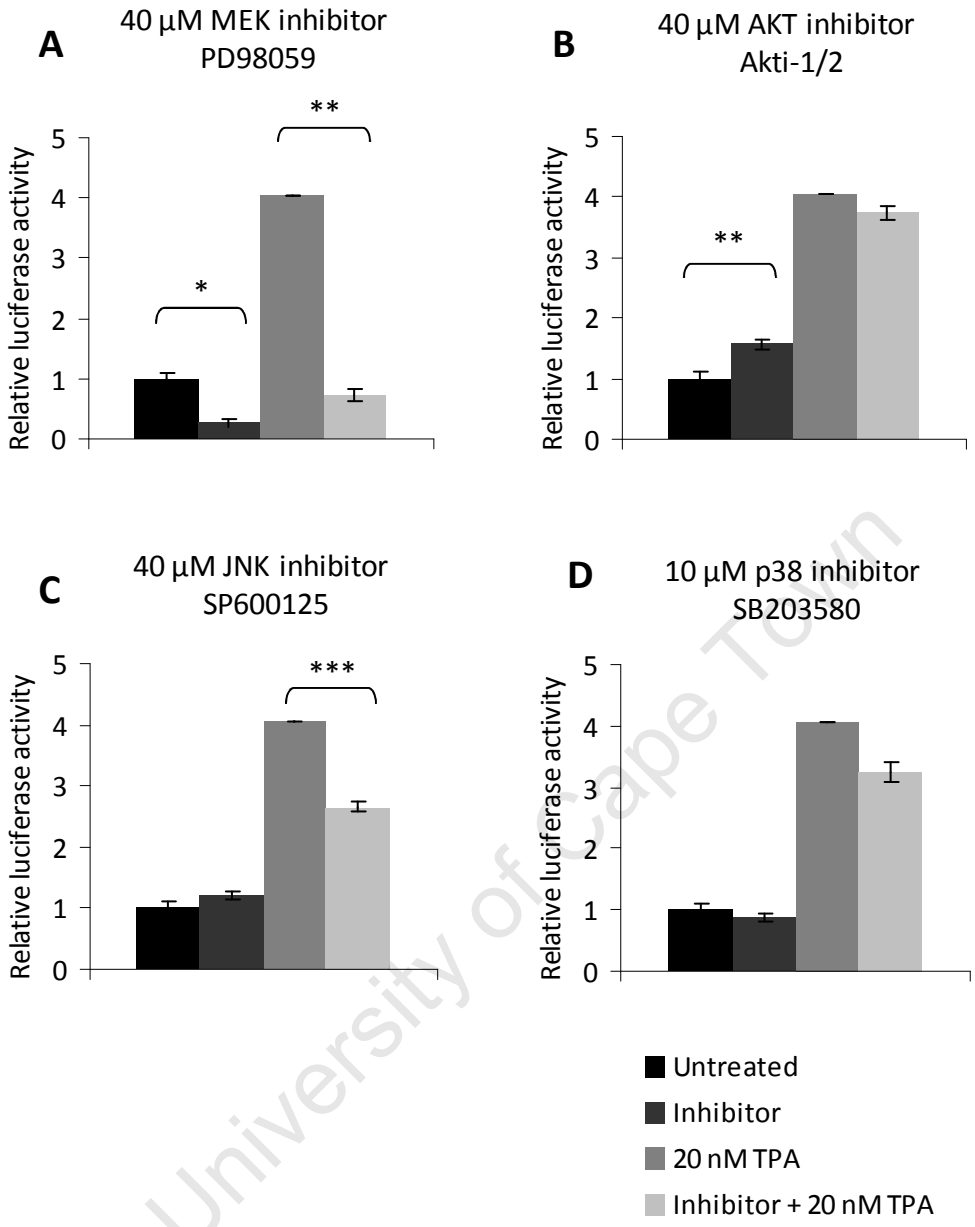

Figure 4.10. TPA-induced NDRG1 promoter activity is stimulated through MEK/ERK and JNK MAPK pathways. NDRG1 luciferase reporter activity was determined in KYSE450 cells transiently co-transfected with the (-2100 to +12) NDRG1 reporter construct and pRL-TK. The day after transfection cells were pre-treated for 1 hour with the indicated concentrations of inhibitors, followed by treatment with 20 nM TPA for 8 hours. The MEK and AKT inhibitors had a significant effect on basal activity of the NDRG1 (-2100 to +12) promoter, while the MEK and JNK inhibitors were able to inhibit, to different extents, TPA-induced NDRG1 promoter activity. The results show the mean ± standard deviation of experiments performed in triplicate, three times (* $p<0.001$, ** $p<0.005$, *** $p<0.05$).

algorithm)[197]. Multiple candidate transcription factor binding sites were retrieved including those for c-Ets-1, TGF-β, E2-F, AP-1 as well as EGR-1 (data not shown).

Since the TPA-stimulated expression of NDRG1 is mediated by MEK/ERK and JNK, particular focus was placed on transcription factors known to lie downstream of these MAPK pathways. In particular, we examined the role of EGR-1 and AP-1, specifically cJun, in modulating NDRG1 expression.

It has been shown that EGR-1 lies downstream of ERK and responds to TPA in other systems[198]. Likewise, TPA activates JNK MAPK, which is responsible for the transactivation of the AP-1 transcriptional complex[199;200], comprising of Jun homodimers and Jun/Fos heterodimers[201]. To elucidate whether EGR-1 and/or cJun were necessary for NDRG1 gene expression following TPA exposure, a siRNA approach was used. KYSE450 cells were transiently transfected with 20 nM control, EGR-1 or cJun siRNA. Twenty-four hours later transfectants were either left untreated or treated with 20 nM TPA for 8 hours. Western blot analysis on whole cell lysates revealed that TPA-induced NDRG1 expression was downregulated by 30 % in the presence of EGR-1 and cJun siRNA compared with cells transfected with control siRNA (Fig. 4.11.A.). Immunoblotting with antibodies against EGR-1 and cJun confirmed the efficient knockdown (although not complete) effect of the target specific siRNA. Interestingly, it appeared that the presence of cJun siRNA also resulted in a downregulation of EGR-1 expression in the presence of 20 nM TPA. This suggests that

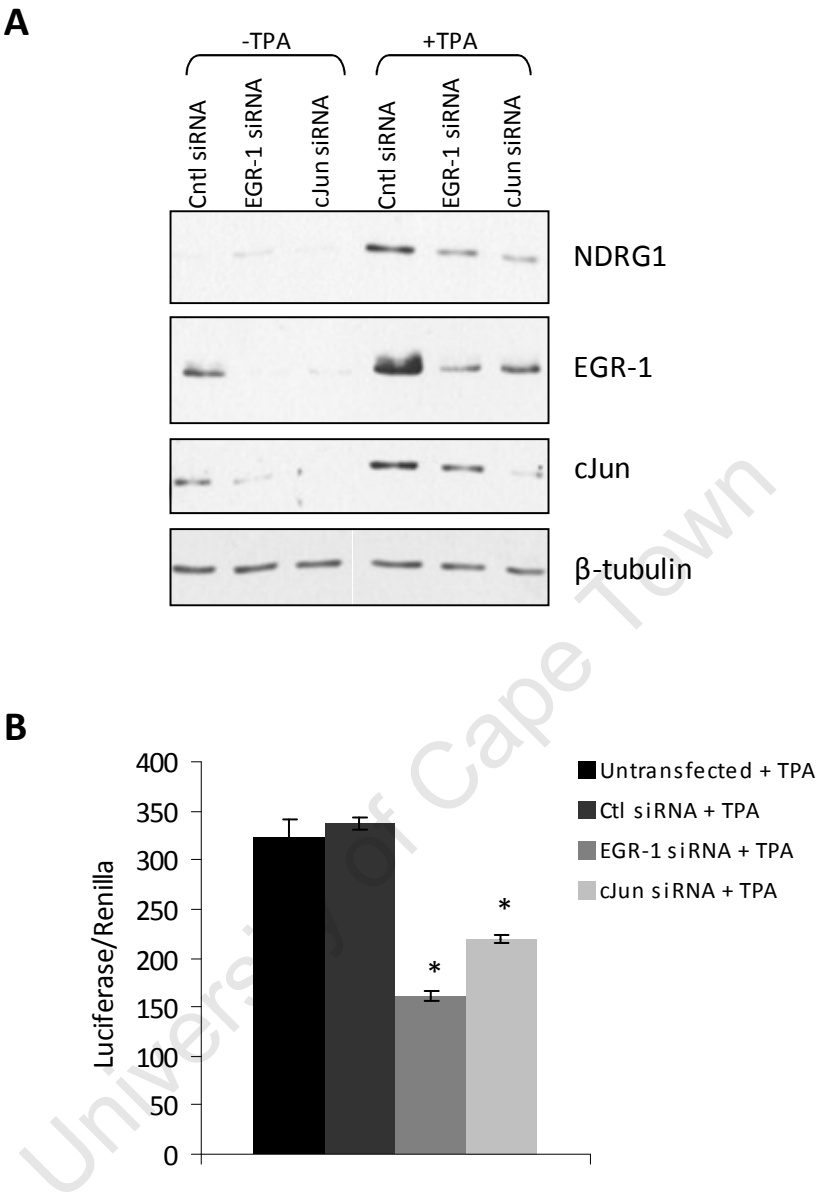

Figure 4.11. EGR-1 and cJun mediate TPA-stimulated up-regulation of NDRG1. A. KYSE450 cells transfected with 20 nM control (Ctl) siRNA, EGR-1 siRNA or cJun siRNA, and left untreated or treated for 8 hours with 20 nM TPA, were examined by Western blot. Whole cell lysates were subjected to SDS-PAGE and immunoblotted with antibodies against EGR-1, NDRG1, cJun and β-tubulin. B. NDRG1 promoter activity was determined in KYSE450 cells transiently co-transfected with the NDRG1 (-2100 to +12) promoter construct alone or the NDRG1 promoter construct with either 20 nM of control siRNA, EGR-1 siRNA or cJun siRNA. TK driven *Renilla* luciferase served as an internal control. Twenty four hours after transfection, cells were treated with 20 nM TPA for 8 hours and assayed for luciferase activity (* $p < 0.001$). The results show the mean ± standard deviation of experiments performed in triplicate, three times.

cJun may affect NDRG1 expression directly through regulation of the promoter as well as indirectly, through modulation of EGR-1 expression.

The effect of EGR-1 and cJun siRNA on NDRG1 (-2100 to +12) reporter activity was next determined by luciferase reporter assay. KYSE450 cells transiently transfected with either the NDRG1 (-2100 to +12) reporter construct alone or the reporter construct and control siRNA, showed no significant difference in luciferase activity when treated with 20 nM TPA (Fig. 4.11.B.). However, luciferase reporter assays performed in the presence of either EGR-1 or cJun siRNA resulted in a 53 and 36 percent decrease in TPA-induced luciferase activity ($p < 0.001$). Taken together these results suggest that both EGR-1 and cJun regulate NDRG1 expression in response to TPA, and this effect is mediated at the transcriptional level.

To confirm that this observation was in fact true in other OSCC cell lines, and not an artefact of cell culture, Western blot analysis was performed on whole cell lysates from WHCO1, KYSE70 and KYSE180 cell lines that had been transiently transfected with control, EGR-1 or cJun siRNA and treated with 20 nM TPA. Results showed that, as in KYSE450 cells, both EGR-1 and cJun mediate the TPA-induced upregulation of NDRG1 expression (Fig. 4.12.).

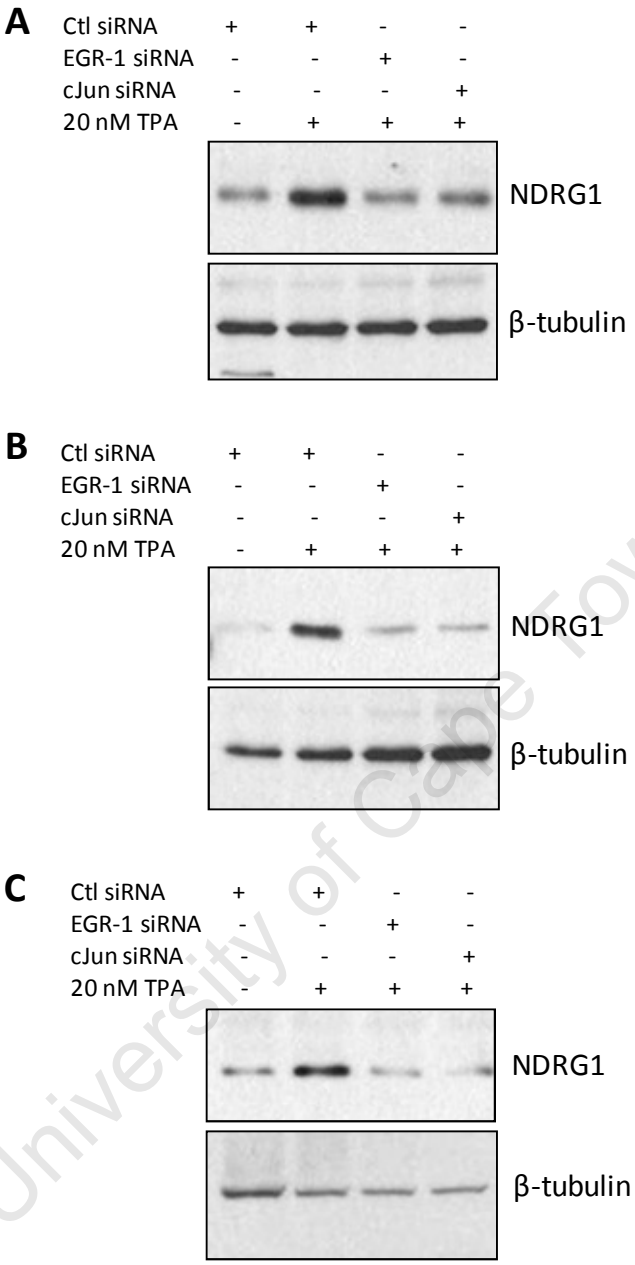

Figure 4.12. TPA-stimulated NDRG1 expression is mediated by EGR-1 and cJun in WHCO1 (A), KYSE70 (B) and KYSE180 (C) cells. Cells were transfected with 20 nM of either control (Ctl), EGR-1 or cJun siRNA. The next day transfectants were treated with 20 nM TPA for 8 hours. Western blot analysis of whole cell lysates showed that TPA-induced upregulation of NDRG1 is abrogated by the presence of EGR-1 or cJun siRNA. β-tubulin was used as a control for protein loading.

4.2.8. An EGR-1 site and two AP-1 sites are important regulatory elements within the NDRG1 -2100 bp to +12 bp region

Since the siRNA approach had shown that both EGR-1 and cJun relayed the TPA-induced signal to the NDRG1 promoter, we next showed that this was a direct effect on the promoter by mutating the predicted EGR-1 and AP-1 (cJun) transcription factor binding sites within the NDRG1 (-2100 to +12) reporter plasmid. Site-directed mutagenesis was employed to alter respective sites by mutating at least one base of the site of interest, without disrupting any other transcription factor binding sites and so as not to introduce any new transcription factor binding sites. Mutagenesis of the EGR-1 site was carried out as reported previously[153], and mutations were confirmed by restriction digestion analysis (data not shown). The sequence of wildtype and mutated sites, as well as their relative positions, are depicted in Figure. 4.13.A.

Mutated NDRG1 (-2100 to +12) promoter constructs were transiently transfected into KYSE450 cells. Figure 4.13.B shows that mutation of the EGR-1 binding site in the proximal NDRG1 promoter resulted in a 90 percent downregulation in NDRG1 (-2100 to +12) luciferase activity in response to TPA ($p < 0.001$). In addition, mutation of either the (-788 to -778) AP-1 site or the (-1123 to -1113) AP-1 site resulted in approximately 50 and 40 percent decrease in promoter activity, respectively ($p < 0.01$; $p < 0.05$). While the cumulative effect of the AP-1 sites was not examined, the data presented here suggests that the predominant regulator of the NDRG1 -2100 bp to +12 bp promoter region is EGR-1.

A

Mutation	Sequence	Position	Restriction Enzyme used to confirm identity
EGR1-WT	5'…GGAGGGGCGAGGCGCGGGGGCGGGCCGCGGCGCC…3'	-49 to -41	*Bfm*I
EGR1-mut	5'…GGAGGGGCGAGGCTATAGGGCGGGCCGCGGCGCC…3'		
AP1(1)-WT	5'…TAAGGTTGGAAAGGGTGAGTCATGAAAGTTCAGGAAA…3'	-788 to -778	*Sch*I
AP1(1)-mut	5'…TAAGGTTGGAAAGGGTGCGCCATGAAAGTTCAGGAAA…3'		
AP1(2)-WT	5'…TGACGGTGCCAGCTGTGAGTCAGACTTCCTTTA TTCA…3'	-1123 to -1113	*Sch*I
AP1(2)-mut	5'…TGACGGTGCCAGCTGTGCGTCAGACTTCCTTTA TTCA…3'		

B

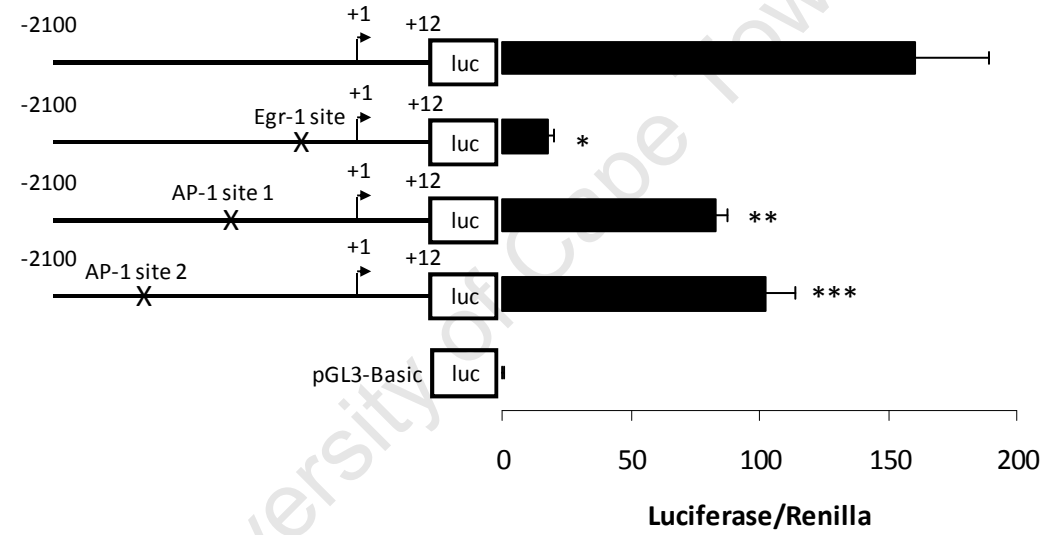

Figure 4.13. Site-directed mutagenesis of EGR-1 and AP-1 transcription factor binding sites in the (2100 to +12) NDRG1 promoter abrogate the TPA-induced transcriptional activity in KYSE450 cells. A. Site-directed mutagenesis was performed on the NDRG1 (2100 +12) promoter construct, using mutagenic primers. The consensus binding sites are in red, with the bases chosen for mutation analysis in green. Positions of the binding sites and restriction enzymes used to identify mutants are shown. Mutagenesis was performed to eliminate the potential EGR-1 and two AP-1 sites within the -2100 bp to +12 bp region of the NDRG1 promoter. B. Luciferase activity of wildtype and mutated NDRG1 (-2100 to +12) promoters in response to 8 hours treatment with 20 nM TPA (*$p < 0.001$, **$p < 0.01$, *** $p < 0.05$). The parental vector pGL3-Basic showed no significant activity. Schematic depiction of the positions of mutations on the NDRG1 (-2100 to +12) promoter are shown. The results show the mean ± standard deviation of experiments performed in triplicate, three times.

4.2.9. EGR-1 binds to the proximal promoter of *NDRG1* following TPA stimulation

As EGR-1 is necessary for TPA-induced up-regulation of NDRG1, we sought to verify that EGR-1 bound the *NDRG1* promoter *in vivo* following TPA stimulation. First, we examined the time course of EGR1 protein response to 20 nM TPA treatment in KYSE450 and WHCO1 cells. Treatment with TPA led to a strong and transient upregulation of EGR-1 protein in both KYSE450 and WHCO1 cells, within 1 hour of exposure (Fig. 4.14.). Maximal levels were achieved after 2 hours of exposure in KYSE450 cells, and 1.5 hours in WHCO1 cells, after which EGR-1 levels declined to basal levels by 10 to 16 hours.

Having determined the time of maximal induction of EGR-1 we performed Chromatin Immunoprecipitation (ChIP) assays using an antibody to EGR-1 with extracts from KYSE450 and WHCO1 cultured cells, untreated or treated for 2 hours with 20 nM TPA. Crosslinked chromatin was isolated from cells and sonicated to generate DNA fragments ranging in size from 500-700 bp. DNA was then immunoprecipitated using an α-EGR-1 antibody, and DNA, bound to EGR-1, was precipitated using protein G agarose beads. Following dissolution of cross-links, the DNA was subjected PCR analysis using primers spanning the EGR-1 site in the NDRG1 promoter (Fig. 4.15.A). A positive band of the correct size of 142 bp was detected in TPA treated KYSE450 and WHCO1 cell lines after immunoprecipitation with the anti-EGR-1 antibody, confirming that EGR-1 binds in the NDRG1 promoter following TPA treatment (Fig. 4.15.B). No PCR product was obtained from untreated cells. Input chromatin served as a positive control, while DNA immunoprecipitated without antibody was included as a negative

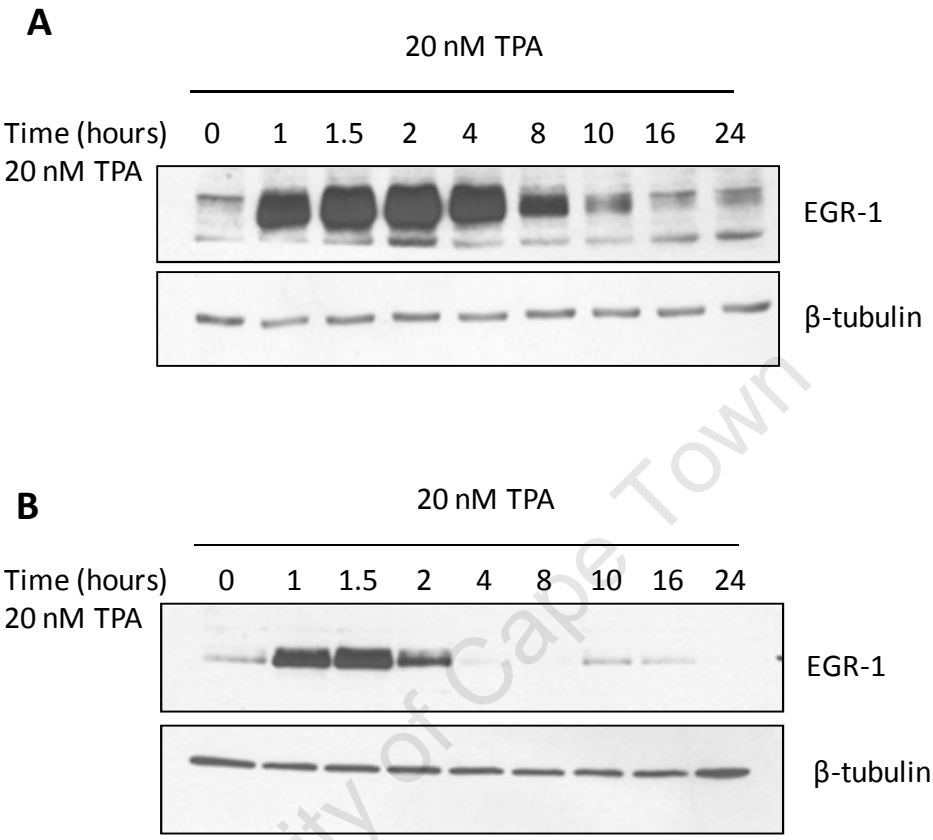

Figure 4.14. Timecourse induction of the EGR-1 protein response to TPA in KYSE450 (A) and WHCO1 (B) cells. Western blot analysis of EGR-1 expression from whole cell lysates of cells treated over time with 20 nM TPA. EGR-1 is rapidly and strongly induced between 1 and 4 hours after TPA treatment. β-tubulin was used as a loading control.

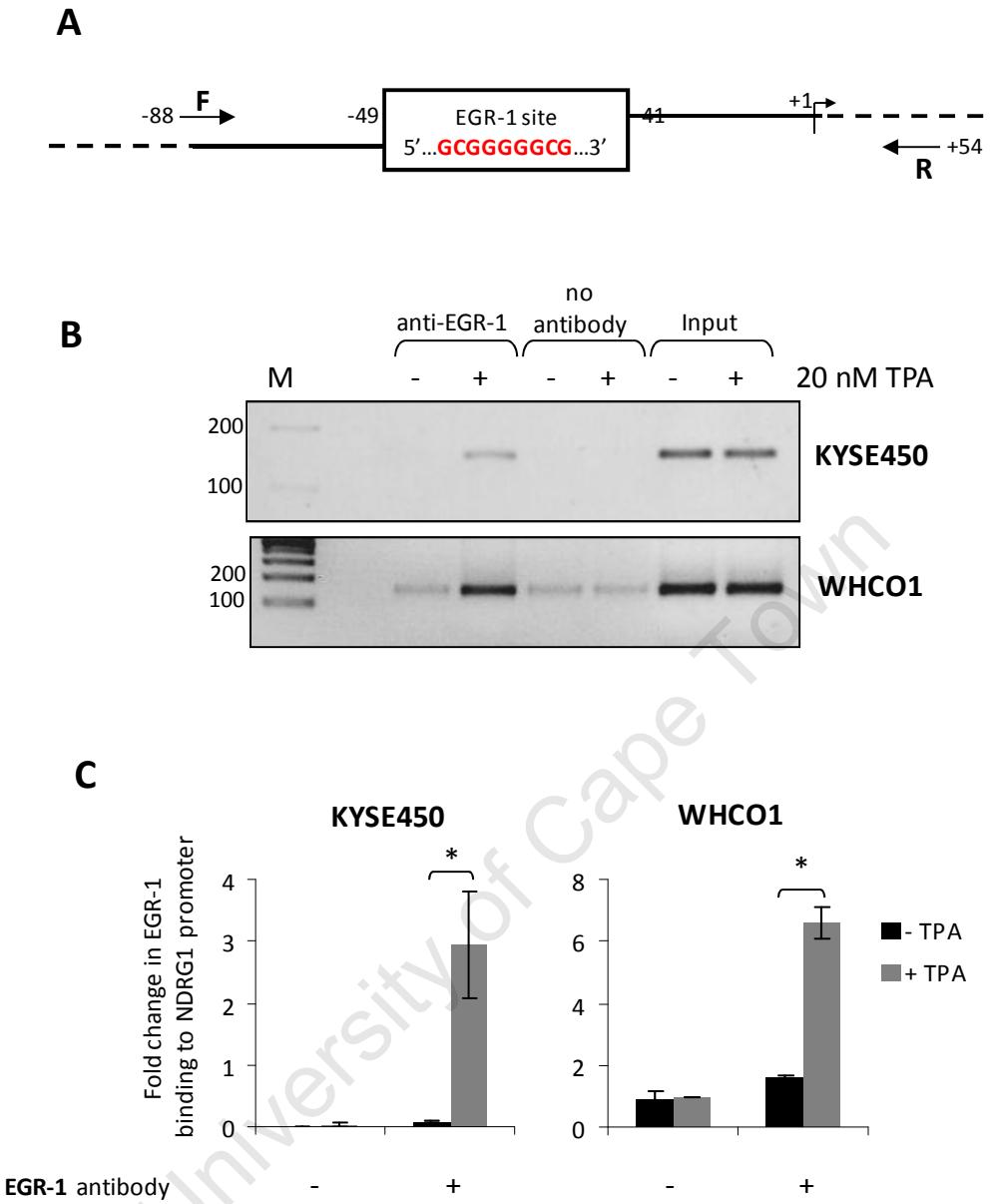

Figure 4.15. ChIP assay identifies the *NDRG1* promoter as an EGR-1 target in KYSE450 and WHCO1 cells. A. Schematic representation of the location of the primer set used in the ChIP assay in relation to the EGR-1 binding site. B. ChIP of EGR-1 was performed with KYSE450 and WHCO1 cells. Chromatin from untreated cells or cells treated for 2 hours with 20 nM TPA was immunoprecipitated with EGR-1 antibody or no antibody as a control. PCR was performed with primers flanking the putative EGR-1 binding site within the *NDRG1* proximal promoter region. C. Real-time RT-PCR using ChIP DNA and primers flanking the EGR-1 binding site within the *NDRG1* promoter. The data shown represents the fold change in EGR-1 binding to the NDRG1 promoter relative to ChIP input DNA (*$p < 0.05$). The results show the mean ± standard deviation of experiments performed in triplicate, three times.

control. The near absent presence of bands in the negative control confirmed specific immunoprecipitation of EGR-1 bound DNA.

Quantitative real-time PCR was performed to demonstrate the increase in EGR-1 binding to the endogenous *NDRG1* promoter between untreated cells and cells treated with TPA (Fig. 4.15.C). The C_T method was used for the calculation of expression fold change between samples relative to respective input DNA. Results showed that in both KYSE450 and WHCO1 cells, EGR-1 binding to the NDRG1 promoter *in vivo* increased by approximately 3-fold in response to TPA treatment ($p < 0.05$).

4.3. DISCUSSION

In order to understand the factors that drive the enhanced expression of NDRG1 in OSCC we cloned and partly characterised the putative NDRG1 promoter. This study is novel in that it is the first, to our knowledge, that describes transcriptional regulation of NDRG1 in oesophageal cancer cells.

Using 12-O-tetradecanoylphorbol 13-acetate as a stimulus, we identified the -2100 bp to +12 bp region of the NDRG1 promoter as responsible for induced transcription of NDRG1. Within this region we identified two AP-1 sites at -788 bp to -778 bp and -1123 bp to -1113 bp as significant regulatory elements stimulating the TPA response. In addition, an EGR-1 regulatory element was identified as essential for driving NDRG1 transcription in response to TPA, and binding of this transcription factor to the NDRG1 -49 bp to -41 bp promoter region was confirmed with ChIP assays *in vivo*. Since target specific siRNA, as well as site-directed mutagenesis implicated both EGR-1 and AP-1 in regulating NDRG1 in response to TPA, we propose that these factors may be in part responsible for the elevated expression of NDRG1 seen in tumour tissue of our cohort of OSCC patients. Although our initial results indicated that treatment of cells with TPA resulted in phosphorylation of ERK1/2, JNK and p38 (Fig. 4.3 and 4.5) we excluded p38 as an important mediator of the TPA-induced NDRG1 response. Phosphorylation was only detected 2 hours post-TPA treatment, and maximal levels of p38 phosphorylation was only observed 4 hours post-TPA treatment. In contrast, maximal levels of ERK1/2 and JNK phosphorylation was observed 1 hour post-TPA treatment, consistent with

elevated levels of NDRG1 detected 1 hour post-TPA treatment (Fig. 4.5). Furthermore, although the AKT inhibitor (Akti1/2) had no effect on the induction of NDRG1 in response to TPA treatment, blockade of AKT was associated with a significant increase in basal NDRG1 expression (Fig. 4.9 and 4.10).

AP-1 has been implicated in many tumourigenic processes including metastasis, enhanced proliferation, apoptosis and angiogenesis[159;202;203] and the transactivation of AP-1 has been shown to be an essential component of tumour progression in epidermal keratinocytes[204]. Of the AP-1 constituent proteins, c-Jun, c-Fos and Fos B are highly efficient in transforming cells[205-207], and enhanced c-Jun and c-Fos expression has been associated with oesophageal cancer[208]. Although we do not show specific binding of cJun to the NDRG1 promoter, our finding, using siRNA and site-directed mutagenesis, that AP-1 regulates NDRG1 at the transcriptional level supports a previous report that a dominant-negative AP-1 weakened the response of NDRG1 to hypoxia[86]. Specific binding of cJun at the AP-1 sites (-788 to -778) and (-1123 to -1113 bp) will be addressed in the future.

Although evidence by others indicates that EGR-1 plays an important role in regulating NDRG1 expression in response to hypoxic conditions[153], we have shown that this transcriptional factor also modulates NDRG1 expression in response to other signalling conditions. Indeed, this is the first *in vivo* demonstration of EGR-1 binding to the NDRG1 proximal promoter region, and reports that the EGR-1 binding motif within the NDRG1 promoter is conserved between human, mouse, rat, chimpanzee and bovine

species[153] suggests that this transcription factor is important for NDRG1 regulation. As with AP-1, EGR-1 has been implicated in tumour growth, proliferation and angiogenesis[186;209]. In fact, our group has recently shown that EGR-1 forms a critical link in proliferative autocrine GRO/CXCR2 signalling in oesophageal cancer[186;210]. Moreover, using the same cohort of patients as in Chapter 2, EGR-1 was shown to be overexpressed in 80 % of the oesophageal tumour tissue studied[186]. Thus, there appears to be a correlation between the frequency of NDRG1 and EGR-1 overexpression in oesophageal tumour tissue compared to normal tissue.

Interestingly, while the AP-1 sites within the NDRG1 promoter were shown to play a part in TPA-induced NDRG1 expression, cJun siRNA appeared to have a repressive effect on EGR-1 expression in KYSE450 cells treated with TPA. We propose that cJun may regulate NDRG1 indirectly, at least in part, through the modulation of EGR-1 expression. Since cJun has been implicated in the regulation of EGR-1 in other systems[211] and the EGR-1 promoter does contain AP-1 binding sites[211;212], this possibility will be explored further, and in additional cell lines.

Taken together, we have characterised factors that regulate the upstream promoter region of NDRG1, leading to its induced expression in response to TPA. Both EGR-1 and AP-1 have been implicated in carcinogenesis and are associated with oesophageal cancer. We show that TPA-induced NDRG1 expression is mediated by MEK/ERK – EGR-1 and JNK-cJun/AP-1 and that this signalling converges at the NDRG1 promoter. We

are however cognisant that TPA induces multiple MAPK pathways. Therefore, in order to more accurately understand the regulation of the NDRG1 promoter, further work will be carried out to investigate the effects of exogenous EGR-1 and AP-1 on NDRG1 expression.

CHAPTER 5

CONCLUSIONS

Over the last decade, evidence presented in the literature has implicated NDRG1 in tumourigenesis. This has not been without controversy, where the reported expression of NDRG1 in some cancers, as well as its relationship to metastasis is not always consistent. Since a preliminary study in our laboratory, using differential-display RT-PCR and microarray technology, identified NDRG1 as differentially expressed in OSCC tissue compared to normal tissue, we sought to characterise its role and regulation in OSCC further.

Analysis of NDRG1 mRNA expression in 8 oesophageal cancer tissue biopsies compared to 6 normal tissue biopsies, by quantitative real-time RT-PCR, revealed that NDRG1 was significantly overexpressed in tumour tissue compared to normal tissue. This observation was consistent with our immunohistochemical analysis of NDRG1 protein expression on a cohort of eighty-three OSCC patients, where NDRG1 expression was found to be 2.6-fold higher in tumour tissue compared to normal tissue. These results are in contrast with others describing NDRG1 expression in OSCC[104;105] which only adds to the controversy surrounding NDRG1's role in cancer. Indeed, this highlights the need for further population based studies on NDRG1 expression in OSCC, where the population's genetic milieu, environment and aetiological agents may differ.

Moreover, the methodology of these studies should be synchronised to reduce the potential of variability.

Our immunohistochemical study also revealed that NDRG1 localises to different compartments within oesophageal epithelial cells, and this localisation tracks with the maturation of the cells. In normal oesophageal epithelium, cells in the basal and parabasal layers display plasma membrane-localised NDRG1 while maturing cells are positive for NDRG1 largely in the cytoplasm and nucleus. Interestingly, both dysplastic tissue as well as poorly differentiated OSCC displayed plasma membrane-associated NDRG1, whilst moderately and well differentiated tumours stained positively for NDRG1 in the cytoplasm, nucleus and plasma membrane. The predominant association of NDRG1 with the plasma membrane of dysplastic cells could suggest that OSCC arises through the malignant expansion of the basal layer of the epithelium where stem cells are proposed to reside[109;175]. Indeed, the fact that NDRG1 is associated with early changes in oesophageal cancer suggests that this protein could probably be used as an early marker for this disease. Moreover, since NDRG1 shows a positive correlation with differentiation in other systems, one might speculate that the cytoplasmic and nuclear localisation of NDRG1 is associated with a commitment of cell fate to differentiate. Interestingly, a recent report by Sibold *et al*[101] showed that while hepatocellular carcinoma cells cultured *in vitro* displayed cytoplasmic localisation of NDRG1, *in vivo* growth of the same cells as xenografts gave rise to plasma membrane-associated NDRG1. This implicated the tumour microenvironment in

influencing NDRG1 localisation. Indeed, it may be useful to examine the localisation and function of NDRG1 in cultured cells grown on denuded, acellular oesophageal connective tissue, which has been shown to give rise to reconstituted oesophageal epithelium[109]. To this end, we examined NDRG1 expression in cultured OSCC cell lines cultured under anchorage-independent conditions, since the function of NDRG1 expression in cultured OSCC cells has, to date, not been demonstrated. Anchorage-independent cell culture resulted in a strong upregulation of NDRG1 protein expression that was sustained for at least 72 hours in WHCO1, WHCO6, KYSE70, KYSE180 and KYSE450 cell lines. Interestingly, immunocytochemistry performed on sections of cultured cells that had been embedded in paraffin blocks, revealed that in WHCO1 and WHCO6 cells, anchorage-independent growth resulted in strong cytoplasmic and nuclear localisation of NDRG1. In KYSE70 and KYSE180 cells, cultured in the same manner, NDRG1 appeared to localise to the plasma membrane. This is, to our knowledge, the first description of NDRG1 expression in cells cultured under anchorage-independent conditions. Interestingly, NDRG1 displayed markedly different localisation in cultured cells derived from the same tissue type, suggesting that even cells from the same tissue may express NDRG1 differently.

To determine whether anchorage-independent upregulation of NDRG1 expression imparted a biological effect on cultured OSCC cell lines, small interfering RNA was used to specifically knock down NDRG1 expression. Effective knock-down of NDRG1 expression was achieved with siRNA but had no effect on anchorage-independent

proliferation or apoptosis of cultured OSCC cell lines. Since no effect was observed here, we next examined the expression of genes involved in angiogenesis and invasion in cell lines cultured under-anchorage-independent conditions. Real-time RT-PCR results indicated that mRNA expression of invasion genes, MMP-2 and MMP-9 decreased with time of anchorage-independent cell culture. Likewise, genes involved in angiogenesis, Ang-1, PDGF-B and VEGF-C also exhibited a downward trend in mRNA expression in cells cultured under anchorage-independent conditions. However, in contrast, mRNA expression of the angiogenic cytokine, VEGF-A, increased with time of anchorage-independent cell culture, reminiscent of the increase observed for NDRG1 mRNA under the same culture conditions. A link between NDRG1 and VEGF-A expression was demonstrated, again using NDRG1 siRNA. Specific knock-down of NDRG1 expression with siRNA resulted in reduced expression of VEGF-A mRNA, as well as reduced levels of VEGF-A protein secreted into the media of cell lines cultured under anchorage-independent conditions. Luciferase reporter assays demonstrated that VEGF-A promoter activity, induced by anchorage-independent cell culture, was NDRG1-dependent.

NDRG1 expression did not appear to have an impact on tumour cell biology (i.e. proliferation and apoptosis*) in vitro*, but since *in vitro* cell culture does not depend on angiogenesis it is reasonable that no phenotypic changes would be observed. In fact, it would be useful to examine whether NDRG1 modulates neovascularisation and VEGF-A expression in an *in vivo* mouse xenograft model, using the same cell lines stably

transfected with control or NDRG1 siRNA. Moreover, it is of interest to us by what mechanism NDRG1 modulates VEGF-A expression. Since Hosoi *et al*. [137] reported that NDRG1 abrogates VEGF-A expression in cultured pancreatic cells, through the attenuation of NF-κB signalling, it may be useful to determine whether the inverse is true in our culture system. In fact, our group recently reported the upregulation of p65 (one of the subunits of the NF-κB heterodimeric complex) in the same cohort of OSCC patients used in this study[186]. Indeed, this may implicate a role for NDRG1 in the angiogenic switch essential for OSCC growth and provide a new target for cancer therapy since targeting VEGF-A using neutralising antibodies and tyrosine kinase inhibitors has been successful in the treatment of colorectal carcinoma, and has shown promising results for other cancers[213].

Our evidence that NDRG1 plays an oncogenic role in OSCC provided us with the impetus to examine what factors may be responsible for its upregulation in this disease. Using TPA as a system to drive NDRG1 expression, we showed that induced NDRG1 lies downstream of the ERK1/2 and JNK MAPK pathways. By cloning and analysing the NDRG1 promoter we showed that TPA-induced NDRG1 expression is largely dependent on EGR-1 and cJun/AP-1 transcription factors. Since EGR-1 and AP-1 have both been associated with OSCC[186;208] it will be useful to further examine their role in the modulation of NDRG1 expression. Specifically, since it has been reported that EGR-1 is a key regulator in GRO/CXC proliferative signalling in oesophageal cancer[186], the expression of NDRG1 in this system may be of interest.

Indeed, this may provide further evidence that EGR-1 contributes to tumourigenesis of oesophageal epithelial cells through the upregulation of NDRG1, and therefore VEGF-A. Another point to consider is that in other cell systems, namely prostate cancer cells, hypoxia resulted in an EGR-1-dependent transcriptional activation of HIF-1α[214]. Since VEGF-A is a transcriptional target of HIF-1 and is also induced by low oxygen tension[184], a link between EGR-1, HIF-1α and VEGF-A seems apparent. This will be a useful pathway to examine in oesophageal cancer, in the context of NDRG1 induction. Indeed, experiments exploring NDRG1, EGR-1, HIF-1α and VEGF-A expression in cell lines cultured in a hypoxic chamber will answer this question.

The study has given rise to new questions with regards to NDRG1 regulation and expression in OSCC. In the first instance, we know that in a subset of our cell lines NDRG1 expression is induced by TPA through PCK/MEK/ERK- EGR-1 and cJun/AP-1. However, both WHCO5 and KYSE520 cell lines exhibit no NDRG1 response to TPA, at both the protein expression and transcriptional level. Whether this is due to a lack of EGR-1 and AP-1 activation by TPA, or whether TPA induces expression of factors that dampen the EGR-1 and AP-1 effect, should be explored. Indeed, this observation could be a reflection of the different internal milieus within the cells. In addition, while the NDRG1 TPA response has been, in part, characterised, the factors responsible for NDRG1 expression under conditions of anchorage-independent cell culture should be examined. Specifically, we will address the possible role of EGR-1 and AP-1, amongst

others, in regulating NDRG1 expression under anchorage-independent cell culture conditions.

The possible role of NF-κB in mediating the VEGF-A response to NDRG1 expression has been discussed. However, a time course microarray study should be performed to determine what other effectors may respond to NDRG1 upregulation, under conditions of anchorage-independent cell culture, and to determine what proteins may result in changes in phenotype, specifically related to angiogenesis.

In conclusion, this study describes the transcriptional regulation of NDRG1 expression by EGR-1 and cJun/AP-1 and implicates an oncogenic role for NDRG1 in the development of OSCC by modulating VEGF-A cytokine expression. The mechanism by which NDRG1 induces VEGF-A transcription and expression must be investigated further.

CHAPTER 6

MATERIALS AND METHODS

6.1. Tissue samples for immunohistochemistry and real-time quantitative PCR

Archived paraffin embedded oesophageal tissues (squamous cell tumour tissue and matched normal tissue from the same patient) were derived from 83 patients who underwent oesophageal resection at the Department of Cardiothoracic Surgery, Groote Schuur Hospital (Observatory, South Africa), with histologically confirmed oesophageal squamous cell carcinoma. These patients, comprised of 20 females and 63 males, were treated between 1986 and 2006 with ages ranging from 23 to 80 years (mean 53.3 ± 10.1 years). Sections from the tumour-spanning region of the oesophagus occasionally contained regions of epithelium with dysplasia. Normal sections were obtained from the resection margins of the tissue. Oesophageal tissue biopsies from which RNA was prepared were snap frozen in liquid nitrogen and stored at -70^{o}C. Ethics approval for this study was granted by the Research Ethics Committee of the University of Cape Town (REC. REF: 320/2004).

6.2. Immunohistochemistry

Oesophageal tumour sections (2 µM thickness) and corresponding adjacent normal oesophageal epithelium from 83 patients who had undergone oesophagectomies were

used for the immunohistochemical analysis. After sections were dewaxed and rehydrated, antigen retrieval was carried out by pressure-cooking the sections in 10 mM citrate buffer (pH 6.0) for 2 minutes. The sections were blocked for endogenous peroxidase using 1 % hydrogen peroxide and subsequently blocked for non-specific binding by incubation in 5 % normal goat serum (DakoCytomation, Denmark) for 20 minutes. Staining was performed as previously described using a rabbit polyclonal antiserum (diluted 1:500) raised to NDRG1 that has been used previously to detect NDRG1 in cancer cell lines[113]. This was a generous gift from Prof. T. Commes (University of Montpellier, France). The tissue sections were stained in an automated DAKO Universal stainer using the IHC software (DakoCytomation). The primary antibody was detected using Envision^{TM} rabbit/mouse peroxidase (DakoCytomation) and the development of colour carried out using diaminobenzidine (DAB) (DakoCytomation). The slides were briefly counterstained in hematoxylin, mounted in Entellen (Merck, Germany) and examined under various magnifications using an Axioskop 2 Mot microscope (Zeiss, Germany). Images were captured with a Zeiss AxioCamHR camera and Axiovisio (version 4.7) software (Zeiss). The specificity of the NDRG1 stain was confirmed by using two additional primary antibodies against NDRG1, namely rabbit anti-Cap43 (1:50; 52-3557, Zymed, San Francisco, CA, USA) and mouse anti-NDRG1 (1:100; sc-100786, Santa Cruz Biotechnology, Santa Cruz, CA, USA).

6.3. RNA isolation from tissue biopsies

Total RNA was prepared from tissue biopsies using TRIzol reagent (phenol/guanidine isothiocyanate) (Invitrogen, Rockville, MD, USA), according to the manufacturer's recommendations. In short, tissue was weighed and 1 ml of TRIzol added to 100 mg tissue. Tissue samples were homogenised and left to stand at room temperature for 5 minutes. Centrifugation was then carried out at 10 000 x g for 10 minutes at 4°C and the supernatant transferred to a new tube while the insoluble material was discarded. One fifth of a millilitre of chloroform per ml TRIzol was added and the samples shaken vigorously, by hand, for 15 seconds and then placed on ice for 10 minutes. Separation of the mixture into three phases: an upper colourless, aqueous phase containing RNA, an interphase containing DNA, and a lower phase containing protein, was performed by centrifugation at 10 000 x g for 15 minutes at 4°C. The aqueous phase was removed to a new tube and RNA precipitated using 0.5 ml isopropanol/ ml TRIzol. Samples were incubated at -20°C overnight and then centrifuged at 10 000 x g for 20 minutes at 4°C. RNA pellets were washed with 75 % ethanol, air-dried and resuspended in 300 µl 0.01 % diethylpyrocarbonate(DEPC)-treated dH_2O. To further purify the RNA 200 µl isopropanol and 20 µl 3 M Sodium Acetate was added and the solution incubated for 1 hour at -20°C. Centrifugation was then carried out at 12 000 x g for 30 minutes at 4°C to pellet the RNA, followed by washing with 70 % ethanol. Lastly, RNA was air-dried and resuspended in 30 µl DEPC-treated dH_2O. RNA was quantified using a UV spectrophotometer and RNA integrity established by denaturing MOPS/formaldehyde agarose gel electrophoresis.

6.4. Cell culture

6.4.1. Cell lines and medium requirements

The human oesophageal squamous cell carcinoma cell lines WHCO1, WHCO5 and WHCO6, derived from South African patients, were a gift from Prof. R. Veale (University of Witwatersrand)[215]. KYSE30, KYSE70, KYSE180, KYSE450 and KYSE520 cell lines, established by Shimada *et al*.[216] were purchased from German Resource Centre for Biological Material, DSMZ GmbH (Braunschweig, Germany). All oesophageal cancer cell lines were maintained in Dulbecco's Modified Eagle's Medium (DMEM) supplemented with streptomycin (100 µg/mL), penicillin (100 U/mL) and 10 % Fetal Calf Serum (FCS) (Gibco, Paisley, Scotland). HUVEC cells, a gift from Dr. N. Davies (University of Cape Town) were grown in DMEM supplemented with streptomycin (100 µg/mL), penicillin (100 U/mL), 10 % Fetal Calf Serum (FCS), epidermal growth factor (10 ng/ml), hydrocortisone (1 µg/ml) and 2 mM L-Glutamine (Sigma-Aldrich Inc., St Louis, USA). All cell lines were cultured in a humidified atmosphere of 5 % carbon dioxide at 37^{o}C and routinely tested for mycoplasm contamination using Hoechst 33258 fluorochrome stain (Sigma-Aldrich, Inc.).

6.4.2. Subculturing cells

Cells in a 100 mm culture dish were washed with 2 ml of trypsin-EDTA trypsinisation solution and the solution aspirated off. Three millilitres of fresh trypsin-EDTA solution was added to the cells and trypsinisation monitored with a microscope (Zeiss). When

70-80% of cells were trypsinised, the reaction was stopped with the addition of 3 ml of fresh DMEM medium containing serum. The cell suspension was transferred to a 10 ml Falcon tube and centrifuged at 250 x g for 5 min at 4^{o}C. The medium/trypsin solution was aspirated off and the cells resuspended in 1 ml of culture medium. Approximately 200 µl of this cell suspension was then inoculated into 10 ml of fresh medium in a 100 mm culture dish. For anchorage-independent cell growth assays, cell lines were cultured at a concentration of 0.5 x 10^{6} cells/ml in culture dishes coated with Poly(2-hydroxyethyl methacrylate) (poly-HEMA; Sigma-Aldrich Inc.) that had been dissolved in 96 % ethanol (10 mg/ml)[217].

6.4.3. Freezing and thawing cells

A confluent dish of cells was trypsinised, neutralised with complete medium, followed by centrifugation to remove cells from trypsinisation solution. Cells were suspended in 5 ml of pre-chilled freezing medium (70 % culture medium, 20 % FCS and 10 % dimethylsulfoxide (DMSO)) and transferred into cryotubes. Tubes were left at -80^{o}C overnight and then transferred to liquid nitrogen.

To thaw cells, the frozen cell suspension was quickly thawed in a 37^{o}C waterbath and then cells transferred to a 10 ml tube containing 8 ml of complete growth medium. Cells, pelleted by centrifugation at 250 x g for 5 min at 4^{o}C, were resuspended in 2 ml

of complete growth medium and inoculated into 10 ml of fresh medium in a 100 mm culture dish.

6.5. Drugs and inhibitors

12-*o*-tetradecanoylphorbol-13-acetate (TPA) was purchased from Sigma (Sigma-Aldrich Inc.). PKC inhibitor (GF109203x), JNK inhibitor (SP600125), MEK inhibitor (PD98059), Akt inhibitor VIII (Akti1/2) and p38 inhibitor (SB203580) were purchased from Calbiochem (EMD Biosciences, Inc. San Diego, USA). EGFR inhibitor (AG1478) was purchased from Biomol International (Exeter, UK). All drugs were resuspended in tissue culture grade DMSO (Sigma-Aldrich Inc.) unless otherwise stated.

6.6. Preparation of cultured cell blocks for immunocytochemistry

Cells were cultured under anchorage-dependent or -independent conditions for 48 hours. Adherent cells were lifted from plates using 0.2 % (w/v) EDTA in PBS. Cells from both conditions were then collected by gentle centrifugation for 5 min at 100 x g in 50 ml tubes. All but 5 ml of PBS was aspirated off, and to this 5 ml of ice cold buffered 4 % paraformaldehyde. After gentle mixing, the cells were transferred to a 12 ml tube and centrifuged as before. The supernatant was discarded and 10 ml of fresh ice cold 4 % paraformaldehyde was gently added on top of the cell pellet. This was left to stand for two hours at 4^{o}C. Again, the supernatant was removed and the cell pellet was gently flushed with PBS, without mixing. After recentrfugation, 10 ml of room

temperature 80 % ethanol was added to the cell pellet. Fixed cells were embedded in paraffin blocks and sectioned at American HistoLabs (Gaithersburg, MD, USA).

6.7. RNA isolation from cultured cells

RNA was harvested from cells, subjected to the appropriate treatment, using Qiazol (Qiagen, Hilden, Germany), according to the manufacturer's recommendations. In short, 0.2 ml chloroform was added per ml of Qiazol used, samples were mixed vigorously for 15 seconds and left on ice for 10 minutes. Centrifugation was carried out at 10 000 x *g* and the upper aqueous phase removed to a new eppendorf tube. RNA was precipitated using 0.5 ml isopropanol per ml Qiazol at -20°C overnight. The next day, samples were centrifuged at 10 000 x g for 20 minutes and RNA pellets washed with 75 % ethanol. The RNA pellets were subsequently air-dried and resuspended in 30 µl 0.01 % DEPC-treated dH_2O. RNA was quantified using a UV spectrophotometer and RNA integrity established by denaturing MOPS/formaldehyde agarose gel electrophoresis.

6.8. RNA quantification and MOPS/formaldehyde agarose gel electrophoresis

RNA was quantified using an ultra violet (UV) spectrophotometer. The RNA suspension was diluted 1:250 and the UV absorbance measured at 260 nm and 280 nm on a Beckman DU 650 Spectrophotometer (Beckman, Brea, CA, USA). The concentration of

RNA was calculated as follows:

$$\text{RNA } (\mu g/ml) = OD_{260\ nm} \times e \times \text{dilution factor}$$

Where *e* (extinction coefficient) for RNA = 40

The purity of RNA was tested by measuring $OD_{260\ nm}/OD_{280\ nm}$ where only ratios of less than 2.0 were considered for use.

RNA quality was determined by MOPS/formaldehyde agarose gel electrophoresis. Briefly, 2 µg of each RNA sample was prepared in a final volume of 13 µl of 1 x RNA loading buffer. To prepare a 50 ml gel, 1.5 % (w/v) agarose was dissolved by heating in 1 x MOPS solution and allowed to cool. Two and a half microlitres of ethidium bromide (10 mg/ml) and 2.7 ml of 37 % formaldehyde were then added, and the gel cast. Once the gel had set, RNA samples were electrophoresed using 1 x MOPS buffer until 28s, 18s and 5s rRNA bands could be visualised under UV light. Samples were only considered for use if bands were visible and of a good quality as seen in Figure 6.1.

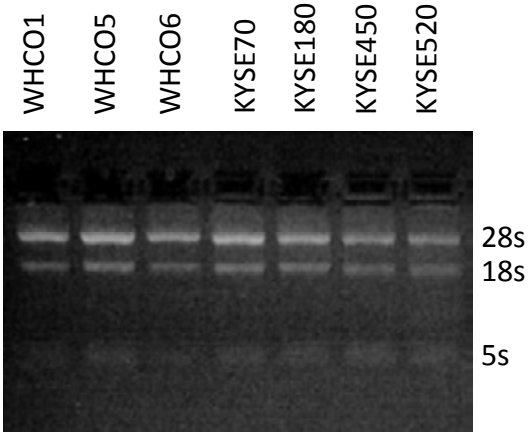

Figure 6.1. MOPS/formaldehyde agarose gel electrophoresis of RNA samples prepared using Qiazol. RNA prepared from cultured cell lines (WHCO1, WHCO5, WHCO6, KYSE70, KYSE180 and KYSE450) was subjected to electrophoresis on a MOPS/formaldehyde agarose gel to assess RNA quality. Positions of 28s, 18s and 5s rRNA are indicated.

6.9. Quantitative real-time RT-PCR

Quantitative real-time RT-PCR analysis on RNA extracted from tissue biopsies and cell lines was carried out using the StepOne Real-time PCR System (Applied Biosystems, Foster City, CA, USA). Reverse transcription cDNA synthesis was performed using 2 µg of total RNA from each sample, 2.5 µM oligo $(dT)_{20}$ primer, 2 mM $MgCl_2$, 1 mM dNTPs, 1 µl ImPromII Reverse Transcriptase II (Promega, Madison, WI, USA), 1 µl RNAsin (Promega) and 1 X ImPromII reaction buffer (Promega) in a final volume of 20 µl. cDNA was subsequently amplified using the KAPA SYBR Fast qPCR Master Mix (KAPA Biosystems, Woburn, MA, USA) and 200 nM of the primer pairs presented in Table 6.1. All primer pairs were designed to span introns to exclude amplification of contaminating genomic DNA. PCR cycling conditions were 95°C for 3 minutes, followed by 40 cycles of 95°C for 1 second and T_a for 20 seconds. Results were

Table 6.1. Real-time RT-PCR primer sequences, annealing temperatures and product sizes

Gene/Primer	Sequence	PCR product size (bp)	T_a (°C)
NDRG1 Forward	5’ GTGCGGAAGGCTGGATGG 3’	144	60
NDRG1 Reverse	5’ ACAATGTGCTGGCGGTAGG 3’		
VEGF-A Forward	5’ TTCATGGATGTCTATCAGCG 3’	236	60
VEGF-A Reverse	5’ GCTCATCTCTCCTATGTGCT 3’		
VEGF-C Forward	5’ GCCAACCTCAACTCAAGGAC 3’	200	60
VEGF-C Reverse	5’ CCCACATCTGTAGACGGACA 3’		
Ang-1 Forward	5’ GGACAGCAGGAAAACAGAGC 3’	292	60
Ang-1 Reverse	5’ TAATCGCTTCTGACATTGCG 3’		
PDGF-B Forward	5’ TTATGAGATGCTGAGTGACCAC 3’	156	55
PDGF-B Reverse	5’ CCTTCTTCCACGAGCCAAG 3’		
MMP-2 Forward	5’ CCCTCGCAAGCCCAAGT 3’	102	60
MMP-2 Reverse	5’ GCACGAGCAAAGGCATCAT 3’		
MMP-9 Forward	5’ CCTGGGCAGATTCCAAACCT 3’	88	53
MMP-9 Reverse	5’ GCAAGTCTTCCGAGTAGTTTTGGAT 3’		
Cyclophilin D Forward	5’ TGAGACAGCAGATAGAGCCAAGC 3’	94	60
Cyclophilin D Reverse	5’ TCCCTGCCAATTTGACATCTTC 3’		
GusB Forward	5’ CTCATTTGGAATTTTGCCGATT 3’	81	60
GusB Reverse	5’ CCGAGTGAAGATCCCCTTTTTA 3’		

T_a refers to the annealing temperature used in the cycling stage of the real-time RT-PCR

standardised using the house-keeping genes, *β-glucuronidase* (*gusB*) and/or *cyclophilin D*. Data was analysed using the comparative threshold cycle (C_T) method to compute the expression fold change between samples[218].

6.10. Immunofluorescent analysis of cultured cells

For immunofluorescent analysis of protein expression and localisation, cultured cells were seeded, at a density of 2 x 10^5, on sterile coverslips in 35 mm dishes and left to grow for 36 hours. Cells were fixed in 4 % paraformaldehyde at room temperature for 20 minutes. To permeabilise the cells, coverslips were soaked in 0.1 % Triton X-100 in PBS for 5 minutes followed by 50mM NH_4Cl in PBS for 5 minutes to quench the reaction, and blocked in 0.2 % gelatin for 45 minutes. Coverslips were then incubated with primary antibody; specifically, rabbit α-NDRG1 primary antibody (1:500) and/or mouse α-E-cadherin primary antibody (1:2; 08-1223, Zymed) overnight in a humidified chamber at 4^{o}C. The next day, primary antibody was removed by 3 washes in PBS, and secondary antibodies, Cy3-conjugated goat anti-rabbit antibody (1:300; Jackson ImmunoResearch, West Grove, PA, USA), Cy3-conjugated goat anti-mouse antibody, (1:300; Jackson ImmunoResearch) or Alexa488-conjugated goat anti-rabbit antibody (1:400; Invitrogen), were applied for a further 45 minutes. Cell nuclei were stained with DAPI (100 ng/ml) for 5 minutes, followed by washing in PBS. Coverslips were mounted on slides with Mowiol. Slides were examined under various magnifications using an Axiovert 200M microscope (Zeiss). Images were captured with a Zeiss AxioCamHRm camera and Axiovisio (version 4.7) software (Zeiss).

6.11. Anchorage-independent cell proliferation (MTT) assay

The effect of control and NDRG1 siRNA on anchorage-independent cell proliferation was measured using the MTT (3-[4,5-dimethylthiazol-2-yl]-2,5-diphenyltetrazolium bromide) assay. In short, cells were transfected with 20 nM of either control or NDRG1 siRNA. The next day, transfectants were seeded into poly-HEMA coated 96-well plates, in a final volume of 100 µl, at a concentration of 10 000 cells/well. After the prescribed time of growth, 10 µl of MTT reagent (Roche, Basel, Switzerland) was added per well, and the plates were incubated at 37^{o}C for 4 hours. One hundred microlitres of solubilisation solution was then added to each well. After overnight incubation at 37^{o}C, absorbencies were read at $OD_{595\ nm}$ using a microplate reader (BioTek, Winooski, VT, USA).

6.12. Caspase-Glo®3/7 Apoptosis assay

The extent of apoptosis was determined by measuring Caspase-3/7 activity, using the Caspase-Glo®3/7 Assay (Promega), according to the manufacturer's instructions. Cells were seeded into normal, or poly-HEMA coated 96-well plates, in a final volume of 100 µl, at a concentration of 8000 cells/well. After 72 hours of anchorage-dependent or -independent growth, 100 µl of Caspase-Glo 3/7 reagent was added to each well. The plates were left at room temperature for 1 hour, after which 100 µl of cell/Caspase-Glo 3/7 suspension was transferred to a white 96-well plate (Nunc, Rochester, NY, USA). Luminescence was measured using the Glomax 96 Microplate Luminometer

(Promega). To determine the effect of control or NDRG1 siRNA on apoptosis, cells were first transfected with 20 nM of control or NDRG1 siRNA. The next day cells were seeded into poly-HEMA coated 96-well plates. The cells were then cultured for 72 hours, and the Caspase-Glo®3/7 Assay performed as described above.

6.13. *In vitro* transwell migration assay

Transwell inserts with 8 µM pores were used in this assay (Greiner bio-one, Solingen Germany). Conditioned medium, to act as HUVEC chemoattractant, was prepared by culturing OSCC cell lines, at a density of 0.5 x 10^6 cells/ml, in an anchorage-independent manner for 72 hours. Cells were removed from the medium by centrifugation (100 x g, 5 min) and 1 ml of the cell-free supernatant transferred to each well of a 12-well transwell plate. HUVECs, which had been starved overnight in complete medium containing 5 % FCS, were seeded into the top chambers of the transwell plate at a density of 2.0 x 10^5 cells/well. After an 8 hour incubation, non-migrated cells, on the upper surface of the transwell filter, were gently removed with a cotton swab. Cells which had migrated through the filter were fixed in 100 % methanol, for 10 minutes at room temperature, after which the filters were air dried. Cells were stained with crystal violet (2 % (v/v) ethanol, 0.2 % (w/v) crystal violet) for 20 minutes and then washed gently with distilled water to remove excess stain. Cell were then visualised under a microscope and counted in four fields of view, on duplicate filters. To neutralise VEGF-A, 5 µg/ml of rabbit anti-human VEGF-A antibody

(PeproTech Asia, Rehovot, Israel) was added to the conditioned medium in the bottom wells, where applicable.

6.14. VEGF-A ELISA

VEGF-A ELISA, to measure the concentration of VEGF-A secreted into the medium, was performed as described by the manufacturer (PeproTech Asia). Briefly, cell lines were cultured under anchorage-dependent or -independent conditions for the indicated times. Media, with or without cells, was removed to a tube and centrifuged (200 x g, 5 min) to remove cells. The supernatant was transferred to a new tube and kept at -80^{o}C. ELISA microplates (Nunc) were coated with capture antibody overnight at room temperature, and then washed. After blocking for 1 hour, and washing, standards and 100 µl of each sample (thawed to room temperature) were added to wells, in triplicate, and left at room temperature for 2 hours. Following incubation with the detection antibody for 2 hours, avidin-HRP conjugate was added, and the colour development carried out using ABTS liquid substrate (Sigma-Aldrich Inc.). Absorbance was measured on a microplate reader (BioTek) at 405 nm.

6.15. Western blot analysis

6.15.1. Preparation of whole cell lysates and protein quantification

For anchorage-dependent cultured cells, cells were treated with drug, or grown in the prescribed fashion, for the indicated times. Medium was removed, cells rinsed twice

with chilled phosphate-buffered saline (PBS), and rinses and media were subjected to centrifugation (150 x g, 5 min) to pellet any non-adherent cells. Cells in the culture dish were lysed using a rubber policeman, on ice, in radioimmunoprecipitation assay (RIPA) buffer containing 1 x complete protease inhibitor cocktail (Roche) and 1 mM sodium orthovanadate and 20 mM sodium fluoride, to inhibit the action of phosphatases. The pellet of non-adherent cells was taken up in the resulting lysis solution. For cells cultured in an anchorage-independent manner, cells were grown for the indicated times and then pelleted by centrifugation (150 x g, 5 min). The resulting cell pellet was washed twice with chilled PBS and the cells then resuspended in RIPA buffer using a pipette. All lysates were subjected to sonication at 4^{o}C and stored at -80^{o}C.

Protein quantification was carried out in 96-well plates using the Bicinchoninic Acid (BCA) protein assay kit (Pierce, Thermo Scientific, Rockford, IL, USA), according to the manufacturer's instructions. Absorbencies of BSA protein standards and cell lysates were read at $OD_{595\ nm}$ using a microplate reader (BioTek).

6.15.2. Sodium dodecyl sulphate polyacrylamide gel electrophoresis (SDS-PAGE) and protein transfer

The SDS-PAGE was performed using the BioRad MINI PROTEIN II gel system (BioRad, Hercules, CA, USA). Protein samples were prepared by mixing equivalent amounts of

protein with protein loading dye, and boiling for 5 minutes at 90^{o}C. SDS-polyacrylamide gels were prepared with 10 % acrylamide separating and 4 % acrylamide stacking gels. Samples were loaded into the wells of SDS-10 % polyacrylamide gels and subjected to electrophoresis at 150 volts, for the appropriate time. Kaleidoscope protein molecular weight marker (BioRad) was used to determine the size of the proteins. Following separation, proteins were transferred to HybondTM-ECL^{TM} nitrocellulose membrane (Amersham Biosciences, Buckinghamshire, UK) using a buffered tank transfer system, at 100 volts for 1 hour.

6.15.3. Immunoblotting and chemiluminescent detection

Following protein separation and transfer, membranes were blocked with a solution of 5 % (w/v) fat free milk (referred to from now on as milk) diluted in Tris-buffered saline (pH 7.4) containing 0.1 % Tween-20 (TBST), for 1 hour at room temperature. Subsequent to blocking, primary antibody was added (Table 6.2) and the membranes left overnight at 4^{o}C, with shaking. The next day, after primary antibody was removed and the membrane washed three times for 10 minutes with TBST, the secondary antibody was added for 1 hour at room temperature. After another three washes with TBST antibody detection was performed, using the Supersignal West Pico or Supersignal West Dura kits (Pierce), depending on the strength of the signal. Chemiluminescent light emission was detected on X-ray film (AGFA) and visualised by developing the film by hand, for 2 minutes in developer (AGFA G128), washed for 2

Table 6.2. Antibodies and conditions used for Western blot analysis

Primary Antibody	Primary Antibody Conditions	Secondary Antibody	Secondary Antibody Conditions	Substrate
NDRG1 [sc-30040, SCBT*]	1:1000 in 5 % Milk in TBST	Goat anti-Rabbit [BioRad]	1:1000 in 5 % Milk in TBST	West Dura
β-Tubulin [sc-9104, SCBT]	1:1000 in TBST	Goat anti-Rabbit [BioRad]	1:1000 in 5 % Milk in TBST	West Pico
EGR-1 [4153, CST**]	1:1000 in 5 % BSA in TBST	Goat anti-Rabbit [BioRad]	1:1000 in 5 % Milk in TBST	West Dura
phospho-ERK1/2 (Thr 202/Tyr 204) [9106, CST]	1:750 in 2.5 % BSA in TBST	Goat anti-Mouse [BioRad]	1:1000 in 2.5 % Milk in TBST	West Dura
ERK2 [sc-154, SCBT]	1:1000 in 1 % Milk in TBST	Goat anti-Rabbit [BioRad]	1:1000 in 2.5 % Milk in TBST	West Pico
phospho-cJun (Ser 63/73) [sc-16312-R, SCBT]	1:1000 in 5 % BSA in TBST	Goat anti-Rabbit [BioRad]	1:1000 in 5 % Milk in TBST	West Pico
cJun [sc-1694, SCBT]	1:1000 in 5 % BSA in TBST	Goat anti-Rabbit [BioRad]	1:1000 in 5 % Milk in TBST	West Pico
phospho-p38 (Thr 180/ Tyr 182) [9211, CST]	1:1000 in TBST	Goat anti-Rabbit [BioRad]	1:1000 in 5 % Milk in TBST	West Dura
p38 [M 0800, Sigma]	1:5000 in TBST	Goat anti-Rabbit [BioRad]	1:1000 in 5 % Milk in TBST	West Pico
phospho SAPK/JNK (Thr 183/ Tyr 185) [9251,CST]	1:1000 in 5 % Milk in TBST	Goat anti-Rabbit [BioRad]	1:1000 in 5 % Milk in TBST	West Dura
SAPK/JNK [9258, CST]	1:1000 in 5 % Milk in TBST	Goat anti-Rabbit [BioRad]	1:1000 in 5 % Milk in TBST	West Pico
phospho-AKT (Ser 473) [9271,CST]	1:1000 in 5 % Milk in TBST	Goat anti-Rabbit [BioRad]	1:1000 in 5 % Milk in TBST	West Dura
AKT [9272, CST]	1:1000 in 5 % Milk in TBST	Goat anti-Rabbit [BioRad]	1:1000 in 5 % Milk in TBST	West Dura

*SCBT - Santa Cruz biotechnology **CST - Cell Signaling Technology, Danvers, MA, USA BSA - Bovine serum albumin

minutes with water, and then fixed for 5 minutes in AGFA G333C fixative, as recommended by the manufacturer.

6.15.4. Stripping and reprobing blots

After detection blots were stripped by soaking in stripping buffer at room temperature for 20 minutes, without shaking. Membranes were then washed four times with TBST after which blocking and reprobing with a new antibody could proceed.

6.16. RNA interference

Small interfering RNA was purchased from Santa Cruz Biotechnology. EGR-1 (sc-29303) and cJun (sc-29223) siRNAs are 20-25 nucleotides designed to specifically knock down expression of target genes. Control siRNA (sc-37007) is non-targeting 20-25 nucleotide siRNA designed as a negative control. Transient transfection of siRNA was performed using Transfectin transfection reagent (BioRad). Depending on the application, either 35 mm or 60 mm culture dishes containing 40-60 % confluent cells were transfected. For a 35 mm culture dish or a single well of a 6-well plate, 0.625 µl of Transfectin reagent was added to 50 µl of serum-, penicillin- and streptomycin-free medium in an eppendorf tube. After a 5 minute incubation at room temperature, 2 µl of 10 µM siRNA was added and the tube left again at room temperature for 20 minutes. The transfection cocktail was then added dropwise to the cells in 1 ml of media (with 10 % FCS and streptomycin (100 µg/mL), penicillin (100 U/mL)), giving a

final concentration of 20 nM siRNA. The next day media was changed and the cells were treated or grown as described. To transfect cells plated in 60 mm culture dishes, the reaction was scaled up accordingly.

6.17. VEGF-A reporter assay

The VEGF-A promoter (-2018 to +50) reporter construct, pVEGF-Luc, was a generous gift from Prof. Alan Knox, University of Knottingham, UK. To examine the activity of the VEGF-A promoter (-2018 to +50) reporter construct in cultured cells, Effectene transfection reagent (Qiagen) was used to transfect cells, at 70 % confluence, in 60 mm culture dishes. Briefly, 1 µg of pVEGF-Luc or pGL3-Basic, 10 ng of pRL-TK (that encodes *Renilla* luciferase) and 8 µl of Enhancer solution were added to 150 µl of EC buffer and left at room temperature for 5 minutes. Twenty-five microlitres of Effectene reagent was then added to the transfection mix. After 10 minutes at room temperature, 1 ml of complete growth medium was added and the transfection mix added dropwise to the cells in 4 ml of complete growth medium. The next day, cells were trypsinised and subjected to anchorage-dependent or -independent growth for 48 hours. Total cell lysates were prepared in 200 µl of 1 X Passive Lysis Buffer (Promega) and firefly luciferase activity was assayed using the Dual Luciferease Kit (Promega) and the Glomax 96 microplate luminometer (Promega). Activity was normalised to the *Renilla* luciferase activity from pRL-TK in the same lysate.

To determine the effect of control or NDRG1 siRNA on pVEGF-Luc activity in cells cultured under anchorage-independent conditions, cells, at 40 % confluence in 60 mm dishes were first transfected with siRNA as described in section 6.16. The next day, media was changed and the cells were transfected with pVEGF-Luc and pRL-TK and subjected to anchorage-independent growth and analysis as described above.

6.18. Preparation of NDRG1 5' regulatory region reporter plasmids

6.18.1. PCR amplification of NDRG1 (-2100 to +12), (-1500 to +12), (-1200 to +12), (-900 to +12) and (-298 to +12) regulatory regions

Primers were designed to amplify the NDRG1 -2100 bp to +12 bp promoter fragment, and deletion mutants thereof, from the published genomic sequence for NDRG1 and its contiguous regions (GenBank accession number NT_008046; appendix 1). The primer sequences, relative positions and annealing temperature used for PCR are listed in Table 6.3.

The DNA template, used for PCR amplification of the 5' NDRG1 regions, was genomic DNA that had previously been extracted from the blood of a normal individual. The PCR reactions were performed using the Expand High Fidelity^{PLUS} PCR System (Roche, Mannheim, Germany) as follows: 400 ng of template DNA, 0.5 µM of the appropriate forward primer, 0.5 µM of +12 reverse primer, 5 % (v/v) DMSO, 0.2 mM dNTPs, 2.5 U Expand^{PLUS} high fidelity DNA Polymerase, 3 mM $MgCl_2$ and 1 X Polymerase Reaction

Table 6.3. Primers used to amplify NDRG1 regulatory sequences

Primer name	Sequence	Position	PCR product size (bp)	Ta (°C)
-2100 F	5' GTCTCATTATGTTGCTCAGA 3'	-2100 to -2080	2112	57
-1500 F	5' CTCTCCCTTTGCCAGTGAGA 3'	-1500 to -1480	1512	57
-1200 F	5' TTGCCCTGGGTCTGGTCCTG 3'	-1200 to -1180	1212	57
-900 F	5' CATATGCAGTAGGGGTTGAG 3'	-900 to -880	912	57
-298 F	5' CCCGCTGCACAGGCCGAG 3'	-298 to -280	310	57
+12 R	5' GCGAGGTTTGTTTACGTCCG 3'	-8 to +12	-	

PCR product size refers to the size of PCR product using the listed forward primers with the +12R reverse primer

Buffer. PCR cycling conditions were: 94°C for 4 minutes, followed by 30 cycles of 94°C for 40 seconds, 57°C for 40 seconds and 72°C for two and a half minutes, and a final extension step of 72°C for 7 minutes. PCR products were subjected to 1 % agarose gel electrophoresis. Bands of the correct size were cut out of the gel and purified using the Wizard^{R} SV Gel and PCR Clean-Up System (Promega) and eluted in 40 µl of distilled water.

6.18.2. 3'-Adenine tailing reactions

Since a high fidelity, proof reading polymerase was used to generate the PCR products, a 3' adenine tailing reaction was performed, to facilitate thymidine/adenine cloning

into the TOPO-XL PCR cloning vector (Invitrogen). Briefly, 3' adenine residues were added to 10 µl of purified PCR product in a reaction containing 5 U Taq polymerase (Stratagene, La Jolla, CA, USA), 1 X Taq buffer, 2.5 mM $MgCl_2$ and 0.2 mM dATP. Reactions proceeded at 70°C for 30 min.

6.18.3. Subcloning of A-tailed promoter PCR products into pCR-TOPO-XL

After the A-tailing reaction, PCR products were ligated directly with the pCR-TOPO-XL vector. In short, 4 µl of A-tailed reaction was ligated with 1 µl of pCR-TOPO-XL vector. After 5 minutes at room temperature, 1 µl of 6 x TOPO Cloning Stop Solution (Invitrogen) was added, and the tubes placed on ice. Two microlitres of the TOPO cloning reaction was used to transform one vial of One Shot cells (Invitrogen) by incubating on ice for 30 minutes, followed by heat shock at 42^{o}C for 30 seconds, and then placed on ice for a further 2 minutes. To the transformation reaction 250 µl of S.O.C. medium (Invitrogen) was added followed by incubation of the bacterial cells at 37^{o}C for 1 hour with shaking (200 rpm). One hundred microlitres of each transformation was spread on a pre-warmed LB agar plate containing 50 µg/ml kanamycin, for clone selection.

6.18.4. Small scale plasmid preparation of pCR-TOPO-XL-NDRG1 promoter constructs

The next day, colonies were selected and inoculated into 5 ml of LB broth containing 50 µg/ml kanamycin. After approximately 16 hours of incubation at 37^{o}C, with shaking

(220 rpm), glycerol stocks were prepared by mixing 500 µl of overnight culture with 500 µl sterile 80 % Glycerol and storing at -80°C. The remaining cultures were subjected to small scale plasmid preparation using the QIAGEN Miniprep Kit (Qiagen), as recommended by the manufacturer.

The identity of correct pCR-TOPO-XL-NDRG1 promoter constructs was confirmed by *Apa*I restriction digestion (Promega). Since *Apa*I cuts once in pCR-TOPO-XL and once in the 3' end of all PCR products, two restriction products were expected for all plasmids generated. *Apa*I restriction fragment sizes of pCR-TOPO-XL-NDRG1 promoter constructs, with NDRG1 promoter fragments in the correct orientation, are listed in Table 6.4.

Table 6.4. *Apa*I restriction products of pCR-TOPO-XL-NDRG1 promoter constructs

Plasmid	*Apa*I restriction products
TOPO(-2100 to +12)	5304 bp and 308 bp
TOPO(-1500 to +12)	4704 bp and 308 bp
TOPO(-1200 to +12)	4404 bp and 308 bp
TOPO(-900 to +12)	4092 bp and 308 bp
TOPO(-298 to +12)	3490 bp and 308 bp

6.18.5. Sequence analysis

Plasmids with inserts of the correct size and orientation were subjected to sequence analysis using the UCT Human Genetics Sequencing Unit. The sequencing reaction was performed with the ABI PRISM BigDye Terminator v3.0 Cycle Sequencing Ready Reaction Kit (Applied Biosystems). Sequencing reactions were performed with 4 µl of Big Dye Mix on 300 ng of template DNA with 2 µM of primer in a total volume of 20 µl. Primers used in independent sequencing reactions on each sample are listed in Table 6.5. The cycling conditions were as follows: 96^{o}C for 1 min, followed by 25 cycles of T_a for 15 sec and 60^{o}C for 4 min. Samples were subjected to automated sequencing and data collected using ABI Prism Model 3100, Version 3.7 collection software.

Table 6.5. Primers used in pCR-TOPO-XL-NDRG1 promoter construct sequencing

Primer	Sequence	Position in promoter	T_a (°C)
T7 primer	5’ TAATACGACTCACTATAGGG 3’	In pCR-TOPO-XL	45
M13 Reverse	5' CAGGAAACAGCTATGAC 3'	In pCR-TOPO-XL	45
-1500 F	5’ CTCTCCCTTTGCCAGTGAGA 3’	-1500 to -1480	57
-900 F	5’ CATATGCAGTAGGGGTTGAG 3’	-900 to -880	57
-298 F	5’ CCCGCTGCACAGGCCGAG 3’	-298 to -280	57

6.18.6. Preparation of pGL3-NDRG1-promoter reporter plasmids

Sequence confirmed NDRG1 promoter fragments were released from recombinant pCR-TOPO-XL-NDRG1 constructs by restriction enzyme digestion with *Kpn*I and *Xho*I (Invitrogen). Released promoter fragment inserts with 5' *Kpn*I and 3' *Xho*I restriction overhangs were gel purified and ligated with pGL3-Basic, which had also been digested with *Kpn*I and *Xho*I, upstream of the *luciferase* gene.

Using the equation:

ng vector/Kb vector X Kb insert X molar ratio (insert(4):vector(1)) = ng insert

and using 100 ng of vector, insert and vector DNA were combined and ligations were performed using 3 U T4 DNA ligase (Promega) and 1 X T4 DNA ligase buffer in a final volume of 10 µl. Ligations were performed overnight at 16°C. The next day, 5 µl of ligation reaction was transformed into highly competent JM109 cells and positive clones selected on LB agar plates containing 50 µg/ml ampicillin. Colonies were picked the next day, glycerol stocks prepared, and screened for the correct inserts by *Kpn*I and *Apa*I restriction enzyme digestion analysis (data not shown), and *Bam*HI in the case of pGL3-NDRG1-(2100 to +12) (Chapter 4, Fig. 4.2) based on restriction enzyme availability at the time.

6.18.7. Large scale plasmid preparation of pGL3-NDRG1-promoter reporter plasmids

Positive clones identified above were cultured for large-scale plasmid preparation using the Qiagen Plasmid Maxi-Prep Kit. Plasmid DNA was prepared as recommended

by the manufacturer (QIAGEN). Starter cultures were prepared by inoculating 5 µl of glycerol stock into 5 ml of LB Broth containing 50 µg/ml ampicillin. Cultures were grown for approximately 8 hours at 37^{o}C with shaking at 200 rpm. The starter culture was then diluted 1/500 to 400 ml with LB broth containing 50 µg/ml ampicillin. Cultures were grown at 37^{o}C for approximately 12 hours with shaking (200 rpm). Bacterial cells were harvested by centrifugation (6000 x g, 15 min, 4^{o}C) in a Beckman JA-10 rotor (Beckman, J-21B centrifuge) and the supernatant discarded. The cell pellet was resuspended in 10 ml of Buffer P1 (containing RNaseA) followed by lysis with the addition of 10 ml Buffer P2. After 5 minutes at room temperature, 10 ml of chilled Buffer P3 was added and the solution left on ice for 20 minutes. The solution was then centrifuged (20 000 x g, 30 min, 4^{o}C) in a Beckman JA-20 rotor after which the supernatant was removed to a new tube and centrifuged as before for 15 minutes. Applying 10 ml Buffer QBT and allowing it to enter the column by gravity flow equilibrated the QIAGEN-tip 500 column. The supernatant was then applied and allowed to enter the resin by gravity flow. The column was washed twice with 30 ml Buffer QC to remove contaminants. Plasmid DNA was then eluted with 15 ml of high salt Buffer QF and precipitated with the addition of 10.5 ml of room-temperature isopropanol. Precipitated plasmid DNA was collected by centrifugation at 15 000 x g for 30 minutes at 4^{o}C and the supernatant discarded. The DNA pellet was washed with 5 ml of room temperature 70 % ethanol and centrifuged at 15 000 x g for 10 minutes at 4^{o}C. The supernatant was discarded and the DNA pellet left to air-dry. Finally, the plasmid DNA was resuspended in an appropriate amount of TE, pH 8.0. Isolation of the

correct plasmids was again confirmed by *Kpn*I and *Apa*I restriction enzyme digestion and *Bam*HI digestion in the case of pGL3-NDRG1-(-2100 to +12).

6.18.8. Preparation of pGL3-NDRG1-(-2100 to +305) reporter plasmid

Primers were designed to PCR amplify the NDRG1 regulatory region from -296 to +305 for subcloning into the pGL3-NDRG1(-2100 to +12) reporter plasmid. Primers were designed against the published genomic sequence for NDRG1 and its contiguous regions (appendix 1). The reverse primer was designed to generate a PCR product containing a 3' *Xho*I restriction site. Primers are described in Table 6.6.

PCR reactions and cycling conditions were as described in section 6.18.1, using a T_a of 62^{o}C The resulting PCR product was cloned into pCR-TOPO-XL as described in section 6.18.3. and sequence confirmed using the T7 primer. Correct clones were cultured and large scale plasmid preparations performed. The -243 to +305 NDRG1 regulatory region was released from the pCR-TOPO-XL-NDRG1(-296 to +305) plasmid by *Apa*I and *Xho*I restriction enzyme digestion, and isolated by agarose gel electrophoresis and gel purification. This fragment was cloned into *Apa*I and *Xho*I digested pGL3-NDRG1(-2100 to +12) plasmid to generate the pGL3-NDRG1(-2100 to +305) reporter construct. Identity of this construct was confirmed by *Nco*I digestion, which gave the correct size fragment of 1683 bp and 5521 bp (data not shown).

Table 6.6. Primers used to PCR amplify the NDRG1 -296 to +305 regulatory region

Primer	Sequence	Position in promoter	T_a (°C)
NDRG1-300FWD	5’ CGCTGCACAGGCCGAG 3’	-296 to -281	62
NDRG1+300REV	5' GACTCGAGCGGTGTCTGCACCCAA 3'	+288 to +305	62

The *Xho*I restriction site incorporated into the reverse primer is underlined

6.18.9. Preparation of pGL3-NDRG1-(-4818 to +12) and (-4818 to +305) reporter plasmids

Primers were designed to PCR amplify the NDRG1 regulatory region from -4819 to -1280 for subcloning into the pGL3-NDRG1(-2100 to +12) and pGL3-NDRG1(-2100 to +305) reporter plasmids. Primers were designed against the published genomic sequence for NDRG1 and its contiguous regions (appendix 1). The forward primer was designed to generate a PCR product containing a 5’ *Kpn*I restriction site. Primers are described in Table 6.7 below.

Table 6.7. Primers used to PCR amplify the NDRG1 -4819 to -1280 regulatory region

Primer	Sequence	Position in promoter	T_a (°C)
NDRG1 proForward	5’ CAGGTACCGGCATGCTTGCAGATAAC 3’	-4819 to -4793	48
NDRG1 proRevNco	5' TCTGTGCCAACCCATGC 3'	-1297 to -1280	48

The *Kpn*I restriction site incorporated into the forward primer is underlined

PCR reactions and cycling conditions were as described in section 6.18.1, using a T_a of 48^{o}C The resulting PCR product was cleaned using the Wizard^{R} SV Gel and PCR Clean-Up System and digested with *Kpn*I and *Nco*I restriction enzymes, releasing the -4819 to -1319 NDRG1 promoter fragment. This fragment was cloned into the *Kpn*I and *Nco*I restriction sites of the pGL3-Basic vector as described in section 6.18.6. Correct plasmid constructs were identified by *Nco*I restriction enzyme digestion (data not shown) analysis and prepared by large scale plasmid preparation. The plasmids listed in Table 6.8 were digested with the appropriate enzymes to release NDRG1 promoter fragments. These were ligated with the *Kpn*I and *Xho*I digested pGL3-Basic vector to generate the pGL3-NDRG1(-4819 to +12) reporter plasmid. To generate the pGL3-NDRG1(-4819 to +305) construct, the pGL3-NDRG1(-2100 to +305) was digested with *Nco*I and *Xho*I to release the NDRG1 -1319 to +305 regulatory region. This was ligated with the -4819 to -1319 NDRG1 region and the *Kpn*I/*Xho*I digested pGL3-Basic vector as for pGL3-NDRG1(-4819 to +12). The identity of

Table 6.8. Plasmids and restriction enzymes used to generate pGL3-NDRG1(-4819 to +12)

Plasmid	Restriction enzymes	Fragment
pGL3-NDRG1(-4819 to -1319)	*Kpn*I and *Nco*I	-4819 to -1319
pGL3-NDRG1(-2100 to +12)	*Nco*I and *Xho*I	-1319 to +12
pGL3-Basic	*Kpn*I and *Xho*I	Linearised pGL3-Basic

the pGL3-NDRG1(-4819 to +12) and pGL3-NDRG1(-4819 to +305) reporter plasmids was confirmed by *Nco*I restriction enzyme digestion, which generated expected DNA fragments of 8269 bp and 1350 bp or 1650 bp, respectively. Correct clones were then sequence confirmed using the primers listed in Table 6.9. and prepared by large-scale plasmid preparation.

Table 6.9. Primers used to sequence the -4819 to -1297 NDRG1 region in pGL3-NDRG1(-4819 to +12) and pGL3-NDRG1(-4819 to +305)

Primer	Sequence	Position in promoter	T_a (°C)
RVprimer3	5’ CTAGCAAAATAGGCTGTCCC 3’	In pGL3-Basic	55
NDRG1 proRevNco	5' TCTGTGCCAACCCATGC 3'	-1297 to -1280	48

6.19. Luciferase assays

Cells were seeded at a density of approximately 1 x 10^5 cells per well of a 6-well plate and trasfected with luciferase reporter plasmids using Effectene Transfection Reagent (Qiagen). Briefly, 0.3 µg of pGL3-NDRG1-promoter plasmid, 10 ng of pRL-TK (that encodes *Renilla* luciferase) and 3.2 µl of Enhancer solution were added to 100 µl of EC buffer and left at room temperature for 5 minutes. Ten microlitres of Effectene reagent was then added to the transfection mix. After 10 minutes at room temperature, 600 µl of complete growth medium was added and the transfection mix added dropwise to the cells in 1.6 ml of complete growth medium. The next day, cells were subjected to treatment conditions, as described. Total cell lysates were prepared

by vigorous scraping in 100 µl of 1 X Passive Lysis Buffer (Promega) and firefly luciferase activity was assayed using the Dual Luciferease Kit (Promega) and Glomax 96 microplate luminometer (Promega). Activity was normalised to the *Renilla* luciferase activity from pRL-TK in the same lysate.

To determine the effect of control, EGR-1 or cJun siRNA on NDRG1 promoter reporter activity cells, at 40 % confluence in 6-well culture plates were first transfected with siRNA as described in section 6.16. The next day, media was changed and the cells were transfected with the pGL3-NDRG1(-2100 to +12) reporter plasmid and pRL-TK, using Effectene Transfection Reagent and subjected to TPA treatment and analysis as described.

6.20. Site-directed mutagenesis

Mutations of putative transcription factor binding sites in the NDRG1 (-2100 bp to +12 bp) promoter region were performed by site-directed mutagenesis. Primers were designed to incorporate the appropriate mutation, to specifically disrupt the transcription factor binding site and not any other site, and without incorporating an additional site into the promoter region. Primer design and melting temperature calculation was performed using Primer X software (http://www.bioinformatics.org/primerx/) and these are described in Table 6.10 below. Mutation of the EGR-1 site was performed as described before[153].

Mutagenesis was performed by PCR as recommended by the Stratagene QuikChange site-directed mutagenesis kit, using the Expand High Fidelity^{PLUS} PCR System (Roche). Reaction conditions were as follows: 100 ng template pGL3-NDRG1-(-2100 to +12), 125 ng forward primer, 125 ng reverse primer, 0.2 mM dNTPs, 2.5 U Expand^{PLUS} high fidelity DNA Polymerase and 1 X Polymerase Reaction Buffer. PCR cycling conditions were: 95°C for 30 seconds, followed by 18 cycles of 95°C for 30 seconds, 55°C for 1 minute and 72°C for 6 minutes, and a final extension step of 72°C for 1 hour. After cooling the PCR reaction, 10 U of *Dpn*I enzyme (Promega) was added directly to the PCR product and parental template DNA digested at 37^{o}C for 2 hours. Highly competent JM109 bacterial cells (Promega) were transformed with 5 µl of the *Dpn*I digest and plated on LB agar plates containing 50 µg/ml ampicillin. The identity of the EGR-1 mutant plasmid was confirmed by *Bfm*I digest (Fermentas, Ontario, Canada)

Table 6.10. Primers used for site-directed mutagenesis

Name	Sequence	Tm (^{o}C)
EGR1-mut-F	5' GAGGGGCGAGGC**tata**GGGCGGGGCCGC 3'	76
EGR1-mut-R	5' GCGGCCCCGCCC**tata**GCCTCGCCCCTC 3'	76
AP1(1)-mut-F	5' CTAAGGTTGGAAAGGGTG**c**G**c**CATGAAAGTTCAGGAAATC 3'	76
AP1(1)-mut-R	5' GATTTCCTGAACTTTCATG**g**C**g**CACCCTTTCCAACCTTAG 3'	76
AP1(2)-mut-F	5' GGTGCCAGCTGTG**c**GTCAGACTTCC 3'	76
AP1(2)-mut-R	5' GGAAGTCTGAC**g**CACAGCTGGCACC 3'	76

Mutated bases are highlighted in bold, lowercase.

while the AP1(1) and AP1(2) mutants were both confirmed using *Sch*I restriction enzyme (Fermentas).

6.21. Chromatin Immunoprecipitation Assay

Cells were seeded at 1 x 10^7 cells per 150 mm tissue culture dish and left overnight. The next day cells were grown in the presence or absence of 20 nM TPA for 2 hours. Cross-linking of protein-DNA complexes was performed with 1 % formaldehyde, added directly to the culture medium, for 10 minutes at room temperature followed by neutralization with Glycine, pH 2.5, to a final concentration of 0.125 M, for 5 minutes. Cells were washed twice with ice-cold PBS, like cells combined and pelleted at 200 x g for 5 min at 4^{o}C. The pellet was resuspended in 300 µl of lysis buffer and left on ice for 10 min. Each lysis solution was sonicated four times on maximum power with a probe sonicator (Heat System-Ultrasonics, Inc., Plainview, NY), and cell debris was pelleted at 4^{o}C for 10 min at 15 000 x g. Twenty microlitres of the soluble chromatin preparation was set aside as the input fraction while the reminder was diluted 1:10 in dilution buffer. Protein G Plus-Agarose beads (Calbiochem, EMD Biosciences) were blocked in a 1:10 solution of lysis buffer:dilution buffer containing 5 % BSA and 100 µg/ml sheared salmon sperm DNA (Invitrogen), for 8 hours at 4^{o}C. Beads were pelleted at 200 x g for 5 min at 4^{o}C, washed with twice with ice-cold PBS and finally resuspended in a 1:10 solution of lysis buffer:dilution buffer. The soluble chromatin was precleared with blocked protein G beads for 2 hours at 4^{o}C. The beads were then removed by centrifugation at 4^{o}C for 1 min at 15 000 x g. Twenty microlitres of EGR-1 antibody

(no. 4152, Cell Signaling Technology), or no antibody, was added to the pre-cleared chromatin and the solution was incubated at 4^{o}C overnight. The next day 45 µl of blocked Protein G Plus-Agarose beads were added and the solution left for a further 2 hours at 4^{o}C. The beads were collected by centrifugation and washed successively for 10 min each with TSE I, TSE II, buffer III, and TE, pH7.4. DNA was eluted from the beads twice at room temperature with 100 µl elution buffer, followed by incubation overnight at 65^{o}C to reverse cross-links. DNA was purified with the Wizard^{R} SV Gel and PCR Clean-Up System (Promega) as per the manufacturer's instructions. Purified DNA was amplified by real-time PCR using NDRG1 promoter primers, designed to span the EGR-1 binding site (Table 6.11), on a StepOne Real Time PCR System (Applied Biosystems) using the KAPA SYBR qPCR Universal Kit (KAPA Biosystems). Real-time RT-PCR cycling conditions were 95°C for 3 minutes, followed by 40 cycles of 95°C for 1 second and 55°C for 20 seconds.

Table 6.11 Primers used in ChIP assay

Primer	**Sequence**	**Position**	**PCR product size (bp)**	**Ta (°C)**
EGR1ChIPF	5' CTGCGTGCTGGGACTGC 3'	-88 to -72	142	55
EGR1ChIPR	5' CGGATGGTGAACTGACGAG 3'	+36 to +54		

6.22. Statistical Analyses

Experiments were performed in triplicate (or quadruplicate) and results are the mean ± standard deviation (SD) or standard error (SE) of two or more independent experiments. For data comparisons the Student's t-test (unpaired or paired) was performed, where appropriate. A *P* value of <0.05 was considered statistically significant.

6.23. Solutions

6.23.1. Tissue culture solutions

Trypsin-EDTA

0.5 g trypsin

8 g NaCl

1.45 g $Na_2HPO_4.2H_2O$

0.2 g KCl

0.2 g KH_2PO_4

10 mM EDTA, pH 8.0

Made up to 1 litre with PBS

PBS

137 mM NaCl

2.7 mM KCl

4.3 mM $Na_2HPO_4.7H_2O$ (pH 7.4)

1.4 mM KH_2PO_4

4 % paraformaldehyde

40 g paraformaldehyde dissolved in 900 ml PBS.

Heat to 50^{o}C and add 1-2 NaOH pellets

6.23.2. RNA solutions

10 X MOPS Buffer

0.2 M [N-morpholino]propanesulfonic acid (MOPS)

0.05 M NaAcetate

0.01 M EDTA

RNA Loading Buffer

0.72 ml Formamide

0.16 ml 10 X MOPS Buffer

0.26 ml 37 % Formaldehyde

0.18 ml dH_2O

0.1 ml 80 % Glycerol

0.08 ml 0.25 % Bromophenol Blue

1.5 % MOPS/formaldehyde agarose gel

0.75 g Agarose

50 ml 1 X MOPS

2.7 ml 37 % Formaldehyde

2.5 µl Ethidium Bromide (10 mg/ml)

6.23.3. VEGF-A ELISA solutions

Wash Buffer

0.05 % Tween-20 in PBS

Block Buffer

1 % BSA in PBS

6.23.4. Protein and Western blot solutions

RIPA Buffer

150 mM Sodium Chloride

1 % Triton X-100

1 % Sodium Deoxycholate

0.1 % SDS

10 mM Tris-Cl, pH 7.4

4 X Protein Loading Dye

250 mM Tris-Cl, pH 6.8

6 % SDS

0.005 % Bromophenol Blue

40 % Glycerol

10 % β-mercaptoethanol

4 % Acrylamide Stacking Gel

7.3 ml dH_2O

1.25 ml 1 M Tris-Cl, pH 6.8

100 µl 10 % SDS

1.3 ml 30 % Acrylamide

120 µl 10 % Ammonium Persulphate

12 µl TEMED

10 % Acrylamide Separating Gel

5.5 ml dH_2O

7.5 ml 1 M Tris-Cl, pH 8.8

200 µl 10 % SDS

6.7 ml 30 % Acrylamide

400 µl 10 % Ammonium Persulphate

40 µl Temed

Acrylamide/Bisacrylamide (37.5:1, 30%)

30 g Acrylamide

0.8 g Bisacrylamide

0.1 g SDS

Up to 100 ml with dH_2O

10 X Running Buffer

20 g Glycine

31.6 g Tris

50 ml 10 % SDS

Up to 500 ml with dH_2O

10 X Transfer Buffer

72 g Glycine

19 g Tris

Up to 500 ml with dH_2O

1 X Transfer Buffer

100 ml 10 X Transfer Buffer

200 ml Isopropanol/Methanol

700 ml dH_2O

Stripping Buffer

100 mM β-Mercaptoethanol

2 % SDS

62.5 mM Tris-HCl, pH 6.7

Rapid Coomassie Staining Solution

0.024 % Coomassie Brilliant Blue

10 % Acetic Acid

90 % dH_2O

Destain

10 % Glacial Acetic Acid

10 % Methanol

TBST

50 mM Tris-Cl, pH 7.5

150 mM NaCl

0.1 % Tween-20

6.23.5. DNA solutions

TE Buffer

10 mM Tris-Cl, pH 8.0

1 mM EDTA, pH 8.0

10 X TBE

108 g Tris

55 g Boric Acid

7.4 g EDTA

Up to 1 *l* with dH_2O

10 x TAE Buffer

0.4 M Tris

0.01 M EDTA

pH to 7.8 with acetic acid

6.23.6. Bacterial solutions

Luria Broth (LB) medium

10 g Tryptone

5 g Yeast Extract

10 g NaCl

1 mM NaOH

Up to 1 litre with dH_2O

LB agar

Same as LB medium, but with 15 g Agar

Ampicillin (10 mg/ml) and Kanamycin (10 mg/ml)

1 mg Ampicillin or Kanamycin

10 ml dH_2O

Filter-sterilised

Store at -20°C

6.23.7. ChIP Solutions

Lysis buffer

1 % SDS

5 mM EDTA

50 mM Tris-Cl, pH 8.1

1 X Complete Protease Inhibitor (Roche)

Dilution buffer

1 % Triton X-100

2 mM EDTA

150 mM NaCl

20 mM Tris-Cl, pH 8.1

1 X Complete Protease Inhibitor

TSEI

0.1 % SDS

1 % Triton X-100

2 mM EDTA

20 mM Tris-Cl, pH 8.1

150 mM NaCl

TSEII

0.1 % SDS

1 % Triton X-100

2 mM EDTA

20 mM Tris-Cl, pH 8.1

500 mM NaCl

Buffer III

0.25 M LiCl

1 % NP-40

1 % Sodium Deoxycholate

1 mM EDTA

10 mM Tris-Cl, pH 8.1

Elution Buffer

1 % SDS

0.1 M $NaHCO_3$

APPENDIX 1

Exert from NT_ 008046 Chromosome 8 genomic contig.
mRNA is in bold, capital letters
The -2100 bp to +1 bp region is highlighted in turquoise
TATA box is highlighted in purple

LOCUS NT_008046 63001 bp DNA linear CON 20-AUG-2004
DEFINITION Homo sapiens chromosome 8 genomic contig.
ACCESSION NT_008046 REGION: complement(47467000..47530000)
VERSION NT_008046.15 GI:51467074
KEYWORDS .
SOURCE Homo sapiens (human)
ORGANISM Homo sapiens
Eukaryota; Metazoa; Chordata; Craniata; Vertebrata; Euteleostomi;
Mammalia; Eutheria; Euarchontoglires; Primates; Catarrhini;
Hominidae; Homo.
REFERENCE 1 (bases 1 to 63001)
AUTHORS International Human Genome Sequencing Consortium.
TITLE The DNA sequence of Homo sapiens
JOURNAL Unpublished (2003)
COMMENT GENOME ANNOTATION REFSEQ: Features on this sequence have been
produced for build 35 version 1 of the NCBI's genome annotation
[see documentation].
On Aug 20, 2004 this sequence version replaced gi:37555983.
The DNA sequence is part of the third release of the finished human
reference genome. It was assembled from individual clone sequences
by the Human Genome Sequencing Consortium in consultation with NCBI
staff.
FEATURES Location/Qualifiers
gene 2324..62408
/gene="NDRG1"
/note="Derived by automated computational analysis using
gene prediction method: BestRefseq. Supporting evidence
includes similarity to: 1 mRNA"
/db_xref="GeneID:10397"
/db_xref="MIM:605262"
mRNA join(2324..2445,15250..15330,19312..19347,34927..35032,
37412..37532,40349..40411,41153..41213,42716..42802,
44984..45040,49036..49139,50808..50864,51653..51704,
52916..52963,55189..55224,57505..57556,60460..62408)
/gene="NDRG1"
/product="N-myc downstream regulated gene 1"
/note="unclassified transcription discrepancy; Derived by
automated computational analysis using gene prediction
method: BestRefseq. Supporting evidence includes
similarity to: 1 mRNA"
/transcript_id="NM_006096.2"
/db_xref="GI:37655182"
/db_xref="GeneID:10397"
/db_xref="MIM:605262"
CDS join(15268..15330,19312..19347,34927..35032,37412..37532,
40349..40411,41153..41213,42716..42802,44984..45040,
49036..49139,50808..50864,51653..51704,52916..52963,
55189..55224,57505..57556,60460..60701)
/gene="NDRG1"

ORIGIN

```
       1 atgcacctgt agaaaatgtt tttgcctttt cagtcctttc ccagtggcgg agtacaggac
      61 ccagctcata agagcagctc aattctgtca tttgtggaat gacagaataa ataagtttca
     121 gggcctaggg aggcaaggct cctgccttag cctcccaagt agctggaact acagctgcat
     181 gccactaagc ccacctgatt ttttattttc ttgtagagat gatgtctcat tatgttgctc
     241 agacttttct ggaactcctg ggctcaagca atcctcccac ctctgcctct gaagtagctg
     301 ggactacagg tacttgccac caggcctggc tagctttcat ctttttttgta gagatgggac
     361 atcactatgt tgtgaaggct ggtctcaaac tcctggactc aagagaggct tctgcattgg
     421 cctcccaaag tgctgggatt acaggtgtaa gccactctac ctggacacaa cattttattt
     481 gaaataagaa aaattttccc tcactgggaa tgctgcagtt gaactagttc aaatccataa
     541 agaatggaag actgcccagt ggtcattcat tcacttatta attctagatg ttaaattttc
     601 tagggtgggg gaatgtgctc ctacattcaa ggcattcttg aatgtagcca aactttgtag
     661 tttagccaaa cttcatagct aatagccaaa ctttgtagtt tagccaaact cttctagcag
     721 caaaacccat gacactggaa ctctgttctt cacactggtc atttgtaata gaataacaga
     781 gctttagcac tagataggtt ctgaaagatc attgaatcta atcctctccc tttgccagtg
     841 agaattctga agcccagatt tgttgatttg tgatcgatag tgtcaaagac aggcctgaaa
     901 cacagatgtc ctgggtccta gaggtgctgt ttgcccctct ccatatttct tttgttccag
     961 aaaaccttc tccaaaactg gccctaataa tcagagggga aagccatggc ccctgccttg
    1021 gggacagcat gggttggcac agaaaagagg tttacaattc agcaggaagt gttgtgcgtg
    1081 cgcgcgtgtg tgtctgtgga ggcgcaggga gggtcacctg agcttgccct gggtctggtc
    1141 ctgggctcag tggcaaattc aacgctgggc aggtggcctg aggacaatga cggtgccagc
    1201 tgtgagtcag acttccttta ttcataaaat catgttcctc catgcagtgc ttctcaacct
    1261 ggctgcacgt caggagccac ctgggtagct ttgtaaaaac cccaatgccc agttggtttg
    1321 caccccctga gattctgatt aaactgttct ggagtccatc tctctctttt tattatctat
    1381 ctatttattt atttttaat ttggcggctc ctctgggact tctcatatgc agtaggggtt
    1441 gagaattgct ggtttctttg gccagatggg aacatgcagg ccaatagtta cgcacaaaca
    1501 gagcagcaga gcaggacggt gctaaggttg gaaagggtga gtcatgaaag ttcaggaaat
    1561 cagaatagga aggggtgaga atcctctcat ctgggcttgt ggggcaggag agaagagccc
    1621 agtgggcaag gtccagtgag tgtgcttaga actgggaaga tgaggggaag ggtaagcgct
    1681 gggcggcggt gggcaagatg gacgagatta aacgggagcg aggatttcag cgagagcttt
    1741 ggcgacacgg aaggctgaga atcggaggga gcctgtcggg cgaaagcgaa ggcggctgct
    1801 gggcaggcag ccgaatccgg ctggagagcc gagctggtga gacctacagg aagtgaaggg
    1861 agtcgctcag ggcgtggcgc aacgagactc ttagaagaaa ctctgaggca gagatggggg
    1921 gcctccgccc atacggagac acaaggaagt ccacatgcac acgcacgagc gcgcacatga
    1981 acacgcacaa gcacacaaac gcctcctccg ggcagggcac acgcgcccgc tgcacaggcc
    2041 gaggccctgg actcggaggg gactgcagag ccgacccaca acccgggccc cgatgccct
    2101 cccggccgcg cccctacgac tgcttgcgca acaggcggcg gctccagtgg gcgcccgccg
    2161 cgcgctgccg gagcccagcc cagccggcg cgcccgggag gagggagcag ggagcgggga
    2221 aggggtgtgt cccggctgcg tgctgggact gcgagggtct gggaggggcg aggcgcgggg
    2281 gcggggccgc ggcgcctata aagtcgccct ccgcccggac gtaAACAAAC CTCGCCTGGC
    2341 TCCCAgctgg tgctgaagct cgtcagttca ccatccgccc tcggcttccg cggggcgctg
    2401 ggccgccagc ctcggcaccg tcctttcctt tctccctcgc gttaggtaag cccgcgccct
    2461 cttctcccag gcgcgacgcg gagcagaaag gggccgcccg tgcggtgccg ctggagcgcc
    2521 aggaccgccc tttgtagccc cgcgtactcc aggagtaagc gccccggagc tgcaagtgcg
    2581 cggtcacccc ggggcgcggg cgcgaggggg ctttgggtgc agacaccgct gaagtggggg
    2641 gttcaattac ggaaagggag gaaaaaaaga cagggtccca ttcatctccc ccctagctgg
    2701 ggattggggt tctggaggtc gggaaggggg cgatgagacg gtccgaaaaa ataccaggat
```

REFERENCES

1. Boyle,P. and Levin,B. (2008) *World Cancer Report 2008*. International Agency for Research on Cancer.

2. Parkin,D.M., Bray,F., Ferlay,J., and Pisani,P. (2005) Global cancer statistics, 2002. *CA Cancer J.Clin.*, **55**, 74-108.

3. Parkin, D. M., Whelan, S. L., Ferlay, J., and Storm, H. Cancer Incidence in Five Continents, Volumes I to VIII. 2005. Lyon, France, International Agency for Research on Cancer. IARC cancerBase No 7.

4. Ferlay, J., Bray, F., Pisani, P., and Parkin, D. M. GLOBOCAN 2002 Cancer Incidence, Mortality and Prevalence Worldwide. 2004. IARC Cancer Base No.5, version 2.0, International Agency for Research on Cancer, Lyon, France.

5. Meltzer,S.J. (1995) Biology of Barrett's Esophagus and Adenocarcinoma. *Gastrointestinal Cancers: Biology, Diagnosis and Therapy*. Lippincott-Raven Publishers, Philadelphia.

6. Glickman,J.N. (2003) Section II: pathology and pathologic staging of esophageal cancer. *Semin.Thorac.Cardiovasc.Surg.*, **15**, 167-179.

7. Chow,W.H., Blot,W.J., Vaughan,T.L., Risch,H.A., Gammon,M.D., Stanford,J.L., Dubrow,R., Schoenberg,J.B., Mayne,S.T., Farrow,D.C., Ahsan,H., West,A.B., Rotterdam,H., Niwa,S., and Fraumeni,J.F., Jr. (1998) Body mass index and risk of adenocarcinomas of the esophagus and gastric cardia. *J.Natl.Cancer Inst.*, **90**, 150-155.

8. Gabbert HE, Shimoda T, Hainaut P, Nakamura Y, Field JK, and Inoue H (2000) Squamous cell carcinoma of the oesophagus. *Pathology and Genetics. Tumours of the Digestive System (WHO Classification of Tumours, Volume 2 IARC WHO Classification of Tumours, No 2)*. International Agency for Research on cancer (IARC) Press, Lyon.

9. Stages of oesophageal cancer. www.cancer.gov, National Cancer Institute, National Institutes of Health . 2009. National Cancer Institute, National Institutes of Health. 9-11-2009.

10. Enzinger,P.C. and Mayer,R.J. (2003) Esophageal cancer. *N.Engl.J.Med.*, **349**, 2241-2252.

11. Willett,C.G. and Czito,B.G. (2009) Combined-modality Therapy for Esophageal Cancer. *ASCO Educational Book*, **2009**, 243-249.

12. Takemura,M., Osugi,H., Takada,N., Kinoshita,H., and Higashino,M. (2003) Prognostic factors in patients with squamous oesophageal cancer associated with solitary lymph node metastasis after oesophagectomy and extended lymphadenectomy. *Oncol.Rep.*, **10**, 75-80.

13. Mqoqi, N., Kellet, P., Sitas, F., and Jula, M. Incidence of Histologically Diagnosed Cancer in South Africa, 1998-1999. 2004. Johannesburg, National Cancer Registry of South Africa, National Health Laboratory Service.

14. Burrell,R.J.W. (1962) Esophageal cancer among Bantu in the Transkei. *J Natl.Cancer Inst.*, **28**, 495-514.

15. Kneebone,R.L. and Mannell,A. (1985) Cancer of the oesophagus in Soweto. *S.Afr.Med.J.*, **67**, 839-842.

16. Rose,E.F. (1973) Esophageal cancer in the Transkei: 1955-69. *J Natl.Cancer Inst.*, **51**, 7-16.

17. Somdyala, N. I. M., Bradshaw, D., Curtis, B., and Gelderblom, W. C. A. Cancer Incidence in selected municipalities of the Eastern Cape Province.PROMEC Cancer Registry Technical Report. 2008. Cape Town, South African Medical Research Council.

18. Fernandes,M.L., Seow,A., Chan,Y.H., and Ho,K.Y. (2006) Opposing trends in incidence of esophageal squamous cell carcinoma and adenocarcinoma in a multi-ethnic Asian country. *Am J Gastroenterol.*, **101**, 1430-1436.

19. van,W.C. (2002) Recent trends in smoking prevalence in South Africa--some evidence from AMPS data. *S.Afr.Med.J*, **92**, 468-472.

20. Semnani,S., Sadjadi,A., Fahimi,S., Nouraie,M., Naeimi,M., Kabir,J., Fakheri,H., Saadatnia,H., Ghavamnasiri,M.R., and Malekzadeh,R. (2006) Declining incidence of esophageal cancer in the Turkmen Plain, eastern part of the Caspian Littoral of Iran: a retrospective cancer surveillance. *Cancer Detect.Prev*, **30**, 14-19.

21. Lalloo,R., Myburgh,N.G., Smith,M.J., and Solanki,G.C. (2004) Access to health care in South Africa--the influence of race and class. *S.Afr.Med.J*, **94**, 639-642.

22. Disease and Mortality in Sub-Saharan Africa. Jamison, D. T., Feachem, R. G., Makgoba, M. W., Bos, E. R., Baingana, F. K., Hofman, K. J., and Rogo, K. O. 2006. Washington, D.C., The International Bank for Reconstruction and Development/The World Bank.

23. Makaula,N.A., Marasas,W.F., Badenhorst,C.J., Bradshaw,D., and Swanevelder,S. (1995) Oesophageal and other cancer patterns in four selected districts of Transkei, Southern Africa: 1985-1990. *Afr.J.Health Sci.*, **2**, 333-337.

24. Hendricks,D. and Parker,M.I. (2002) Oesophageal cancer in Africa. *Iubmb Life*, **53**, 263-268.

25. Larsson,S.C., Giovannucci,E., and Wolk,A. (2006) Folate intake, MTHFR polymorphisms, and risk of esophageal, gastric, and pancreatic cancer: a meta-analysis. *Gastroenterology*, **131**, 1271-1283.

26. Stolzenberg-Solomon,R.Z., Qiao,Y.L., Abnet,C.C., Ratnasinghe,D.L., Dawsey,S.M., Dong,Z.W., Taylor,P.R., and Mark,S.D. (2003) Esophageal and Gastric Cardia Cancer Risk and Folate- and Vitamin B12-related Polymorphisms in Linxian, China. *Cancer Epidemiology Biomarkers & Prevention*, **12**, 1222-1226.

27. Stoner,G.D. and Gupta,A. (2001) Etiology and chemoprevention of esophageal squamous cell carcinoma. *Carcinogenesis*, **22**, 1737-1746.

28. Marasas,W.F., Jaskiewicz,K., Venter,F.S., and Van Schalkwyk,D.J. (1988) Fusarium moniliforme contamination of maize in oesophageal cancer areas in Transkei. *S.Afr.Med.J.*, **74**, 110-114.

29. Marasas,W.F. (1996) Fumonisins: history, world-wide occurrence and impact. *Adv.Exp.Med.Biol.*, **392**, 1-17.

30. Shephard,G.S., Marasas,W.F.O., Burger,H.M., Somdyala,N.I.M., Rheeder,J.P., Van der Westhuizen,L., Gatyeni,P., and Van Schalkwyk,D.J. (2007) Exposure assessment for fumonisins in the former Transkei region of South Africa. *Food Additives and Contaminants*, **24**, 621-629.

31. Gelderblom,W.C., Snyman,S.D., Lebepe-Mazur,S., van der,W.L., Kriek,N.P., and Marasas,W.F. (1996) The cancer-promoting potential of fumonisin B1 in rat liver using diethylnitrosamine as a cancer initiator. *Cancer Lett.*, **109**, 101-108.

32. Bever,R.J., Jr., Couch,L.H., Sutherland,J.B., Williams,A.J., Beger,R.D., Churchwell,M.I., Doerge,D.R., and Howard,P.C. (2000) DNA adduct formation by Fusarium culture extracts: lack of role of fusarin C. *Chem.Biol.Interact.*, **128**, 141-157.

33. Islami,F., Pourshams,A., Nasrollahzadeh,D., Kamangar,F., Fahimi,S., Shakeri,R., bedi-Ardekani,B., Merat,S., Vahedi,H., Semnani,S., Abnet,C.C., Brennan,P., Moller,H., Saidi,F., Dawsey,S.M., Malekzadeh,R., and Boffetta,P. (2009) Tea drinking habits and oesophageal cancer in a high risk area in northern Iran: population based case-control study. *BMJ*, **338**, b929.

34. Rolon,P.A., Castellsague,X., Benz,M., and Munoz,N. (1995) Hot and cold mate drinking and esophageal cancer in Paraguay. *Cancer Epidemiol Biomarkers Prev*, **4**, 595-605.

35. Sammon,A.M. (1992) A case-control study of diet and social factors in cancer of the esophagus in Transkei. *Cancer*, **69**, 860-865.

36. Dandara,C., Ballo,R., and Parker,M.I. (2005) CYP3A5 genotypes and risk of oesophageal cancer in two South African populations. *Cancer Lett.*, **225**, 275-282.

37. Dandara,C., Li,D.P., Walther,G., and Parker,M.I. (2006) Gene-environment interaction: the role of SULT1A1 and CYP3A5 polymorphisms as risk modifiers for squamous cell carcinoma of the oesophagus. *Carcinogenesis*, **27**, 791-797.

38. Li,D., Dandara,C., and Parker,M.I. (2005) Association of cytochrome P450 2E1 genetic polymorphisms with squamous cell carcinoma of the oesophagus. *Clin Chem.Lab Med.*, **43**, 370-375.

39. Li,D.P., Dandara,C., Walther,G., and Parker,M.I. (2008) Genetic polymorphisms of alcohol metabolising enzymes: their role in susceptibility to oesophageal cancer. *Clin Chem.Lab Med.*, **46**, 323-328.

40. Matsha,T., Erasmus,R., Kafuko,A.B., Mugwanya,D., Stepien,A., and Parker,M.I. (2002) Human papillomavirus associated with oesophageal cancer. *J Clin Pathol*, **55**, 587-590.

41. Yao,P.F., Li,G.C., Li,J., Xia,H.S., Yang,X.L., Huang,H.Y., Fu,Y.G., Wang,R.Q., Wang,X.Y., and Sha,J.W. (2006) Evidence of human papilloma virus infection and its epidemiology in esophageal squamous cell carcinoma. *World J.Gastroenterol.*, **12**, 1352-1355.

42. Genuis,S.J. (2007) An ounce of prevention: A pound of cure for an ailing health care system. *Can Fam Physician*, **53**, 597-599.

43. Gescher,A.J., Sharma,R.A., and Steward,W.P. (2003) Cancer prevention and delay are as important as cure. *The Lancet Oncology*, **4**, 72-73.

44. Sitas, F, Madhoo, J, and Wessie, J. Incidence of Histologically Diagnosed Cancer in South Africa, 1993-1995. 1998. Johannesburg, National Cancer Registry of South Africa, National Health Laboratory Service.
Ref Type: Report

45. Mannell,A. and Murray,W. (1989) Oesophageal cancer in South Africa. A review of 1926 cases. *Cancer*, **64**, 2604-2608.

46. Mackay,S. and Stefanou,G. (2006) Management of oesophageal carcinoma. *Aust.Fam.Physician*, **35**, 202-206.

47. Leonard,G.D., McCaffrey,J.A., and Maher,M. (2003) Optimal therapy for oesophageal cancer. *Cancer Treat.Rev.*, **29**, 275-282.

48. Kon,Z.R. and Lackan,N. (2008) Ethnic Disparities in Access to Care in Post-Apartheid South Africa. *Am J Public Health*, **98**, 2272-2277.

49. Hanahan,D. and Weinberg,R.A. (2000) The hallmarks of cancer. *Cell*, **100**, 57-70.

50. Harada,H., Nakagawa,H., Oyama,K., Takaoka,M., Andl,C.D., Jacobmeier,B., von,W.A., Enders,G.H., Opitz,O.G., and Rustgi,A.K. (2003) Telomerase induces immortalization of human esophageal keratinocytes without p16INK4a inactivation. *Mol.Cancer Res*, **1**, 729-738.

51. Bannon,J.H. and Mc Gee,M.M. (2009) Understanding the role of aneuploidy in tumorigenesis. *Biochem.Soc.Trans.*, **37**, 910-913.

52. Kokame K, Kato H, and Miyata T (1996) Homocysteine-respondent Genes in Vascular Endothelial Cells Identified by Differential Display Analysis. *J Biol Chem.*, **271**, 29659-29665.

53. van Belzen N, Dinjens WN, Diesveld MP, Groen NA, van der Made AC, Nozawa Y, Vlietstra R, Trapman J, and Bosman FT (1997) A novel gene which is up-regulated during colon epithelial cell differentiation and down-regulated in colorectal neoplasms. *Lab Invest.*, **77**, 85-92.

54. Kurdistani SK, Arizti P, Reimer CL, Sugrue MM, Aaronson SA, and Lee SW (1998) Inhibition of tumor cell growth by RTP/rit42 and its responsiveness to p53 and DNA damage. *Cancer Res.*, **58**, 4439-4444.

55. Zhou D, Salnikow K, and Costa M (1998) Cap43, a novel gene specifically induced by Ni2+ compounds. *Cancer Res.*, **58**, 2182-2189.

56. Park H, Adams MA, Lachat P, Bosman F, Pang SC, and Graham CH (2000) Hypoxia induces the expression of a 43-kDa protein (PROXY-1) in normal and malignant cells. *Biochem Biophys Res Commun.*, **276**, 321-328.

57. Kovacevic Z and Richardson DR (2006) The metastasis suppressor, Ndrg-1: a new ally in the fight against cancer. *Carcinogenesis*, **27**, 2355-2366.

58. Li,J. and Kretzner,L. (2003) The growth-inhibitory Ndrg1 gene is a Myc negative target in human neuroblastomas and other cell types with overexpressed N- or c-myc. *Mol.Cell Biochem.*, **250**, 91-105.

59. Qu X, Zhai Y, Wei H, Zhang C, Xing G, Yu Y, and He F (2002) Characterization and expression of three novel differentiation-related genes belong to the human NDRG gene family. *Mol Cell Biochem.*, **299**, 35-44.

60. Zhou RH, Kokame K, Tsukamoto Y, Yutani C, Kato H, and Miyata T (2001) Characterization of the human NDRG gene family: a newly identified member, NDRG4, is specifically expressed in brain and heart. *Genomics*, **73**, 86-97.

61. Lin TM and Chang C (1997) Cloning and characterization of TDD5, an androgen target gene that is differentially repressed by testosterone and dihydrotestosterone. *Proc Natl Acad Sci U S A.*, **94**, 4988-4993.

62. Shimono A, Okuda T, and Kondoh H (1999) N-myc-dependent repression of ndr1, a gene identified by direct subtraction of whole mouse embryo cDNAs between wild type and N-myc mutant. *Mech Dev.*, **83**, 39-52.

63. Yamauchi Y, Hongo S, Ohashi T, Shioda S, Zhou C, Nakai Y, Nishinaka N, Takahashi R, Takeda F, and Takeda M (1999) Molecular cloning and characterization of a novel developmentally regulated gene, Bdm1, showing predominant expression in postnatal rat brain. *Brain Res Mol Brain Res.*, **68**, 149-158.

64. Wilson R, Ainscough R, Anderson K, Baynes C, Berks M, Bonfield J, Burton J, Connell M, Copsey T, Cooper J, and et al. (1994) 2.2 Mb of contiguous nucleotide sequence from chromosome III of C. elegans. *Nature*, **368**, 32-38.

65. Chou,M.Y., Hsiao,C.D., Chen,S.C., Chen,I.W., Liu,S.T., and Hwang,P.P. (2008) Effects of hypothermia on gene expression in zebrafish gills: upregulation in differentiation and function of ionocytes as compensatory responses. *J Exp Biol*, **211**, 3077-3084.

66. Tian Y, Xu M, Fu Y, Yuan A, Wang D, Li G, Liu G, and Lu L (2008) Mapping and expression analysis of chicken NDRG1 and NDRG3 genes. *Biochem Genet.*, **46**, 677-684.

67. Krauter-Canham R, Bronner R, Evrard JL, Hahne G, Friedt W, and Steinmetz A (1997) A transmitting tissue- and pollen-expressed protein from sunflower with sequence similarity to the human RTP protein. *Plant Science*, **129**, 191-202.

68. Zoroddu MA, Kowalik-Jankowska T, Kozlowski H, Salnikow K, and Costa M (2001) Ni(II) and Cu(II) binding with a 14-aminoacid sequence of Cap43 protein, TRSRSHTSEGTRSR. *J Inorg Biochem.*, **84**, 47-54.

69. Zoroddu MA, Peana M, Kowalik-Jankowska T, Kozlowski H, and Costa M (2004) Nickel(II) binding to Cap43 protein fragments. *J Inorg Biochem.*, **98**, 931-939.

70. Shaw E, McCue LA, Lawrence CE, and Dordick JS (2002) Identification of a novel class in the alpha/beta hydrolase fold superfamily: the N-myc differentiation-related proteins. *Proteins*, **47**, 163-168.

71. Lachat P, Shaw P, Gebhard S, van Belzen N, Chaubert P, and Bosman FT (2002) Expression of NDRG1, a differentiation-related gene, in human tissues. *Hiarochem Cell Biol.*, **118**, 399-408.

72. Sugiki T, Taketomi Y, Kikuchi-Yanoshita R, Murakami M, and Kudo I (2004) N-myc downregulated gene 1 is a phosphorylated protein in mast cells. *Biol Phaem Bull.*, **27**, 624-627.

73. Agarwala KL, Kokame K, Kato H, and Miyata T (2000) Phosphorylation of RTP, an ER stress-responsive cytoplasmic protein. *Biochem Biophys Res Commun.*, **272**, 641-647.

74. Murray JT, Campbell DG, Morrice N, Auld GC, Shpiro N, Marquez R, Peggie M, Bain J, Bloomberg GB, Grahammer F, Lang F, Wulff P, Kuhl D, and Cohen P (2004) Exploitation of KESTREL to identify NDRG1 family members as physiological substrates for SGK1 and GSK3. *Biochem J.*, **384**, 477-488.

75. Murray JT, Cummings LA, Bloomberg GB, and Cohen P (2005) Identification of different specificity requirements between SGK1 and PKBalpha. *FEBS Lett.*, **579**, 991-994.

76. Guan RJ, Ford HL, Fu Y, Li Y, Shaw LM, and Pardee AB (2000) Drg-1 as a differentiation-related, putative metastasis suppressor gene in human colon cancer. *Cancer Res.*, **60**, 749-755.

77. Tu LC, Yan X, Hood L, and Lin B (2007) Proteomics analysis of the interactome of N-myc downstream regulated gene 1 and its interactions with the androgen response program in prostate cancer cells. *Mol Cell Proteomics.*, **6**, 575-588.

78. Kachhap SK, Faith D, Qian DZ, Shabbeer S, Galloway NL, Pili R, Denmeade SR, DeMarzo AM, and Carducci MA (2007) The N-Myc down regulated gene1 (NDRG1) is a Rab4a effector involved in vesicular recycling of E-cadherin. *PLoS ONE.*, **2**, e844.

79. Zerial,M. and McBride,H. (2001) Rab proteins as membrane organizers. *Nat.Rev.Mol.Cell Biol*, **2**, 107-117.

80. Cangul H (2004) Hypoxia upregulates the expression of the NDRG1 gene leading to its overexpression in various human cancers. *BMC Genet.*, **5**.

81. Sugiki T, Taketomi Y, Kikuchi-Yanoshita R, Murakami M, and Kudo I (2004) Association of N-myc downregulated gene 1 with heat shock cognate protein 70 in mast cells. *Biol Phaem Bull.*, **27**, 628-633.

82. Wang,G., Yang,Z.Q., and Zhang,K. (2010) Endoplasmic reticulum stress response in cancer: molecular mechanism and therapeutic potential. *Am J Transl.Res*, **2**, 65-74.

83. Kaufman,R.J. (1999) Stress signaling from the lumen of the endoplasmic reticulum: coordination of gene transcriptional and translational controls. *Genes Dev.*, **13**, 1211-1233.

84. Harding,H.P., Calfon,M., Urano,F., Novoa,I., and Ron,D. (2002) Transcriptional and translational control in the Mammalian unfolded protein response. *Annu Rev Cell Dev.Biol*, **18**, 575-599.

85. Salnikow K, Blagosklonny MV, Ryan H, Johnson R, and Costa M (2000) Carcinogenic nickel induces genes involved with hypoxic stress. *Cancer Res.*, **60**, 38-41.

86. Salnikow K, Kluz T, Costa M, Piquemal D, Demidenko ZN, Xie K, and Blagosklonny MV (2002) The regulation of hypoxic genes by calcium involves c-Jun/AP-1, which cooperates with hypoxia-inducible factor 1 in response to hypoxia. *Mol Cell Biol.*, **22**, 1734-1741.

87. Kokame K, Kato H, and Miyata T. Nonradioactive differential display cloning of genes induced by homocysteine in vascular endothelial cells. Methods 16(4), 434-443. 1998.

88. Banz,V.M., Medova,M., Keogh,A., Furer,C., Zimmer,Y., Candinas,D., and Stroka,D. (2009) Hsp90 transcriptionally and post-translationally regulates the expression of NDRG1 and maintains the stability of its modifying kinase GSK3beta. *Biochim Biophys Acta*, **1793**, 1597-1603.

89. Bandyopadhyay S, Pai SK, Hirota S, Hosobe S, Takano Y, Saito K, Piquemal D, Commes T, Watabe M, Gross SC, Wang Y, Ran S, and Watabe K (2004) Role of the putative tumor metastasis suppressor gene Drg-1 in breast cancer progression. *Oncogene*, **23**, 5675-5681.

90. Bandyopadhyay S, Pai SK, Hirota S, Hosobe S, Tsukada T, Miura K, Takano Y, Saito K, Commes T, Piquemal D, Watabe M, Gross S, Wang Y, Huggenvik J, and Watabe K (2004) PTEN Up-regulates the tumor metastasis suppressor gene Drg-1 in Prostate and Breast Cancer. *Cancer Res.*, **64**, 7655-7660.

91. Fukahori S, Yano H, Tsuneoka M, Tanaka Y, Yagi M, Kuwano M, Tajiri T, Taguchi T, Tsuneyoshi M, and Kojiro M (2007) Immunohistochemical expressions of Cap43 and Mina53 proteins in neuroblastoma. *J Pediatr Surg.*, **42**, 1831-1840.

92. Angst E, Sibold S, Tiffon C, Weimann R, Gloor B, Candinas D, and Stroka D (2006) Cellular differentiation determines the expression of the hypoxia-inducible protein NDRG1 in pancreatic cancer. *Br J Cancer.*, **95**, 307-313.

93. Maruyama Y, Ono M, Kawahara A, Yokoyama T, Basaki Y, Kage M, Aoyagi S, Kinoshita H, and Kuwano M (2006) Tumor growth suppression in pancreatic cancer by a putative metastasis suppressor gene Cap43/NDRG1/Drg-1 through modulation of angiogenesis. *Cancer Res.*, **66**, 6233-6242.

94. Bandyopadhyay S, Pai SK, Gross SC, Hirota S, Hosobe S, Miura K, Saito K, Commes T, Hayashi S, Watabe M, and Watabe K (2003) The Drg-1 gene suppresses tumor metastasis in prostate cancer. *Cancer Res.*, **63**, 1731-1736.

95. Cangul H, Salnikow K, Yee H, Zagzag D, Commes T, and Costa M (2002) Enhanced overexpression of an HIF-1/hypoxia-related protein in cancer cells. *Environ Health Perspect.*, **110 Suppl 5**, 783-788.

96. Song JY, Lee JK, Lee NW, Jung HH, Kim SH, and Lee KW (2008) Microarray analysis of normal cervix, carcinoma in situ, and invasive cervical cancer: identification of candidate genes in pathogenesis of invasion in cervical cancer. *Int J Gynecol Cancer*, **18**, 1051-1059.

97. Nishio S, Ushijima K, Ushijima K, Takemoto S, Kawano K, Yamaguchi T, Nishida N, Kakuma T, Tsuda H, Kasamatsu T, Sasajima Y, Kage M, Kuwano M, and Kamura T (2008) Cap43/NDRG1/Drg-1 is a molecular target for angiogenesis and a prognostic indicator in cervical adenocarcinoma. *Cancer Lett.*, **264**, 36-43.

98. Koshiji M, Kumamoto K, Morimura K, Utsumi Y, Aizawa M, Hoshino M, Ohki S, Takenoshita S, Costa M, Commes T, Piquemal D, Harris CC, and Tchou-Wong KM (2007) Correlation of N-myc downstream-regulated gene 1 expression with clinical outcomes of colorectal cancer patients of different race/ethnicity. *World J Gastroenterol.*, **13**, 2803-2810.

99. Wang Z, Wang F, Wang WQ, Gao Q, Wei WL, Yang Y, and Wang GY (2004) Correlation of N-myc downstream-regulated gene 1 overexpression with progressive growth of colorectal neoplasm. *World J Gastroenterol.*, **10**, 550-554.

100. Chua MS, Sun H, Cheung ST, Mason V, Higgins J, Ross DT, Fan ST, and So S (2007) Overexpression of NDRG1 is an indicator of poor prognosis in hepatocellular carcinoma. *Mod Pathol.*, **20**, 76-83.

101. Sibold S, Roh V, Keogh A, Studer P, Tiffon C, Angst E, Vorburger SA, Weimann R, Candinas D, and Stroka D (2007) Hypoxia increases cytoplasmic expression of NDRG1, but is insufficient for its membrane localization in human hepatocellular carcinoma. *FEBS Lett.*, **581**, 989-994.

102. Chang JT, Wang HM, Chang KW, Chen WH, Wen MC, Hsu YM, Yung BY, Chen IH, Liao CT, Hsieh LL, and Cheng AJ (2005) Identification of differentially expressed genes in oral squamous cell carcinoma (OSCC): overexpression of NPM, CDK1 and NDRG1 and underexpression of CHES1. *Int J Cancer*, **114**, 942-949.

103. Dang C, Gottschling M, Manning K, O'Currain E, Schneider S, Sterry W, Stockfleth E, and Nindl I (2006) Identification of dysregulated genes in cutaneous squamous cell carcinoma. *Oncol Rep.*, **16**, 513-519.

104. Ando T, Ishiguro H, Kimura M, Mitsui A, Kurehara H, Sugito N, Tomoda K, Mori R, Takashima N, Ogawa R, Fujii Y, and Kuwabara Y (2006) Decreased expression of NDRG1 is correlated with tumor progression and poor prognosis in patients with esophageal squamous cell carcinoma. *Dis Esophagus*, **19**, 454-458.

105. He F, Zhang L, Gao D, Chen K, Li H, Zhang S, and Zhang Y (2006) The Protein Expression of NDRG1 in Esophageal Squamous Cell Carcinoma and Its Relationship with Clinical Pathology Factors. *Life Science Journal*, **3**, 18-22.

106. Jankowski,J., Hopwood,D., Dover,R., and Wormsley,K.G. (1993) Development and Growth of Normal, Metaplastic and Dysplastic Esophageal Mucosa - Biological Markers of Neoplasia. *European Journal of Gastroenterology & Hepatology*, **5**, 235-246.

107. Marques-Pereira J.P., Leblond, and C.P. (1965) Mitosis and differentiation in the stratified epithelium of the rat esophagus. *Am.J.Anat.*,73-87.

108. Jones,S.J., Dicker,A.J., Dahler,A.L., and Saunders,N.A. (1997) E2F as a regulator of keratinocyte proliferation: implications for skin tumor development. *J.Invest Dermatol.*, **109**, 187-193.

109. Seery,J.P. and Watt,F.M. (2000) Asymmetric stem-cell divisions define the architecture of human oesophageal epithelium. *Curr.Biol.*, **10**, 1447-1450.

110. Chen,B., Nelson,D.M., and Sadovsky,Y. (2006) N-myc down-regulated gene 1 modulates the response of term human trophoblasts to hypoxic injury. *J.Biol.Chem.*, **281**, 2764-2772.

111. Chen,S., Han,Y.H., Zheng,Y., Zhao,M., Yan,H., Zhao,Q., Chen,G.Q., and Li,D. (2008) NDRG1 contributes to retinoic acid-induced differentiation of leukemic cells. *Leuk.Res.*.

112. Zhang,J., Chen,S., Zhang,W., Zhang,J., Liu,X., Shi,H., Che,H., Wang,W., Li,F., and Yao,L. (2008) Human differentiation-related gene NDRG1 is a Myc downstream-regulated gene that is repressed by Myc on the core promoter region. *Gene*, **417**, 5-12.

113. Piquemal,D., Joulia,D., Balaguer,P., Basset,A., Marti,J., and Commes,T. (1999) Differential expression of the RTP/Drg1/Ndr1 gene product in proliferating and growth arrested cells. *Biochim.Biophys.Acta*, **1450**, 364-373.

114. Gomez-Casero,E., Navarro,M., Rodriguez-Puebla,M.L., Larcher,F., Paramio,J.M., Conti,C.J., and Jorcano,J.L. (2001) Regulation of the differentiation-related gene Drg-1 during mouse skin carcinogenesis. *Mol.Carcinog.*, **32**, 100-109.

115. Nishie,A., Masuda,K., Otsubo,M., Migita,T., Tsuneyoshi,M., Kohno,K., Shuin,T., Naito,S., Ono,M., and Kuwano,M. (2001) High expression of the Cap43 gene in

infiltrating macrophages of human renal cell carcinomas. *Clin.Cancer Res.*, **7**, 2145-2151.

116. Xu,B., Lin,L., and Rote,N.S. (1999) Identification of a stress-induced protein during human trophoblast differentiation by differential display analysis. *Biol.Reprod.*, **61**, 681-686.

117. Sawai,S., Shimono,A., Wakamatsu,Y., Palmes,C., Hanaoka,K., and Kondoh,H. (1993) Defects of embryonic organogenesis resulting from targeted disruption of the N-myc gene in the mouse. *Development*, **117**, 1445-1455.

118. Arvanitis,C. and Felsher,D.W. (2006) Conditional transgenic models define how MYC initiates and maintains tumorigenesis. *Semin.Cancer Biol*, **16**, 313-317.

119. Fotovati A, Fujii T, Yamaguchi M, Kage M, Shirouzu K, Oie S, Basaki Y, Ono M, Yamana H, and Kuwano M (2006) 17Beta-estradiol induces down-regulation of Cap43/NDRG1/Drg-1, a putative differentiation-related and metastasis suppressor gene, in human breast cancer cells. *Clin Cancer Res.*, **12**, 3010-3018.

120. Morgan,D.O. (2007) *The cell cycle:principles of control*. Published by New Science Press Ltd in association with Oxford University Press, London.

121. Yang,X., Wang,W., Fan,J., Lal,A., Yang,D., Cheng,H., and Gorospe,M. (2004) Prostaglandin A2-mediated Stabilization of p21 mRNA through an ERK-dependent Pathway Requiring the RNA-binding Protein HuR. *Journal of Biological Chemistry*, **279**, 49298-49306.

122. Chen,X., Barton,L.F., Chi,Y., Clurman,B.E., and Roberts,J.M. (2007) Ubiquitin-independent degradation of cell-cycle inhibitors by the REGgamma proteasome. *Mol.Cell*, **26**, 843-852.

123. Kim K, Ongusaha PP, Hong YK, Kurdistani SK, Nakamura M, Lu KP, and Lee SW (2004) Function of Drg1/Rit42 in p53-dependent mitotic spindle checkpoint. *J Biol Chem.*, **279**, 38597-38602.

124. Stein S, Thomas EK, Herzog B, Westfall MD, Rocheleau JV, Jackson RS 2nd, Wang M, and Liang P (2004) NDRG1 is necessary for p53-dependent apoptosis. *J Biol Chem.*, **279**, 48930-48940.

125. Motwani M, Sirotnak FM, She Y, Commes T, and Schwartz GK (2002) Drg1, a novel target for modulating sensitivity to CPT-11 in colon cancer cells. *Cancer Res.*, **62**, 3950-3955.

126. Shah MA, Kortmansky J, Motwani M, Drobnjak M, Gonen M, Yi S, Weyerbacher A, Cordon-Cardo C, Lefkowitz R, Brenner B, O'Reilly E, Saltz L, Tong W, Kelsen DP, and Schwartz GK (2005) A phase I clinical trial of the sequential

combination of irinotecan followed by flavopiridol. *Clinical Cancer Research*, **11**, 3836-3845.

127. Shah MA, Kemeny N, Hummer A, Drobnjak M, Motwani M, Cordon-Cardo C, Gonen M, and Schwartz GK (2005) Drg1 expression in 131 colorectal liver metastases: correlation with clinical variables and patient outcomes. *Clin Cancer Res.*, **11**, 3296-3302.

128. Zheng,Y., Wang,L.S., Xia,L., Han,Y.H., Liao,S.H., Wang,X.L., Cheng,J.K., and Chen,G.Q. (2009) NDRG1 is down-regulated in the early apoptotic event induced by camptothecin analogs: the potential role in proteolytic activation of PKC delta and apoptosis. *Proteomics.*, **9**, 2064-2075.

129. Bergers,G. and Benjamin,L.E. (2003) Tumorigenesis and the angiogenic switch. *Nat.Rev.Cancer*, **3**, 401-410.

130. Mustonen,T. and Alitalo,K. (1995) Endothelial receptor tyrosine kinases involved in angiogenesis. *J Cell Biol*, **129**, 895-898.

131. Polette,M., Nawrocki-Raby,B., Gilles,C., Clavel,C., and Birembaut,P. (2004) Tumour invasion and matrix metalloproteinases. *Crit Rev.Oncol.Hematol.*, **49**, 179-186.

132. Sato,F., Shimada,Y., Watanabe,G., Uchida,S., Makino,T., and Imamura,M. (1999) Expression of vascular endothelial growth factor, matrix metalloproteinase-9 and E-cadherin in the process of lymph node metastasis in oesophageal cancer. *Br.J Cancer*, **80**, 1366-1372.

133. Ferrara,N. and Gerber,H.P. (2001) The role of vascular endothelial growth factor in angiogenesis. *Acta Haematol.*, **106**, 148-156.

134. Jones,N., Iljin,K., Dumont,D.J., and Alitalo,K. (2001) Tie receptors: new modulators of angiogenic and lymphangiogenic responses. *Nat.Rev.Mol.Cell Biol*, **2**, 257-267.

135. Neufeld,G. and Kessler,O. (2006) Pro-angiogenic cytokines and their role in tumor angiogenesis. *Cancer and Metastasis Reviews*, **25**, 373-385.

136. Yu,J., Ustach,C., and Kim,H.R. (2003) Platelet-derived growth factor signaling and human cancer. *J Biochem.Mol.Biol*, **36**, 49-59.

137. Hosoi,F., Izumi,H., Kawahara,A., Murakami,Y., Kinoshita,H., Kage,M., Nishio,K., Kohno,K., Kuwano,M., and Ono,M. (2009) N-myc downstream regulated gene 1/Cap43 suppresses tumor growth and angiogenesis of pancreatic cancer through attenuation of inhibitor of kappaB kinase beta expression. *Cancer Res.*, **69**, 4983-4991.

138. Arao T, Yanagihara K, Takigahira M, Takeda M, Koizumi F, Shiratori Y, and Nishio K (2006) ZD6474 inhibits tumor growth and intraperitoneal dissemination in a highly metastatic orthotopic gastric cancer model. *Int J Cancer*, **118**, 483-489.

139. Domhan S, Muschal S, Schwager C, Morath C, Wirkner U, Ansorge W, Maercker C, Zeier M, Huber PE, and Abdollahi A (2008) Molecular mechanisms of the antiangiogenic and antitumor effects of mycophenolic acid. *Mol Cancer Ther.*, **7**, 1656-1668.

140. Agrawal,S., Unterberg,M., Koschmieder,S., zur Stadt,U., Brunnberg,U., Verbeek,W., Buchner,T., Berdel,W.E., Serve,H., and Muller-Tidow,C. (2007) DNA Methylation of Tumor Suppressor Genes in Clinical Remission Predicts the Relapse Risk in Acute Myeloid Leukemia. *Cancer Res*, **67**, 1370-1377.

141. Yang,B., House,M.G., Guo,M., Herman,J.G., and Clark,D.P. (2004) Promoter methylation profiles of tumor suppressor genes in intrahepatic and extrahepatic cholangiocarcinoma. *Mod Pathol*, **18**, 412-420.

142. Ellen TP, Ke Q, Zhang P, and Costa M (2008) NDRG1, a growth and cancer related gene: regulation of gene expression and function in normal and disease states. *Carcinogenesis*, **29**, 2-8.

143. Maxwell,P.H. (2005) Hypoxia-inducible factor as a physiological regulator. *Experimental Physiology*, **90**, 791-797.

144. Wang,G.L., Jiang,B.H., Rue,E.A., and Semenza,G.L. (1995) Hypoxia-inducible factor 1 is a basic-helix-loop-helix-PAS heterodimer regulated by cellular O2 tension. *Proceedings of the National Academy of Sciences of the United States of America*, **92**, 5510-5514.

145. Ivan,M., Kondo,K., Yang,H., Kim,W., Valiando,J., Ohh,M., Salic,A., Asara,J.M., Lane,W.S., and Kaelin,W.G., Jr. (2001) HIFalpha targeted for VHL-mediated destruction by proline hydroxylation: implications for O2 sensing. *Science*, **292**, 464-468.

146. Lando,D., Peet,D.J., Whelan,D.A., Gorman,J.J., and Whitelaw,M.L. (2002) Asparagine Hydroxylation of the HIF Transactivation Domain: A Hypoxic Switch. *Science*, **295**, 858-861.

147. McNeill,L.A., Hewitson,K.S., Claridge,T.D., Seibel,J.F., Horsfall,L.E., and Schofield,C.J. (2002) Hypoxia-inducible factor asparaginyl hydroxylase (FIH-1) catalyses hydroxylation at the beta-carbon of asparagine-803. *Biochem.J*, **367**, 571-575.

148. Cummins,E.P. and Taylor,C.T. (2005) Hypoxia-responsive transcription factors. *Pflugers Arch.*, **450**, 363-371.

149. Salnikow K, Su W, Blagosklonny MV, and Costa M (2000) Carcinogenic metals induce hypoxia-inducible factor-stimulated transcription by reactive oxygen species-independent mechanism. *Cancer Res.*, **60**, 3375-3378.

150. Le NT and Richardson DR (2004) Iron chelators with high antiproliferative activity up-regulate the expression of a growth inhibitory and metastasis suppressor gene: a link between iron metabolism and proliferation. *Blood*, **104**, 2967-2975.

151. Ratcliffe,P.J. (2002) From erythropoietin to oxygen: hypoxia-inducible factor hydroxylases and the hypoxia signal pathway. *Blood Purif.*, **20**, 445-450.

152. Masuda K, Ono M, Okamoto M, Morikawa W, Otsubo M, Migita T, Tsuneyoshi M, Okuda H, Shuin T, Naito S, and Kuwano M (2003) Downregulation of Cap43 gene by von Hippel-Lindau tumor suppressor protein in human renal cancer cells. *Int J Cancer*, **105**, 803-810.

153. Zhang P, Tchou-Wong KM, and Costa M (2007) Egr-1 Mediates Hypoxia-Inducible Transcription of the NDRG1 Gene through an Overlapping Egr-1/Sp1 Binding Site in the Promoter. *Cancer Res.*, **67**, 9125-9133.

154. Glover,J.N. and Harrison,S.C. (1995) Crystal structure of the heterodimeric bZIP transcription factor c-Fos-c-Jun bound to DNA. *Nature*, **373**, 257-261.

155. Shaulian,E. and Karin,M. (2002) AP-1 as a regulator of cell life and death. *Nat Cell Biol*, **4**, E131-E136.

156. Karin,M., Liu,Z., and Zandi,E. (1997) AP-1 function and regulation. *Curr Opin Cell Biol*, **9**, 240-246.

157. van,D.H. and Castellazzi,M. (2001) Distinct roles of Jun : Fos and Jun : ATF dimers in oncogenesis. *Oncogene*, **20**, 2453-2464.

158. Hartl,M., Bader,A.G., and Bister,K. (2003) Molecular targets of the oncogenic transcription factor jun. *Curr Cancer Drug Targets.*, **3**, 41-55.

159. Angel,P. and Karin,M. (1991) The role of Jun, Fos and the AP-1 complex in cell-proliferation and transformation. *Biochim.Biophys.Acta*, **1072**, 129-157.

160. Thiel,G. and Cibelli,G. (2002) Regulation of life and death by the zinc finger transcription factor Egr-1. *J Cell Physiol*, **193**, 287-292.

161. Lo,L.W., Cheng,J.J., Chiu,J.J., Wung,B.S., Liu,Y.C., and Wang,D.L. (2001) Endothelial exposure to hypoxia induces Egr-1 expression involving PKCalpha-mediated Ras/Raf-1/ERK1/2 pathway. *J Cell Physiol*, **188**, 304-312.

162. Yan,S.F., Lu,J., Zou,Y.S., Soh-Won,J., Cohen,D.M., Buttrick,P.M., Cooper,D.R., Steinberg,S.F., Mackman,N., Pinsky,D.J., and Stern,D.M. (1999) Hypoxia-

associated Induction of Early Growth Response-1 Gene Expression. *Journal of Biological Chemistry*, **274**, 15030-15040.

163. Sinsheimer,R.L. (1989) The Santa-Cruz Workshop - May 1985. *Genomics*, **5**, 954-956.

164. White House Press Release - First Survey of the Human Genome. http://www.ornl.gov . 6-25-2000. The White House, Office of the press secretary. 9-11-0090.

165. Venter,J.C., Adams,M.D., Myers,E.W., Li,P.W., Mural,R.J., Sutton,G.G., Smith,H.O., Yandell,M., Evans,C.A., Holt,R.A., Gocayne,J.D., Amanatides,P., Ballew,R.M., Huson,D.H., Wortman,J.R., Zhang,Q., Kodira,C.D., Zheng,X.Q.H., Chen,L., Skupski,M., Subramanian,G., Thomas,P.D., Zhang,J.H., Miklos,G.L.G., Nelson,C., Broder,S., Clark,A.G., Nadeau,C., McKusick,V.A., Zinder,N., Levine,A.J., Roberts,R.J., Simon,M., Slayman,C., Hunkapiller,M., Bolanos,R., Delcher,A., Dew,I., Fasulo,D., Flanigan,M., Florea,L., Halpern,A., Hannenhalli,S., Kravitz,S., Levy,S., Mobarry,C., Reinert,K., Remington,K., bu-Threideh,J., Beasley,E., Biddick,K., Bonazzi,V., Brandon,R., Cargill,M., Chandramouliswaran,I., Charlab,R., Chaturvedi,K., Deng,Z.M., Di Francesco,V., Dunn,P., Eilbeck,K., Evangelista,C., Gabrielian,A.E., Gan,W., Ge,W.M., Gong,F.C., Gu,Z.P., Guan,P., Heiman,T.J., Higgins,M.E., Ji,R.R., Ke,Z.X., Ketchum,K.A., Lai,Z.W., Lei,Y.D., Li,Z.Y., Li,J.Y., Liang,Y., Lin,X.Y., Lu,F., Merkulov,G.V., Milshina,N., Moore,H.M., Naik,A.K., Narayan,V.A., Neelam,B., Nusskern,D., Rusch,D.B., Salzberg,S., Shao,W., Shue,B.X., Sun,J.T., Wang,Z.Y., Wang,A.H., Wang,X., Wang,J., Wei,M.H., Wides,R., Xiao,C.L., Yan,C.H., Yao,A., Ye,J., Zhan,M., Zhang,W.Q., Zhang,H.Y., Zhao,Q., Zheng,L.S., Zhong,F., Zhong,W.Y., Zhu,S.P.C., Zhao,S.Y., Gilbert,D., Baumhueter,S., Spier,G., Carter,C., Cravchik,A., Woodage,T., Ali,F., An,H.J., Awe,A., Baldwin,D., Baden,H., Barnstead,M., Barrow,I., Beeson,K., Busam,D., Carver,A., Center,A., Cheng,M.L., Curry,L., Danaher,S., Davenport,L., Desilets,R., Dietz,S., Dodson,K., Doup,L., Ferriera,S., Garg,N., Gluecksmann,A., Hart,B., Haynes,J., Haynes,C., Heiner,C., Hladun,S., Hostin,D., Houck,J., Howland,T., Ibegwam,C., Johnson,J., Kalush,F., Kline,L., Koduru,S., Love,A., Mann,F., May,D., McCawley,S., McIntosh,T., McMullen,I., Moy,M., Moy,L., Murphy,B., Nelson,K., Pfannkoch,C., Pratts,E., Puri,V., Qureshi,H., Reardon,M., Rodriguez,R., Rogers,Y.H., Romblad,D., Ruhfel,B., Scott,R., Sitter,C., Smallwood,M., Stewart,E., Strong,R., Suh,E., Thomas,R., Tint,N.N., Tse,S., Vech,C., Wang,G., Wetter,J., Williams,S., Williams,M., Windsor,S., Winn-Deen,E., Wolfe,K., Zaveri,J., Zaveri,K., Abril,J.F., Guigo,R., Campbell,M.J., Sjolander,K.V., Karlak,B., Kejariwal,A., Mi,H.Y., Lazareva,B., Hatton,T., Narechania,A., Diemer,K., Muruganujan,A., Guo,N., Sato,S., Bafna,V., Istrail,S., Lippert,R., Schwartz,R., Walenz,B., Yooseph,S., Allen,D., Basu,A., Baxendale,J., Blick,L., Caminha,M., Carnes-Stine,J., Caulk,P., Chiang,Y.H., Coyne,M., Dahlke,C., Mays,A.D., Dombroski,M., Donnelly,M., Ely,D., Esparham,S., Fosler,C., Gire,H., Glanowski,S., Glasser,K., Glodek,A., Gorokhov,M., Graham,K., Gropman,B., Harris,M., Heil,J., Henderson,S.,

Hoover,J., Jennings,D., Jordan,C., Jordan,J., Kasha,J., Kagan,L., Kraft,C., Levitsky,A., Lewis,M., Liu,X.J., Lopez,J., Ma,D., Majoros,W., McDaniel,J., Murphy,S., Newman,M., Nguyen,T., Nguyen,N., and Nodell,M. (2001) The sequence of the human genome. *Science*, **291**, 1304-1351.

166. Macgregor,P.F. and Squire,J.A. (2002) Application of Microarrays to the Analysis of Gene Expression in Cancer. *Clin Chem*, **48**, 1170-1177.

167. Tricarico,C., Pinzani,P., Bianchi,S., Paglierani,M., Distante,V., Pazzagli,M., Bustin,S.A., and Orlando,C. (2002) Quantitative real-time reverse transcription polymerase chain reaction: normalization to rRNA or single housekeeping genes is inappropriate for human tissue biopsies. *Anal.Biochem.*, **309**, 293-300.

168. Livak,K.J. and Schmittgen,T.D. (2001) Analysis of relative gene expression data using real-time quantitative PCR and the 2(-Delta Delta C(T)) Method. *Methods*, **25**, 402-408.

169. Luo,A., Kong,J., Hu,G., Liew,C.C., Xiong,M., Wang,X., Ji,J., Wang,T., Zhi,H., Wu,M., and Liu,Z. (2004) Discovery of Ca2+-relevant and differentiation-associated genes downregulated in esophageal squamous cell carcinoma using cDNA microarray. *Oncogene*, **23**, 1291-1299.

170. Waxman,S. and Wurmbach,E. (2007) De-regulation of common housekeeping genes in hepatocellular carcinoma. *BMC Genomics*, **8**, 243.

171. Hansen,C.N., Ketabi,Z., Rosenstierne,M.W., Palle,C., Boesen,H.C., and Norrild,B. (2009) Expression of CPEB, GAPDH and U6snRNA in cervical and ovarian tissue during cancer development. *APMIS*, **117**, 53-59.

172. Ruan,W. and Lai,M. (2007) Actin, a reliable marker of internal control? *Clin Chim.Acta*, **385**, 1-5.

173. Barber,R.D., Harmer,D.W., Coleman,R.A., and Clark,B.J. (2005) GAPDH as a housekeeping gene: analysis of GAPDH mRNA expression in a panel of 72 human tissues. *Physiol.Genomics*, **21**, 389-395.

174. Wamunyokoli, F. Differentially expressed genes in oesophageal cancer. 2002. PhD thesis/dissertation, University of Cape Town.
Ref Type: Thesis/Dissertation

175. Seery,J.P. (2002) Stem cells of the oesophageal epithelium. *J.Cell Sci.*, **115**, 1783-1789.

176. Yan X, Chua MS, Sun H, and So S. N-Myc down-regulated gene 1 mediates proliferation, invasion, and apoptosis of hepatocellular carcinoma cells. Cancer Lett. 2008.
Ref Type: Generic

177. Du,J.R., Jiang,Y., Zhang,Y.M., and Fu,H. (2003) Vascular endothelial growth factor and microvascular density in esophageal and gastric carcinomas. *World J Gastroenterol.*, **9**, 1604-1606.

178. Nagata,J., Kijima,H., Hatanaka,H., Tokunaga,T., Kamochi,J., Abe,Y., Takagi,A., Mine,T., Yamazaki,H., Nakamura,M., and Ueyama,Y. (2002) Angiopoietin-1 and vascular endothelial growth factor expression in human esophageal cancer. *Int.J Mol.Med.*, **10**, 423-426.

179. Shih,C.H., Ozawa,S., Ando,N., Ueda,M., and Kitajima,M. (2000) Vascular endothelial growth factor expression predicts outcome and lymph node metastasis in squamous cell carcinoma of the esophagus. *Clin Cancer Res*, **6**, 1161-1168.

180. Shimada,Y., Imamura,M., Watanabe,G., Uchida,S., Harada,H., Makino,T., and Kano,M. (1999) Prognostic factors of oesophageal squamous cell carcinoma from the perspective of molecular biology. *Br.J Cancer*, **80**, 1281-1288.

181. Ferrara,N. (1996) Vascular endothelial growth factor. *Eur.J Cancer*, **32A**, 2413-2422.

182. Roberts,W.G. and Palade,G.E. (1995) Increased microvascular permeability and endothelial fenestration induced by vascular endothelial growth factor. *J Cell Sci.*, **108 (Pt 6)**, 2369-2379.

183. Senger,D.R., Van de,W.L., Brown,L.F., Nagy,J.A., Yeo,K.T., Yeo,T.K., Berse,B., Jackman,R.W., Dvorak,A.M., and Dvorak,H.F. (1993) Vascular permeability factor (VPF, VEGF) in tumor biology. *Cancer Metastasis Rev.*, **12**, 303-324.

184. Jung,J.E., Lee,H.G., Cho,I.H., Chung,D.H., Yoon,S.H., Yang,Y.M., Lee,J.W., Choi,S., Park,J.W., Ye,S.K., and Chung,M.H. (2005) STAT3 is a potential modulator of HIF-1-mediated VEGF expression in human renal carcinoma cells. *FASEB J.*,04-3099fje.

185. Kurokawa,T., Miyamoto,M., Kato,K., Cho,Y., Kawarada,Y., Hida,Y., Shinohara,T., Itoh,T., Okushiba,S., Kondo,S., and Katoh,H. (0 AD) Overexpression of hypoxia-inducible-factor 1[alpha](HIF-1[alpha]) in oesophageal squamous cell carcinoma correlates with lymph node metastasis and pathologic stage. *Br J Cancer*, **89**, 1042-1047.

186. Wang,B., Khachigian,L.M., Esau,L., Birrer,M.J., Zhao,X., Parker,M.I., and Hendricks,D.T. (2009) A key role for early growth response-1 and nuclear factor-kappaB in mediating and maintaining GRO/CXCR2 proliferative signaling in esophageal cancer. *Mol Cancer Res*, **7**, 755-764.

187. Iervolino,A., Trisciuoglio,D., Ribatti,D., Candiloro,A., Biroccio,A., Zupi,G., and Del,B.D. (2002) Bcl-2 overexpression in human melanoma cells increases

angiogenesis through VEGF mRNA stabilization and HIF-1-mediated transcriptional activity. *FASEB J*, **16**, 1453-1455.

188. Stein,I., Neeman,M., Shweiki,D., Itin,A., and Keshet,E. (1995) Stabilization of vascular endothelial growth factor mRNA by hypoxia and hypoglycemia and coregulation with other ischemia-induced genes. *Mol.Cell Biol*, **15**, 5363-5368.

189. Yu,X., Luo,A., Zhou,C., Ding,F., Wu,M., Zhan,Q., and Liu,Z. (2006) Differentiation-associated genes regulated by TPA-induced c-Jun expression via a PKC/JNK pathway in KYSE450 cells. *Biochem.Biophys.Res.Commun.*, **342**, 286-292.

190. Levy,S., Hannenhalli,S., and Workman,C. (2001) Enrichment of regulatory signals in conserved non-coding genomic sequence. *Bioinformatics.*, **17**, 871-877.

191. Hall,T.A. (1999) BioEdit: a user-friendly biological sequence alignment editor and analysis program for Windows 95/98/NT. *Nucl.Acids.Symp.Ser.*, **41**, 95-98.

192. Thompson,J.D., Higgins,D.G., and Gibson,T.J. (1994) CLUSTAL W: improving the sensitivity of progressive multiple sequence alignment through sequence weighting, position-specific gap penalties and weight matrix choice. *Nucleic Acids Res*, **22**, 4673-4680.

193. Barbosa,L.A., Goto-Silva,L., Redondo,P.A., Oliveira,S., Montesano,G., De,S.W., and Morgado-Diaz,J.A. (2003) TPA-induced signal transduction: a link between PKC and EGFR signaling modulates the assembly of intercellular junctions in Caco-2 cells. *Cell Tissue Res*, **312**, 319-331.

194. Xian,W., Kiguchi,K., Imamoto,A., Rupp,T., Zilberstein,A., and DiGiovanni,J. (1995) Activation of the epidermal growth factor receptor by skin tumor promoters and in skin tumors from SENCAR mice. *Cell Growth Differ.*, **6**, 1447-1455.

195. Kumar,S., Jiang,M.S., Adams,J.L., and Lee,J.C. (1999) Pyridinylimidazole compound SB 203580 inhibits the activity but not the activation of p38 mitogen-activated protein kinase. *Biochem.Biophys.Res Commun.*, **263**, 825-831.

196. Cartharius,K., Frech,K., Grote,K., Klocke,B., Haltmeier,M., Klingenhoff,A., Frisch,M., Bayerlein,M., and Werner,T. (2005) MatInspector and beyond: promoter analysis based on transcription factor binding sites. *Bioinformatics.*, **21**, 2933-2942.

197. Berezikov,E., Guryev,V., Plasterk,R.H., and Cuppen,E. (2004) CONREAL: conserved regulatory elements anchored alignment algorithm for identification

of transcription factor binding sites by phylogenetic footprinting. *Genome Res*, **14**, 170-178.

198. Bauer,I., Hohl,M., Al-Sarraj,A., Vinson,C., and Thiel,G. (2005) Transcriptional activation of the Egr-1 gene mediated by tetradecanoylphorbol acetate and extracellular signal-regulated protein kinase. *Arch.Biochem.Biophys.*, **438**, 36-52.

199. Lamph,W.W., Wamsley,P., Sassone-Corsi,P., and Verma,I.M. (1988) Induction of proto-oncogene JUN/AP-1 by serum and TPA. *Nature*, **334**, 629-631.

200. Pulverer,B.J., Kyriakis,J.M., Avruch,J., Nikolakaki,E., and Woodgett,J.R. (1991) Phosphorylation of c-jun mediated by MAP kinases. *Nature*, **353**, 670-674.

201. Chiu,R., Boyle,W.J., Meek,J., Smeal,T., Hunter,T., and Karin,M. (1988) The c-Fos protein interacts with c-Jun/AP-1 to stimulate transcription of AP-1 responsive genes. *Cell*, **54**, 541-552.

202. Ozanne,B.W., Spence,H.J., McGarry,L.C., and Hennigan,R.F. (2007) Transcription factors control invasion: AP-1 the first among equals. *Oncogene*, **26**, 1-10.

203. Wisdom,R., Johnson,R.S., and Moore,C. (1999) c-Jun regulates cell cycle progression and apoptosis by distinct mechanisms. *EMBO J*, **18**, 188-197.

204. Behrens,A., Jochum,W., Sibilia,M., and Wagner,E.F. (2000) Oncogenic transformation by ras and fos is mediated by c-Jun N-terminal phosphorylation. *Oncogene*, **19**, 2657-2663.

205. Eferl,R. and Wagner,E.F. (2003) AP-1: a double-edged sword in tumorigenesis. *Nat.Rev.Cancer*, **3**, 859-868.

206. Jochum,W., Passegue,E., and Wagner,E.F. (2001) AP-1 in mouse development and tumorigenesis. *Oncogene*, **20**, 2401-2412.

207. Smeal,T., Binetruy,B., Mercola,D.A., Birrer,M., and Karin,M. (1991) Oncogenic and transcriptional cooperation with Ha-Ras requires phosphorylation of c-Jun on serines 63 and 73. *Nature*, **354**, 494-496.

208. Hussain,S., Bharti,A., Salam,I., Bhat,M., Mir,M., Hedau,S., Siddiqi,M., Basir,S., and Das,B. (2009) Transcription factor AP-1 in esophageal squamous cell carcinoma: Alterations in activity and expression during Human Papillomavirus infection. *BMC Cancer*, **9**, 329.

209. Fahmy,R.G., Dass,C.R., Sun,L.Q., Chesterman,C.N., and Khachigian,L.M. (2003) Transcription factor Egr-1 supports FGF-dependent angiogenesis during neovascularization and tumor growth. *Nat Med.*, **9**, 1026-1032.

210. Wang,B., Hendricks,D.T., Wamunyokoli,F., and Parker,M.I. (2006) A growth-related oncogene/CXC chemokine receptor 2 autocrine loop contributes to cellular proliferation in esophageal cancer. *Cancer Res*, **66**, 3071-3077.

211. Hoffmann,E., Ashouri,J., Wolter,S., Doerrie,A., ttrich-Breiholz,O., Schneider,H., Wagner,E.F., Troppmair,J., Mackman,N., and Kracht,M. (2008) Transcriptional Regulation of EGR-1 by the Interleukin-1-JNK-MKK7-c-Jun Pathway. *Journal of Biological Chemistry*, **283**, 12120-12128.

212. Aicher,W.K., Sakamoto,K.M., Hack,A., and Eibel,H. (1999) Analysis of functional elements in the human Egr-1 gene promoter. *Rheumatol.Int*, **18**, 207-214.

213. Donovan,E.A. and Kummar,S. (2006) Targeting VEGF in cancer therapy. *Curr Probl.Cancer*, **30**, 7-32.

214. Sperandio,S., Fortin,J., Sasik,R., Robitaille,L., Corbeil,J., and de,B., I (2009) The transcription factor Egr1 regulates the HIF-1alpha gene during hypoxia. *Mol Carcinog.*, **48**, 38-44.

215. Veale,R.B. and Thornley,A.L. (1989) Increased single class low-affinity EGF receptors expressed by human esophageal squamous cell carcinoma cell lines. *S.Afr.J.Sci.*, **85**, 375-379.

216. Shimada,Y., Imamura,M., Wagata,T., Yamaguchi,N., and Tobe,T. (1992) Characterization of 21 newly established esophageal cancer cell lines. *Cancer*, **69**, 277-284.

217. Ishida,K., Nagahara,H., Kogiso,T., Aso,T., Hayashi,N., and Akaike,T. (2003) Cell adhesion aside from integrin system can abrogate anoikis in rat liver cells by down-regulation of FasL expression, not by activation of PI-3K/Akt and ERK signaling pathway. *Biochemical and Biophysical Research Communications*, **300**, 201-208.

218. Livak,K.J. and Schmittgen,T.D. (2001) Analysis of relative gene expression data using real-time quantitative PCR and the 2(-Delta Delta C(T)) Method. *Methods*, **25**, 402-408.